

STRESS INTENSITY FAILURE RATE PROPAGATORS OF FLEXIBLE PAVEMENT

SAMUEL OLUGBENGA ABEJIDE (*Jnr*)

Doctoral thesis submitted in partial fulfilment of the requirement for the Degree

DOCTOR OF ENGINEERING IN CIVIL ENGINEERING

at the Central University of Technology,

Faculty of Engineering, Built Environment and Information Technology,

Department of Civil Engineering, Bloemfontein Campus,

Free State

Promoter: Prof. Mohamed M H Mostafa (University of KwaZulu-Natal, South Africa)

Co- Promoters: Dr Rahman Mujib (Brunel University, United Kingdom)

Prof. Dillip K Das (University of KwaZulu-Natal, South Africa)

APRIL 2020

Bloemfontein

DECLARATION

I, Samuel Olugbenga Abejide, student number , declare, this day, the 23rd of April 2020, this dissertation, submitted to Central University of Technology, Faculty of Engineering Built Environment and Information Technology, Civil Engineering Department, Bloemfontein campus Free State for the award of the degree of Doctor of Engineering in Civil Engineering, is my independent work. This thesis submission conforms with the code of conduct for academic integrity, diligence, excellence and true workmanship alongside other relevant policies, procedures, rules and regulations of the Central University of Technology, Free State. This thesis has not been submitted previously to any institution by myself or any other person in fulfilment of the requirements for the attainment of any qualification. All the sourced work cited and quoted is duly acknowledged through the provided list of references.



27th APRIL, 2020

SIGNATURE OF STUDENT

DATE

DEDICATION

The submitted thesis is dedicated to Almighty God, who gives life, wisdom and understanding freely. To Him be all Praise, Honour and Glory forever (*Amen*).

ACKNOWLEDGEMENTS

God has been my strongest advocate throughout my entire Doctoral experience. All glory to the Almighty for supporting me through this journey.

The work completed in this dissertation would not have been possible without the guidance of my wonderful supervisory committee members, Prof. M. Mostafa, Dr Mujib Rahman and Prof. Das Dillip. Thank you for your support throughout my Doctoral study. Your knowledge in this field is immense and you have been an excellent resource throughout my research. Prof Mostafa, I have studied your professionalism and have acquired more than just academic knowledge in your presence. You have been a great mentor, in direct and indirect ways, and have been an exemplary icon of excellence in teaching, learning and supervision. I appreciate your assistance as my supervisor and highly value your input towards my Doctoral degree.

In addition, I will like to recognise the effort of the Head of Department Civil Engineering, through the Faculty of Engineering, Built Environment and Information Technology; Central University of Technology for providing me with financial support, but most importantly, allowing me the opportunity to gain valuable experience as a researcher. Thank you for your support, academically, financially and in my professional development.

A big 'thank you' goes to the Research Group in Evolvable Manufacturing Systems (*RGEMS*) that assisted with the MISRA v1.1 setup build.

My deepest and profound gratitude goes to Miss Nour Mostafa and to Ms Elizabeth le Sueur, who assisted with language editing of this thesis. Your input and professionalism are highly recognised.

Furthermore, a huge gratitude goes to my Co-Promoters, Dr Rahman Mujib and Prof, Das Dillip for their endless support and critique: without your input this thesis would not be as fine-tuned. I also extend my gratitude to the many graduate students and doctoral students who assisted me in my work. Thank you to the SURT research group for their input in my research throughout my career at CUT, and special thanks to MERSETA for their support. Please continue to assist the many graduate students of the future and keep changing lives for the better.

I would like to take this opportunity to express my heart-felt gratitude to everyone who helped make this thesis a success. I am thankful for their guidance, constructive criticism and friendly advice throughout the project.

I cannot forget to thank my Mother, Mrs Comfort Onize Abejide, and my Father, Prof. O.S. Abejide, for their love and tireless support throughout my research as well as that of my colleagues.

I would like to extend my heart-felt gratitude to my fiancée, God bless you. You mean much to me. Thank you for your love, care, support and prayers.

I would also like to extend a big gratitude to Dr Yinka O.J and his caring wife for their prayers love and support; Dayo Adedeji, Dr Akanbi, Mr Bongani G, and the unforgettable assistance, endless backdoor reviews and support of Prof. Bankole Awuzie, as well as everyone who supported me throughout this project. Mangut Pablo Gonzalez.

I also want to use this section to express gratitude to Walter Sisulu University MERSETA study fellowship scheme; assisting with accommodation and travel visit to Bloemfontein for consultation with my supervisors.

ABSTRACT

A responsive pavement management infrastructure is essential for providing durable pavement infrastructure. This need has been accentuated by the quest for sustainability through the adoption of Road Traffic Management System (RTMS) patterns as employed by the various Departments of Transportation (DOT) in South Africa. It can be summarised that increasing humidity/moisture content resulting in percentage increase in saturation content of the underlying base, subbase or subgrade layers will significantly result to a reduction of the Resilient Modulus (M_R) of the entire pavement structure weather flexible or rigid. However, this scenario poses a great threat to the structural carrying capacity of the pavement structure. Therefore, it is imperative to provide a solution to such critical problems as they occur and when there is no control to avert them. This can, only be made possible by identifying the exact cause of the problem and providing a feasibly efficient and achievable solution. In the design of roads, flexible pavement has overtime experienced associated distress failure modes resulting in potholes, loss of skid resistance, and reduction in riding quality, noise and road surface ponding. Many of these have being tackled by research, both in the past and currently. The structural collapse of pavement is as a result of distress modes caused by human factors, construction error, excessive traffic loading, environmental factors, cumulative design and geometric errors results to unnecessary loss of strength and stability during the estimated design pavement service life. The objective of this current study is to develop stress intensity failure rate propagators induced by the factors of distress earlier mentioned in order to develop performance functions of asphaltic pavement model using the finite element method followed by a semantic stream-web data analysis (JAVA Expert System Shell analysis JESS). Multivariable transfer functions are generated in order to assess the different modes of failure for Mode I where the onset of crack begins to develop. Moisture sensors are embedded into the pavement in other to determine the real time failure modes populated under service loading and environmental conditions. Damage models are obtained to evaluate the evolution of crack growth and the strain energy release rate for failure mode I (crack initiation). The analysis of this study is further modelled in Abaqus CAE 6.13 as well as a proposed web-based computation analysis of pavement failure (JESS). The FE model indicates that at 20% moisture ingress, the vertical deformation of the subgrade is stable with a value $6.65 \text{ E-}05$. With further increase in moisture, the pavement stiffness reduces and the deformation increases with a failure rate value of $9.68 \text{ E-}05$. The difference indicates that there is a high percentage correlation between moisture content

or saturation content increase in pavement and the resilient modulus of the pavement (Stiffness coefficient). Further subjecting the pavement to the same load or increasing load cycles will result in gradual delamination and further yield to total deformation. The results are as presented and discussed as the data obtained from the sensor probes are discretised for analysis in the workbench. A network level pavement management system to contribute to the development of a framework for evaluating pavements' quality index (PQI) and service life capacity with varying environmental and climatic conditions is presented. The results indicate variation of stiffness with increasing moisture content. Increase in moisture propagation increased saturation of the unbound granular base which reduced the elastic modulus of the subbase layer and reduced the strength of the pavement leading to formation of bottom-up cracks and cracking failure. The horizontal tensile strain (E11) at the asphalt layer at 20% was 69.57×10^{-4} , which increased to 140.8×10^{-4} at 60% moisture content. The horizontal deformation (E22) reduced, assuming that the material is experiencing work-hardening and no further stress can result to any significant damage. The damage remained at a constant value of 96.8×10^{-4} at 60% saturation. Consequently, the performance of the pavement is affected by temperature gradient. This implies that increasing temperature gradient results in reduction in stiffness of the asphalt layer. In tropical regions, this can result to immediate rutting failure of the asphalt layer, which overtime leads to formation of top-down cracks and potholes with increasing moisture content, even if it is a newly constructed road less than two years old. The web data architecture analysis provides deflection values for failure occurring within the pavement underlying layers. The findings indicate that there is a high correlation between Environmental Condition and road pavement (Asphalt Concrete). The result indicates that increasing temperature gradient of the pavement reduces the fracture energy of the pavement, which results in delamination and collapse over a longer period of time. On the contrary, reduced temperature gradient increases the fracture Energy, making the pavement stiffness high and resistant to failure, but at very low temperatures a compromise is reached and the strength is breached resulting in a brittle material (glass). Although the failure is not visible at the onset of crack propagation, but continual exposure to increasing temperatures as well as increasing moisture content will lead to failure of the pavement before the design life is reached. There is also a surge in the relationship between Pavement Fracture Energy and the Pavement Resilient Modulus. Further, it is found that, the higher the temperature, the higher the rate of deflection and the lower the temperature, the lower the deflection.

TABLE OF CONTENTS

| | |
|---|--------|
| DECLARATION | ii |
| DEDICATION | iii |
| ACKNOWLEDGEMENTS | iv |
| ABSTRACT | vi |
| TABLE OF CONTENTS | viii |
| PUBLICATIONS | xii |
| TABLES | xiii |
| LIST OF FIGURES | xiv |
| ABBREVIATIONS | xvii |
| CHAPTER ONE: BACKGROUND | - 1 - |
| 1.0 Introduction | - 1 - |
| 1.1 Problem Statement | - 3 - |
| 1.2 Aim and Objective of study | - 4 - |
| 1.3 Justification of Study | - 4 - |
| 1.4 Scope of Study | - 5 - |
| 1.5 Limitations of Study | - 6 - |
| 1.6 Outline of Dissertation | - 8 - |
| <i>1.6.1 Chapter One</i> | - 8 - |
| <i>1.6.2 Chapter Two</i> | - 8 - |
| <i>1.6.3 Chapter Three</i> | - 8 - |
| <i>1.6.4 Chapter Four</i> | - 8 - |
| <i>1.6.5 Chapter Five</i> | - 8 - |
| <i>1.6.6 Chapter Six</i> | - 8 - |
| CHAPTER TWO: LITERATURE REVIEW | - 9 - |
| 2.0 Introduction | - 9 - |
| 2.1 Stress and Strain Measurement in Pavement | - 13 - |
| 2.1.1 Pavement Condition Monitoring | - 16 - |
| 2.2 South African Transportation Systems | - 18 - |
| 2.3 Pavement Management Systems | - 19 - |
| 2.3.1 Network and Project Level Pavement Management System | - 20 - |
| 2.3.2 Pavement Management Decision Making | - 22 - |

| | |
|---|-------------|
| 2.3.3 Artificial Neural Networks (ANN) in Pavement Management System | 23 - |
| 2.3.4 Monte Carlo Simulation Approach and Randomized Sections Selection | 24 - |
| 2.4 Pavement Performance and Instrumentation Parameters | 25 - |
| 2.4.1 Pavement Cracking Consideration and Pavement Cracking Initiation | 27 - |
| 2.4.2 Reflective cracking failure patterns | 30 - |
| 2.4.3 Flexible Pavement Design Methods..... | 31 - |
| 2.5 Empirical and Mechanistic Empirical Pavement Design Overview..... | 35 - |
| 2.6 Trésaguet Road Design Philosophy | 36 - |
| 2.7 Telford Road Design Philosophy | 36 - |
| 2.8 Macadam Road Design Philosophy | 37 - |
| 2.9 The AASHO Road Test | 37 - |
| 2.10 Mechanistic-Empirical Pavement Design Method..... | 39 - |
| 2.10.1 Distress Prediction in M-E Design Method | 42 - |
| 2.11 Analysis of Flexible Pavement Base Materials | 42 - |
| 2.11.1 Asphalt-Stabilised Base Material..... | 42 - |
| 2.11.2 Cement- Stabilized Base Materials..... | 43 - |
| 2.11.3 Bound Granular Base Materials..... | 43 - |
| 2.11.4 HMA Pavement Failure Investigation modes..... | 44 - |
| 2.11.5 Moisture Impairment/Damage in Hot Mix Asphalt Pavements | 46 - |
| 2.12 Two-Dimensional Stress State..... | 48 - |
| 2.12.1 Three-Dimensional Stress State | 49 - |
| 2.13 Concept of Reliability | 50 - |
| 2.13.1 Reliability Index | 52 - |
| 2.13.2 Simulation Techniques | 52 - |
| 2.14 First Order Reliability Unconstrained Method (FERUM) | 53 - |
| 2.14.1 First Order Reliability Method (FORM)..... | 53 - |
| 2.15 Summary..... | 56 - |
| CHAPTER THREE: METHODOLOGY..... | 57 - |
| 3.0 Research Design | 57 - |
| 3.1 Linear Elastic Fracture Mechanics | 59 |
| 3.2 Strain Energy Release rate for Flexible Pavement | 60 |
| 3.3 Climatic Effect on Highway Structures | 61 |
| 3.4 Evaluation of Water Flow within Pavement System | 61 |

| | |
|---|------------|
| 3.5 Conventional Infiltration Mode | 63 |
| 3.6 Hydraulic Conductivity Curve Models | 64 |
| 3.7 General Design for Combating Moisture Damage | 65 |
| 3.7.1 Moisture Subsurface Drainage | 65 |
| 3.7.2 Water flow Analysis within pavement structures | 66 |
| 3.8 Finite Element Analysis of Pavement Drainage | 67 |
| 3.8.1 Pavement Impulse Response | 68 |
| 3.8.2 Static Impulse Analysis | 68 |
| 3.8.3 Dynamic Impulse Analysis | 68 |
| 3.8.4 Stochastic Processes | 69 |
| 3.8.5 Reliability of Highway structures | 69 |
| 3.9 Summary | 71 |
| CHAPTER FOUR: INSTRUMENTATION AND DEVICE SETUP | 72 |
| 4.0 Instrumentation and Analysis | 72 |
| 4.1 Pavement Instrumentation Using Moisture Sensors | 72 |
| 4.1.1 Instrumentation Consideration Overview | 72 |
| 4.1.2 Arduino Technology | 74 |
| 4.2 Microcontroller configuration and build up | 75 |
| 4.3 Hydraulic Water Content and Humidity Potential | 76 |
| 4.4 Measurement of Volumetric Moisture Content | 78 |
| 4.5 Pavement Temperature Gradient | 78 |
| 4.6 Components of Pavement Instrumentation | 80 |
| 4.7 Pavement material geometry configuration | 81 |
| CHAPTER FIVE: DATA EXPERIMENTATION AND DATA ANALYSIS | 84 |
| 5.0 Introduction | 84 |
| 5.1 Data Experimentation and Data Analysis | 84 |
| 5.2 Damage Model for Simulation of flexible pavement | 89 |
| 5.2.1 Damage model for delamination onset and crack propagation | 95 |
| 5.2.2 Damage Criterion and growth prediction in HMA flexible pavement | 99 |
| 5.3 Summary | 108 |
| CHAPTER SIX: DISCUSSION OF RESULTS | 109 |
| 6.0 Introduction | 109 |
| 6.1 Discussion of Objectives | 110 |

| | |
|---|------------|
| 6.1.1 Build/Fabricate Sensor Probes to Collect Moisture and Temperature Data from Hot Mix Asphalt Flexible Pavement using Smart Technology. | 110 |
| 6.1.2 Install sensor probes to a road pavement test section to collect pavement response | 115 |
| 6.1.3 Examine the response of the pavement using Finite element method and multi layered elastic transfer functions for appropriate pavement design. | 115 |
| 6.1.3.1 Web Integrated Source Code Program To Calculate Pavement Failure Using Moisture And Temperature Stress Intensity Propagators | 117 |
| 6.1.4 Develop a program to run pavement failure considering Temperature and moisture variables using Visual Studio Software package and propose a frame work for pavement failure response and maintenance plans based on pavement environmental conditions..... | 118 |
| CHAPTER SEVEN: CONCLUSION AND RECOMMENDATION | 119 |
| 7.0 Conclusion | 119 |
| REFERENCES..... | 121 |
| APPENDIX I | 147 |
| GRIFFITH ENERGY RELEASE FOR PAVEMENT FAILURE CONSIDERING TEMPERATURE AS ENVIRONMENTAL INPUT PARAMETERS..... | 147 |
| APPENDIX II..... | 162 |
| INPUT VALUES FOR CALCULATING PAVEMENT DEFLECTION CONSIDERING TEMPERATURE AND AXLE LOAD | 162 |
| APPENDIX III: INPUT VALUES FOR FIELD CALIBRATION CONSTANT KZ | 165 |
| APPENDIX IV: PROCEDURE FOR INSTRUMENTATION AND INSTALLATION | 166 |
| APPENDIX V: MOISTURE AND TEMPERATURE SENSOR DATA OBTAINED FROM PAVEMENT SUBGRADE LAYER..... | 168 |

PUBLICATIONS

- Abejide S.O. and M. Mostafa Hassan (2017) “Moisture Content Numerical Simulation on Structural Damage of Hot Mix Asphaltic Pavement” Materials and Science Engineering Proceedings of the Second International Conference on Civil Engineering and Materials Science (ICCEMS 2017), May 26-28, Seoul, South Korea; pp 279-282; <https://doi.org/10.1088/1757-899X/216/1/012048>.
- Heyns M, S.O. Abejide and M. Mostafa Hassan (2018) “Sustainable Waste Alternative as Cement Replacement in Pavement Stabilization” JOURNAL OF CONSTRUCTION PROJECT MANAGEMENT AND INNOVATION; Vol 8, No 1, June 18, pp 1767 – 1778; ISSN: 2223-7852; <https://hdl.handle.net/10520/EJC-10a49a808d>
- Abejidi S.O., Mostafa M.M.H., Adedeji J. (2019) Development of an ontology based expert system for determining the performance indicator for HMA pavements. In proceedings of the 12th conference on asphalt pavements for southern Africa CAPSA 2019, 13-16 Oct, Sun City, pp. 1179-1187.
- Abejide S.O., M. Mostafa Hassan, B. Auwize (2019) “SMART PAVEMENT PROCUREMENT STRATEGY IN PLANNING DESIGN AND CONSTRUCTION OF SUSTAINABLE TRANSPORTATION AND INNOVATION TECHNOLOGY” in proceedings of International Council for Research and Innovation in Building and Construction CIB conference; CONSTRUCTING SMART CITIES, Hong Kong, 17-21 June 2019
- Abejide O.S., M. M. H. Mostafa, R. Mujib. (In view). Moisture damage stress intensity failure rate propagator of hot mix asphaltic pavement using fracture mechanics. SUCI, GeoMeast, Conference.
- Abejide O.S, Mostafa M.M.H, D.Das , Awuzie B.O. (In view). Pavement Quality Index rating strategy for Implementing Smart Pavement Infrastructure. (*Proposed Journal Publication 2020*)

Abejide O.S. Mostafa M.M.H, D. Das, Mlanga V.T. (In View). Semantic Stream Reasoning for Developing Pavement Stress Intensity Propagators 2019. (*Proposed Publication 2020*)

TABLES

| | |
|--|-----|
| Table 2.0: Components of a Pavement Drainage System..... | 10 |
| Table 2.1: Factors Influencing Moisture Damage | 45 |
| Table 3.0: Material Properties of Pavement Layers | 62 |
| Table 3.1: Strain and resilient modulus for different Percent Saturation Coefficient levels..... | 63 |
| Table 5.0 Pavement Failure Modes | 105 |
| Table 5.1: Relationship between Griffith Failure Mode and Asphalt Concrete Failure Mode..... | 107 |

LIST OF FIGURES

| | |
|--|----|
| Figure 1.0: Moisture and temperature instrumentation for pavement stress intensity failure rate propagation..... | 6 |
| Figure 2.0: Description diagram for Implementing Internet of Things into Pavement Instrumentation..... | 26 |
| Figure 2.1: Stress pulses caused by a passing wheel on a cracked underlying pavement (Lytton, 1989) | 29 |
| Figure 2.2: Reflective cracking due to thermal stresses (Lytton, 1989) | 29 |
| Figure 2.3: Typical Pavement Layer Interphase. (Yesuf, 2014) | 32 |
| Figure 2.4: Basic Layout for Multilayers in Flexible Pavement System | 33 |
| Figure 2.5: Stresses beneath a rolling wheel load (Gu, Cui and Cai, 2019) | 49 |
| Figure 2.6: Three-Dimensional stress state distribution of pavement assembly (Abaqus, CAE) | 50 |
| Figure 2.7: The 3-D view of Two Random Joint Density Function (rs), (Bergstrom, 2006) | 54 |
| Figure 2.8: Distribution for the variable M. Failure occurs when $M < 0$. (Bergstrom, 2006) | 55 |
| Figure 2.9 The Standardized Normal Distribution Function Safety Index β , is connected to a certain Probability of Failure, P_f, β (Bergstrom, 2006) | 56 |
| Figure 3.0: Schematic Research Design Process | 58 |
| Figure 4.0: Sensor embedded into road with Faraday casing | 73 |
| Figure 4.1: Arduino Block Diagram Programming Language Setup | 74 |
| Figure 4.2: Arduino Block Diagram for determining Moisture and Temperature Values | 75 |
| Figure 4.3: Configuration of the proposed microcontroller | 76 |

Figure 4.4: Straight line approximation of the stress-strain curve for AC. Source: (FHWA, 2009)79

Figure 4.5: Pavement Strain under cyclic loading (Rahman, 2014)82

Figure 5.0: Cumulative Laboratory Temperature gradient analysis of pavement sensor84

Figure 5.1: Cumulative Laboratory Humidity gradient of moisture sensors85

Figure 5.2: Relationship between Pavement Temperature and Humidity86

Figure 5.3: Horizontal tensile Strain at bottom of Asphalt of subgrade. (Source: Abejide and Mostafa, 2017)88

Figure 5.4: Vertical Compressive Strain at Top of Subgrade. (Source: Abejide and Mostafa, 2017)89

Figure 5.5: Asphalt Concrete Temperature Gradient Sensor I and Fracture Energy90

Figure 5.6: Asphalt Concrete Temperature Gradient Sensor II and Fracture Energy90

Figure 5.7: Asphalt Concrete Temperature Gradient Sensor III and Fracture Energy90

Figure 5.8: AC Temperature Gradient Sensor I and Resilient Modulus91

Figure 5.9: AC Temperature Gradient Sensor II and Resilient Modulus92

Figure 5.10: AC Temperature Gradient Sensor III and Resilient Modulus92

Figure 5.11: AC Fracture Energy and Resilient Modulus I93

Figure 5.12: AC Fracture Energy and Resilient Modulus II94

Figure 5.13: AC Fracture Energy and Resilient Modulus III95

Figure 5.14: M-E flexible pavement design flow chat (Source: MEPDG: 2004)101

Table 5.15: Relationship between pavement deflection and temperature gradient I102

Table 5.16: Relationship between pavement deflection and temperature gradient II102

| | |
|--|-----|
| Figure 5.17: Design infographic for moisture and temperature pavement instrumentation algorithm (Researcher, 2019) | 104 |
| Figure 5.18: Web Data Architecture Model for HMA pavement failure mode. (Researcher, 2019) | 106 |
| Figure 6.0: Front Elevation of MISRA v1.1 | 110 |
| Figure 6.1: Full Elevation MISRA v1.1 | 111 |
| Figure 6.2: Aerial View of MISRA v1.1 | 112 |
| Figure 6.3: Moisture Sensor Detector | 112 |
| Figure 6.4: Temperature Sensor | 113 |
| Figure 6.5: MISRA v1.1 Microprocessor | 113 |
| Figure 6.6: MISRA v1.1 Prototype Developed | 114 |
| Figure 6.7: MISRA v1.1 Full Setup with Solar Panel | 114 |

ABBREVIATIONS

3D – Three dimensional.

A – Maximum value of the failure ratio R .

a – crack width

AASHTO – American Association of State Highway and Transportation Officials.

AC – Asphalt concrete.

APT – Accelerated Pavement Testing.

ASG – Asphalt Strain Gauges.

BC – Base course.

c – Cohesion.

C – Material parameter.

d_{max} – Maximum diameter.

E – Young's modulus / soil stiffness.

FE- Finite Element.

FWD – Falling Weight Deflectometer.

GWT – Ground Water Table. h – Height.

HMA - Hot Mix Asphalt. HVS – Heavy Vehicle Simulator.

k_1, k_2 and k_3 – Experimentally determined constants.

k_m – Regression parameter.

KT – Korkiala-Tanttu.

LVDT - Linear Variable Differential Transducers. m – Power for stress-level dependency of stiffness.

M-E – Mechanistic Empirical.

MEPDG – Mechanistic Empirical Pavement Design Guide.

MLET – Multi Layer Elastic Theory.

mm – Unit for Length.

M_R – Resilient modulus.

M_{Ropt} – Resilient modulus at a reference condition.

N – Load repetitions.

N_{eq} – Equivalent number of load repetitions.

p – Normal stress (Deviator stress ($q = (s_1 - s_3)$)).

q_f – Deviator stress at failure ($q_f = (q_0 + m \times p)$).

F_R - Failure ratio ($R = q/q_f$).

RLT – Repeated Load Triaxial Test.

S% - Degree of saturation at a given time.

Sb – Subbase.

Sg – Subgrade.

S_{opt} – Degree of saturation at a reference condition.

SPC – Soil Pressure Cell.

VTI – The Swedish National Road and Transport Research Institute.

w – Moisture content.

W_c – Water content.

z – Thickness.

β – Material parameter. β_I – Calibration factor.

Δt – Small time steps

\hat{d}_p – Permanent deformation.

ε – Axial strain. ε_{MU} – Strain Measuring Unit.

ε_p – Accumulated plastic strain.

ε_r – Recoverable (resilient) strain.

ε_v – Vertical strain.

θ – Bulk stress ($q = (s_1 + 2s_3)$).

ν – Poisson's ratio.

ρ – Material parameter.

σ – Axial stress.

σ_1, σ_2 and σ_3 – Principal stresses.

σ_d – Deviator stress ($s_d = \frac{s_1 - s_3}{2}$).

Accumulated permanent or plastic vertical displacement in the HMA layer/sublayer, in

$\varepsilon_{p(HMA)}$ = Accumulated permanent or plastic axial strain in the HMA layer/sublayer, in/in

$\varepsilon_{r(HMA)}$ = Resilient or elastic strain calculated by the structural response model at the mid-depth of each HMA layer/sublayer, in/in

β_{1r} = local or mixture field calibration constants; for the global calibration these constants were all set to 1.0

$k_{1r,2r,3r}$ = Global field calibration parameters (from the NCHRP 1-40D recalibration; $K_{1r} = 3.35412$, $K_{2r} = 0.4791$, $k_{3r} = 1.5606$)

k_z = Depth confinement factor

h_{HMA} = Thickness of HMA layer/sublayer, in

T = Pavement Temperature

$$k_z = (C_1 + C_2 D) 0.328196^D$$

D = depth below the surface, in

H_{HMA} = total HMA thickness, in

= Permanent or plastic deformation for the layer/sublayer, in

n = Number of axle-load repetition

ε_0 = Intercept determination from laboratory repeated load permanent deformation tests, in/in

ε_r = Resilient strain imposed in laboratory test to obtain material properties ε_0 , ε_r and p , in/in

ε_v = Average vertical resilient or elastic strain in the layer/sublayer and calculated by the structural response model, in/in

h_{soil} = Thickness of the unbound layer/sublayer, in

$\varepsilon_{p(HMA)}$ = local calibration constant for the rutting in the unbound layers; the local calibration constant was set to 1.0 for the global calibration effort

K_{s1} = Global calibration coefficient; $k_1 = 1.673$ for granular materials and 1.35 for fine grained materials

B_{s1} = local or mixture field calibration constant; for the global calibration these constants were all set to 1.0

$$\log\beta = (-0.6119 - 0.017638W_c)$$

ρ = soil parameter factor

wc = water content, %

$a_{1,9}$ = Regression constant; $a_1 = 0.15$ and $a_9 = 20.0$

$b_{1,9}$ = Regression constant; $b_1 = 0.0$ and $b_9 = 0.0$

CHAPTER ONE: BACKGROUND

1.0 Introduction

In the past decade, sustainability of road, transportation came with advances using monitoring devices in the form of instrumentation to monitor pavement response as well as bridge responses while in service. Very little information is available about the performance of these instruments, considering — environmental conditions. Environmental and climatic conditions as well as human activities has exacerbated negative effects on the performance and durability of road pavements (Maharaj, Rean, Mahase, M., and Maharaj, Chris, 2019; Mohamed N., Maharaj R. and Ramlochan D., 2017; Zapata, P. and Gambatese, J.A., 2005; Gang, Z. 2003). Thus, it is important to identify degradation mechanisms (i.e. under the influence of traffic loads, weather conditions and aging materials, road pavements deteriorate. The rate of deterioration or degradations can be of different kinds: fatigue rutting, fatigue cracking). in order to minimize cost-overrun in pavement maintenance. The incidence of varying climate change produces variations in environmental and atmospheric conditions, resulting in hazardous conditions, which require human efforts to provide sustainable solutions. Global warming and climate change variations affect pavements exposure in various ways, ranging from positive to negative actions, reducing pavement stiffness and significantly resulting in increased degradation over time (Bumjoon Kang, Moudon, Hurvitz, and Saelens, ., 2017; Akhter, and Witezak, 1985; Kim, *et al.*, 2009; Witezak, 1985). The effects may have direct impacts or induced effects; on road safety (pavement quality, stiffness and design life expectancy) or traffic noise (roughness). The occurrence of changing climate conditions makes it necessary to apply modern technology to determine pavement response resulting from expected climate and its effects (Field *et al*, 2014; Hajek and Haas, 1987).

The common flexible pavement design in South Africa is the conventional Hot Mix Asphalt (HMA) prior to this time has been in use since the 1920's (Sabita Manual, 2005). As far back as 1978, the National Institute for Transport and Road Research, now CSIR (Council for Scientific and Industrial Research) developed the Technical Recommendations for Highways (TRH8). The technical recommendation document was under the Committee of the State Road Authorities (CSRA) approved to serve as a reference material for the design of HMA surfaces. TRH8:19871 serves as the most recent and improved edition of the approved document, which is centred on the

Marshall Design method, including but not limited to additional information and design criteria for component assessment.

New technology and improvement in the road construction industry has exposed deficiencies and or loop holes in the scope and depth of the methodology contained in TRH8:1987 (Technical Recommendations for Highways). These changes include: an aggressive design causing increase in traffic capacity volumes. The inundation of pre-existing information and innovative methods often times result to fragmentation of methods used within the South Africa mix design. Increasing use of Asphalt design mixes such as the Stone Mastic Asphalt (SMA), Large Aggregate Mix Bases (LAMBS), Ultra-Thin Friction Courses (UTFC) and other thin layer asphalt surface (<25mm) having no adequate provision as documented in the TRH8:1987 can greatly affect the design specifications needed. However, the basic issues experienced with HMA are: certain mixes (Semi-open Graded Mix) are not in alignment with the IGHMA (Interim Guideline for Hot Mix Asphalt in South Africa) or the TRH8 Code of Practice for flexible pavement mixes. The difficulties experienced with the design density measurement of thin layers (<25mm); the mix design process for HMA is not fully integrated with the structural design process (stress-strain values). These related concerns have resulted in an increasing need to construct and design highway facilities especially where accessibility is needed to link a rural region to an urban region (Sabita, 2005).

Scarcity of highway infrastructure funds and public expectation surge for improved ballyhoo and peculiarity has made it critical to understand the effect of environmental pavement conditions on Hot Mix Asphalt pavement performance. In view of the salient contributions of roadway infrastructure to the economy and communication activities within modern societies, researchers have been studying earnestly to find alternative measures to attain the most suitable road pavement behaviour patterns (Shafabakhsh *et al.*, 2013a), and consequently design and construct safe, stable, cost-effective and environmentally friendly roads. Structural failure in a highway infrastructure is caused by a number of damage mechanisms: fatigue cracking, advanced crushing, pavement temperature variation, changing load cycles and varying moisture content resulting in delamination or degradation of the pavement surface over time. The standard of design adopted for this study is based on the South African road pavement design manual (COLTO manual). The utilization of Finite Element Method (FEM) to evaluate the stress-strain non-linear response behaviour of the pavement model structure is developed considering Mechanistic-Empirical Pavement Design

Guide. The evaluation of pavement structures, using the FEM; enables enactment of constitutive models that take account of the unsystematic behaviour of unbound aggregate layers. ABAQUS bench work tool, is adopted to evaluate pavement conditions (Saevarsdottir, 2014; Oscarsson, 2011; Lekarp *et al.*, 2000a, 2000b; Erlingsson, 2010 & 2007). These conditions are increasing varying axle wheel loads, unbound aggregate material stiffness, unsystematic material behaviour is adopted to evaluate the stress deformation obtained from the road. Specific data required for the analysis is acquired within specific study test points. The data collected forms the basis of the design for sustainable design. Furthermore, a standardized hybrid pavement design is adopted in this study. This goes a long way to enhance sustainable development growth and development of the South African economic sector in the transportation of goods and agricultural products from province to province within the country.

1.1 Problem Statement

The total axle load anticipated over the design life of a roadway needs to be evaluated based on prevailing Equivalent Standard Axle Loads (ESAL) and traffic growth projections (future traffic loading, which is given in the form of ESAL 80 over a period of time, t). Most often, this is usually taken care of in the design method considered for the pavement design. However, the estimated magnitude of total axle loads over the pavement design service life is expressed in terms of an equivalent number of 18-kip single-axle loads ESALs (Hall, 2000); this is why many newly constructed roads do not meet the required life span before failure. It has been observed, that flexible pavements usually experience fatigue cracking and/or deformation of the subgrade at premature ages. This scenario is generally caused by: soil expansion due moisture ingress into the underlying layers, inadequate soil stabilisation, inappropriate material specification in the base course, inadequate thickness of pavement layers, pavement temperature variations, especially in tropical and cold regions, and increasing growth rate of axle wheel loads, etc. This is to note that the roads need regular maintenance to attain the design life span, which in turn increases the operational cost of the roads. In order to enhance sustainable transportation and sustainable pavement design, this study focuses on developing stress intensity failure propagation models in flexible pavement using environmental condition-variable data (temperature and moisture variables) collected in real-time. Consequently, the principle of stress concentration factors, (*maximum shear — Von Mises Criterion*) is considered, assuming the pavement is represented as

a brittle material in the Finite Element analysis *model* environment in *Abaqus CAE 6.13*. Transfer equation models are developed using JESS script to determine the deflection of the pavement considering real-time data obtained from the sensor devices.

1.2 Aim and Objective of study

The conducted study aims to develop stress intensity failure propagators as variables promoting crack growth in Hot Mix Asphalt pavement design. The objectives of the study are to:

- Build/fabricate sensor probes to collect moisture and temperature data from Hot Mix Asphalt flexible pavement using smart technology.
- Install the sensor probes to a road pavement test section to collect pavement response data.
- Examine the response of the pavement using: Finite element method and multi-layered elastic methods for appropriate pavement design.
- Develop a framework for pavement response with regards to failure and maintenance plans based on the pavement response considering environmental conditions.

1.3 Justification of Study

The majority of the primary roadways in the Republic of South Africa are constructed using Hot Mix Asphalt laid over selected granulated under lying base material. The strength of the pavement matrix is governed by the environmental conditions (Saevarsdottir and Elingsson 2013). Uncontrolled humidity/moisture in the underlying base layer results in loss of its structural load bearing capacity. This in turn reduces the spread, which the traffic load is distributed. The surge in humidity/moisture level over time decreases the Resilient Modulus and increases irreversible deformation (Miller and Bellinger, 2014; Davies, 2004). Humidity/moisture and fine particles that cannot be accounted for in most cases, get hauled by hydrostatic pressure to the surface layers, thus reducing the strength of the overlying HMA by increasing strain under service conditions (Miller and Bellinger, 2014). Furthermore, uncontrolled moisture ingress in the HMA surface layers causes deterioration through stripping and ravelling of the bitumen binder from the aggregates. An understanding of the environmental effects of moisture on HMA allows better

service performance and failure prediction of pavement under working loads as it is evident that the performance of a pavement while in service with prejudice is affected by the presence of moisture within underlying layers (Tam, Ibrahim, Rahman and Mazura, 2014; Davies, 2004). There is, therefore, a need to investigate how environmental conditions impact the flexible pavements in order to improve their design. In this study, therefore, a reliability-based analysis is carried out to determine the safety index margins using stochastic response surface method to determine the onset of failure and crack propagation with regards to the flexible pavement.

1.4 Scope of Study

Pavement instrumentation has not gained popularity in the past decades. In the United States of America, some full-scale testing has been conducted at different facilities to monitor pavement response. Examples of these are the Naardo Experiment, the Transport and Road Research Laboratory, United Kingdom (TRRL) Road Test and the Finnish Road Test (Tabatabee et al, 1992); the exercitation of an innovative pavement section on Motorway A10 (Duong, N., Blanc, J. and Hornyh, P., 2016). Variables such as instrumentation schemes, pavement structures, truck speed and axle load configuration have not been fully addressed (Sohm, Hornyh, Kerzrého., Cottineau, Le Cam, Hautière, De La Roche, and Van Damme. 2012b; Duong *et al.*, 2016). Information regarding pavement response while in service for evaluation pavement is limited. Pavement design and construction are generally carried out to keep the underlying layers unsaturated. For this study, the underlying layers are categorised into three states: unsaturated, semi-saturated and saturated states respectively. The source of information is moisture sensor probes buried inside selected test core and monitored over a period of one complete seasonal year (12 months) to obtain data on the variation of moisture content and temperature gradient of the pavement layer subjected to hygroscopic content in different seasonal changes. The moisture probes are designed to collect data every 10 minutes per day and 30 minutes in off-peak periods of rainfall precipitation. The data received is inputted into pre-set design models programed to ascertain the pavement behaviour or response pattern: horizontal tensile strain at the bottom of the Asphalt Concrete layer as well as vertical compressive strain at the top of the asphalt subbase layer. Figure 1.0 presents the process which harnesses road pavement with information technology and the proposed sensor device.

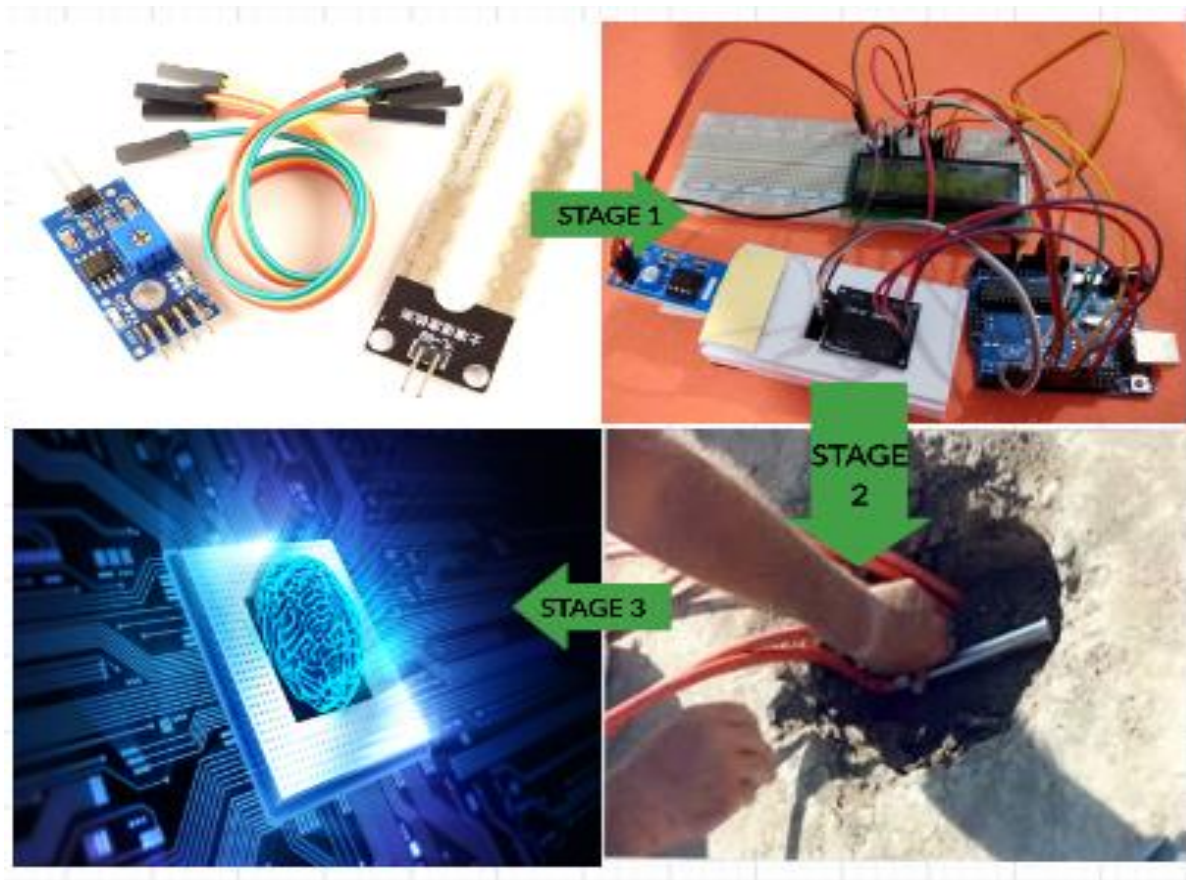


Figure 1.0: Moisture and temperature instrumentation for pavement stress intensity failure rate propagation.

1.5 Limitations of Study

As previously mentioned, instrumentation of pavement is not a common practice (Reza *et al*, 2006: Tabatabaee, N., Al-Qadi, I. L., Sebaaly, P. EE. 1992). Full-scale Asphalt Concrete pavement tests have been conducted on selected strain measuring devices, pressure cells and deflection-measuring devices. The principle made use of technology that can be correlated with pavement design principles, but there has not been any case considering pavement instrumentation and environmental condition. This research study is restricted to failure of flexible pavements (Hot Mix Asphalt — HMA). The focus was centred on deterioration of flexible pavement due to fatigue cracking, rutting and pavement deformation under excessive working loads due to increasing moisture/hydration coefficient and temperature gradient change as the primary environmental factors resulting in pavement deterioration while the road is in use during its designed life. The test region is located within the Eastern Cape (East London-Road Section

MN508) where the instrumentation was performed. The choice of the location was due to its proximity to be able to monitor the panels and the device so that neither of the two could be stolen by chance. The technical limitation was very challenging with regards to the choice of casing (sensor-enclosure) and the type of sensor to be used to collect the data. Due to the exposure condition, a Faraday casing was specified as the enclosure to safely secure the sensor components when embedded inside the underlying road pavement layers.

The computation of the pavement response was performed using a Java Expert Shell System (JESS) script and coded via a web architecture domain system. Currently, static analysis is employed in pavement design using multi-layered elastic packages as well as finite element analysis which are fixed programs that determine failure response based on an input-output system. This study considers real-time analysis of environmental condition data as they remain a constant variable affecting pavement structural stability and performance over time.

1.6 Outline of Dissertation

1.6.1 Chapter One

The background of the thesis is presented in this chapter. This chapter aims at unveiling the general problems associated with pavement deterioration considering the major causes as specified in the aim of the conducted study. Consequently, associated problems facing pavement failure is presented to introduce the justification of the conducted study. The objective of this thesis is presented in a step-by-step format which will be adequately tackled in the course of the study. The scope and restriction of the study is also presented.

1.6.2 Chapter Two

In this chapter, a further and deeper background of the problem is discussed. Related research on pavement life, pavement failure, distress effects, their causes as well as remedial actions previously taken to avert the outlined failure mode as evident from literature were discussed. Consequently, the methods used previously also discussed.

1.6.3 Chapter Three

Given the previously discussed literature and background study, the methodology is presented in the chapter. It includes an explicit background on Finite Element Analysis and reliability of Hot Mix Asphalt pavement. Also, moisture sensitivity saturation models for flexible pavement are presented. This is followed by the development of the transfer function models which are used to introduce damage models for flexible pavement subject to data obtained from the installed moisture and temperature sensors.

1.6.4 Chapter Four

This chapter focuses on the instrumentation technique needed for the study and the procedure for the instrumentation is given in Appendix V.

1.6.5 Chapter Five

The resulting analysis is presented and discussed in this chapter. Failure models as obtained from the Finite Element workbench is also analysed. The data is compared with the previous study on damage criteria for flexible pavement.

1.6.6 Chapter Six

The chapter constitutes the findings, discussions, recommendation and conclusion.

CHAPTER TWO: LITERATURE REVIEW

2.0 Introduction

Highway infrastructure system constructed previously during the Roman Empire was the first recorded account of road pavement network in human history. The success recorded in road construction during this era was predicated on the notion of drainage. The importance of road pavement drainage control systems (verges, side drains, grade/slope and/or road camber) cannot be over emphasized (Toryila, 2016; Finn, Buckley, Kelly, McDaid, Mullaney, Power, 2004; North East Somerset Council, 2016; NCHRP, 1998). In recent times, Finn *et al.*, (2004) proposed specifications for road drainage design and construction. This centred on principles that drainages form the basic parameter towards design and construction of highway structural platforms and this needs to be strictly adhered to especially new road construction projects. It also means that pavement structures are designed in such a way as to easily drain water away by introducing camber or pavement gradient. The underlying weaker layers (subgrade, subbase and base course) must be properly protected. In other words, the pavement surface must possess features to prevent flooding, ponding and seepage by providing adequate slope, thereby keeping the carriageway and/or shoulders free of ponding water occurring in the course of flood times (Bath & North East Somerset Council, 2016; Finn *et al.*, 2004). A deeper insight of the pavement material properties results to an efficient and economical sustainable design (Maharaj *et al.*, 2019; NCHRP, 2004, 2010). Ingress of increasing moisture saturation can be extremely dangerous to pavements as it affects service life performance. Proper design, construction, and maintenance of pavement drainage has the ability to prolong pavement performance. In the design and construction of a proposed roadway, drainage issues are addressed by incorporating subsurface drainage mediums into the pavement structural matrix. In other to attain proper drainage design, pavement design engineers carefully need to evaluate the rate of permeability of the drainage layer as well as selectively assess the hydraulic conductivity of the drainage materials. Globalisation and the need for sustainable development, results to an increase in urbanisation causing green fields to be converted to urban settlement and industrial use which increases stormwater runoff. Advancement in technology has resulted to Engineers and Scientists introduce innovative thinking to manage urban runoff and harvest stormwater for productive purposes (irrigation, storage tanks, reservoirs, etc.). Meanwhile, with developments in urbanisation, there is the occurrence of associated pull factor i.e. attraction to urban living) and push factor i.e. (dissatisfaction with rural life). This

contributes to the increasing distortion of the ecosystem as well as disruption of the ozone layer resulting in global warming which has its associated repercussion (Lean, 2010; Lockwood, 2009). Uncontrolled runoff occurs resulting from inefficiency of the drainage systems to handle peak flows during high precipitation (Zhang, 2006). Table 2.0 shows the components of a sustainable drainage system for sustainable transportation.

Table 2.0: Components of a Pavement Drainage System

| Basic Components | Variable Components |
|--|--|
| Wearing course | Rigid Surface: Portland Cement Concrete Flexible Surface: Asphaltic Concrete |
| Permeable Base Course | Destabilized or Unbound Granular Base Asphalt Stabilised Granular Base (Bitumen Treated Base, Emulsion Treated Base) Cement Stabilised Granular Base |
| Filter Layer | Dense-Graded Granular Base(Sub-base) Geotextile Base (polyethylene components) |
| Subgrade | Bearing capacity of Subgrade Soil Depth of Water Table Grade formation layer |
| Edge drains (including outlets with headwalls) | Aggregate Trench Drain with Geotextile Filter & Drain Pipes Prefabricated Geo-Composite Side-drain |

The components of a drainage system as well as its variable parameters are presented. The requirement followed must ensure that the top asphaltic concrete surface layer type does not retain water, dust, snow or ice and its material properties should be water-resistant. The base must possess water-resistant properties, either as an impermeable material or as a semi-porous layer which allows for water drainage through its pores (bitumen-treated bases or cement treated bases). The underlying layers should be designed to standard specification for road bases as well as subgrade design.

From Table 2.0, it can be concluded that; there is a paramount need for the material components used in the pavement matrix to be selected thoughtfully and properly placed on site to provide for permeability and uniform stability. It is needful to also note that, inadequate material compaction of the drainage layer possesses tendency to alter the gradation (particle size distribution) and create additional fines, which may result in lower permeability (Porous Asphalt Pavement, 2015). Construction activities associated with storage, haulage and compaction of aggregate largely results to segregation, non-uniform permeability and stability of the pavement over time (Sharma, A. and Sharma, D., 2017).

The efficacy of runoff drainage layers after being spread and compacted on site is imperative. Quality Assessment and Quality Control (QA/QC) protocols for simple, rapid, *in-situ* testing of permeability and stability are needed (IOWA State University, 2003).

In the study conducted by David (2004), he postulated that the stability of pavement layers is enhanced considering aggregate properties; angularity, abrasion, durability, specific gravity, toughness, density, as well as aggregate shape and size. Angular aggregates resist degradation under persistent loading and possess dense gradation that interlock together under compaction. A densely graded sample has the ability to enhance stability and reduce permeability. Secondly, Reclaimed Crushed Concrete Aggregate samples were found to have lower permeability, lower strength, and lower resistance to particle size degradation compared with limestone and gravel-stone samples. Laboratory and field measurements indicate that with accentuated fines content (material passing No. 200 sieve) increase, permeability decreases dramatically. The results were obtained from the concept of Accelerated Pavement Testing (APT), which requires *in-situ* input variables of Dry-Density and humidity/moisture variation to ascertain the saturated Hydraulic-Conductivity state of the Sample. Approximated variable parameters for an expansive variation of

the underlying base materials are available. Considerably, best accuracy will require actual measurements to be taken. Thus, the choice of selecting sensor probes to collect time-domain data from the pavement while traffic load is applied to it in real-time (Duong *et al.*, 2016; ASTM D7369 2011; Liu *et al.*, 2004; Muñoz-Carpena, 2004).

Depending on the particular environmental condition, a possibility arises when analytical variables considered in derivation equations change due to varying environmental and climatic changes, especially moisture variation, caused by water retention properties (Tam *et al.*, 2014; Yang *et al.*, 2008). In principle, it means that the structural damage in the pavement takes the form of cracking and deformation due to the changing climate or environmental condition as well as constant loading repetitions over the infiltrated weak underlying pavement bases (Su, Xiao, Wang, and Amirghanian, 2017). Common cracks in Hot Mix Asphalt pavements are fatigue cracking, thermal cracking. Contrary to fatigue cracking, thermal cracks are traditionally referred to as reflective cracks (Golestani, Nam, Noori, An and Tatari, 2016; Greene, *et al.*, 2012; Amini, 2005a, 2005b). Fatigue in pavements can be referred to as fracture failure under repeatedly changing traffic load cycles (Miller and Bellinger, 2014). Furthermore, Miller and Bellinger (2014) alongside Himeno and Watnabe (1987) postulated an innovative criterion of fatigue failure, “it was stated that, fatigue pavement failure can initiate at the top of the pavement slab when the pavement stiffness or resilient modulus is low”. Reduction in the stiffness ratio or resilient modulus can be as a result of poor compaction and/or inadequate methods or compaction equipment. At tropical regions, reduction in the temperature gradient (freeze and thaw) can incite pavement thermal cracking. The essential mechanisms of low-temperature cracking have been explored by Kucukvar *et al.* (2014), Wu *et al.* (2014), Noori *et al.* (2014), and Christison, 1972. Pavement sections subjected to low temperature gradient, develop micro-cracks which occur at the surface of the pavement. These cracks propagates through the full depth of the asphalt layer with successive repeated thermal cycles. Although excessively low temperatures initiates micro-cracks. The initiation of cracks develops over time resulting from poor compaction. This has the tendency to significantly accelerate full development of these cracks (Noori *et al.*, 2014). Symons and Herrin, (2009), and Mostafa *et al.*, (2005) in their study concluded that surface cracking has the tendency to consequentially result to reactions that affect the service life of the Hot Mix Asphalt Concrete. However, the occurrence of surface cracks induced at the time of construction is usually not the reason for the development of the varying types of crack failure in Hot Mix Asphalt pavements.

The generated surface cracks serve as catalyst which over time accelerates the development of bottom-up-cracking and eventually results in failure of the pavements (Mostafa and Abd El Halim, 2004). The effects of moisture on asphalt concrete pavements resulting in crack development have been examined extensively (Kucukvar *et al.*, 2014; Noori *et al.*, 2014; Mostafa *et al.*, 2005). Increasing moisture causes the asphalt concrete mixture to exhibit a segregation of the asphalt binder film from the aggregate surface area in a phenomenon better known as stripping. Stripping of the aggregate from the Asphalt Concrete Layer is one of the key contributors to loss of the structural integrity, which ultimately accelerates the deterioration/delamination failure of the pavement.

2.1 Stress and Strain Measurement in Pavement

The design consideration of pavements around the 1920's was solely centred on experience (Huang, 2004; Ghosni *et al.*, 2014); standard pavement layer thickness was adopted in this study regardless of the type of subgrade formation soils. The empirical methods have been ameliorated to consider the effect of subgrade soils using different soil classification methods and strength tests. These test vary from: The California Bearing Ratio (CBR) test, among others etc. There is a perception shift in the construction of highway facilities from the empirical methods to the use of semi-analytical methods as well as the fully optimised analytical methods (Ghosni *et al.*, 2014; Saevarsdottir, 2014). It is necessary to ascertain the particular mode for pavement failure, either resulting from crack growth or as a result of inadequate compaction (Dobriyal,,Qureshi,,Badola,, and Hussain,,2012; Colliander,, Jackson,, Bindlish,, Chan,, Das,, Kim, 2017).

Electrical Strain Gauges.

Previously, electrical resistance strain gauges were introduced to measure strain in flexible pavement. For this reason, strain gauges were selected based on their gauge length. For pavement application, the criterion then was based on the maximum aggregate size of the pavement mixture matrix, usually taken as 25.4mm. The length of the gauge ranges from three to five times the maximum nominal aggregate size. The electrical strain gauge was further developed into the Asphalt Concrete Strain Gauge.

Time-Domain Reflectometry Sensor (TDR)

The Time-Domain Reflectometry Sensor is a conventional sensor. Many of the Time Domain Reflectometry Sensors have more than two or more metal rods extending from the sensor casing or enclosure to be embedded into the test point. This occurs when a pulse wave is transmitted onto the metal rods. The wave propagates along the metal rods and is reflected at the end of the metal rods. Taking measurement of the wave propagation time back and forth along the metal rods, the dielectric constant of the soil that holds the metal rods can be calculated. The dielectric constant provides the moisture content value of the soil. The success of this method considers a high cost incurred and the complicated electronics of TDR sensors.

H- Gauges and Strip Gauges.

These are strain gauges in the form of a foil glued to carrier blocks prepared in the laboratory and also referred to as Soil Strain Gauges. The commonly used gauge is the H-gauge. This is manufactured by Kyowa ("Kyowa gages"). H-gauges consists of a 120 Ω unbounded metallic-filament (wire) synchronized in acryl possessing modulus of elasticity value of 2800 MPa (400 000 psi). Aluminium, Steel, or Brass fastener bars are usually attached to both ends of the strip. At the Technical University of Denmark, H-gauges have been modified to improve data collection accuracy, and durability (OECD, 1985). The H-gauge is fully synchronized in a strip of fibreglass reinforced with epoxy possessing minimal stiffness, high-rise flexibility and strength (Tabatabaee *et al.*, 1992).

Piezoelectric Transducers.

This device is used to measure the strain value of a material. This consist of metallic-foil strain gauge bonded and embedded into thin sheets of Asphalt mastic. This is further used to measure longitudinal strain at the bottom of the Asphalt Concrete layer (Liu *et al.*, 2004).

Pressure Cells.

Further research led to the development of pressure cells which measure the electrical output that can be generated from the device with regards to the stress applied to the diaphragm of the cell in a mechanical bench calibration test. The requirements and the design for the pressure cell can be found in Tabatabee *et al.*, (1992) and Liu *et al.*, 2004.

Linear Variable Differential Transformer — LVDT.

Other forms of measuring devices have been noted which range from velocity devices to detect driver speed as well as deflection devices: (Linear variable Differential Transformer – LVDT; Multi-Depth Deflectometer – MDD and Single Layer Deflectometer — SLD) to determine the pavement deflection under moving loads. These principles make use of static devices which are used periodically and not permanently as they are very sophisticated and fragile. Certain parameters deter the reliability of the strain being measured and makes this approach not sustainable. Some of the parameters: the different station meter of the installed gauges, the non-uniformity of pavement composition matrix, the individual layer thickness of the pavement, the pavement surface roughness resulting from dynamic load profile, varying load cycles, truck suspensions; axle configuration. and tyre pressure rating (Wu *et al.*, 2014; Tabatabee *et al.*, 1992).

Parallel Transmission-Line Moisture Sensors (PTL)

The Parallel Transmission-line moisture sensor is usually composed of three sub categories. Firstly, the sensor electronics which includes the transmitter, receiver, amplifier, filter, power supplies, etc. Secondly, the sensor enclosure that protects the sensor from crushing, water invading and eroding. Thirdly, the sensor head made up of a parallel-plate transmission line which usually protruding out of the sensor enclosure in order to directly make contact with the soil sample for which readings are to be collected. The sensor electronic board is usually installed within the enclosure. The sensors operate at a frequency of 1GHz depending on the type of data and condition of exposure. The simulation and experimental results as conducted by the researcher demonstrates that output voltage of the sensor is directly proportional to the moisture content in the soil (Liu *et al.*, 2004).

Parallel-Plate Transmission-Line sensor (PPTL)

This sensor configuration has similar working concept as the PTL sensors as previously discussed. The distinctive discrepancy between the PTL and PPTL gauge is in their structural configuration. The PPTL sensor possesses a layer of low-loss dielectric material in between two parallel copper plates, with a confined fraction of the wave energy. The design of the PPTL does not guarantee reliability and stability of the transmitted signals, but also compromises the sensors' sensitivity and measuring dynamic range. This is performed in such a way that a PPTL sensor is designed to accurately measure the moisture content value of the soil sample from 0 to 100%. These sensors were installed in the Bryan and Waco districts in Texas, USA, at the SPS-8 test location as well as the Texas APT test location to monitor increasing humidity/moisture variation as well as saturation content in the underlying pavement layer. The PPTL are affordable compared to the PTL, relatively small in size and remotely accessible.

2.1.1 Pavement Condition Monitoring

Decreasing temperature, results to the formation of micro-cracks at the surface of the Hot Mix Asphalt. These cracks disseminate through entire depth of the Asphalt Concrete with increasing as well as varying thermal cycles. On the other hand, low temperatures changes can result to the initiation of micro-cracks. The occurrence of the cracks can be induced by, poor layer compaction, which has the tendency to accelerate full scale maturity of these cracks under service load. Pavement reflective cracking has been traditionally envisaged to be initiated at the bottom of the Asphalt Concrete layer at the same location of previously existing cracks in the under layers which propagate to the surface. Consequently, recent research engagement has shown that reflective cracking is initiated at the surface of the wearing course which over time finds its way to the bottom of the Asphalt Concrete layer (Von Quintus, Mallela, and Lytton, 2003; Wu *et al.*, 2014; Noori *et al.*, 2014).

Pavement analysis and design following crack prevention centres its principles on a combination of Mechanistic and empirical theories. Furthermore, Multi layered Linear and Non-Linear elastic concepts served as the foundation platform towards the development of the AASHTO 1973 interim design guide and its subsequent revision in 1993. Recently, modified pavement design methods are explicitly taken account of in the recent Mechanistic-Empirical Pavement Design Guide. This was developed under the National Cooperative Highway Research Program (NCHRP) Project 1-

37A (Papadopoulos and Santamarina, 2019; Cortes, Shin, and Santamarina, 2012). In general, HMA pavement structures are analysed considering two major factors. Firstly, the HMA pavement structural response which is determined using Mechanistic and constitutive material models developed from design layer properties. Secondly, the output parameters obtained from the analysis in the form of horizontal tensile strains at the bottom/top of the bound aggregate layers and compressive vertical strain at the top of the subgrade layers. The values obtained serve as input design parameters to model distress prediction based on scenarios of empirical field data, from which the expected pavement life is determined (Cortes *et al.*, 2012; NCHRP, 2010, 2004; Kim *et al.*, 2009).

Highway infrastructures in the United States in recent times, have been designed using Empirical design methods that were established based on performance data measured during the 1950s at the AASHTO road test in Ottawa, Illinois. Owing to the changing specification in varying truck axle loads combination, tyre specification, construction practices and materials, in addition to climate and subgrade soil differences from one location to another. These Empirical Design procedures have become unsuitable for the current design of new and rehabilitated pavement structures (Jadoun, 2011). Furthermore, the shortcomings associated with the Empirical pavement design procedures have been studied by Jadoun, 2011; Lu *et al.*, 2014; Zhang *et al.*, 2015. In view of this, the AASHTO Joint Task Force on pavements initiated an initiative in 1996 to develop an alternative pavement design guide that takes account of previous construction practice and mechanistic design model. The resultant effect of the intervention was made public in 2004 in the form of mathematical model workbench called the *Mechanistic-Empirical Pavement Design Guide* (MEPDG). The design equation solver subroutine of the MEPDG evaluates critical pavement responses relating to subjected pavement layer stiffness properties and magnitude of traffic loading experienced. The Mechanistic-Empirical component alternative bridges the gap between laboratory observed responses and *in-situ* field performance values (Jadoun, 2011).

The purpose of Hot Mix Asphalt design consideration is designed to select choice material properties to be used as the separation layers. This principle enables the heterogeneous layer differences function together as a single composite matrix to sustain the service loads calculated in expressions of traffic volume for a specified design life. There are two principal pavement design methods: empirical methods and mechanistic methods which is later discussed. Empirical

design methods were previously the foundation rock of flexible pavement structural design. This principle was developed based on Empirical quantities; pavement materials and individual layer thickness. The AASHTO, 1993; Guide for Design of Pavement Structures implemented an Empirical approach which is still widely in use by most Highway Department of Transportation worldwide. The Mechanistic Design principles centres itself on Pavement responses. These pavement response models form the skeleton of the Mechanistic Design. In addition, the introduction of pavement failure response models; the resultant stresses, vertical and/or compressive strains, and deflections in the pavement structure can be calculated (Qin, 2010; Murana and Olowosulu, 2015). There is, an increasing negative effect of inadequate drainage system on road pavement. Although, road pavement is classified as either flexible pavement or rigid pavement, poor drainage system results in loss of serviceability over a period of time when subjected to poor drainage control system adopted along the pavement section. This study develops measures to detect the effect of increasing moisture content with increase ingress of water seeping into the pavement or from capillary rise from the water table within the soil geometric region considering real-time pavement performance response (Toryila, 2016; Finn *et al.*, 2004; Liu *et al.*, 2004; Muñoz-Carpena, 2004).

2.2 South African Transportation Systems.

Highway transportation system, amongst other transportation modes has expanded within the last two decades, both for passengers and freight transportation (Rodrigues *et al.*, 2016). South Africa has approximately 746, 978 kilometres in length of road network coverage. Approximately ten million vehicles which provide haulage across most sectors of the economy; depend largely on the roadway transportation infrastructure to transport goods. In South Africa, 83 percent of the goods produced and manufactured are transported by road. Future economic predictions reveal that freight transport demand will appreciate by 200 percent to 250 percent over the next 20 years (Ndebele, 2012). This intervention makes road infrastructure very important for socio-economic development. This has resulted in pavement specialist searching for innovative means to determine the most suitable, durable, and economically friendly road design (Shafabakhsh *et al.*, 2013a). Despite advancement in research and design of pavement infrastructure, Hot Mix Asphaltic pavement experience abrupt failure before the estimated design life. This may result from decreasing bearing capacity of the soil (Kordi *et al.* 2010), excessive traffic loading of the pavements, variations in design specification and unsuitable construction materials used (Kordi *et*

al., 2010; Shafabakhsh *et al.*, 2013a). Pavement design and construction requires huge lumps of funding to be implemented. With the appropriate approach to soil stabilisation, the soil's strength is greatly improved resulting in a stable pavement matrix as well as reduced cost of construction and maintenance (Heyns *et al.*, 2018; Alfatlawi, 2015; Magdi and Zumrawi, 2016). In addition, challenges pertaining to the parameters in the design of road pavements persist. Considering technological evolution of sophisticated design tools, advanced modelling and pavement life prediction models based on a number of methods such as the Stochastic Response Surface Method, Discrete Element Method, Finite Difference Method, Finite Element Analysis, and Boundary Layer Element Methods. Taking note of these methods, the outcome of a sustainable design and construction of quality Hot Mix Asphalt pavement structures is achieved. This study, puts forward an attempt made to simulate the behaviour of Hot Mix Asphalt pavement life assessment. This is done by considering Fracture Mechanics and stochastic response surface methods to predict pavement life performance and crack growth. This simulation is based on real-time data obtained from probes instrumented into the pavement system to monitor the variation of moisture and temperature gradient (Toryila, 2016; Noori *et al.*, 2014)

2.3 Pavement Management Systems

The performance and functionality of Hot Mix Asphalt pavement condition considering the viability and implementation of modern and outdated technologies cannot be exhausted (Kim *et al.*, 2009). However, certain investigations in the past, such as data processing, electromagnetic speed and movement waves, nuclear assessment, laser travel, spin-up/spin-down, eddy current and motion detector waves, have gained wide application in pavement condition monitoring and investigation (Zhang, Gaspard and Elseifi, 2016; Saha and Ksaibati, 2016; Al-Qadi *et al.*, 1992; Al-Qadi *et al.*, 1994, , 1996). An important part of the pavement management system, the Pavement Condition Survey (PCS), is performed by devices walking and/or driving along the road and classifying the pavement condition based on their visual observations. This method is usually time-consuming, subjective, and open to transcription error (poor interpretation of the data or information generated). To overcome these limitations, methods were devised by various agencies to speed up the process by automating the recording, processing and storing of the data. The advent of these methods resulted in a revolution in PCS (Zafar, Shah, Jaffar, Muhammad and Rindr and Soomro, 2019; Al-Qadi *et al.*, 2004). Drones and vehicular-mounted sensors were implemented in PCS to take photographs of the pavement. Some of the vehicles carrying on-board computers for

recording and storing the data directly in the field were deployed at the PCS investigation site (Wu, Yang and Zhang, 2013; Al-Qadi *et al.*, 2004). The condition survey equipment records the pavement condition periodically and determines the rate of deterioration. The instrumentation and technique used, and the performance criteria based on field testing should be properly documented and analysed. Furthermore, other factors such as ease of processing, ease of interpretation of output, operating speed, equipment durability and robustness and cost-effectiveness are strongly considered (Zafar *et al.*, 2019).

However, it is argued that many of these factors considered already in use by highway and transportation communities are inefficient to evaluate, detect and analyse pavement distress deterioration (Zafar *et al.*, 2019; Pavement Interactive, 2008; Hajek and Haas, 1987. In this study, a more advanced, and detailed evaluation of pavement distress deterioration considering *multi-variable transfer functions* is developed and analysed with reference to HMA pavement (Zafar *et al.*, 2019; Khattak, Landry, Veazey and Zhang (2013; Wu *et al.*, 2013; Zhang *et al.*, 2016; Karim, Rubasi, and Saleh, 2016).

2.3.1 Network and Project Level Pavement Management System

In a report by the South African National Roads Agency Limited (SANRAL) assets management system, road transportation makes up the largest portion for easy haulage of goods and transportation of people within the country (SAPEM, 2014). The interconnectivity of pavement networks linking towns, states, and even countries together to allow citizens to meet with their daily demand in the need for an adequate reach of goods and services is of primary importance. The desire and need to cater for domestic services is one of the primary factors in the mode of transportation to be selected. This makes road infrastructure of high priority when it comes to maintenance during its design life (Karim *et al.*, 2016; Ramandeep, 2012).

The knowledge of an entire pavement network would require a nearly impossible amount of manual distress surveys. Innovative advancements in mobile data collection technology have led to increased departmental usage of automated distress surveys. This automated process allows for a department to obtain distress criteria as well as other pavement characteristics at a network level (Zafar *et al.*, 2019; Karim *et al.*, 2016; Kazmierowski *et al.*, 2010). Many methods to capture pavement performance values have been employed. These methods range from mathematical models to methods involving the use of a computerized and programmed data collection system.

The first method makes use of an automated data collection system involving driving a Heavy Vehicle Simulator testing van at a specific and /or controlled speed over the road network to determine and observe the strain, stress as well as pavement roughness. Depending on the vehicle suspension, a specific roughness value is calculated and registered to a data storage domain repository at very short incremental lengths (Deduct Points- DP).

The next pavement performance value obtained using an automated data collection system is the Falling Weight Deflectometer (FWD) test method. The method requires the use of an FWD vehicle which contains a load plate and sensors. This method allows Departments of Transportation to predict and also Back-Calculate the modulus of elasticity of pavement layers in order to determine the structural integrity of pavements (*stiffness and deflection*) along the network. This method gives an exact idea on the structural behaviour of the pavement not only that of the wearing surface alone. Lastly, pavement performance distresses are obtained from still images taken by vans as they pass over the network. This method typically involves using third-party software which calculates certain distresses on the surface layer as prescribed by the department or user which allows the department or user to better understand sections/segments where there are greater densities of distresses on the network. Technologies for capturing these images have increased dramatically in recent years with high resolution and three-dimensional images becoming available (Zafar *et al.*, 2019; Fischer *et al.*, 2018; Ramandeep, 2012). These technologies, used with the proper software, will allow having very detailed pavement condition prediction and analysis throughout the network (National Highway Authority of Pakistan, 2019; Babashamsi, Peyman, Yusoff, Ceylan, Nor, and Jenatabadi, 2016).

Image and visual digitisation of a road test section to be analysed for spatial failure and deformation in the form of rutting and crack formation is proposed. This is done in order to give a proper estimation of the extent of damage caused and provide remedial actions needed to avert such problems in future. The images are usually taken by a spectroscopic device and analysed using an X-Ray diffractive machine to indicate the particle and material dispersion in a failed road section and compare with a particle and material dispersion of a non-failed road section (Jelokhani-Niaraki, Alesheikh, Alimohammadi, Sadeghi-Niaraki and Kim, 2011; Janani and Samson 2020; Kamal, Mathavan, Zafar, Moazzam, Ali, Ahmad and Rahman, 2018; Kim, Yang and Kwon, 2017; Kim, Kim, An and Lee, 2019).

2.3.2 Pavement Management Decision Making

Decision making in highway maintenance projects is very important as it is a functional parameter which lies on its dependency on pavement life prediction and analysis. The Pavement Management System supports agency decisions at three different levels: The Strategic Level, Network Level, and the Project Level. The types of decision range from; assets considered, level of detail, and breadth of decisions which differ across individual levels. It is imperative to note that there is no ideal single pavement management system which is best suited for all agencies or transportation departments. Accordingly, it is imperative to develop specific treatment needs as they arise by treating each management system as unique. The philosophy of the pavement management system adopted must be subjective to predictive/preventive maintenance, i.e. treating the pavement distress problems early enough before they develop and become severe. This procedure is cost-effective and beneficial to the highway system in the long run (Janani, 2020; Namgyu Kim, 2019).

Depending on the data and information obtained on the performance level of the pavement in question, the necessary treatment or maintenance remedy to be adopted is determined. One major remedy employed in the pavement management system to be considered is that of crack sealing/filling. This remedy is one of the most widely used treatments in the world due to its low cost and relatively fast application rate. The essence of this management system is to prevent water ingress from seeping through the cracks generated due to pavement distress during the service life through the base and underlying inter pavement layers.

Another remedy deployed in pavement management system treatment is the idea of micro-surfacing developed in 1970 in Germany and has been practised in the United States since 1980. This method involves the mixture of polymer-modifying asphalt emulsion, water, mineral filler, and other additives spread over the pavement surface. Its use has picked up significantly because of the flexibility it has in its use; it has no restriction on traffic volume, and only needs one hour to cure before it can handle traffic again (Kazmierowski *et al.*, 2010)

The Network and Project level dichotomy in PMS has resulted in the development in the application of methods of analyzing pavement distress. Some network methods will be discussed further in this study based on the output data generated from the moisture and temperature analysis obtained from the built sensors (Jin, Yang and You, 2017).

2.3.3 Artificial Neural Networks (ANN) in Pavement Management System

A typical ANN structure consists of four primary elements: an input layer, hidden layer, number of neurons, as well as a target layer and is controlled by the training algorithm. Essentially, each neuron will receive a weighted portion of each input element in the layer and attribute a bias towards it creating an input signal. This signal will then be transformed into the output signal by means of a transfer function. There are a vast number of transfer functions which can be applied in this step; however, most networks use either linear or sigmoid. This process repeats itself as the network keeps adjusting the weights and bias to meet performance requirements of the network. The standard function for performance in most neural networks is mean squared error (MSE). Depending on the training algorithm used, the network will adjust weights and biases differently to meet performance requirements. Artificial Neural Networks (ANN) have been a useful tool for researchers all over the world for decades, especially for complex datasets for which manual function designs are unfeasible. Pavement researchers specifically have used neural networks because of the complexities involved in computing and predicting: asphalt binder properties, thermal crack detections, as well as for various elements of pavement management on a large scale (Sakhaei *et al.*, 2009; Underwood *et al.*, 2009). ANN is used to predict the three different pavement performance indicators with the numerous factors obtained in the pavement management system. The ability of the neural network to learn from observed data to improve function approximation makes it fairly unique. The attractive abilities of ANN have drawn much attention to its implementation over the past few decades resulting in numerous analysis types, models, training and algorithms, etc. A typical ANN structure consists of four primary elements: an input layer, hidden layer, number of neurons, as well as a target layer and is controlled by the training algorithm. Essentially, each neuron will receive a weighted portion of each input element in the layer and attribute a bias towards it creating an input signal. This signal will then be transformed into the output signal by means of a transfer function. There are a vast number of transfer functions which can be applied in this step; however, most networks use either linear or sigmoid. This process repeats itself as the network keeps adjusting the weights and bias to meet performance requirements of the network. The standard function for performance in most neural networks is mean squared error (MSE). Depending on the training algorithm used, the network will adjust weights and biases differently to meet performance requirements (Arslan and Yetik, 2014; Bourquin, Schmidli, van Hoogevest and Leuenberger, 1997).

Depending on the type of data collected, the method of data processing and analysis will differ from each other due to several data sources and data formats. Data could range from climatic data, traffic data, axle load data, and pavement geometry data parameters. The data obtained from the proposed instrumentation study will focus on climatic data which is further categorized into pavement temperature response as well as pavement moisture entrainment response (Yang and Wang, 2019; Arslan and Yetik, 2014).

2.3.4 Monte Carlo Simulation Approach and Randomized Sections Selection

The Monte Carlo approach involves the process of creating partitions and breaking the entire pavement into segments to be analysed discretely. In the sampling process, a uniform distribution is used, i.e. each location within a segment had an equal chance of being selected. After each section was created, the cracking data for that section was extracted from the database and saved in the 2D table together with other factors. Finally, in order to facilitate robust and semi-automated analysis, all data is stored in a three-dimensional (3-D) array. All the stored data collected is processed and analysed in the 3-D array using the Finite Element Approach in MATLAB or ANSYS. These work bench involve discretization of the entire pavement system into smaller fragments for better understanding of the behaviour within a confined location (Yang and Wang, 2019).

Pavement Management Systems (PMS) are managerial processes which takes account of the planning, executing operation and maintenance of a network of pavement (Highway Corridor). This is aimed to minimize budget while maximizing pavement life. These systems typically begin by having an understanding of what the current pavement conditions are throughout the network. In order to create a sustainable Pavement Management System, a well-defined and organized pavement assessment route network is needful. This process involves computing pavement condition. The first step for the computation of pavement condition in any PMS is to discretize the pavement network using index values in other to assess the condition of the entire pavement routes within the network. In this case, a Pavement Condition Index (PCI) is created based on the three pavement performance indicators as earlier discussed: longitudinal and transverse cracking together with the International Roughness Index (IRI). In longitudinal and transverse cracking, ASTM D6433-10 can be introduced to evaluate and analyse the number of deduct points to adopted considering the occurrence of crack density in meters considering medium occurrence frequency.

Looking at the fact that IRI is not a distress value and therefore not listed usually in the ASTM D6433-10, deduct points can be computed using a correlation from connecting the PCI with IRI (Yang and Wang, 2019; Arslan and Yetik, 2014; Park *et al.*, 2007).

Lastly, project-level in PMS can be summed up in a system of scenarios whereby a series of management scenarios are used to observe and monitor Pavement Structural Condition over a period of time as well as the associated cost incurred. These four scenarios are

- i. Do Nothing Scenario
- ii. Keep the PCI threshold above 60
- iii. Keep the PCU threshold above 70
- iv. Keep the PCI threshold above 80

The scenarios observed is put forward to estimate the advantages and disadvantages of keeping the pavement condition of the network at a high level and obtaining the most efficient longevity extension treatment models. The above scenarios can be monitored over a period of 20 years depending on the design life of the project. Usually, a random normal lifetime extension can be created each time for each treatment within the ranges of good, fair and poor condition. Furthermore, a comprehensive pre-processing and multiple checks should be performed in order to produce good quality data for the analysis.

2.4 Pavement Performance and Instrumentation Parameters

HMA pavement is a composite structure composed of complex heterogeneous layered material components formed by multiple combinations of different materials subjected to traffic loading and various environmental conditions. Asphalt concrete pavement is one of the most robust infrastructure components in the world, and its design, construction, conservation and rehabilitation depends on the availability of resources including finance. However, future projection of the design service life of the pavement is one of the most demanding tasks for pavement engineers (Kim *et al.*, 2009). Certain components affecting the performance of Hot Mix Asphalt; loading cycle, magnitude of axle load, loading duration, unloading/rest period, temperature variation at time and duration of loading, and increasing humidity/moisture content result in premature pavement failure. As such, different empirical and mechanistic models and

analysis frameworks have been developed in order to predict asphalt concrete responses in-service condition (Janani, 2020; Kim *et al*, 2009). Figure 2.0 shows a description diagram for pavement instrumentation using the concept of Internet of Things.

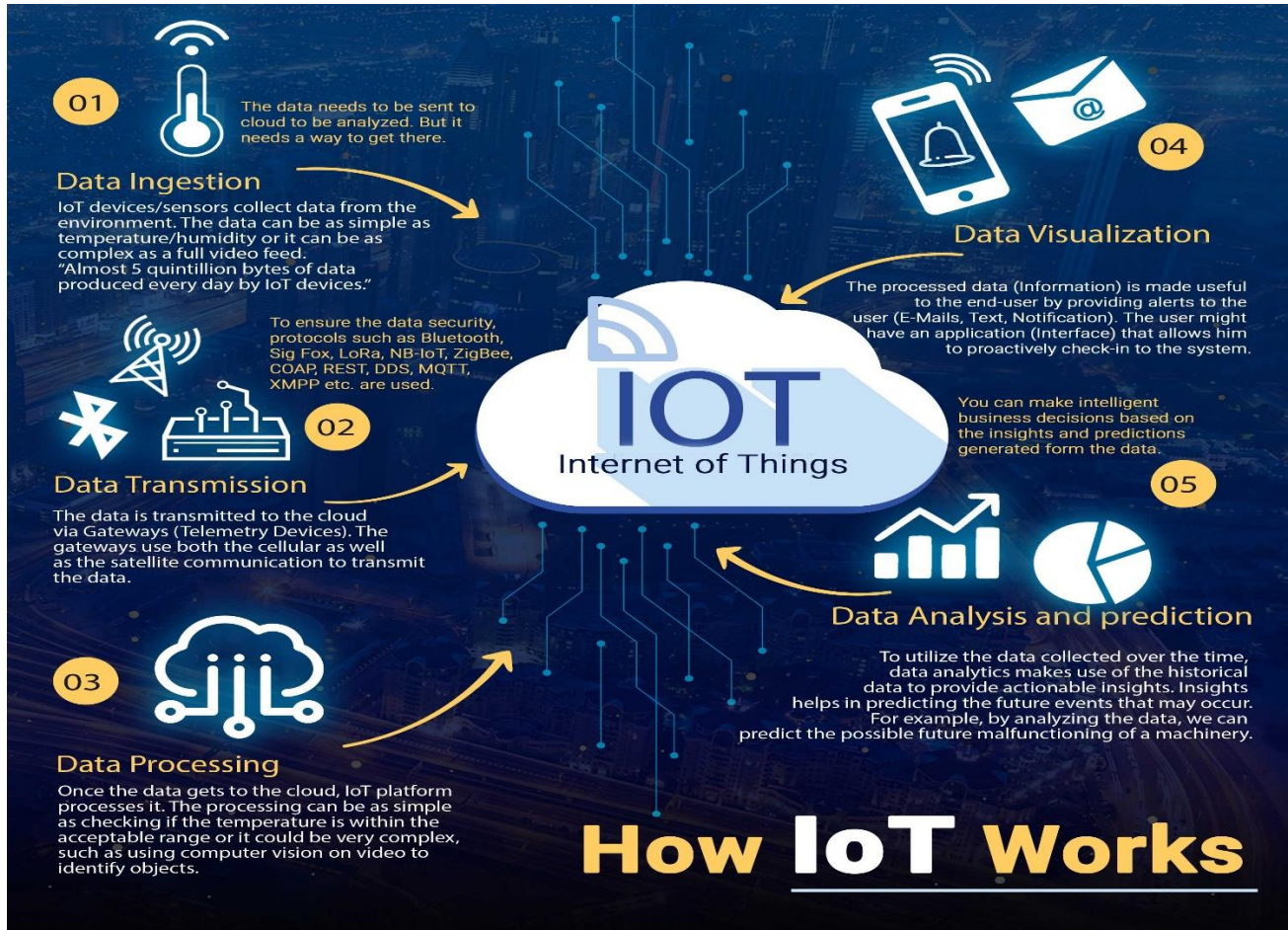


Figure 2.0: Description diagram for Implementing Internet of Things into Pavement Instrumentation

The above diagram illustrates the system of components which is connected by communication protocols. Each components performs a designed function either as a device component, domain, server, storage system, inference or output interface. The instrumentation will take the form of firstly a data receiver or ingestion system, data transmission system, data processing system, data visualisation system and lastly, Data analysis and prediction system. Full illustration is as indicated in the Figure 2.0.

For efficient communication between the Data Ingestion phase to the Data analysis phase a site for this needs to be identified. The site to which the instrumentation will take place considering performance and durability of the pavement is selected to generate results that will assist the Eastern Cape Department of Transportation as well as the District Roads Engineers for pavement efficient analysis and evaluation. The road allocated to this project was made possible by the District Road Engineer resident in East London. The instrumentation needed some form of physical survey necessary to obtain certain boundary conditions as well as constraints where applicable.

2.4.1 Pavement Cracking Consideration and Pavement Cracking Initiation

A major concern resulting in delamination in Hot Mix Asphalt pavement is fatigue cracking. This scenario is very common in all road type categories, interstate roads, municipal roads or residential access roads. The phenomenon of fatigue cracking is related to the material and structural characterization of asphalt concrete pavements. Currently, within South Africa, available test methods and analysis protocols require accurately predicting the fatigue performance of asphalt mixtures during the designed life span (Nascimento, 2015). In Brazil, many researchers have proposed different test methods and specimen geometrics for fatigue damage characterization, such as the bending beam test, indirect tensile test, gyratory compaction test and the trapezoidal test. The results of these test at a single temperature are fitted to power low-cycle fatigue curves (Wöhler curves) and used with simplified pavement layered elastic analysis for performance prediction. The implementation of the findings of this research has been limited in application due to non-validation and poor laboratory-to-field transfer functions (Nascimento, 2015).

It is needful to note that, the efficiency of a fatigue performance model in pavement design and preservation possesses two main components. Firstly, a fatigue damage growth relationship that describes how damage grows as a function of load frequency, temperature, and load level. Secondly, a failure criterion that can be used to define the fatigue life of the asphalt concrete (Norouzi *et al.*, 2014; Kim *et al.* 2014). An example of pavement failure is the occurrence of reflective cracking in the form of distress contours in asphalt pavement. Reflective cracking which is a new concept in pavement failure in the flexible pavement is the inability of the overlay to withstand differential movement across the crack or joint of the underlying pavement, which may be due to traffic loading or thermal loading. This occurs as the pre-existing crack in the old asphalt

pavement or the joint in the underlying Portland cement concrete slab which will propagate upward through the new asphalt overlay (Kucukvar, *et al.*, 2014; Wu, *et al.*, 2014; Jayawickrama and Lytton, 1987). The occurrence of reflective cracking in the Hot Mix Asphalt pavement destroys the structural stiffness of the pavement surface which is observed in most cases as alligator cracks, wrapping and curling of the pavement etc. The resultant of this effect adversely reduces the structural strength (stiffness) of the pavement and consequently allows humidity/moisture ingress to the pavement system resulting in deterioration. This process has the tendency of breaking the bond between the Asphalt binder (bitumen) and the aggregate materials (Lytton, 1989). Crack propagation theory, entails principles as provided by the laws of empirical fracture mechanics. This is expressed as the ratio between the pavement crack length and the number of load cycles to failure equated to a constant. Furthermore, this is a resilient modulus deficiency associated to fracture of the material. There is a need to monitor the ingress of water at the initiation of cracks as well as predicting the length of the crack as this will greatly affect the amount of moisture entrainment into the pavement over time.

$$\frac{dc}{dN} = AK^n \quad (2.1)$$

where: dc = Change in Crack length

d_N = Change in number of load cycles to failure

K = Stress intensity factor at the crack tip

A, n = Fracture property of the material.

The expression is further interpreted such that, if the stress intensity parameter at the crack tip dwindles, pavement crack propagation reduces. This is a theoretical concept with the presence of a reinforced layer which tends to reduce the tensile stress at the crack tip (Barksdale, 1991; Paris and Erdogan, 1963; Kutuk, 1998).

Lytton (1989) was able to develop an experiment to indicate the effect of a load passing through the top of a pavement overlay having a cracked underlying intermediate layer. The Figure 2.1, presents three kinds of high stress pulses experienced within the pavement structure. Two of these pulses are maximum shear pulses that occur at the points A and C and in the opposite direction. However, the wheel load passing point B causes a maximum bending stress pulse. Figure 2.2

indicated that thermal cracks are caused by stresses in the overlay as a result of increases temperature changes occurring along the pavement surface which causes contraction and curling of the underlying pavement surface.

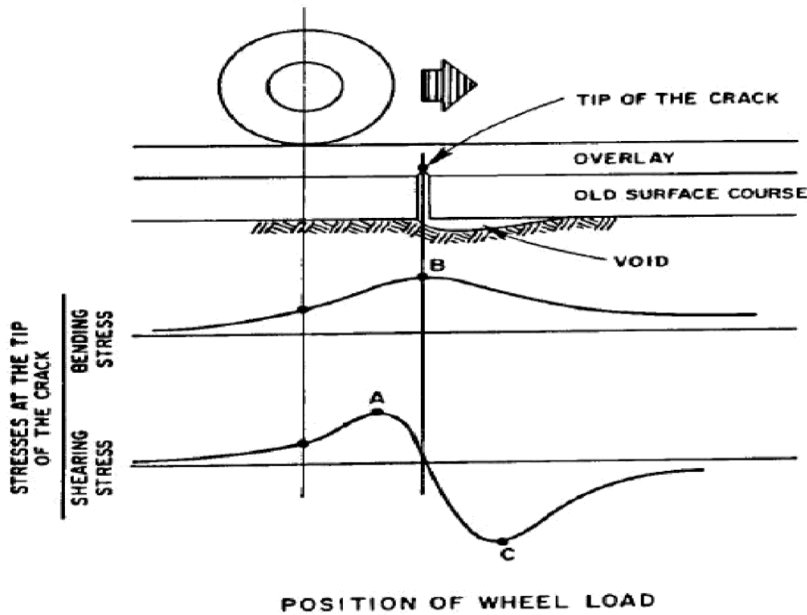


Figure 2.1: Stress pulses caused by a passing wheel on a cracked underlying pavement (Lytton, 1989)

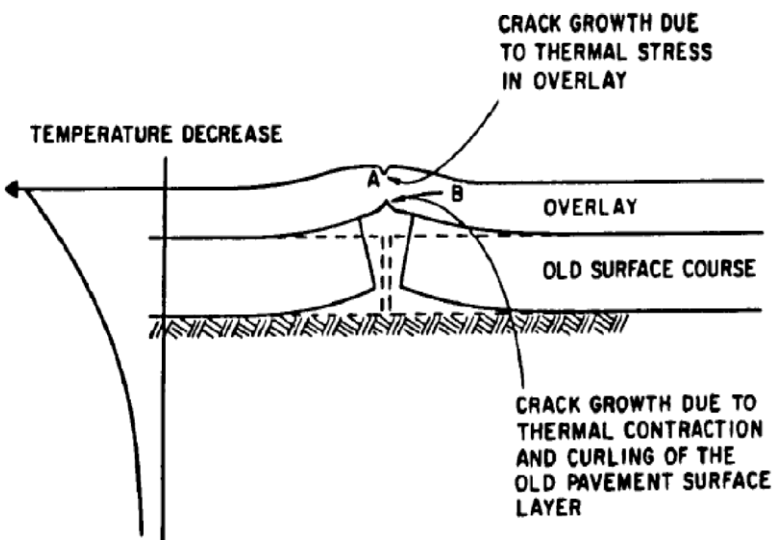


Figure 2.2: Reflective cracking due to thermal stresses (Lytton, 1989)

Although several methods have been identified to prevent reflective pavement cracking (Hesp *et al.*, 2009). Some of these methods range from; introducing a thin layer at the interface of the old and new layer, rubberizing the existing concrete pavement, crack-sealing the existing pavement using interlayer systems and increasing the thickness of the HMA overlay which has always been effective. Amongst these techniques, the interlayer systems have been exceptionally effective. The efficiency of the interlayers depends on proper selection interlayer system (material characterization) and interlayer conditions, construction methods in the installation and condition and characteristics of the existing pavement layer (Hesp *et al.*, 2009).

2.4.2 Reflective cracking failure patterns

Kucukvar *et al.*, (014), Wu, *et al.* (2014), Irwin (1957), Lytton (1989), Griffith (1920) and Jayawickrama *et al.* (1987) identified three failure modes in HMA layers reinforced with a glass-grid interlayer. These failure modes are commonly found in ordinary HMA as well a Hybrid EME performance grade asphalt pavement (Pavement Interactive);

- Mode I: Crack commences at the top of the pavement.
- Mode II: The energy required to open the crack reaches a minimum stable level.
- Mode III: Bottom-up and top-down cracks meet at the middle of the sample.

Modes I and III occur when the interlayer material acts as a strain-relieving material, and Mode II happens when they act as reinforcing material. Two different scenarios are possible when bottom-up cracking reaches the interlayer, depending on the type of Geosynthetic type an interlayer condition. In strain-relieving mode, the crack stalls at the interlayer level for a while and then starts moving upward in the overlay. In a reinforced mode, the crack rotates in a perpendicular manner due to the resulting stress and propagates below the grid to a distance where there is no longer enough energy to propagate the horizontal crack any further (Lytton, 1989). Zhou and Sun (2002) studied reflective cracking in the field and reported that 97 percent of cracked thin overlays had double cracks close to the joint.

Hosseini *et al.* (2009), observed three distinctive stages in the fatigue life of the test samples. Firstly, a fast reduction in stiffness of the samples, which is approximately 10 percent of the total fatigue life. Secondly, there exist linear reduction in the stiffness of the samples resulting from the

number of load cycles. This stage covers almost 90 percent of the fatigue life. The second stage is usually associated with the formation and development of microcracks. Lastly, a sudden decrease in the stiffness of the samples as they approach failure. The outcome of their study also showed that reinforcement of the samples reduced the crack growth rate. Khodaii *et al.* (2009) concluded that specimens with embedded geogrids outperformed the non-reinforced samples in terms of resistance to cracking. Also, they concluded that embedding the geogrid within the overlay is more advantageous than placing it at the bottom of the layer. Moreover, they reported that the occurrence of top-down cracking depends on the geogrid position in the asphalt overlay, relative stiffness of the overlay compared to the old pavement, and temperature (Khodaii *et al.*, 2009).

2.4.3 Flexible Pavement Design Methods

Kim and Drabkin, 1994; de Lima *et al.*, 2013 in their study stipulated that the major detrimental problem in transportation infrastructure investment is concomitant to availability of materials and their haulage material costs. However, with reduced financial strength there is shortage of resources to plan, construct, operate and maintain the transportation facility. Furthermore, The Federal Highway Administration of the U.S. Department of Transportation reported in 2014 “\$ 65 billion dollars was the estimated annual fund set aside to be used in the repairs and maintenance of existing road infrastructure (highways and bridges) in the U.S (Quebec, 2014). This amounted to 40% of the total budget allocation on all related expenses in 2010 (FHWA, 2013). Similar occurrence was observed in the province of Quebec (Canada). In addition, major infrastructure investment in road transportation took 22.8% of the total highway infrastructure investment budget. Furthermore, it was observed that 70% of the earmarked investment was assigned to maintain roadways and structures and to keep them in perfect condition (Quebec, 2014). In European countries such as Denmark, a little above 40% of civic budget was assigned to the road network (ECMT, 1998). 12.5% of the total 4 years’ budget in Sao Paulo - Brazil was disbursed on roadways development and Maintenance (Vasconcellos, 2014). In order to reduce excessive financial resources while still achieving an efficient highway facility, a mechanistic model of the road section is firstly proposed. Linear Elastic or viscoelastic model is used for the pavement analysis. In a number of occurring scenarios, the selection by road category as well as durability and design life requirement of the pavement type depends on different factors such as the number of functional years, availability of funds, proposed traffic load, soil conditions, and environmental

factors. Furthermore, construction and operation cost as well as maintenance cost are also important factors to be taken into account, although they are often neglected (Yesuf, 2014).

Huang (2004) in his study recognized the major principle behind the design of conventional flexible pavement. He based his principle on primarily providing a structurally stable layered matrix with higher stiffness materials on the top where the intensity of stress is high. Also ensuring subservient materials (in terms of strength and quality) at the bottom where the stress intensity is low. For the purpose of this study, an axis-symmetric undeformed model of a typical flexible HMA pavement is shown in Figure 2.3. This comprises the HMA layer; bounded and/or unbounded base layer; sub-base layer and the subgrade layer. Figure 2.3 indicates a diagrammatic representation of a typical South African pavement where the bounded layer is made of a Bituminous Treated Base (BTB) layer and the HMA is made of stable Medium Grade Bituminous Mix

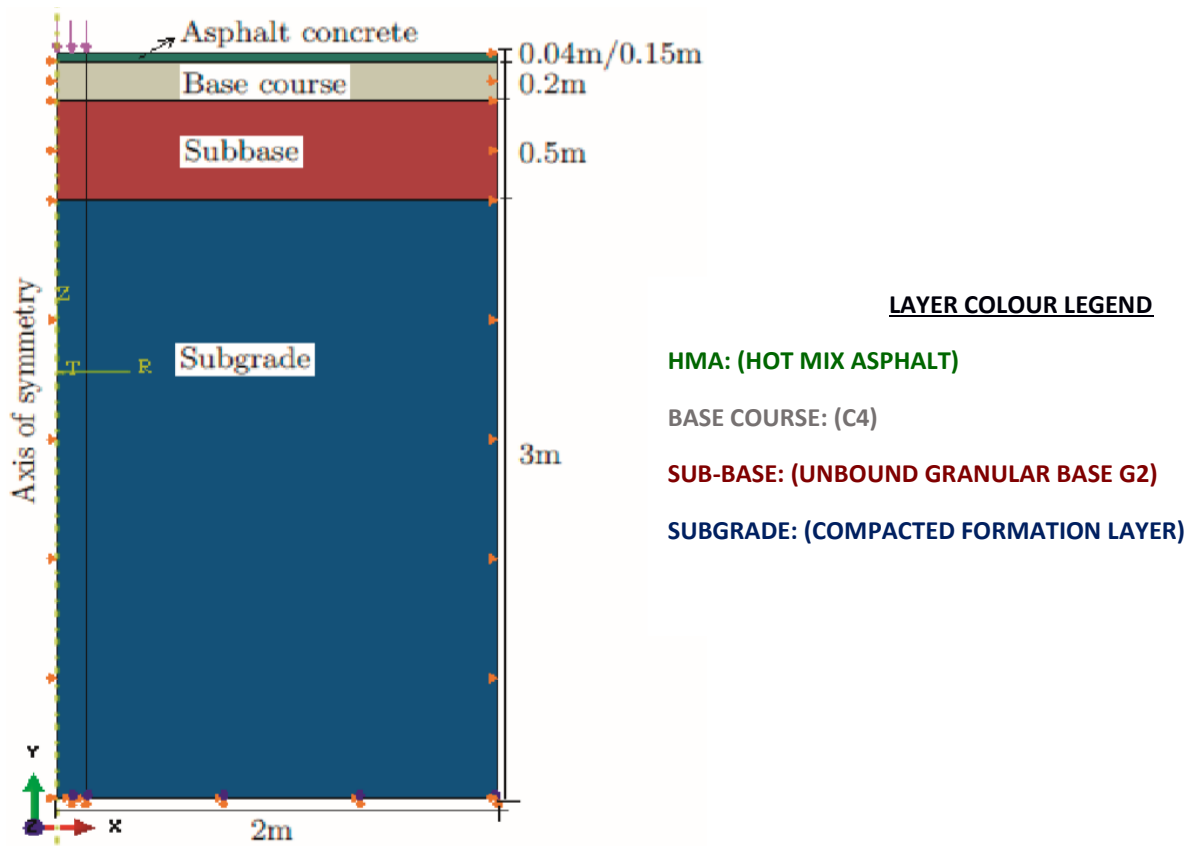


Figure 2.3: Typical Pavement Layer Interphase. (Yesuf, 2014)

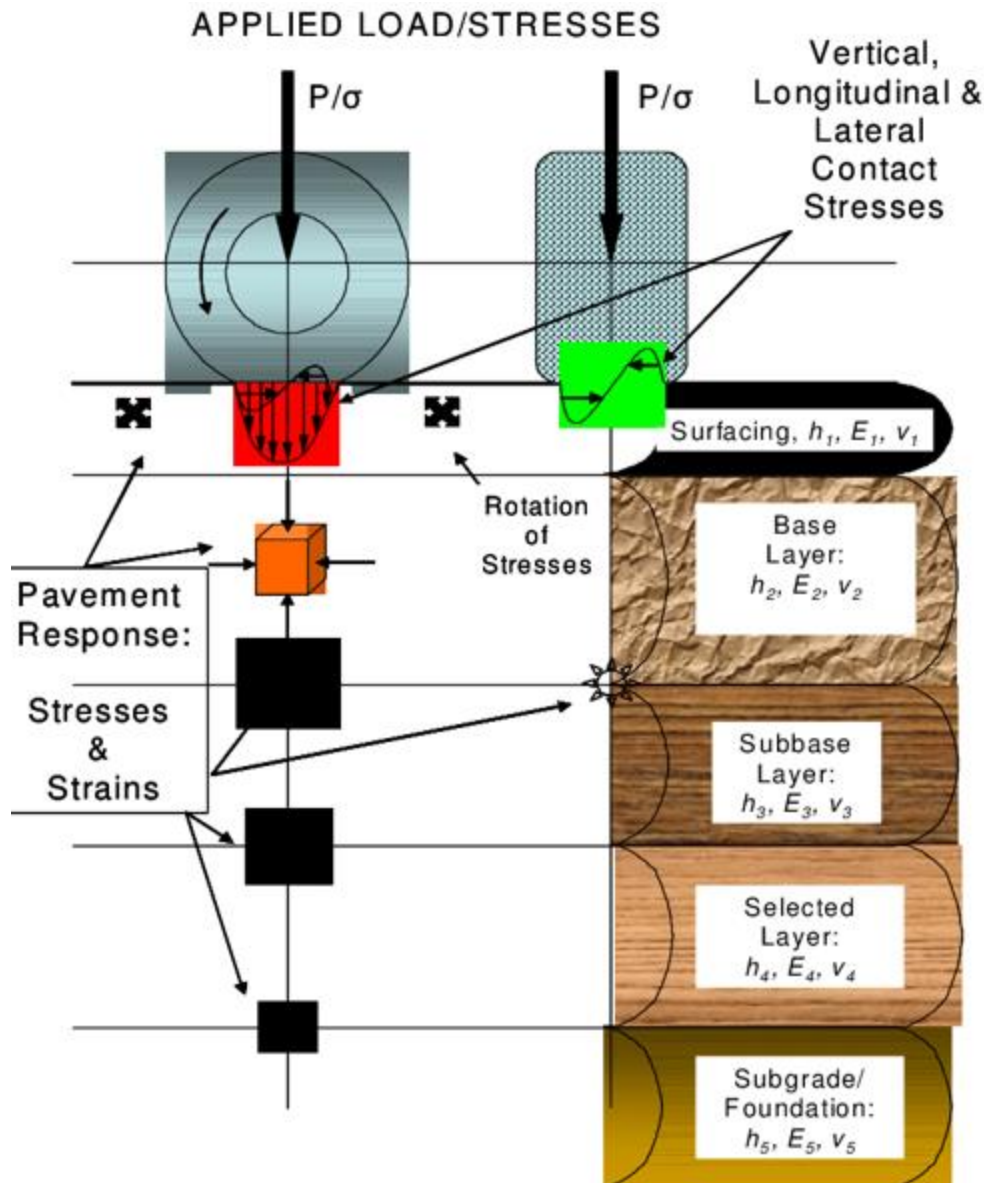


Figure 2.4: Basic Layout for Multilayers in Flexible Pavement system

As shown in Figure 2.4, the surfacing at the top section is the most sensitive part of the pavement and this layer has the highest stiffness property specification requirement in the design. The basis of this is to cater for the excessive high stresses resulting from axle loads as the traffic move over the surface. The underlying layers range from a bounded Base Course (Cement bound or Bitumen Treated Bases as the binder) to an unbounded subbase (UGM-unbound granular material). Sometimes, the subbase is stabilized depending on the material or geographic properties at the site. The subgrade is the least layer with the least stiffness value, the basic aim of the succession layers

is to shield and protect the subgrade from the ingress of moisture and excessive deformation that arise from axle loads. The respective heights for the layers can vary as well as the resilient modulus E .

In addition, the geology of South African soil consists of fines. These range from classical geological features, unique minerals and, significant materials in the form of exploitable industrial and precious minerals has led to the development of different material composition. This is mostly used in the construction of the individual aforementioned layers. The distinct property and thickness of the individual layer has led to optimized structural and economical requirements based on the prevailing geological material used during construction. The wearing course as indicated above is dependent on the grade size analysis used in the design mix: semi-graded, open-graded mix, gap graded mix, etc; as well as the type of bitumen used. The base course is dependent on the type of traffic analysis used in traffic design. However, depending on the riding quality and skid resistance required, the amount of binder needed to provide the design riding surface and prevent moisture from entering into the underlying layers is employed.

The subsequent layers of Hot Mix Asphalt pavements are composed of untreated or stabilised aggregates. Typically, these base layers are mostly composed of variety of different categories of bituminous mixes especially when a structural base layer is required if roads are to be built on weak subgrades. In some occasions, subbase layer is made up of a durable high strength structural aggregates. In addition to stiffness requirements, the subbase course provides improved drainage and prevents the occurrence of frost action in roads. The subgrade is the formation soil or a selected material compacted to the desired density to the design optimum moisture content value. On problematic soils, geotextiles materials are used to provide support to the subgrade. In the construction phase of transportation infrastructure on soft soils, the use of geotextiles as reinforcement can be implemented with sufficient fund in other to place the sub-base layer on the weak layer (Yesuf, 2014). In pavement design, the three cardinal components of major concern essential towards achieving a durable pavement structure are: firstly, material characteristics; secondly, traffic loading and thirdly environmental factors. These design parameters have to be incorporated into the pavement design model in other to obtain a reliable response of the pavement structure (Yesuf, 2014). Thou the theoretical framework of including every aspect of the influencing factors has not been feasible, at least in practice. One of the methods to minimize such

difficulties is to analyse the effect of each individual factor and the combined effect of two or more factors in the design phase (Yesuf, 2014).

2.5 Empirical and Mechanistic Empirical Pavement Design Overview

The Mechanistic Empirical Pavement Design Guide (MEPDG), was developed under National Cooperative Highway Research Program *NCHRP* project 1-37A (NCHRP, 2004) as a state-of-the-art practice for asphalt pavement evaluation. MEPDG used a traditional approach divided into two steps: pavement response prediction and pavement performance prediction. The first approach applies a multi-layered elastic analysis-based procedure to compute the stresses and strains at critical points in a specific damage model for performance prediction. In the second approach, the output generated is plugged into specific damage models for performance predictions. Each step is performed for the different period of the pavement service life since MEPDG is integrated with a climatic module, traffic loading spectra, seasonal complexities and hourly input data distribution log. This approach has been inefficient due to several weaknesses resulting from; damage evolution in the complex structures and new material properties not captured properly by the Mechanistic-Empirical models (Olowosulu, 2005; Kim, 2009; Papagiannakis and Masad, 2008, Papagiannakis, 2013). For example, different combinations of layers, material types, and thicknesses in perpetual pavements make it difficult to predict the failure mechanisms accurately using conventional Hot Mix Asphalt performance prediction models and pavement response models (Kim, 2009). A shortcoming of the MEPDG's two-step approach is the mode-of-loading dependency of most of the inherent performance models. These models were developed using results obtained from laboratory tests that were conducted under specific conditions of loading (Tseng and Lytton, 1989). Moreover, the Mechanistic-Empirical laboratory test protocols were designed to simulate specific boundary conditions of pavement structures rather than to capture the fundamental properties of the materials. Therefore, numerous tests are required to cover the wide range of pavement conditions.

2.6 Trésaguet Road Design Philosophy

Trésaguet, a well-respected and practising French engineer, is considered to be the first man to introduce a modern approach to pavement construction after the Roman influence on road-building methodology (Oglesby, 1975; 1976). Trésaguet is credited for advancing and successfully improving the construction and maintenance of stone roads. He is also believed to have made it possible for Napoleon to build the French highway system. As a result of his considerable experience gained in road pavement design, Trésaguet wrote a treatise on road design in the year 1775. The essence of his proposal and improvement on Roman efforts were focused on better drainage, crowned subgrade as well as crowned foundation and reducing the thickness of the broken stone layer to approximately 0.25m. His treatise addressed designing roads with geographical constraints along the route, suggested a reduction in the width of the carriageway, removing ditches on one side of the road and ensuring the slope was not greater than 7 percent. His main innovations involved gravelling techniques. In summary, his proposal involved a road with three layers of stone on the crowned subgrade (Oglesby, 1975; 1976). On the other hand, Trésaguet in his findings could not provide failure mode predictions of pavement subjected to varied loading and hazardous environmental conditions (O’Flaherty, 2002).

2.7 Telford Road Design Philosophy

In the early 1800s, the Telford then Macadam design philosophies took root. Telford’s school of thought sought to build on the advances made by Trésaguet in the design of pavements and his particular preference was to do so on flat subgrades wherever possible. The reason for taking this position is that he felt it would reduce the number of horses required to haul cargo along the carriageway. The proposed overall pavement thickness of 350mm - 450mm was considerably less than previous attempts at pavement design and like Trésaguet, employed three layers of material above the subgrade. The distinct approach taken by Telford was to have the foundation course, above the subgrade, comprise large cubic shaped stones which were approximately 75mm minimum thickness, 125mm breadth and 175mm in height (Oglesby, 1975). Although in an attempt to reduce the pavement thickness and minimise the cost of construction and materials used, Telford still did not come up with a sustainable measure for predicting or estimating failure mode on the pavement overtime during the design service life (O’Flaherty, 2002).

2.8 Macadam Road Design Philosophy

After Telford, Macadam further advanced road design philosophy from its initial stages of development and as a result, the design methodology was named after him. In his approach, Macadam modified the Telford design by removing the foundation layer of relatively large stones and replaced it with small broken stones not exceeding 75mm, that the smaller stones were more suitable for interlock with each other due to angularity. The practice of designing water-bound Macadam roads was largely discontinued because of some inherent flaws in this philosophy. The overarching effect of the vacuum created under the moving vehicle and the thrust of its wheels resulted in the rapid removal of the binder. In essence, the road surface was reduced to a pile of rubble and was no longer capable of providing acceptable levels of service for the road user. In addition, the cost-effectiveness of the Macadam design was deemed questionable, particularly in parts of the world where labour costs tend to be high (O'Flaherty, 2002).

2.9 The AASHO Road Test

The design of pavement is either flexible or rigid except otherwise specified. The main prohibitive factor against the widespread use of rigid pavements is the overall cost vis-à-vis other options (Parris, 2015). Even though there is an effort to use more mechanistic approaches to pavement design, the use of the 1993 AASHTO Pavement Design Guide is still the most common approach taken by practitioners. Emergent from the AASHTO Road Test, Equation 2.2 was developed for flexible pavement design based on a calculated structural number.

The use of the aforementioned as well other methodologies employed for pavement design underwent a considerable shift in philosophy in the early 1960s with the advent of the American Association of State Highway Officials (AASHO) road test program. The Interstate Highway System (IHS) in the United States is arguably the single greatest and most expensive public works project to date (Hallin *et al.*, 2007). This system is unrivalled in many parts of the world and provides the infrastructural substratum for the relative economic prosperity of the United States. In many ways, the AASHO test program was authorized by IHS legislation enacted in June of 1956 and championed by President Eisenhower. In essence, the public highway system developed concomitantly with the motor vehicle industry. As motor vehicles underwent changes in weight, size, speed, capacity and sheer volume, it became evident that the early methods would not be

adequate and accordingly, new and more advanced methodologies had to be developed. Consistent with the earlier methods of road construction discussed in this chapter, highway engineers in the 1920s were aware that the structural integrity of the road pavement system was premised on the axle loads of vehicles. However, the volume of traffic was so low, it was assumed that the pavements which resisted natural forces were adequate for that traffic loading. Nevertheless, with the surge of vehicular traffic traversing the roadway, a more direct assessment of the relationship between pavement design and axle weights saw practitioners build on initial test efforts initiated throughout the early 1900s such as the Bates Experimental Road Test conducted by the Division of Highways of the Illinois Department of Public Works and Buildings between 1922 and 1923. The tests were conducted from 1958 – 1960 and the compiled results were used to inform more broadly applicable scientific approaches to design. These results formed the basis of the design of most of the IHS post-1961 (Hallin *et al.*, 2007). In fact, all the pavement design guides issued by AASHTO until 1993 are incapable of easily adapting to significant improvements made in pavement engineering, design and materials (Mazumder *et al.*, 2015).

$$\log(W'_{18}) = Z_R \cdot S_0 + 9.36 \cdot \log(SN + 1) - 0.20 + \frac{\log(\Delta PSI)/(4.2 - 1.5)}{0.4 + 1094/(SN + 1)^{5.19}} + 2.32 \cdot \log(MR) - 8.07 \quad (2.2)$$

With the premise of the above-mentioned design methods developed, there has also been the development of the latest mechanistic method which is currently under review for full-scale adoption which seeks to provide a solution for better performance and longevity of pavement structures. Considering several soil parameters for its development; California Bearing Ratio (CBR) of the soil, Shear Strength, Strain and Deflection. Most of the initial pavement design methods were based on empirical methods which rely on strength testing as developed by the California highway department of transportation in 1929 where pavement thickness was related to the CBR (*i.e.*, the penetration resistance of a subgrade soil relative to a standard crushed rock). This method is disadvantageous because it is limited only to a certain set of environmental material and loading conditions (Huang, 1993), and its applications in other situations require a new method to be developed. Consequently, the implementation of CBR in design utilizes limiting shear failure method considering the angle of internal friction and cohesion of subgrade soils as major properties for pavement thickness determination. However, the AASHTO design method is dependent on the variable parameter associated with the Structural Number as well as the equivalent single axle load

considered. The Pavement Serviceability Index to determine the strength parameter for a flexible pavement is given as:

$$\beta = 0.4 + \frac{0.081(L_1 + L_2)^{3.23}}{(D+1)^{5.19}L_2^{3.23}} \quad (2.3)$$

a further approximation to determine the strength of the pavement is given as:

$$\log \rho = 5.93 + 9.36 \log(SN + 1) - 4.79 \log(L_1 + L_2) + 4.33 \log(L_2) \quad (2.4)$$

where: SN = Structural Number

The final design equation for obtaining the structural number of a flexible pavement considering standard single axle load of 18kips equivalent to 80kN is given by:

$$\log W_{t18} = 9.36 \log(SN + 1) - 0.2 + \frac{\log\left(\frac{4.2 - p_f}{4.2 - 1.5}\right)}{0.4 + \frac{1094}{(SN+1)^{5.19}}} \quad (2.5)$$

where: W_{t18} : number of 18kip (80kN) single axle load application times

p_f : the terminal serviceability index

2.10 Mechanistic-Empirical Pavement Design Method

The Mechanistic-Empirical Method (ME-DM) developed by Kerkhoven and Dormon in 1953; (Huang, 1993) takes account of subgrade vertical compressive strain, and horizontal tensile strain at the bottom of the Asphalt Concrete Surface layer and the top of the subgrade. This method makes use of input (a wheel load) and relates to an output (stress/strain) for the design. The Mechanistic-Empirical Design Method partly considers the change of temperature and moisture profiles in the pavement structure and subgrade over the design life of a pavement (Olowosulu, A. T, 2005; MEPDG, 2004). This is furthermore achieved through the use of a climatic modelling software referred to as the Enhanced Integrated Climatic Model (EICM), (MEPDG, 2004). Temperature gradient variations as well as humidity/moisture changes are the two environmentally driven variables that significantly affect the underlying pavement layers. In some occasions

induced effect resulting from the two parameters result to increased stress values from the magnitude of axle loads the pavement is subjected to.

In 1997, Larson *et al.* introduced the *Enhanced Integrated Climatic Model (EICM) version 2.0* work bench program. The EICM 2.0 (Windows 95 version) which is an upgrade to the original Integrated Model developed in a joint effort by the Texas Transportation Institute, Texas A&M University and the University of Illinois in 1989. The EICM functions as a single-dimensional heat and moisture process instance that is purpose designed to analyse pavement soil systems in conjunction with climatic conditions (Liu and Lytton, 1985 1986; Dempsey *et al.*, 1985; Papagiannakis, 2013). The EICM, in contrast with Mechanistic-Empirical Design Methods' has the capability to give rise to accurate estimates of rainfall patterns and precipitation rate, solar radiation, cloud cover, wind speed, and air temperature to faux the upper boundary conditions within the pavement design process. EICM possesses diversity relating to options for specifying the humidity/moisture and temperature at the lower boundary and at the interface between the subgrade and the base course. EICM focusses on the lateral and vertical drainage of the base course, which is a two-dimensional problem. This is used in determining the magnitude of moisture seepage that enters the subgrade by infiltration and percolation through the pavement surface and base course.

ME-DM method has gained global attention over the last decades (Kim 2007). This is as a result of the inaccuracy of the design and failure observed in the implementation of traditional methods, its level of accuracy when compared with traditional methods and its simplicity when compared with the EICM design methods (Huang 2004; Jain *et al.*, 1992, 2013). This increased attention has been attributed to the advantages associated with the use of Mechanistic-Empirical Design Methods. Some of them are, to identify and evaluate stress and strain, analyse static and time-dependent variables, incorporate non-linear material characterization, large strain/deformations, dynamics analysis and environmental parameters. ME-DM method of evaluation is based on standard input parameters such as pavement thickness, material properties, loading condition (in terms of static and dynamic) interacting with it. In other to model pavements correctly considering the ME-DM, it is pertinent to use numerical methods. These methods among others are finite difference method, the boundary element method and Finite Element Method (Áurea *et al.*, 2006,

Holanda *et al.*, 2006; Ameri *et al.*, 2012). FEM is mostly adopted in pavement analysis and will be considered in this study.

Considerably, Finite Element Methods has been introduced extensively in road engineering over time (Peng and He, 2009). Finite Element Method of pavement analysis is seen to be the most versatile of pavement analysis techniques so far. This possess the capabilities to incorporate both 2-Dimension and 3-Dimension geometric modelling which is able to analyse static, time-dependent problems, nonlinear material characterisation, large strains/deformations, dynamics analysis and other sophisticated features (NCHRP, 2004). However, the adoption of Finite Element Method to solve any problem consists of three separate stages. First is the pre-processing (Modelling); secondly, processing (Evaluation) and thirdly; post-processing (Simulation). In view of all these, the use of 3D (Abaqus-Finite Element Analysis) provides a more efficient finite element approach (Wang, 2001; Sukumaran, 2004; Rahman *et al.*, 2011; Shafabakhsh *et al.*, 2013; Holanda *et al.*, 2006).

Research over the years has been conducted in Hot Mix Asphalt pavement inter layers via Finite Element Methods (Gupta and Kumar, 2014). Although, granular materials when discretizing is given priority, as more focus is centred on designing the Asphalt layer and subgrade deformation subjected to service loads (Adu-Osei, 2001; Araya, 2011; Tiliouine and Sandjak, 2014). On the other hand, limited study has been carried out on stabilized base and subbase layers (Peng and He, 2009). Considering all the advances in technology, there exist a level of uncertainty in pavement performance predictions which are more difficult to control than the response model (NCHRP, 2004). In view of this, a reality check through validation of results with field testing or available results is of paramount importance (Sung-Hee Kim *et al.*, 2017).

Finite Element Method over time has been adopted in the analysis of pavement failure such as rutting and fatigue cracking at different layers (Abed and Al-Azzawi 2012; Al-Khateeb *et al.*, 2011 and Walubita and van da Ven 2000). FEM can also be used to determine the accurate positioning of the Geogrid (Geosynthetic) material (Al-Azzawi 2012). This can be extended also to estimate the thickness of each layer (Shafabakhsh *et al.*, 2013; Sinha *et al.*, 2014) and the interaction between pavement and its instrumentation (Yin, 2013 and Zafar *et al.*, 2005). Advancement in technology has resulted to researchers considering the strict use of Finite Element Method for the design of sustainable highway pavement. In a study by Jagtap and Nagrale (2013), FEM was found to be of

benefit as using it for optimized pavement design which reduces the construction cost by 11-15%. With high success rate attained in the introduction of FEM, it is needful to feature the design of optimization in Finite Element Method for sustainable urban pavement structure.

2.10.1 Distress Prediction in M-E Design Method

The evaluation of pavement distress can be evaluated from observation and performance of the underlying load and service conditions of the pavement in line with observed failure and strain under varying load combinations. This phenomenon results to computing the number of loading cycles to failure (Mamlouk and Mobasher, 2004; NCHRP, 2004; Pavement Interaction, 2008). There exist numerous failure trend models to compute pavement distress. Nonetheless, two are widely recognized; fatigue cracking in the Asphalt Concrete layer and the deformation (*in the form of deflection*) occurring at the top of the subgrade (Pavement Interaction 2008; Ekwulo and Eme 2009; South African National Road Agency Ltd. (SANRAL, 2013). Furthermore, the Asphalt Institute damage model (Asphalt Institute, 1982) is commonly accepted (Ekwulo & Eme, 2009; Pavement Interaction 2008). Asphalt Institute models are presented in Equation 2.6 (Fatigue Failure) and Equation 2.7 (Rutting Failure). Overall, the distress prediction models are used to define the point at which failure occurs in pavement by determining the incremental damage.

$$N_f = 0.0796(\varepsilon_t)^{-3.291}(E)^{-0.854} \quad (2.6)$$

where; N_f = Number of load repetitions to fatigue cracking; ε_t = Tensile strain at the bottom of the asphalt surface in microstrain; E = resilient modulus of asphalt in psi

$$N_r = 1.365 \times 10^{-9}(E_c)^{-4.477} \quad (2.7)$$

where; N_r = Number of load repetitions to subgrade rutting failure; E_c = Vertical Compressive strain at the top of subgrade

2.11 Analysis of Flexible Pavement Base Materials

2.11.1 Asphalt-Stabilised Base Material

Asphalt-stabilised base layer materials have been found to possess stiffness three times higher than typically compacted unbound granular base materials with the same thickness. However, laboratory test results (Ashteyat, 2004) clearly indicates a strong dependence on the strength and stiffness of asphalt stabilized materials on the service temperature. A considerable reduction in the

strength and stiffness is observed in the stabilised base material with an increasing temperature gradient. Consequently, since asphalt- stabilised material shows a tendency for bond loss due to moisture and freezing-thawing cycles, leading to a high probability of pre-mature pavement failure (Ashteyat, 2004). This study focuses on instrumenting the pavement layer while subjected to varying temperature and moisture gradient the data obtained is used to determine the service life expectancy of the pavement using a real-time model (*transfer-functions*).

2.11.2 Cement- Stabilized Base Materials

The materials properties of the cement-stabilized granular base indicated that both flexural strength and resilient moduli are not significantly affected by normal temperature changes. In general, a surge in the moisture saturation content results to a reduction in the modulus of elasticity of the unbound granular base materials. It is also needful to note that, moisture variation has two major distinctive effects on cement stabilised bases. Firstly, moisture variations can affect the state of stresses, through suction or pore water pressure. Coarse-grained and fine-grained materials can exhibit more than a fivefold increase in modulus due to the soils being drying out. This indicates that the resilient modulus of cohesive soils is strongly influenced by a complex clay-water electrolyte interaction. Secondly, moisture can alter the entire structure of the soil through the destruction of the cementation bond between aggregate material molecules (MEPDG, 2004).

2.11.3 Bound Granular Base Materials

Bound granular base materials are usually not affected by the presence of moisture due to the property of the binder material used (cement or bitumen). However, excessive moisture can lead to stripping in asphalt stabilized mixtures. Cement bound granular materials may also be damaged during freeze-thaw and wet-dry cycles, as reflected in modulus reduction. Studies conducted on bound granular base materials stipulates a considerable reduction in the compressive strength of cement-treated materials after being subjected to 15 cycles of freezing/thawing cycles. Following this, results show that the amount of unconfined compressive strength reduction of cement stabilized granular base materials due to freezing/thawing was found to be up to 60% at 35 cycles (Eshkeveri Salimi S, Abbo, Andrew, J., and Kouretzis, George, 2019: Ashteyat, 2004).

2.11.4 HMA Pavement Failure Investigation modes

The aim in the design of Hot Mix Asphaltic pavement is to solve the impairment mechanism related to failure and or delamination modes, pavement distresses parameters and the probable scenarios resulting in these irregularities. HMA damage investigation should be able to highlight the mechanisms causing the distress and takeout discrepancies as well as unrelated mechanisms (Crampton, 2001). The important tasks involved in an HMA pre-construction investigation are shown in Table 2.1.

Table 2.1: Pavement Failure Catalyst

| Major Factors | Description |
|--|--|
| Aggregate Properties | <ul style="list-style-type: none"> • Chemical properties (degree of acidity or pH, surface chemistry, type of minerals, source of aggregate. • Physical characteristics (angularity, surface roughness, surface area, gradation, porosity and permeability) • Dust and clay coatings • Resistance to degradation |
| Asphalt Binder Properties | <ul style="list-style-type: none"> • Grade or stiffness • Chemical composition • Crude source and refining process |
| Hot Mix Asphalt Void Content Characteristics | <ul style="list-style-type: none"> • Air void level and compaction • Type of HMA (dense-graded, gap-graded, open-graded) |
| Environmental Factors | <ul style="list-style-type: none"> • Temperature gradient • Freeze-thaw cycles • Moisture saturation • Dampness/wetness • Pavement age/design life • Ion content in surrounding free water |
| Traffic | <ul style="list-style-type: none"> • Percent of truck passing • Gross vehicle weight of trucks • Truck tire pressure |
| Hot Mix Asphalt Construction | <ul style="list-style-type: none"> • Compaction value • Drainage allowance • Weather condition • Segregation parameter • Contractor Experience, years of experience |
| Design of HMA | <ul style="list-style-type: none"> • Voids in Mix (VIM) • Subsurface Drainage for runoff • HMA Mix Design • Designer experience and Designer Site visit |

Source: (SAPEM, 2014)

2.11.5 Moisture Impairment/Damage in Hot Mix Asphalt Pavements

Impairment in Hot Mix Asphalt (*HMA*) pavements can be as a result of loss of strength and durability due to the effects of increasing moisture content (Little and Jones, 2003). This is usually caused by loss of cohesion (strength) of the asphalt film which results to loss of the adhesion (bond) between the aggregate and bitumen, as well as degradation of the aggregate particles subjected to freezing (Terrel and Al-Swailmi, 1994). Moisture damage is most commonly manifested in the form of stripping-off of the binder from the aggregate and filler material as a result of presence of induced friction caused between the two surfaces. This can occur in the form of displacement, spontaneous emulsification, pore pressure, and hydraulic scour (Majidzadeh and Brovold, 1968; Taylor and Khosla 1983; Cho and Kim, 2010; Tarrer and Wagh, 1991; Terrel and Al-Swailmi, 1994; Cheng *et al.*, 2002; Birgisson *et al.*, 2005). A number of related factors that affect the performance of HMA pavement subjected to moisture damage can be seen in the study carried out by Stuart (1990) and Hicks (1991).

Following recent studies, it can be said that humidity/moisture impairment customarily is initiated at the base of the Asphalt Concrete or at the interface of two Asphalt Concrete surface layers (Khosla *et al.*, 1999). This further manifest into the creation of localized potholes resulting in pavement ravelling or rutting. When compared with high strength Asphalt binders (Rubberized Asphalt, PG Bitumen etc.), localized fatigue cracking (longitudinal cracking that progresses to alligator cracking) may occur resulting in loss of strength and stiffness of the pavement structure. Subsequent water intrusion into the localised voids impaired with water, together with traffic loading, further depletes the structural integrity of the pavement layer. This among many other factors can deter the underlying layers, if not repaired. In addition, it may result to substantial localized failure of the pavement structure (Scholz, 1995; Lui and Lytton, 1985). Surface ravelling or a loss of surface aggregate can also occur, especially with chip seals, bitumen emulsion or areas prone to excessive precipitation. In tropical regions with high-temperature conditions, binder from within the pavement will migrate to the pavement surface resulting in flushing or bleeding (Stuart, 1990).

Loss of pavement structural capacity can be as a result of unbridled humidity/moisture in the underlying pavement base layer which in turn reduces the cover over which the imposed traffic load will be distributed. The increased saturation level as a result of moisture ingress has a

significant effect on pavement structure which decreases pavement Resilient Modulus (M_R) and increases permanent deformation (Seavarsdottir and Elingsson, 2013). Excessive moisture and fine grained particles is often times transported by hydrostatic pressure within the pavement matrix to the underlying layers This effect reduces the strength of the overlying HMA layers by increasing the vertical compressive strain under service conditions. A proper apprehension of the environmental effects on Hot Mix Asphalt pavements allows better forecast of pavement performance and behaviour under different environmental conditions (Davies, 2004). Regardless of the strength of the HMA surface course, the stability and durability of a pavement depend on the strength of its subbase and subgrade (Kiehl and Briegleb, 2011). A strong surface layer will undoubtedly fail prematurely if constructed over a weak foundation as the strength of pavement may fluctuate with changes in the humidity/moisture content of its underlying layers (Ahmed *et al.*, 2012). It is needful to note that the performance of pavement surfaces is adversely affected by the presence of moisture within underlying layers (Saevarsdottir and Elingsson, 2013). The design and construction of Hot Mix Asphaltic surfaces are generally performed with the notion of keeping the inter pavement layers dry or unsaturated. This serves to ensure that the pavement surface is drained efficiently. Unfortunately, uncontrolled humidity/moisture seeps into the pavement structure, this deficiency over a period of time affects the performance of the structure. (Charlier *et al.*, 2009; Ekblad, 2007; Lekarp, Isacson, and Dawson, 2000a, 2000b; Rahman and Erlingsson, 2012; Salour and Erlingsson, 2013; Theyse, 2002) concluded that increasing humidity/moisture content reduces the Resilient Modulus, M_R of the underlying base granular materials. They further stated that humidity/moisture ingress over time results to loss of frictional strength and decreases resistance to deformation. The Mechanistic-Empirical Pavement Design Guide put forward that the changes in humidity/moisture content is the important factor accounting for the rutting of unbound granular materials, as increasing moisture content results to a dwindling effect in the Resilient Modulus, M_R (MEPDG, 2004).

The response of highway infrastructure platforms subjected to traffic surge loading is analysed by computing the stresses and strains parameters within its inter-layers. In most cases, stress values beyond the pavement carrying capacity (Resilient Modulus) result to pavement fatigue cracking and/or surface rutting. This results to structural and functional failure during its intended design life; also posing a safety hazard threat to motorists. Pavement distresses are minimized among others by the use of Stochastic pavement designs mathematical algorithm. Pavement stress-strain

analysis is an ideal tool for analytical modelling of pavement behaviour and thus, constitutes an integral part of pavement design and performance evaluation. Pavement structures are heterogeneous structures built over various geomorphologic, geologic and climate environments. Saevarsdottir (2014) stated that, from top-down, a flexible pavement structure distributes axle loading to the subgrade soil, preventing excessive pavement deformations and controlling environmental degradation effect on the structure's bearing capacity. In addition, from the bottom up, the pavement structure should minimize environmental-related stresses and displacements, such as disparate frost and heave and post-consolidation. Doreand Zubeck (2009), summarised that a structure needs to fulfil its role to maintain good structural and functional performance during its design life.

2.12 Two-Dimensional Stress State

Linear dimensional pavement stress state estimation is centred on a Mechanistic Design (Croney and Croney, 1998; Huang, 1993) and Multi Layered Elastic Pavement Design system. The standard and efficient method to model pavement load response is the Stress-Strain analysis. The induced stress pattern due to a moving wheel load in pavement is complex and usually difficult to simulate (Wang and Grandhi, 1995). Figure 2.5 shows the unbound granular layers as well as the resultant vertical and horizontal stresses while the shear stress is reversed as the load passes causing a rotation of the principal stress axis. This effect further concludes that, the Resilient Modulus (M_R) behaviour of unbound granular materials is affected by factors such as: magnitude of the load, aggregate relative density, grading, maximum aggregate size and shape or angularity properties (Saevarsdottir, 2014).

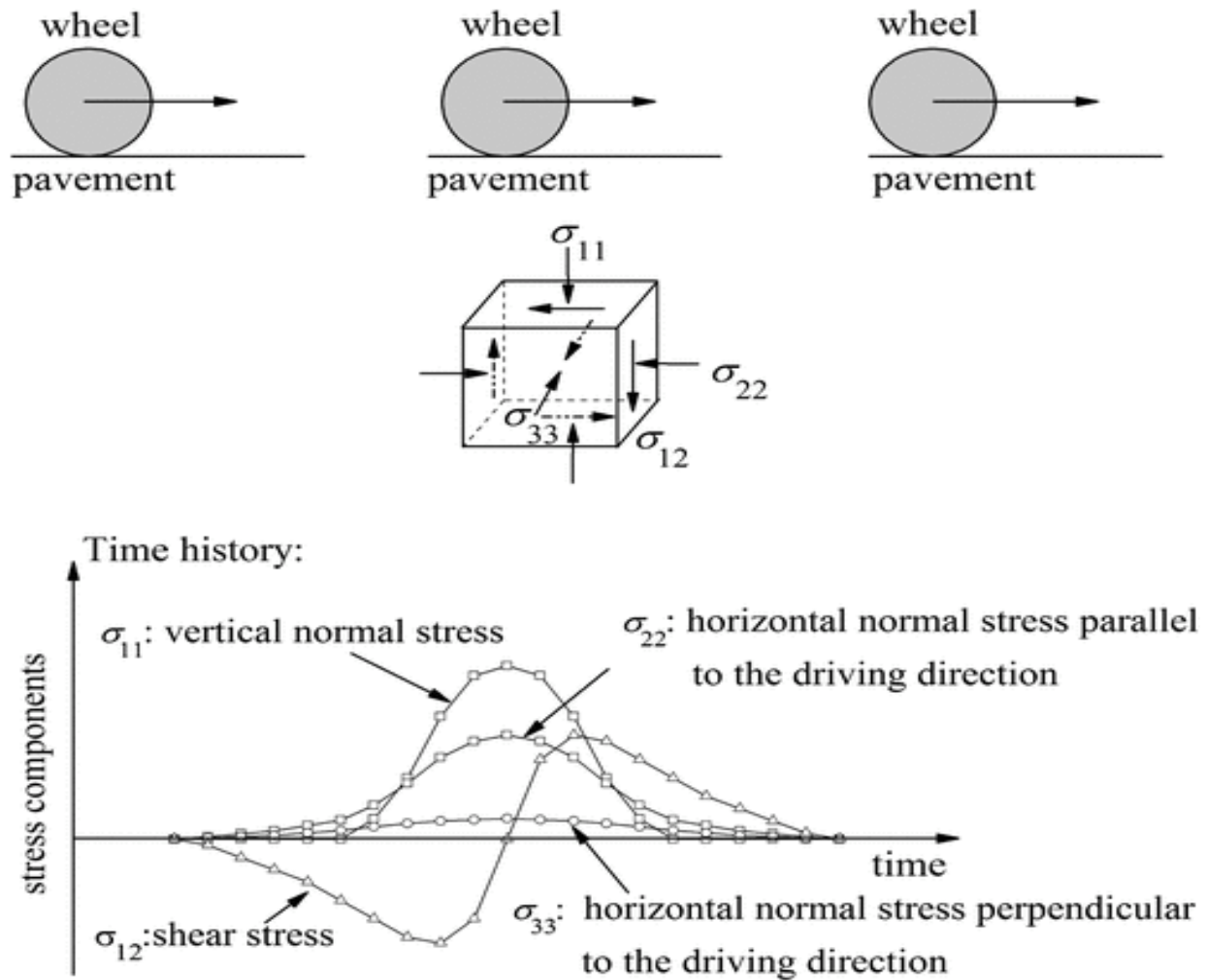


Figure 2.5: Stresses beneath a rolling wheel load (Gu, Cui, and Cai. 2019)

2.12.1 Three-Dimensional Stress State

The initiation of Finite Element Analysis provides a clear visualisation of three Finite Element models following the design standard and objectives with regards to moisture entrainment. A proposed mathematical model was introduced to prove the viability and efficiency of using 3D Finite Element Methods over the Multi Layered Elastic Design method. The adoption of these two methods is important in the design of pavement structure. This can be used to examine the structural response of a stabilized base layer in terms of the stresses and compressive strains at the top of the subgrade and the tensile strain at the bottom of the Asphalt surface layer. The models were developed using the Abaqus® workbench tool as shown in Figure 2.6. Considering design traffic parameter, this study's emphasis was focused on pavement humidity/moisture and temperature variation damage subjected to increasing traffic axle loading. The principle adopted

considered a major factor responsible for most pavement damage world-wide (De Beer *et al.*, 2005). However, a design input value of 80,000N and a pressure distribution of 650Mpa is adopted in the design. A tyre track model is proposed and designed to act along a coverage radius of 195mm² considering a category “A” road with maximum traffic count at peak periods over wet condition environment.

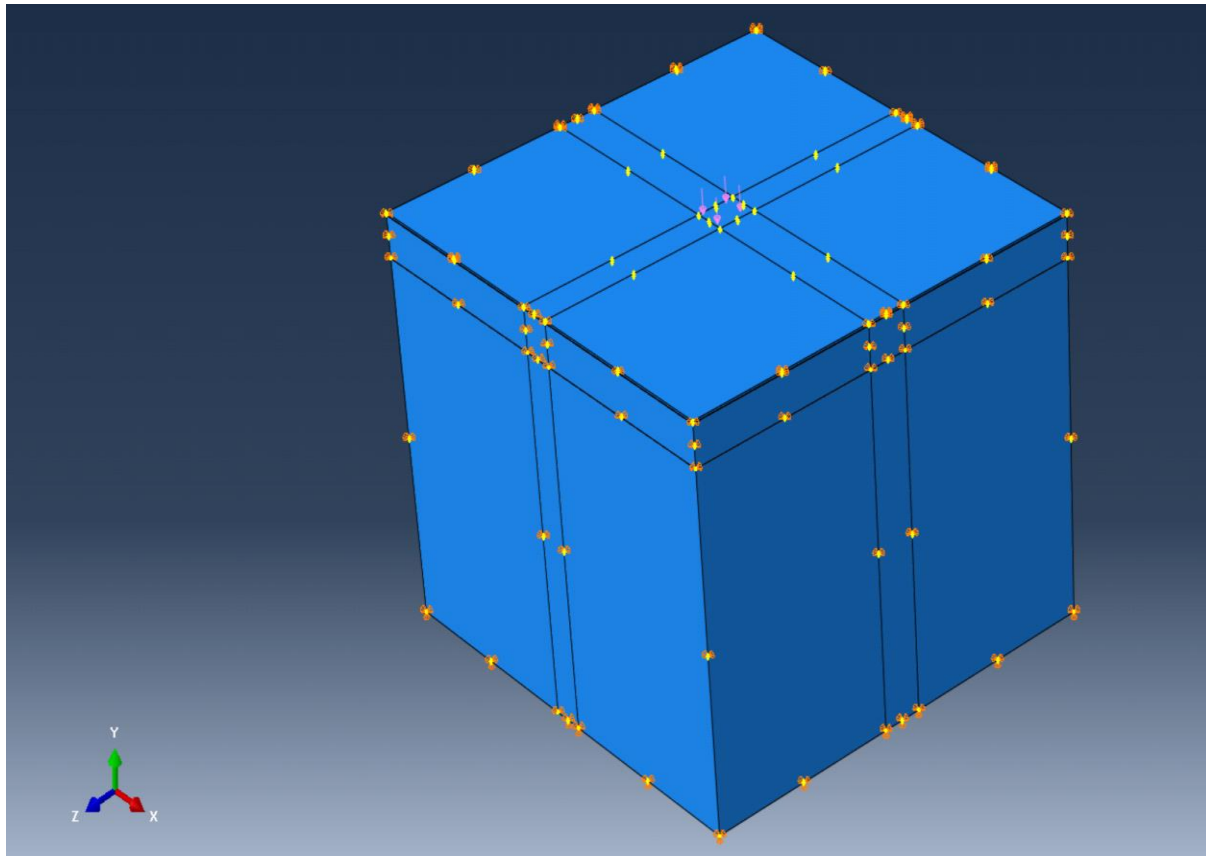


Figure 2.6: Three-dimensional stress state distribution of pavement assembly (Abaqus, CAE)

2.13 Concept of Reliability

The reliability theory in engineering basically deals with the rational treatment of uncertainties in engineering structural components and with the methods for assessing the safety and serviceability of the structures (Belegundu and Chandrupatla, 1999; Skjong, 1995). In other words, pavement reliability is concerned with the calculation and prediction of a limit state violation for highway pavement structures at any stage during their designed lifetime (Ditlevsen and Madson, 2005). The

violation of a Limit State is the attainment of an undesirable condition (failure) for the structure. Such as damage to a part of the structure or total collapse of the structure resulting in loss of human lives. Modern reliability methods provide an alternative design approach by assigning probability distributions to the uncertain variables for computation of the probability of exceeding various limit states and for comparison of this probability with a required reliability level. Computer techniques of structural analysis have improved the accuracy of representing the actual behaviour of pavement structural components. Advanced programs (such as: ABAQUS, NASTRAN, ANSYS, SAP and PYTHON, etc.) are made accessible for Linear and Non-Linear evaluation of complex highway structural pavement systems. A condensed element meshing caters for a more accurate determination of strain/stress at any desired point within the structure. The associated setback is the representation of element boundary conditions and material property geometry. For example, the actual in-situ support or constrain is often different from that assumed in an idealized type, and the strength of material and modulus of elasticity can be different than what is assumed in design. The deterministic approach also provides an efficient analysis, but there is a need to include the randomness of the material property and environmental parameters such as varying moisture content and varying temperature gradient.

Melchers (1987) defined the concept of structural reliability as a phenomenon related with the prediction of the probability of a limit state violation for engineered structures at any stage during their design life. Structural safety is concerned with the non-violation of the ultimate or safety limit state for the structure. The “violation” of a limit state is the attainment of an undesirable condition for the structure, i.e. damage to a part of the structure or total collapse of the structure which could lead to loss of human lives.

The reliability of a pavement structure in this context will refer to the ability to fulfil its designed traffic loading requirements within the design life. Reliability is often understood to equal the probability that a structure will not fail to perform its intended function. The term failure in this regard does not mean catastrophic failure but is used to indicate that the structure does not meet up requirement at the initial design stage to perform efficiently as desired. The reliability of a highway structure can be considered as a rational evaluation criterion which provides a good basis for the decision and judgement on the; maintenance, rehabilitation, or overall improvement of the highway facility (O'Connor, 1995).

Example of some reliability-based methods to analyse and generate reliability model of pavement include:

- First order reliability method; Goldwitzer, (1995)
- Monte Carlo Simulations
- Direct integration method
- First Order Second Moment Method
- Second order Second-Moment Method
- Genetic Algorithm amongst many others etc.

2.13.1 Reliability Index

In general, a suitable definition of the reliability index Z_x represents itself as the shortest distance from the origin of standard space (reduced variable space) to the limit state line $g(Z_R, Z_Q) = 0$, in the reduced variables space, where Z_R is the defined as the reduced random variable for resistance to failure and Z_Q is the reduced random variable for imposed load (Ferrand, 2005; Hasofer and Lind, 1974). The reduced form of a random variable, X , is given by equation (2.8):

$$Z_x = \left| \frac{X - \mu_x}{\sigma_x} \right| \quad (2.8)$$

2.13.2 Simulation Techniques

In many occasions, the computational methods of reliability as earlier defined presents itself to become very complicated and complex. This happens especially when the limit state function is very complex or cannot be expressed in a closed-form. In these situations, simulation methods are used. Examples of simulation methods used in the computation of reliability include: Monte Carlo Simulation (MCS) and Rosenblueth's 2K + 1 Point Estimate Method. A suitable method will be chosen among the above reliability models to generate a reliability function and to calculate a reliability value of the HMA under the effects of moisture and temperature effects.

2.14 First Order Reliability Unconstrained Method (FERUM)

FERUM which is a general-purpose structural reliability method was initiated in 1999 at the University of California at Berkeley. Finite Element Reliability based design can be used to carry out analysis using variable number of workbenches such as: MATLAB, ANSYS and PYTHON. FERUM 4.0 offers Reliability-Based Design Optimization (RBDO) capabilities. It offers new features such as simulation-based techniques (Directional Simulation, Subset Simulation), Global Sensitivity Analysis, Reliability-Based Design and Optimization. Subset Simulation and global Sensitivity Analysis can be carried out either using the original physical model or a Support Vector Machine surrogate. In this method the physical model is computationally demanding. The solutions can be best computed virtually through vectorized calculations in MATLAB or for real with multi-processor computers, provided that a suitable interface is developed (Hasofer and Lind, 1974; Dubourg *et al.*, 2012).

2.14.1 First Order Reliability Method (FORM)

The First-Order Reliability Method (*FORM*) is a mathematical tool designed to provide approximations of probability integrals occurring in structural reliability. In Figure 2.8, the probability that the load effect S , falls into an infinitesimal interval ds at s which is $f_s(s).ds$. Also, the probability that R falls in or under this interval is $\int_{-\infty}^s f_R(r)dr$. The probability that S falls in this interval ds when $R \leq S$ will result to $f_s(s).ds. \int_{-\infty}^s f_R(r)dr$.

The expression gives the probability that $R \leq S$ is:

$$P_f = P(\mathbf{R}-\mathbf{S}) \leq 0 = \int_{-\infty}^{\infty} f_s(s) \cdot \left[\int_{-\infty}^s f_R(r) dr \right] ds \quad (2.9)$$

The equation (2.9) can be viewed as the volume of the two-dimensional joint density functions from the failure surface and can be seen in Figure 2.7. Where R and S are plotted as probability functions on the r and s axes. The limit state equation, $G = R - S = 0$, separates the safe from the unsafe region, dividing the volume into two parts. The volume of the part cut away and defined by $s > r$ corresponds to the probability of failure. The design point (r^* ; s^*) is located on this straight line where the joint probability density is greatest. If failure is to occur, it is likely to be there. The desired safe state is above the failure surface, defined as $R-S=0$, and undesired failure state is below.

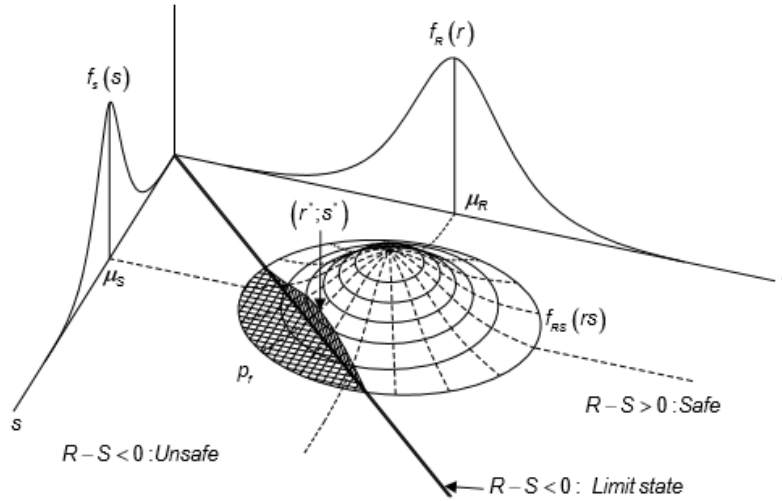


Figure 2.7: The 3-D view of Two Random Joint Density Function $f_{R(S)}(rs)$, (Bergstrom, 2006).

If R and S are normally distributed and statistically uncorrelated, then:

$$R \in N (MR, \sigma R)$$

$$S \in N (MS, \sigma S)$$

The safety margin, M is defined as:

$$M = R - S \tag{2.10}$$

Then it is also valid that:

$$M \in N (MM, \sigma M)$$

$$\text{Where } MM = MR - MS \text{ and } \sigma M = \sqrt{\sigma^2 R + \sigma^2 S} \tag{2.11}$$

The distribution of M is schematically given in Figure 2.8 below. Failure occurs when $M < 0$

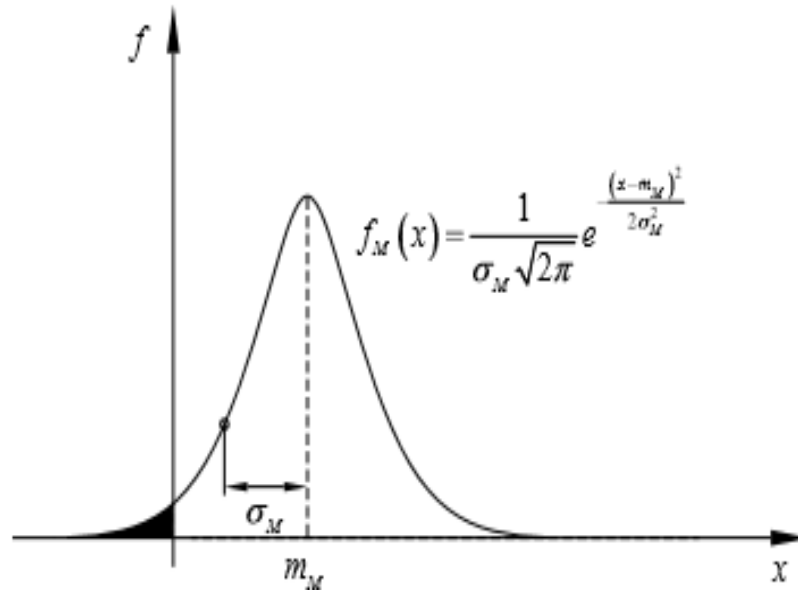


Figure 2.8 Distribution for the variable M. Failure occurs when $M < 0$. (Bergstrom, 2006).

$$P_f = P(M < 0) = \int_{-\infty}^0 f_M(x) dx = \frac{1}{\sigma_M \sqrt{2\pi}} \int_{-\infty}^0 e^{-\frac{x-m_M}{2\sigma_M^2}} dx \quad (2.12)$$

Now let,

$$\frac{x-m_M}{\sigma_M} = y \rightarrow \frac{1}{\sigma_M} dx = dy \quad (2.13)$$

$$P_f = P(M < 0) = \frac{1}{\sqrt{2\pi}} \int e^{-\frac{y^2}{2}} dy = \Phi\left(-\frac{m_M}{\sigma_M}\right) = \Phi(-\beta) \quad (2.14)$$

$\Phi(\cdot)$ is the standardised normal distribution function Figure 2.9. This function, given in Equation 2.15; has mean value 0 and standard deviation 1. If R and S are normally distributed, the safety index, β , is calculated as:

$$\beta = \frac{m_M}{\sigma_M} = \frac{m_R - m_S}{\sqrt{\sigma_R^2 + \sigma_S^2}} \quad (2.15)$$

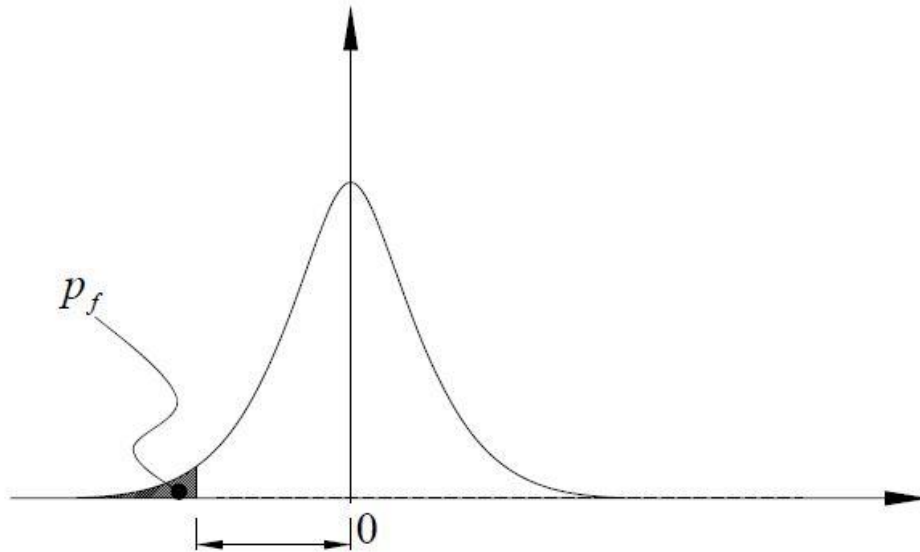


Figure 2.9 The Standardised Normal Distribution Function Safety Index β , is connected to a certain Probability of Failure, P_f (Bergstrom, 2006)

2.15 Summary

In this section, a further and deeper background of the problem is discussed. Related research on pavement life, pavement failure, distress effects, their causes as well as remedial actions previously taken to avert the outlined failure mode evidenced from literature was discussed. Consequently, the methods taken in the literature were reviewed to decipher an action plan which will be discussed in the next chapter. the introduction of the test core drilling location is presented, and the cores sampling details are recorded.

CHAPTER THREE: METHODOLOGY

3.0 Research Design

The research design adopted for this study incorporates Fracture mechanic together with stochastic response analysis of pavement layers under environmental and service conditions. The design principle also allows for the response analysis to be based on characteristic input values of the pavement at the time of analysis. This considers characteristic pavement temperature, pavement saturation level (moisture/humidity content), ground water table (GWT) depth, depth of sensor embedment. The provided values were used to determine the resilient modulus of the pavement at the time of analysis. This process is based on the assumption that the GWT depth varies depending on the topographic location of the pavement as well as the soil properties. The analysis result is developed in form of a reliability reference mode which further provides an indication of the confidence level of the pavement (stiffness value, fracture energy, resilient modulus of the underlying asphalt base layers) down to the subgrade layer.

This research study will bring about a reduction in design and construction cost with the use of Stochastic response models in flexible pavement design. There will also be a reduction in maintenance cost, since the cost of maintaining a road pavement is usually higher than the design and construction cost. Furthermore, the advent of delamination growth prediction, it can be easy to determine the level of maintenance and when to implement maintenance measures before the pavement begins to deteriorate with glaring effects.

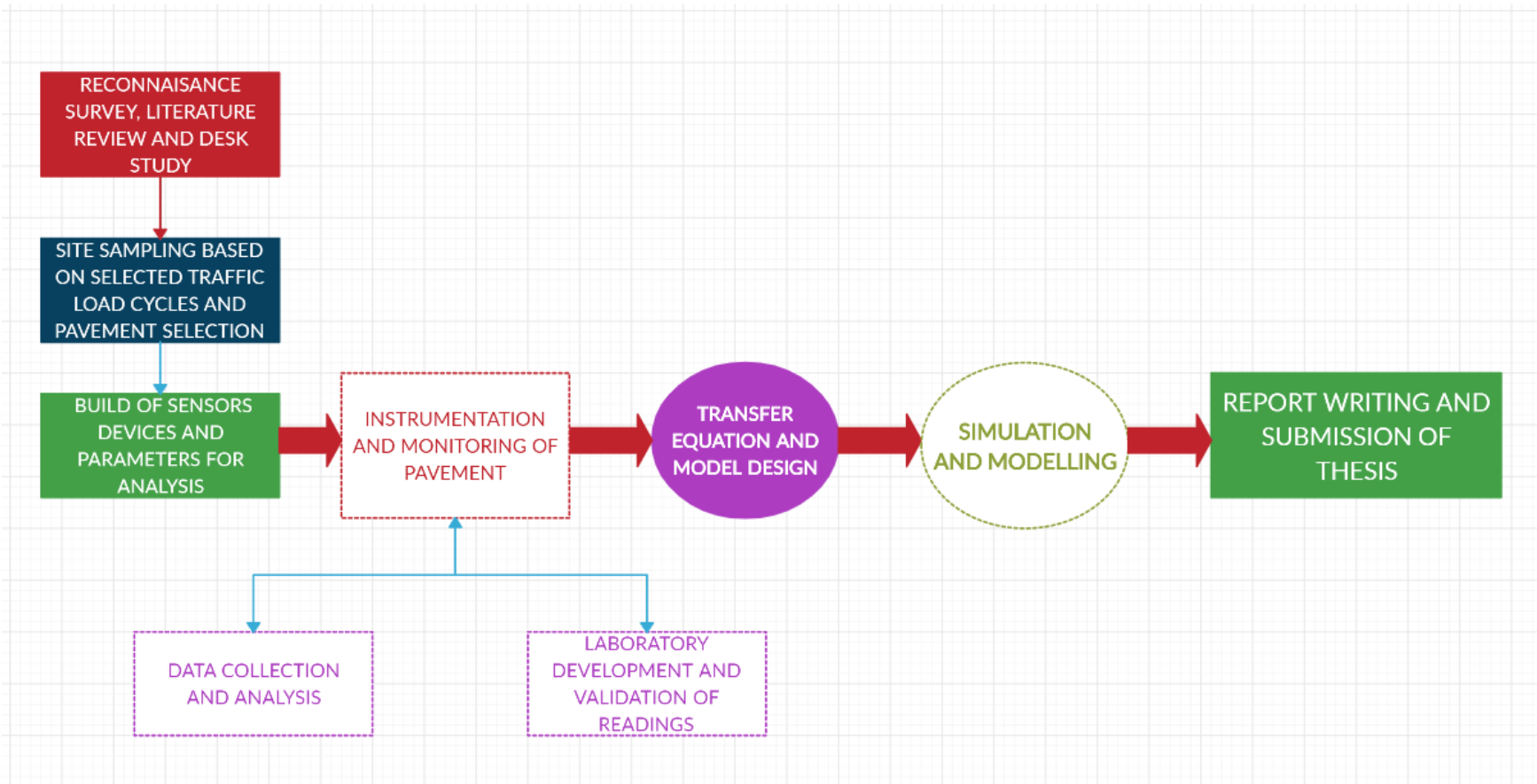


Figure 3.0: Schematic Research Design Process

3.1 Linear Elastic Fracture Mechanics

The behaviour of a pavement structure, when subjected to traffic loads, is dependent on the magnitude of the axle load and the pavement stiffness property. However, in an investigation to determine the effect of surface crack, appearance and pavement deformation; a deterring rupture and failure pattern over time due to the disturbance in the surface molecular structural arrangement of the particles is generated. Previous studies on the problem of rupture of elastic solids draw back to the initiation of “the theorem of fracture energy”. The equilibrium state of an elastic solid material is deformed by specific surface forces, as a result of minimum potential energy formation of the entire structure (Griffith, 1920). In recent times, fracture mechanics is an important tool which is used to analyse the behaviour of materials as well as to improve its mechanical property. The field of fracture mechanics, concerned with the principles of physics, stress, strain as well as the elasticity and plasticity of materials is implemented in the prediction of pavement damage. This is made visible via the formation of crack growth and crack propagation as a function of its durability and long-term performance (Irwin, 1957; Schapery, 1984).

In a pavement section, crack formation is an attribute of the pavement surface in the unstrained state. Although the spread of the crack continuity under traffic load sufficient to cause rupture will result to large change in the shape of its extremities [*longitudinal and transverse profiles*] (Fini *et al.*, 2011). If the crack exceeds a particular size such that its width is greater than the radius of molecular action at all points except very near its ends, such cracks may be inferred to be caused due to the increase of surface energy as a result of the spreading of the crack. This crack scenario will propagate with sufficient accuracy by the product of the increment of surface energy centred into the surface tension of the material caused by the bond between the pavement aggregate material, the filler /fines as well as the bituminous binder (Fini *et al.*, 2011). The concept of surface energy by Griffith (1920) is presented and the determination of a mathematical model that relates the effect of the varying temperature gradient is analysed on the pavement test section.

3.2 Strain Energy Release rate for Flexible Pavement

Griffith, (1920) introduced an expression for the artificial flaw in an experiment conducted whereby, the product of the square root of the flaw length and the stress at failure was nearly constant, and expressed by the equation:

$$\sigma_f = \sqrt{a} \approx C \quad (3.1)$$

where: a is the flaw length and σ_f is the stress at failure.

The growth of a crack, as well as its extension around its surrounding, requires an increase in the surface energy. The expression for the surface energy can be applied to pavement materials based on the discovery Griffith made for brittle materials. The procedure for the surface energy for elastic material can be found in Griffith, 1920.

Griffith further populated the failure in material will occur when the free energy attains a peak value at a critical length, beyond which the free energy decreases as the crack length increases. This can be expressed as:

$$C = \sqrt{\frac{2E\gamma}{\pi}} \quad (3.2)$$

where E is the Young's Modulus of the material and γ is the surface energy density of the material.

Irwin (1957) further made a modification to the Griffith formula considering the fact that plasticity plays a significant role in the deformation of a structure. These became a harmonisation of the total energy dissipation in a material. This expression forms the modified version of Griffiths energy criterion:

$$\sigma_f \sqrt{a} = \sqrt{\frac{E G}{\pi}} \quad (3.3)$$

Since pavement structure behaves like a brittle material considering viscoelastic fracture properties especially pavements in low-temperature regions, the surface energy expression for brittle materials such as glass $G \approx 2\gamma = 2J/m^2$ can be assumed. Jia-Der and Perng (1989), proposed evaluation of asphalt material properties using indirect tensile strength and three-point bending

test. It was also observed that temperature has an adverse effect on the young's modulus of the asphalt material as well as the reduction in the asphalt concrete fracture energy.

3.3 Climatic Effect on Highway Structures

Environmental changes as beautiful as it can be to human survival and growth has a detrimental hazardous effect on highway structures. It is, however, imperative to take note of certain prevailing environmental conditions in the design phase of highway structures, some of which are difficult to estimate. It is, however, necessary to understand these conditions, as it will aid to better achieve a sustainable structure. Climate conditions is an ever-changing environmental factor having variables which differ from region to region with fluctuating changes in precipitation and increase in the number of cloudbursts. In places with decreasing temperatures causing changes in the cryosphere, there exist a reduction of the snow cap within the northern hemisphere with a thinner ice layer in permafrost areas. This results to occurrence of global warming which has triggered uncertain sudden change which makes hydrology engineers unable to determine the soil stability and drainage coefficient (Dipanjan, 2014; Ger *et al.*, 2004).

Pavement fatigue cracking in Hot Mix Asphaltic surfaces is seen as a major structural defect resulting from excessive traffic loading. In addition, constant entrainment of rainwater through the cracks that are formed result to detrimental structural impairment of the pavement intermediate layers with major focus on the unbound granular subbase materials, subgrade and base course. In the course of this study, two primary failure model is considered (Amit, 2016); these are temperature gradient on the performance of the asphalt concrete in its service life as well as percentage moisture saturation with increasing hydraulic content.

3.4 Evaluation of Water Flow within Pavement System

There are two different types of fluid flow, saturated and unsaturated. In the saturated flow, all the material voids are filled with water, therefore the volumetric water content is equal to the material porosity. In reality, the hydraulic conductivity is not a function of the pore suction; hence hydraulic conductivity is considered as a constant value. The driving force causing saturation flow are gravitational and pressure-potential gradients (Tindall and Kunkel, 1999). The table shows the saturation coefficient for a selected soil sample modelled using the axis-symmetric method in

Abaqus FE workbench. Radial strain at the bottom of the asphalt layer and vertical strain at the top of the subgrade was used to control fatigue and rutting of the flexible HMA pavement. This was performed independently using a Multi-layered Elastic Design principle by a work bench tool (*mePADS*) where several fatigues and rutting models were developed to relate the asphalt modulus and the measured strains to the number of load repetition to pavement failure the analysis result is as shown in the Table 3.0.

Table 3.0: Structural Material Properties of Asphalt Pavement Layers

| <i>Layer</i> | <i>Material Code (Colto 2008)</i> | <i>Thickness (mm)</i> | <i>Elastic Modulus (Mpa)</i> | <i>Poisson's Ratio</i> |
|--------------------------|---------------------------------------|-----------------------|----------------------------------|------------------------|
| Asphalt | AC | 30 | 4000 | 0.40 |
| Base C4 | C2 | 200 | 2560 | 0.35 |
| Unbound Granular Base | G4 | 350 | Varied | 0.35 |
| Subgrade | G5 | 5000 | 200 | 0.35 |

(Source: Abejide and Mostafa, 2017)

The investigation was further extended to the magnitude of pavement fatigue cracking to failure as well as the magnitude of fatigue rutting to failure. A distinctive difference is as observed between the normal strain at 70 percent saturation coefficient and 20 percent coefficient; where, it is estimated that the pavement exceeded its yield point resulting in total damage.

Table 3.1: Strain and resilient modulus for different Percent Saturation Coefficient levels

| Saturation Coefficient (S %) | Elasticity Modulus (Mpa) | Horizontal | | Vertical | |
|------------------------------|--------------------------|----------------|--------|----------------|--------------------|
| | | Tensile Strain | Strain | Tensile Strain | Compressive Strain |
| | | Bottom AC | | Top Subgrade | |
| | | <i>MLED</i> | | <i>MLED</i> | |
| | | (Abaqus) | | (Abaqus) | |
| 20 | 441 | 67.8 | 253 | 93.2 | 238.8 |
| 30 | 369.9 | 72.2 | 257 | 99.2 | 244 |
| 40 | 325.5 | 75.2 | 260 | 103.5 | 246.2 |
| 50 | 281.4 | 79.3 | 261 | 108.4 | 247.9 |
| 60 | 237.4 | 83.7 | 260 | 114.2 | 248.2 |
| 70 | 187 | 89.8 | 257 | 122.3 | 245.6 |
| 80 | 130 | 99.2 | 245 | 134.6 | 235.5 |

(Source: Abejide and Mostafa, 2017)

3.5 Conventional Infiltration Mode

In view of saturated flow conditions, there are two distinctive different approaches taken into consideration for the hydraulic design of a permeable base. The first is the Steady-state flow, which assumes uniform flow conditions. However, the difficulty to estimate the proper precipitation frequency and duration makes it not convenient. The second approach is time-to drain. Time-to-drain is a parameter that allows determining the performance of a permeable base. This approach considers the amount of humidity/moisture entering the pavement until the porous base is saturated. The excess runoff resulting from precipitation will not enter the pavement section after is saturated; this flow will simply run off on the pavement surface. After the precipitation event, the base will drain water into the drainage system.

3.6 Hydraulic Conductivity Curve Models

Brutsaert, (1967); Steiakakis *et al.*, (2012), reviewed the different models adopted in the prediction of the hydraulic conductivity of unsaturated soils. In actual sense, there is a distinct discrepancy between two main groups. The first is based on a philosophized postulate by Kozeny's for saturated and unsaturated porous medium according to which the relative hydraulic conductivity K_r is a power function of the effective saturation S_e (Steiakakis *et al.*, 2012; Hubert *et al.*, 1996).

$$K_r = \frac{K}{K_{sat}} = S_e^\alpha \quad (3.4)$$

Where:

$$S_e = \frac{(\theta - \theta_r)}{\theta_{sat} - \theta_r} \quad (3.5)$$

where: S_e and K_r are the actual and the residual water content, respectively. In view of this, (Feng *et al.*, 2020; Averjanov, (1950) proposed the value $a = 3.5$, whereas, Irrnay, (1954) derived Equation 3.6 theoretically with $a = 3.0$. It seems that for a wide variety of soils, $a = 3.5$ leads to a better agreement with observations (Brooks and Corey, 1964; 1966; Mualem, 1976; Jun *et al.*, 2019)

In 1957, Gardner developed one of the first interpolation functions for the hydraulic conductivity curve, namely:

$$k(\psi) = \left(\frac{k_s}{1 + A_k \cdot \psi^\beta} \right) \quad (3.6)$$

Where:

k_s is the saturated hydraulic conductivity.

ψ is the pore suction.

A_k, β are empirical curve fitting coefficients.

Some other well-known hydraulic conductivity curve model includes the Brooks and Corey model, (1966), Green and Corey model, (1971), and the Van Genuchten model, (1980). According to a

study presented by Ariza (2002), the comparison of these four models indicates that Gardner's model is merely empirical, and it is sensitive to its coefficients. The Brooks and Corey model does not perform well at low suction values making it difficult to obtain values close to unity. This difficulty also applies to Van Genuchten's model. Green and Corey's model is the simplest to calculate with the least amount of experience.

3.7 General Design for Combating Moisture Damage

The main objective of proper pavement design is to protect the base, subbase, subgrade and the surfacing layer free from becoming saturated or to prevent the layers from exposure to constant increasing moisture levels over time. Rabab'ah (2007) gave four major approaches to be employed in combating pavement moisture-related problems. These are: prevention of moisture from entering the pavement system, the use of materials that are insensitive to the effect of moisture, incorporation of prevailing environmental design feature to minimise moisture damage complexities, efficient removal of moisture that enters the pavement system.

Rabab'ah (2007) furthermore reported that, excessive water in the pavement base, subbase and subgrade soils easily causes early distress, fault lines and leads to structural or functional failure of the pavement, unless countermeasures are put in place to avert this damage mode. In summary, water-related damage can result to failure distress patterns. These are seen as; reduction of the subgrade and base/subbase strength, differential swelling in expansive subgrade soils, stripping of the asphalt binder in flexible pavements, frost, heave and reduction of strength. This occurs during frost melt and movement of fine particles into the base or subbase course resulting in a reduction of the hydraulic conductivity (Lytton *et al.*, 1993; Khoury *et al.*, 2010; Khoury and Zamman, 2004).

3.7.1 Moisture Subsurface Drainage

In the design of pavement, the most important factor to be accounted for is minimizing pavement contact with water. Thou the presence of water in pavement structures is mainly due to infiltration. This is mainly through the pavement surfaces and shoulders, melting of the ice during freezing/thawing cycles, capillary rise and seasonal changes in the prevailing soil table water. Groundwater conditions affect the moisture content in pavement systems and are responsible for the major factor influencing increasing subgrade water content (Yoder and Witczak, 1975). Furthermore, increasing depth to Ground Water Table results to minimize the moisture content in

base and subbase layers. Although, water is usually present within the soil and granular pavement material, but free water, capillary water, bound moisture, and water vapour are the most concerns to pavement engineers (Ksaibati *et al.* (2002); Rabab'ah, 2007). A method of preventing moisture accelerated pavement damage is to use moisture insensitive or non-erodible base materials that are less susceptible to moisture detrimental effects. In addition, the materials should be checked for resistance to moisture erosion. This needs to be performed in such a way that the aggregate subbase should be recommended to prevent pumping and loss of fines from beneath the treated base in areas with adverse conditions such as hot climates, high design traffic load and areas with high amount of pumpable fines in the subgrade (Rabab'ah, 2007, MEPDG, 2004).

The subsurface drainage can also be minimised by ensuring adequate binder film thickness within the microstructure connectivity of the aggregates. Ensuring an adequate amount of crushed materials, low fines content, and low plasticity. Open-graded materials serve to provide adequate moisture drainage with reduced fines. The fines are usually ejected through the joints and cracks although this variable should be checked for long term durability due to settlement problems over time. Full-width paving by eliminating the shoulder or pedestrian lane is seen as an effective measure to minimise subsurface infiltration and provision of a granular layer between the subgrade and the base course. This is aimed at reducing erosion and to allow bottom seepage and minimize frost susceptibility that could increase pavement roughness.

3.7.2 Water flow Analysis within pavement structures

The safest and efficient way to prolong pavement life is to shield it from moisture-susceptible scenarios. This process is non-achievable as the earth cannot be hidden from precipitation. However, the efficient means is to bridge the gap between pavement performance and pavement deterioration modes by properly analysing the fluid dynamics within the pavement layers. A common means for minimising surface infiltration is to provide adequate cross-slopes and longitudinal slopes. This helps to drain water away from the pavement surface quickly and efficiently providing side drains along the pavement longitudinal profile. The reduction in the time taken for water to drain; the lower the tendency of the moisture to infiltrate through the joints, cracks and fissures during the pavement life hence increasing the durability and service life capacity of the pavement.

3.8 Finite Element Analysis of Pavement Drainage

A Finite Element Analysis subroutine program for simulating pavement drainage should be capable of handling transient, two-dimensional, saturated/unsaturated flow. The Finite Element program provides relatively sophisticated models for near-surface processes where real-time climatic data can be easily inputted into the FE program. There is a need to incorporate several different functions for describing the moisture characteristic curve (moisture content vs. suction) and unsaturated hydraulic conductivity functions (hydraulic conductivity vs. suction) is also important. In this research, the ABAQUS CAE software program (ABAQUS CAE, 6.13) was used to simulate pavement drainage. The Axis-symmetric model was used in comparison with Layered Elastic Design software (MePads). The Axis-symmetric model is a 2-D Finite Element Analysis in ABAQUS used to model moisture movement and pore-water pressure distribution within the individual pavement layer. The model presented both saturated and unsaturated flow variations within the pavement layer.

A standard sequence equation solver includes three executable programs. DEFINE; for defining the model. SOLVE; for solving the problem. CONTOUR; for presenting the results in a graphical form. The equation solver assumes that flow in unsaturated soil above the water table similarly follows Darcy's Law manner to flow in saturated soil. The flow is proportional to the hydraulic gradient and the hydraulic conductivity (Aurea *et al.*, 2006). The major difference between saturated and unsaturated flow in the equation solver is that, in a saturated soil, the hydraulic conductivity is insensitive to the pore-water pressure; whereas, in an unsaturated soil, the hydraulic conductivity varies greatly with changes in pore-water pressure. The governing equation is Richards' equation.

$$\frac{\partial}{\partial x} \left(k_x \frac{\partial H}{\partial x} \right) + \frac{\partial}{\partial y} \left(k_y \frac{\partial H}{\partial y} \right) + Q = \frac{\partial \Theta}{\partial t} \quad (3.7)$$

where: H = total head, k_x = hydraulic conductivity in the x direction, k_y = hydraulic conductivity in the y direction, Q = the applied boundary flux, Θ = volumetric water content.

This fundamental partial differential equation states that the difference between the flow entering and leaving an elemental volume at a point in time is equal to the change in volumetric water

content. As can be seen, Richards' equation can be used for saturated and unsaturated conditions. The right part of the equation would become zero in steady-state conditions. $t = \text{time}$.

3.8.1 Pavement Impulse Response

One of the most critical decision to be made in the analysis of any pavement type is the ability to identify the mode of failure and its growth progression along the line of loading. Although, several analytical methods have been identified FEA, Deterministic Methods, Monte Carlo Simulations, Genetic Algorithm amongst many others in solving pavement response categorized either as static, dynamic, linear or non-linear, deterministic and stochastic models. These response models can be analysed either individually or could be a combination of two or more models depending on the properties and condition of service (Athanasios, 2010). The response reaction of the pavement will depend on the geometry of the material and the nature of loading subjected to.

3.8.2 Static Impulse Analysis

Athanasios (2010); suggested a general equilibrium equation for static analysis expressed as:

$$\mathbf{K} * \mathbf{r} = \mathbf{R} \quad (3.8)$$

where: \mathbf{K} is the global stiffness matrix formed from the combination of the element stiffness matrices; \mathbf{r} is the vector of unknown nodal displacements and \mathbf{R} is the nodal load vector. Consequently, he further stated that the typical steps in finite element analysis should be followed.

3.8.3 Dynamic Impulse Analysis

The response of a pavement to a moving dynamic load will tend to follow a dynamic response pattern, which is usually established by a convolution integral (Duhamel's Integral) this response pattern can either follow a linear or non-linear system response. Although, pavement dynamic analysis may include the following; time dependency, damping and inertia as local and system effects, the equation below can be used to determine the resistance to dynamic movement which is a function of the global stiffness of the pavement:

$$\mathbf{M}\ddot{\mathbf{r}} + \mathbf{C}\dot{\mathbf{r}} + \mathbf{K}\mathbf{r} = \mathbf{R}(t, \dot{\mathbf{r}}, \ddot{\mathbf{r}}) \quad (3.9)$$

where: $\mathbf{R}(t, \dot{\mathbf{r}}, \ddot{\mathbf{r}})$ is the time-dependent load, $\mathbf{r}(t)$ the displacement, \mathbf{M} the global matrix, \mathbf{C} is the global damping matrix, and \mathbf{K} the global stiffness matrix. Mass and damping properties of the system can be derived as the assembly of the properties of each element. The internal reaction

forces for any element can then be computed by the use of virtual work equations. The above equation is applicable both for linear and non-linear systems.

3.8.4 Stochastic Processes

A more complex and explicit analysis of pavement response is the Stochastic response analysis. In contrast, the deterministic analysis describes the exact magnitude of the load at any given time. A deterministic analysis on a given HMA pavement involves initial determination of the statistical data for environmental loading such as temperature, moisture ingress, traffic loading etc. related to failure distress models. Considering high level response analysis; for example, a suitable event could be defined as the magnitude of force which is expected to cause the most severe response. This process requires that the structural model is exposed to a unidirectional, periodic wave. The estimated loading is calculated in the time domain at given points in time during a wave cycle. Contrary to deterministic processes, a stochastic analysis process is usually described by the use of probabilistic functions. A stochastic load or response may not be fully described by exact magnitude at a given time, but rather by the probability (statistical distribution) by which it will exceed some specified value. Significant developments have been identified in the field of system reliability assessment. HMA pavement structural system with multiple failure paths can be represented by a series of parallel subsystems, with each subsystem representing a failure mode. Starting from a single component reliability level subroutine, to the combined structural reliability of the system (Athanasios, 2010).

3.8.5 Reliability of Highway structures

In a report made by Prozzi *et al.* (2005), it was noted that the AASHTO design equation for the design of flexible pavement structures is based on the results of the AASHTO road test. The road test results were used to develop a deterioration model that provided the basis for flexible and rigid pavement design.

$$p_t = C_0 - (C_0 - C_1) \left(\frac{W_t}{\rho} \right)^\beta \quad (3.10)$$

p_t : serviceability value at time t ($C_1 \leq p_t \leq C_0$)

C_0 : initial serviceability value

C_1 : serviceability level at which a test section was considered have failed

W_t : accumulated axle load applications at the time t

β, ρ : regression parameters or functions.

Structural Serviceability in the context of a highway structure is defined as the ability of a specific section of pavement to sustain the resultant stresses (traffic load, environmental conditions, material quality, Resilient Modulus etc.) during its design life (Huang, 1993). Equation (3.10) estimates P_t in terms of Present Serviceability Index (PSI), defined as a mathematical combination of values obtained from certain distress measurements so formulated as to predict the Present Serviceability Rating (PSR) for certain pavements within prescribed limits (Huang, 1993). On the other hand, PSR is the mean of the individual ratings (by individuals of a specific panel) of the present serviceability of a specific section of roadway. The individual ratings varied between 5 (Excellent) to 0 (Very Poor). Equation (3.11) was used by AASHO to determine PSI (HRB, 1962).

$$P_t = 5.03 - 1.91 \log(1 + SV) - 0.01 \sqrt{C + P} - 1.38 RD^2 \quad (3.11)$$

SV : mean of the slope variance

C : linear cracking

P : patching area

RD : average rut depth

β and ρ are given by Equations (3.11) and (3.12).

$$\beta = 0.4 + \frac{\beta_0 + (L_1 + L_2) \beta_2}{(D + 1) \beta_1 L_2 \beta_3} \quad (3.12)$$

$$\rho = \frac{A_0 (D + 1)^{A_1} L_2^{A_3}}{(L_1 + L_2)^{A_2}} \quad (3.13)$$

$$D = a_1 D_1 + a_2 D_2 + a_3 D_3$$

D1 : surface thickness (in)

D2 : base thickness (in)

D3 : subbase thickness (in)

L1 : nominal axle load in kips

L2 : axle type (1 for single axles and 2 for tandem axles)

a_i : layer coefficients.

In a study conducted by Prozzi et al, 2005, they discovered that designs failing early had an increased rate of serviceability loss, while more adequate designs, had a decreasing loss rate. The failure parameter was equated to the number of load combination at which $P_t = 1.5$ (failure condition). The failure regression equations for and P_t were obtained using stepwise regression approach, this procedure did not account for uncertainty relating to varying environmental conditions. In addition to load combination and environmental conditions, there are serious inconsistencies in the specification of the regression equations for structural safety. These two aspects have led to the estimation of biased regression parameters. This concludes that, the models are intrinsically linear leading to unnecessary large regression errors. The estimated standard error of Equation 1 was approximately 0.707 PSI according to their study (Prozzi *et al.*, 2005).

3.9 Summary

In view of the previously discussed literature and background study, a methodology is proposed. Firstly, the literature on performance functions is presented on the asphaltic pavement. An explicit background on Finite Element Analysis is presented as well as the reliability of flexible pavement. this study further unveils the transfer function required for the conducted study. However, moisture sensitivity saturation models for flexible pavement is presented based on the fourth objective. this is followed by the development of the transfer function models which are used to introduce damage models for flexible pavement based on the data collected from the installed sensors. However, the damage models are based on the development of strain energy release rate for the method proposed Linear Elastic Fracture Mechanics (LEFM).

CHAPTER FOUR: INSTRUMENTATION AND DEVICE SETUP

4.0 Instrumentation and Analysis

The ability to monitor changes occurring or experienced within a system or systems as a result of external forces in view of this study is termed instrumentation (Researcher). Industrial process control was originally performed manually by use of senses (sight, feelings or touch) making the control totally operator dependent (Dunn, 2006). There has been a drastic change in the industrial process control which evolved from manual assumptions and estimation to the use of complex modern-day microprocessor-controlled system. This has resulted to tremendous improvements in parameters which were unable to be measured previously. Furthermore, it can be monitored with accuracy and control (Dunn, 2006). A wide range of technologies are used in instrumentation and process control depending on the context and situation where the need arises. This ranges from control of a series of events and processes in a material or within a medium; which could be sequential (one step) or continuous (multiple steps) (Battikha, 2004; Dunn, 2006).

4.1 Pavement Instrumentation Using Moisture Sensors

Pavement Instrumentation is defined as the art and science of measurement and control of process variables within a road pavement. These process variables range from deflection height difference, strain values, pressure, temperature, humidity, flow, pH, force, speed (Battikha, 2004). However, for the purpose of this study, instrumentation programs and product design adopted measured pavement's response to loading and environment. Sensors were built to provide technical data needed to validate new design standards and project applications which include accelerated test pavement facilities for highways, airports and bridges. Understanding pavement's response to strain, pavement pressure, in situ moisture and temperature is critical in the design phase.

4.1.1 Instrumentation Consideration Overview

ECHO EC-5 is an instrumentation sensor device obtained from Arduino technology. This device is used to monitor humidity or moisture saturation values within a medium. The accompanying temperature sensor is a device used to measure the temperature gradient within a medium or environment. The pavement sensors used were temperature sensors of the type (*METER GROUP ECH20 EC-5 SOIL MOISTURE SENSOR*). The EC-5 is a basic, reliable and low-cost soil moisture sensor. The EC-5 determines volumetric water content (VWC) by measuring the dielectric constant of the media using capacitance technology. Its 70 MHz frequency minimizes

salinity and textural effects, making this sensor accurate in almost any soil or soilless media. It is just 5 cm long and has a 0.3 L measurement volume.

The technical specification for volumetric water content (VWC) ranges from: 0% - 100%. The resolution is 0.001 m³/m³ VWC in mineral soils, 0.25% in growing media.

The generic calibration for the sensor has an accuracy value range: ± 0.03 m³/m³ typical in mineral soils that have solution EC <8 dS/m. Medium specific calibration: ± 0.02 m³/m³ in any porous medium ($\pm 2\%$).

The sensor temperature gradient ranges from -40 to 60⁰C with an accuracy of $\pm 10^0$ C. The voltage specification ranges from 2.5VDC at 10mA to 3.6 VDC at 10mA.

Both sensors were secured together in a steel faraday casing to prevent breakage or damage due to excessive tyre pressure from the traffic loads as the vehicles pass over the embedded sensors as shown in the Figure 4.0.



Figure 4.0: Sensor embedded into road pavement

4.1.2 Arduino Technology

The instrumentation technology adopted in determining the pavement response to increasing moisture and temperature utilises the Arduino programming language which is composed of two major parts or functions in enclosed blocks of statement. Figure 4.1 presents the Arduino Block Diagram Programming Language setup.

```
Void setup ( )  
  {  
    Statements;  
  } void loop ( )  
  {  
    statements;  
  }
```

Figure 4.1: Arduino Block Diagram Programming Language Setup

The setup () is the preparation, while the loop () is the execution. Both functions are required to run the generated program.

The developed program or script to determine the moisture and temperature coefficient for the conducted study can be seen in the Appendix I.

The developed program is composed of devices; PV panel, Solar Charge Controller, Batteries, Temperature and Moisture sensors, Arduino Micro Controller, connected together to sequentially measure and record the readings and save the data on a memory device. A block diagram of the setup is as shown in the Figure 4.2.

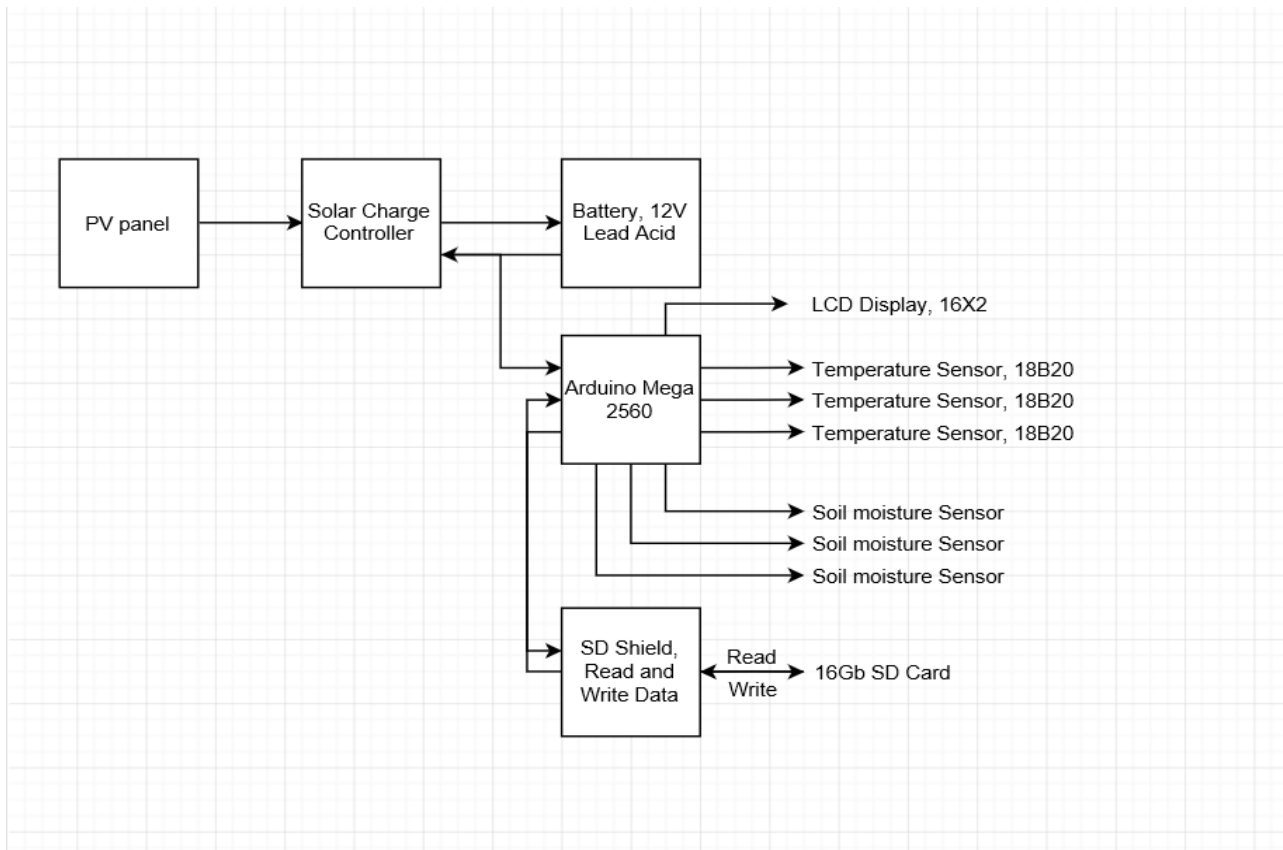


Figure 4.2: Arduino Block Diagram for determining Moisture and Temperature Values

4.2 Microcontroller configuration and build up

A microcontroller setup is a small computer chip linked with a CPU, a storage device unit (RAM, ROM), I/O peripherals, counters, etc., and all these components are assembled into one Integrated Circuit (IC). On the other hand, the microprocessor with these units are combined on board through buses. The microcontroller is interfaced easily with external peripherals having serial ports, ADC, DAC, Bluetooth, Wi-Fi, etc. The microcontroller process is fast when compared to the microprocessor interfacing as shown in Figure 4.3. Most microcontrollers use RISC Architecture. There also exist microcontrollers which use CISC architecture like 8051, Motorola, etc.

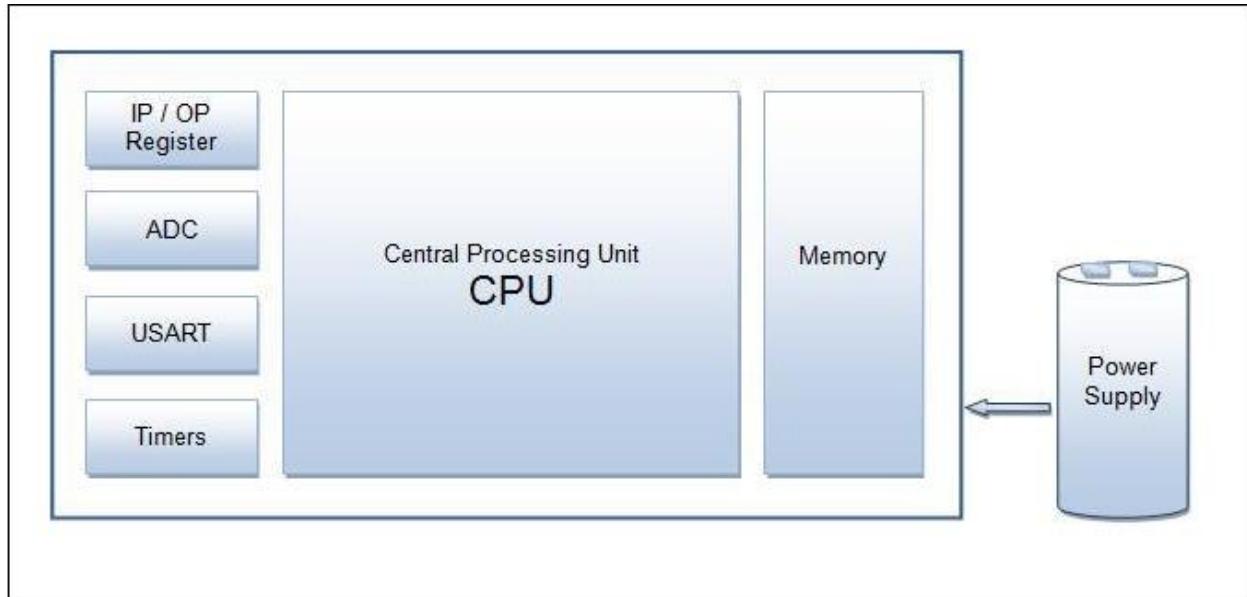


Figure 4.3: Configuration of the proposed microcontroller.

4.3 Hydraulic Water Content and Humidity Potential

In a conducted study by Ponizovsky and Salimgaryeyeva, (2001), they were able to establish the relationship between soil water potential and soil permittivity for leached Chernozem-Podzolic Gray Forest Soils, kaolin and bentonite clays, kaolin-sand and bentonite-sand mixtures. However, the water potential as determined by these researchers were observed to be closely related to the permittivity for soils of similar textures and for clays. This was inconsiderate of the essential difference in the relationship between water potential-water content and between water permittivity-water content. The analysis was performed using the Time Domain Reflector (TDR) measurements.

The amount of moisture/humidity contained in a unit mass or volume of soil and the energy state of the water in the soil serve as the basic factors affecting plant growth. This phenomenon indirectly affects the capillary movement of water to the surface within a confined section. An illustration of the confinement is as seen in a flexible pavement section layout. Although, numerous behavioural soil attributes depend strongly on water content. Some of these attributes can be in the form of mechanical properties seen as; consistency, plasticity, strength, compatibility, penetrability, permeability, stickiness and trafficability. Mostly, clayey soils and some other soil types, swelling and shrinkage are associated related problems caused by the addition and/or extraction of water change which affects the bulk density of the soil induced by the pore-size

distribution. It is necessary to note that soil water content affects the total air content of soil and is compactivity with regards to the maximum attainable density required when necessary (Ponizovsky and Salimgaryeyeva, 2001).

Furthermore, the mass of a soil per volume fraction of moisture present in the soil is expressed in terms of soil wetness or saturation. This physiochemical attribute or state of saturation is categorized in terms of its free energy per unit mass, called the potential (alluding to the variable “potential energy” of water in the soil). This is a function defined by the tendency of soil to retain water within the soil matrix. Saturation and saturation potential are functionally related to each other, and the graphical representation of this relationship is termed the soil-moisture characteristic curve. The graphical interpretation of this scenario is affected by the direction and rate of change of soil moisture and is sensitive to changes in soil volume and structure. Thus, both saturation and matric potential vary widely in space and time as the soil can be saturated by air/precipitation, drained by gravity/leaching and dried by evaporation due to increasing temperatures (Ahuja and Shwartzendruber, 1973).

The lowest saturation point likely to be encountered is a variable state referred to in the laboratory as an arbitrary state (oven-dry condition). Furthermore, the highest humidity/moisture condition of a soil is that of full saturation, defined as a condition in which all soil pores are filled with water. Saturation is relatively easy to define in the case of non-swelling (for example, sandy) soils (Sharma and Sharma, 2017). In most cases it is difficult or near impossible to classify swelling soils. This is mainly due to the fact that soils may continue to absorb moisture and swell even after all pores have been filled. In the field, the soil usually attains complete saturation, as bubbles of air may form and remain occluded or encapsulated within the matrix even when the soil is flooded with excess water. Furthermore, air bubbles may effervesce within the soil whenever the temperature gradient increases, and the solubility of gases is exceeded. For this reason, some investigators (Black, T. N, Gardner, W. R and Thurtell, G. W, 1969; Ahuja and Shwartzendruber, (1973) prefer the term “satiation” to describe the condition of soils in the field in which the soil sample, though not completely saturated, is as wet as it ever gets to be. The study of the soil characteristics for the samples taken for experimentation was obtained from the Eastern Cape site. The results clearly indicate water potential and the water retention properties (Sung-Hee Kim, 2017; Sharma and Sharma 2017).

4.4 Measurement of Volumetric Moisture Content

Soil water availability is a function of the particle size of the soil sample as well as the gravel content. Paruelo *et al.*, (1999) and Sing and Franzini (2012) presented a model for estimating the volumetric water content as a function of soil water potential and gravel content. They concluded that gravel soil can withhold up to 67% soil moisture of the amount held by fine material; thus, water content at field capacity decreases up to 50% when gravel content gradation is less than 11mm.

However, since permeability is a characteristic physical property of a porous medium, one might assume its relationship with pore geometry, which is a measurable soil property. In Gang, (2003), Wang *et al.* (1964), and Scazziga *et al.*, (1987), after numerous attempts to discover a functional relationship between permeability and pore pressure; it was concluded in their work that, the simplest approach is to seek a correlation between permeability and total porosity. Scazziga *et al.* (1987) and Wang *et al.* (1964) provided a method for also eliminating the amount of soil moisture that could be held within the soil particle pore spaces through an improvised porous pavement surface layer which has the capability of draining soil moisture that could be held up via seepage through an Ultra-Thin Film medium grade Asphalt Concrete layer.

4.5 Pavement Temperature Gradient

Asphalt concrete is composed of a viscous mix (binder) and brittle inclusions (aggregates and filler) which makes it behave like a viscoelastic material. The response due to deformation on loading rate and prevailing environmental condition needs to be understood extensively. For the purpose of this study a fracture criterion is proposed which is used to estimate the fracture strength of the HMA pavement. The existence of joint and cracks causes stress concentrations as well as redistribution of stress. Although the prediction of a material to fail should the tensile strength be exceeded is sometimes not reliable; hence a precise estimation of the fracture resistance of the asphalt concrete to failure needs to be generated. Jia-Der and Perng (1989) provided an equation for estimating the distribution of stress in front of a crack tip (Mode I) failure. A proper prediction for determining the fracture resistance of the asphalt material using the Griffith energy criterion is provided and used to analyse the condition of the pavement. Whereby it is assumed that fracture instability of the HMA is reached when the increase in surface energy which is generated by

extension of the crack is balanced by the release of elastic strain energy in the volume surrounding the crack.

The expression for the critical stress (σ_c) at which a crack will propagate based on the Griffith energy criterion as proposed by Griffith in 1920 is given as:

$$\sigma_c = \left(\frac{2\tau E}{\pi a} \right)^{\frac{1}{2}} \quad (4.1)$$

where: τ is the surface energy per unit area and E is the Young's Modulus of the material. This equation led to the development of the cohesive crack model for the asphalt concrete using the Dugdale and Barenblatt cohesive crack model. The following assumptions are made: the process zone starts to develop at one point when the first principal stress reaches the tensile strength f_t , the process zone develops perpendicular to the direction of first principal stress; the properties of the materials outside the process zone are governed by stress-strain relation; the material in the process zone is able to transfer stress and stress-transferring capability depends on its opening according to the stress-separation curve shown in Figure 4.4; in addition, the stress-separation relationship depends on the loading rate and the service temperature.

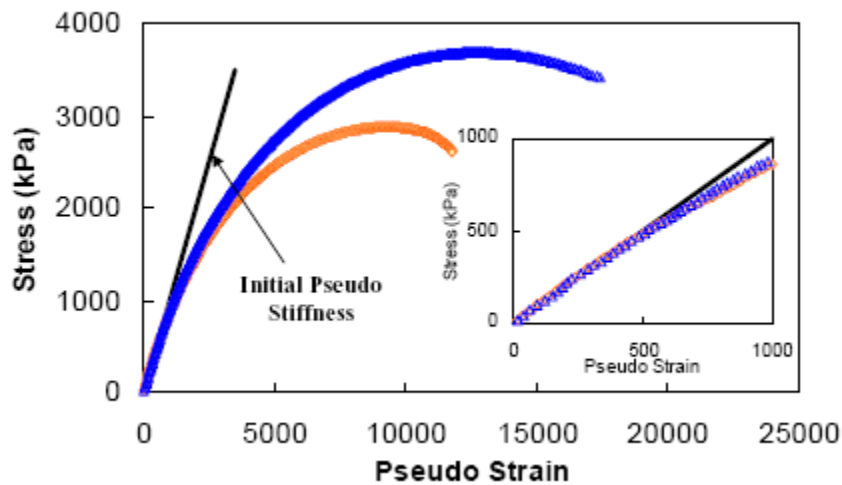


Figure 4.4: Straight line approximation of the stress-strain curve for AC. Source: (FHWA, 2009)

Based on these assumptions, the specific Asphalt Concrete Energy can be shown to be maximum when the material matrix is bonded together. The specific dissipation energy begins to reduce with

an increasing temperature gradient, thus resulting in the disintegration of the material matrix. The HMA mix three-point bend test fracture energy under varying temperature gradient is given by:

$$G_f = 0.355x10^{(1.3226+0.0018T-0.000118T^2)} \quad \text{lb/in} \quad (4.2)$$

$$E_{(T)} = 10^{(5.93906-0.0142T)} \quad \text{psi} \quad (4.3)$$

where: G_f = Asphalt concrete fracture energy, T = asphalt concrete temperature gradient,

E = modulus of Asphalt concrete.

4.6 Components of Pavement Instrumentation

The most critical phase of this study is the pavement instrumentation and the development of scientific computation for the calibration of the sensors. In an attempt to outline the components of the instrumentation system, it is imperative to identify the functionality of each component as identified previously.

Recently, advancement in Micro-Electromechanical Sensors and Systems (MEMS) technology and wireless sensor networks have gained wide application in Structural Health Monitoring (*SHM: a systematic approach that is employed to monitor and prevent rapid deterioration of infrastructure assets for dams, bridges and buildings*), not much application is seen with real-time data generation on road pavement. The objective of a smart component is to generate response models, which can be further analysed either individually or as a combination of all response models, obtained. The response reaction of each failure model will depend on the geometry of the material and the nature of loading it is exposed to. One of the most critical decisions to be made in the analysis of any pavement type is the ability to identify the mode of failure and its growth progression along the line of loading; which entails, instrumentation of the road pavement with tracking and monitoring devices to remotely read and analyse pavement response with changing environmental and loading conditions. The components of the Smart Road Infrastructure sensor device built for this study requires some form of GPRS and a web-based application system to be active. The web application is designed to read, compute and analyse variables associated with environmental conditions, loading cycles as well as material requirements. Thou, such activity is

dependent on the information to be obtained; usually, a sensor is incorporated into the system built with a microprocessor to read, compute and analyse pavement response in a physical scene under specified conditions. The process is such that; the detectable characteristic behaviour is converted into an output signal via a firmware development/gateway. The signal is passed to other parts of the system, which display or record the measurement and or use it for control purpose. Like any other manmade structural system, failure can occur in diverse modes depending on the service condition it is subjected to. Pavement instrumentation will require that, wired sensors are currently in use to track pavement response under environmental and traffic condition, to generate readings for traffic load failure, temperature and moisture stress and strain failure, as well as deflection failure. The use of IoT in pavement response and modelling was used to assist with generating a web-based application data to provide maintenance solution for pavement performance and maintenance.

4.7 Pavement material geometry configuration

Linear material elastic strain response increases with increasing stress value. In its simplest form, the modulus of elasticity of a material is dependent on its stress to strain ratio. In general, the stiffness of a material is a function of its resilient modulus. Since each layer comprises different material geometry, the stiffness varies from top to bottom. The topmost layer having the highest stiffness value and the preceding interlayers with decreasing stiffness. Since most paving materials are not elastic as the materials experience some permanent deformation after each load repetition. If the load is small compared to the strength of the material and repeated often, the deformation under each individual load repetition is almost recoverable and is therefore considered as elastic (Rahman, 2011; Rahman and Erlingsson, 2012; 2014). Figure 4.5 shows the strains under cyclic loading.

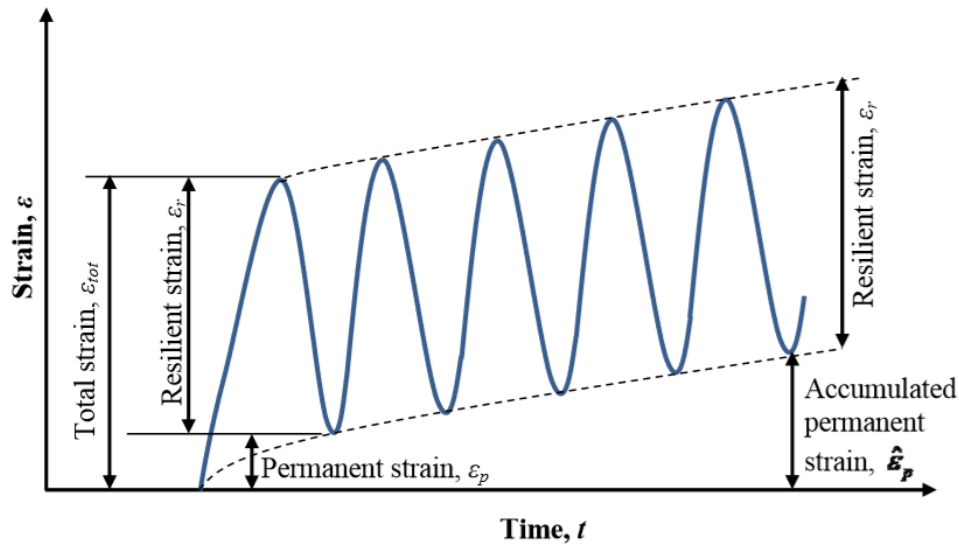


Figure 4.5: Pavement strains under cyclic loading (Rahman and Erlingsson, 2012; 2014)

The resilient modulus is the general categorisation for stiffness based on the recoverable strains encountered under repeated loading. Usually, the resilient modulus for each intermediate layer is defined as

$$\sigma_{ij} = D_{ijkl} \epsilon_{kl} \quad (4.4)$$

where σ_{ij} is the stress tensor, D_{ijkl} are the elastic constants and ϵ_{kl} is the elastic stress tensor.

Although, it is needful to point out that, there are certain factors that affect the resilient response of the pavement granular layers. Lekarp *et al.* (2000a) noted moisture, stress level, density, grading and maximum grain size of the material with regards to the aggregate type, shape and angularity. Since these parameters are dynamic in nature having a non-linear response, a strategic response must be generated to counter the effect on the stress response model. This can be achieved by improving the stiffness index of each independent layer under service loads. The maximum grain size distribution of the aggregate used as well as the percentage of binder content greatly influences the stiffness index. The standards for the bituminous mix as specified by the South African Pavement Design guide should be adhered to as well as the standards as provided by the COLTO manual.

The value of the corresponding fracture energy based on varying temperature gradient from the sensor probe is generated and the effect of the reduction in critical stress due to the result of the

effect of temperature gradient on the effective modulus/stiffness of the asphalt is presented in Chapter Five.

4.8 Summary

This chapter focuses on the instrumentation technique needed for the study and the procedure for the instrumentation taken. The first objective which is to collect data on a test section (Pavement Cores) is analysed and studied to determine the inherent pavement properties. the resulting core is filled with a pavement mix to seal the core. However, the sensors are installed near the cores to be able to study the changes and compare with the data obtained from the drilled core samples. The result obtained from the sensor is simulated and modelled. these models are inserted into the transfer functions developed in Chapter Three for analysis and results are recorded.

CHAPTER FIVE: DATA EXPERIMENTATION AND DATA ANALYSIS

5.0 Introduction

This chapter presents the results obtained from the analysis of the data collected from the instrumentation section of the pavement. The data collected was stored in to a memory repository domain. Furthermore, the data was then transferred to the web domain where stochastic response analysis was performed. The results obtained are provided in the course of the chapter. The algorithm used for the analysis is as shown in the pavement sensor infographics in Figure 5.16.

5.1 Data Experimentation and Data Analysis

The sensor was designed, fabricated, calibrated and validation was performed to determine the efficiency of results, state of validity and checked for any errors before embedding into the pavement subgrade layer. The sensor probes were calibrated using the soil present on the instrumentation site and the value for the moisture change was validated using a full state saturation model (Alexander *et al.*, 2001). In this model, a standard mass of soil was sampled and an amount of water that will indicate full saturation was determined. The amount of water was divided into 10 portions in order to attain a gradient change from 10% saturation up to 100% saturation. This process was carried out to validate the saturation level of the pavement underlying base layer material grade specification (from dry to moist, and finally full saturation). Since soil properties vary from point to point along the longitudinal road profile, it is not realistic to perform *soil-water saturation test* on all instrumented pavement section. Consequently, intermediate saturation was determined by interpolating between two forward and backward saturation points. The results for the moisture and temperature development of the sensors are as indicated in Figure 5.0 and Figure 5.1.

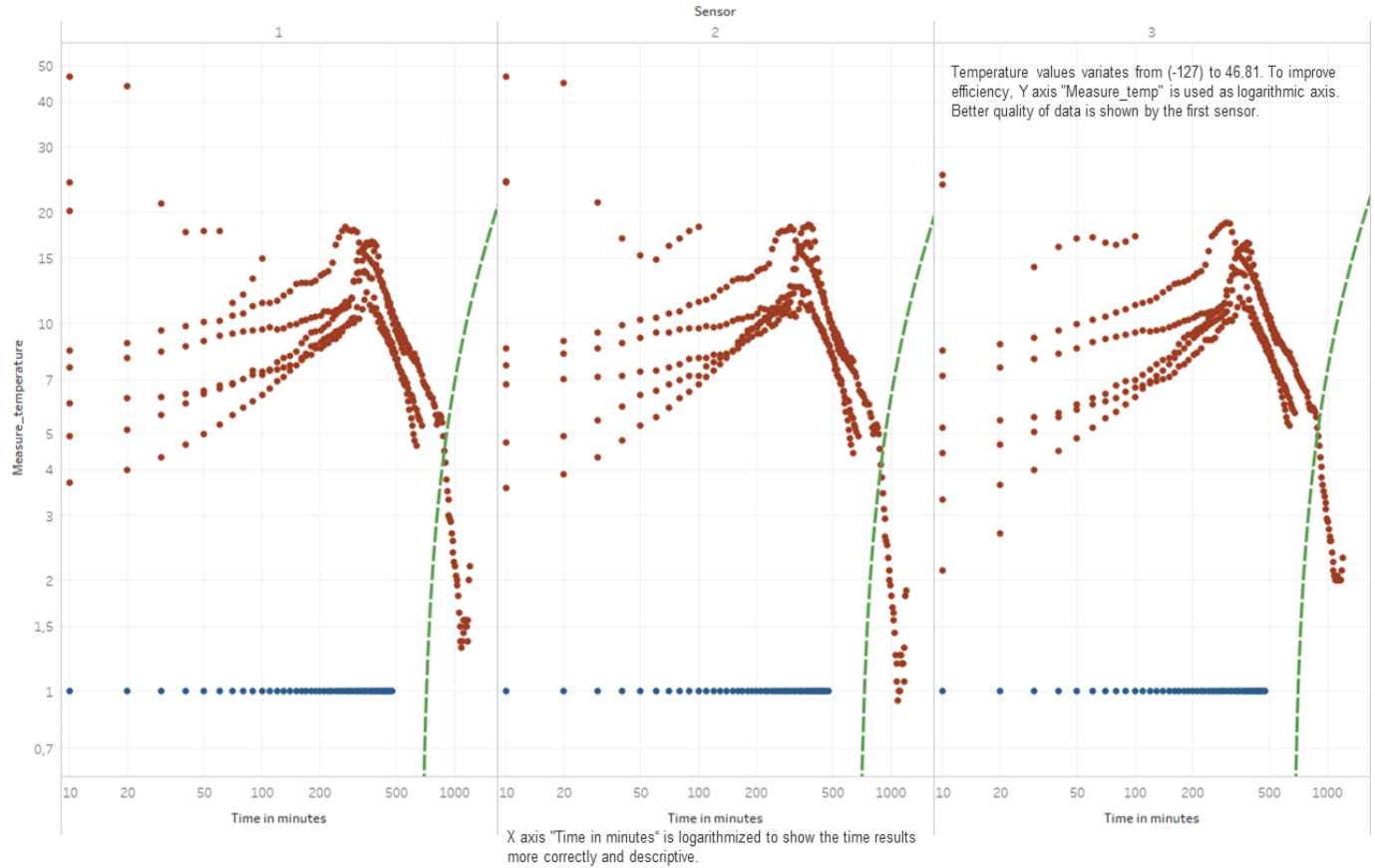


Figure 5.0: Cumulative Laboratory Temperature gradient analysis of pavement sensor

Figure 5.0 presents the temperature gradient data collected from three sensor devices over a period of time. Each column of readings represents the different sensors that were placed into the pavement section. The time interval for collecting temperature readings using modern instrumentation technology was 10 minutes. This implies that at every 10 minutes, the sensor will collect temperature gradient change and send it to the web domain for analysis.

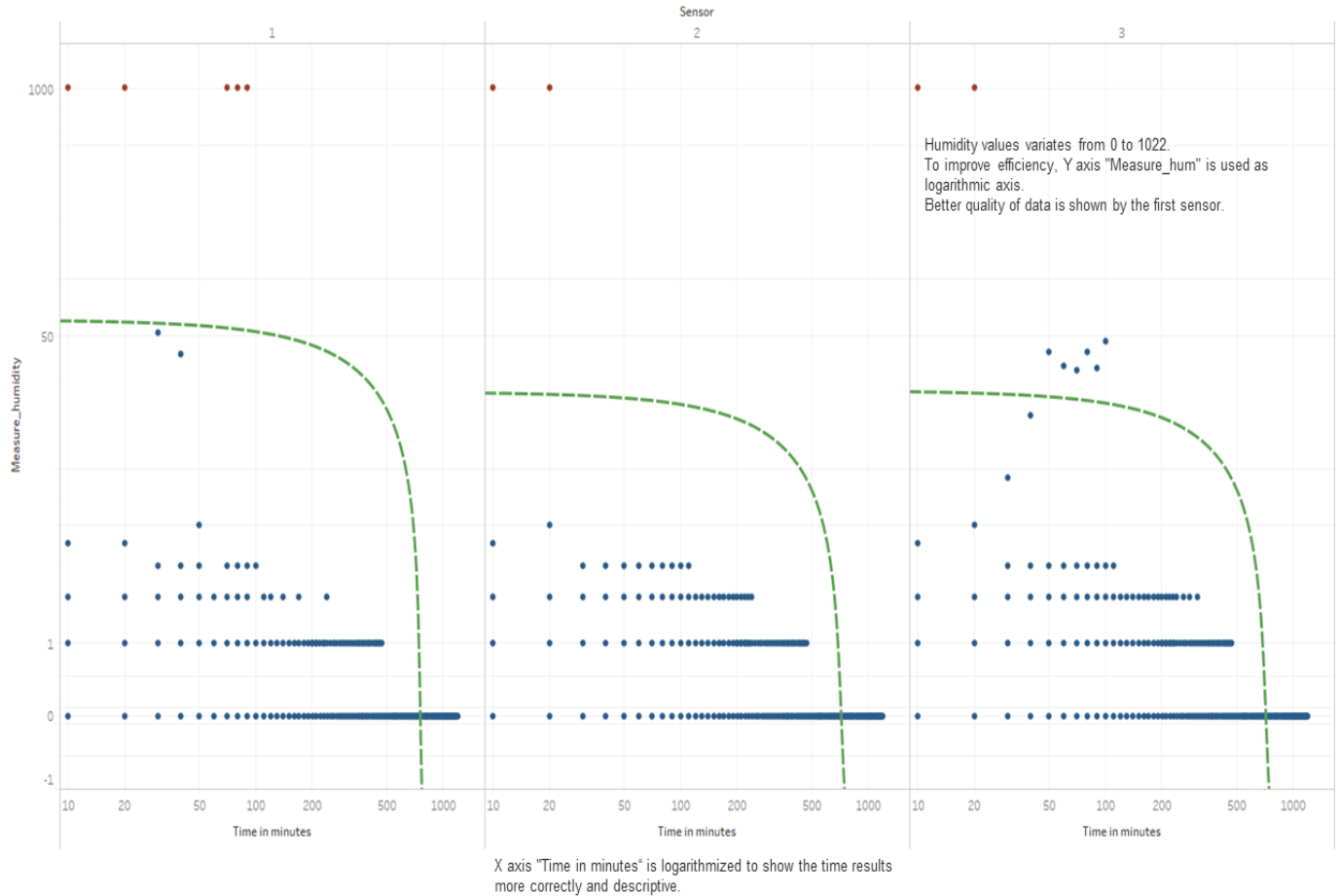


Figure 5.1: Cumulative Laboratory Humidity gradient of moisture sensors

Figure 5.1 represents the pavement humidity data collected from three sensor device over a period of time. Each column of readings represents the different sensors that were placed into the pavement section. The time interval for collecting humidity content using modern instrumentation technology was 10 minutes. This implies that at every 10 minutes, the sensor will collect humidity content of the pavement and send it to the web domain for analysis.

The relationship between the pavement temperature gradient and Pavement Humidity as variable data collected from the sensors is presented in Figure 5.2. The data collected over time indicates that increasing temperature results in reduced pavement humidity Figure 5.3. On the other hand, decrease in temperature gradient results in increase humidity. And the peak period for increasing humidity is during the rainy season and winter because of precipitation or fog and mist during a reduced temperature gradient. The sensors were well calibrated in order to collect exact

atmospheric or environmental data (temperature and moisture/humidity) as it affects the road pavement directly.

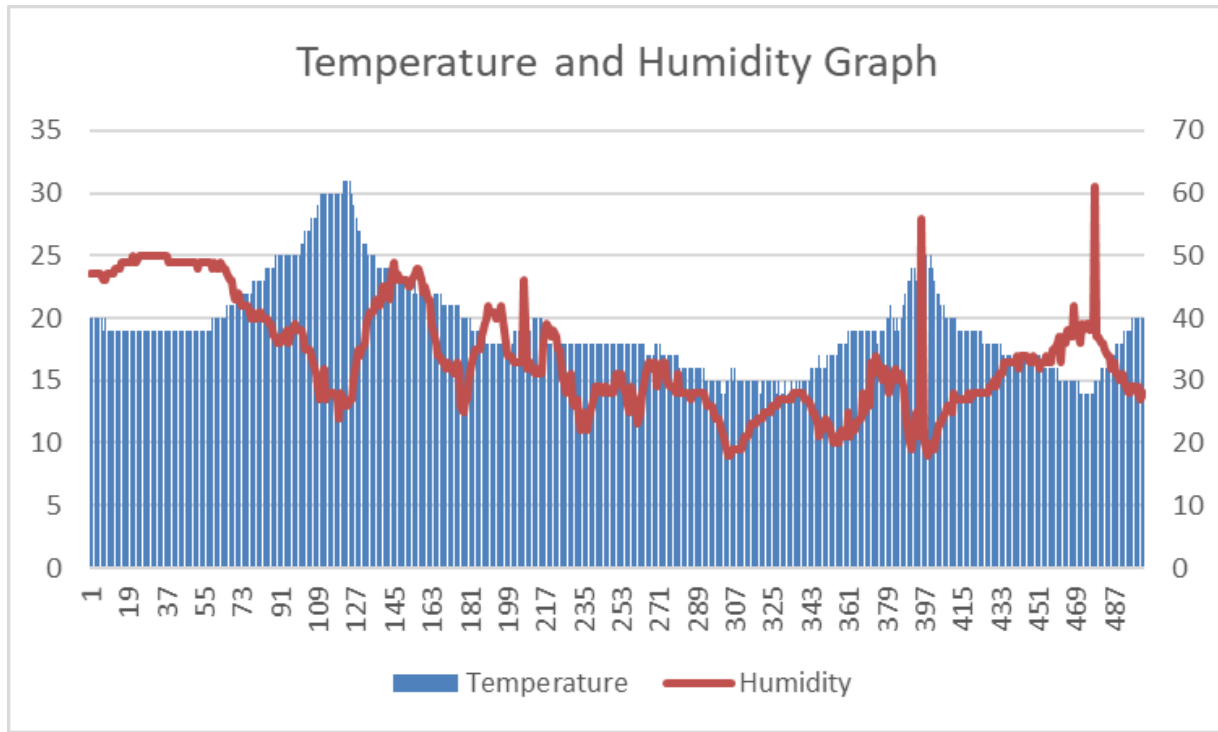


Figure 5.2: Relationship between Pavement Temperature and Humidity

The field temperature and humidity data obtained from the sensors is analysed with reference to the selected traffic route MN508 as provided by the District Road Engineer, Eastern Cape Province, South Africa. Figure 5.3 and Figure 5.4 show the relationship between the horizontal tensile strain and the vertical compressive strain with respect to modelled varying moisture content using Finite Element Analysis. In the Figure 5.4, increasing moisture content results to increase Horizontal Tensile strain at the bottom of the asphalt which results to reduced pavement stiffness. Figure 5.5 indicates that as moisture content increases, there is some form of compaction at first within the subgrade layer under moving traffic resulting to a high compressive strength value at the top of the subgrade. As moisture content increases, compressive strength value increases then reaches maximum at 40% then begins to drop drastically under traffic load due to disintegration of the material particles of the subgrade and the Asphalt Concrete surface layer. This procedure is

further analysed using First Principles Equation as presented by the South Carolina Department of Transportation and the NCHRP Design Guide.

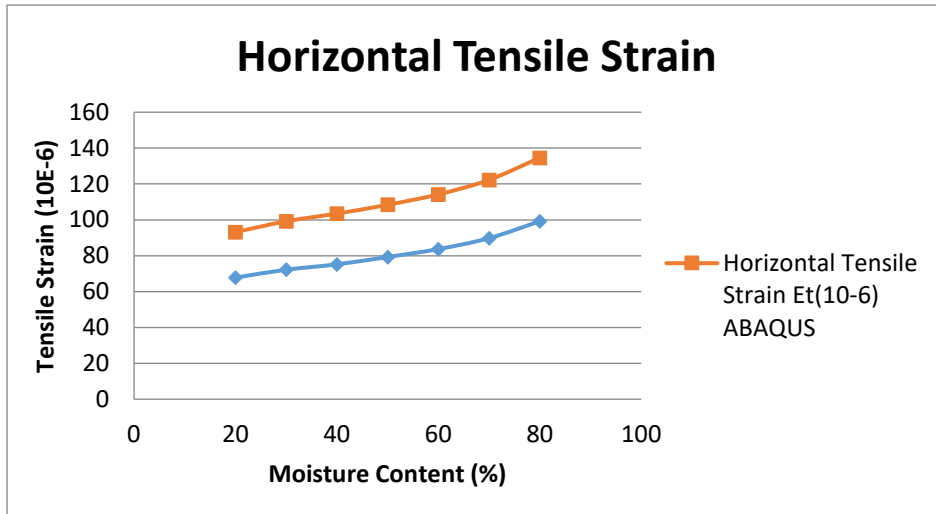


Figure 5.3: Horizontal tensile Strain at bottom of Asphalt of subgrade. (Source: Abejide and Mostafa, 2017)

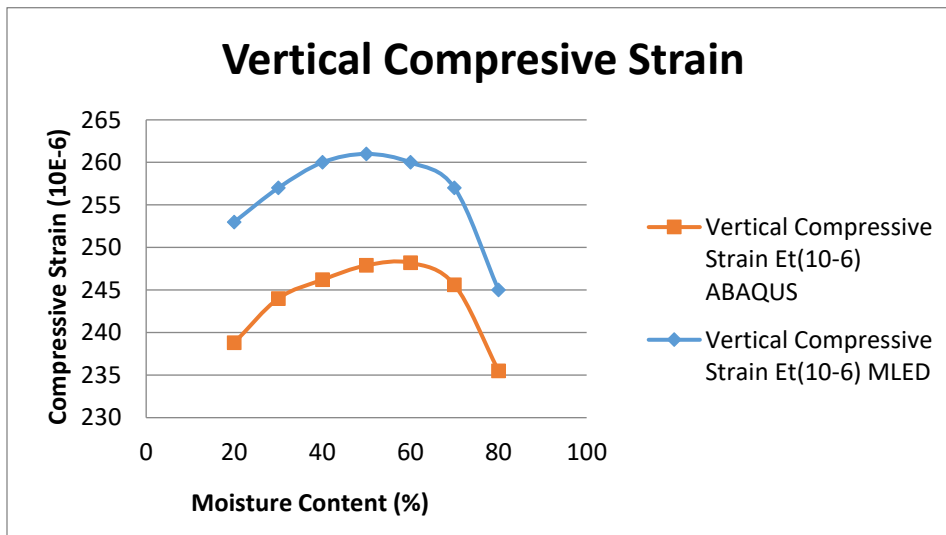


Figure 5.4: Vertical Compressive Strain at Top of Subgrade. (Source: Abejide and Mostafa, 2017)

5.2 Damage Model for Simulation of flexible pavement

In order to determine the damage model for a Hot Mix asphaltic pavement, certain parameters are considered (traffic load cycle, material geometry, design life, and exposure conditions). Damage models vary from failure modes (Model I, Model II and Model III) that would arise during the pavement service life as earlier discussed. However, a very important need should be taken to point out that the tire design configuration plays an important role in the damage criteria of pavement failure patterns based on the tyre width, the number of the axle as well as the axle configuration distribution. The pavement analysis considering (Fracture Energy) is presented using the in-situ pavement response to moisture and varied temperature gradient to model the failure pattern. The vertical compressive strain at the top of the subgrade as well as the horizontal tensile strain at the bottom of the Hot Mix Asphalt is presented using a 3-D Finite Element model and compared with a Two-dimensional/Axis-symmetric model. The procedure and the subroutine model for determining the Griffith fracture energy for the pavement using equation 4.2 and 4.3. the results are presented in Figure 5.5 – Figure 5.7.

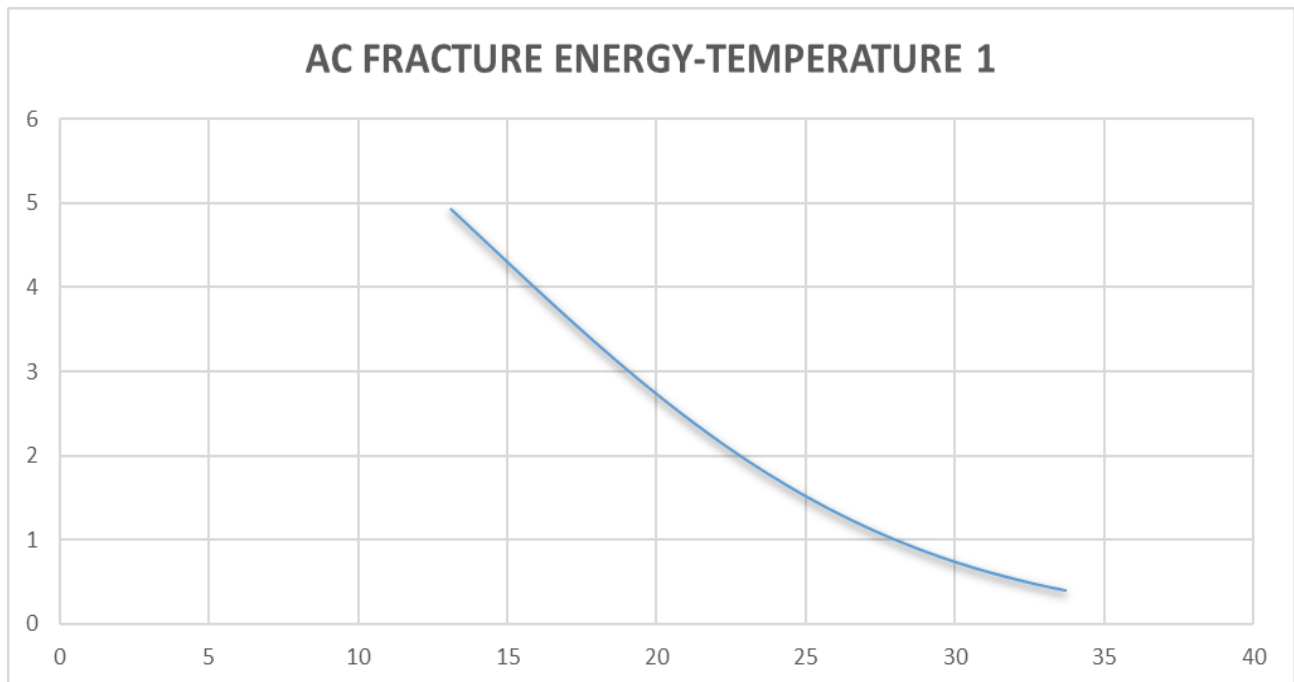


Figure 5.5: Asphalt Concrete Temperature Gradient Sensor I and Fracture Energy

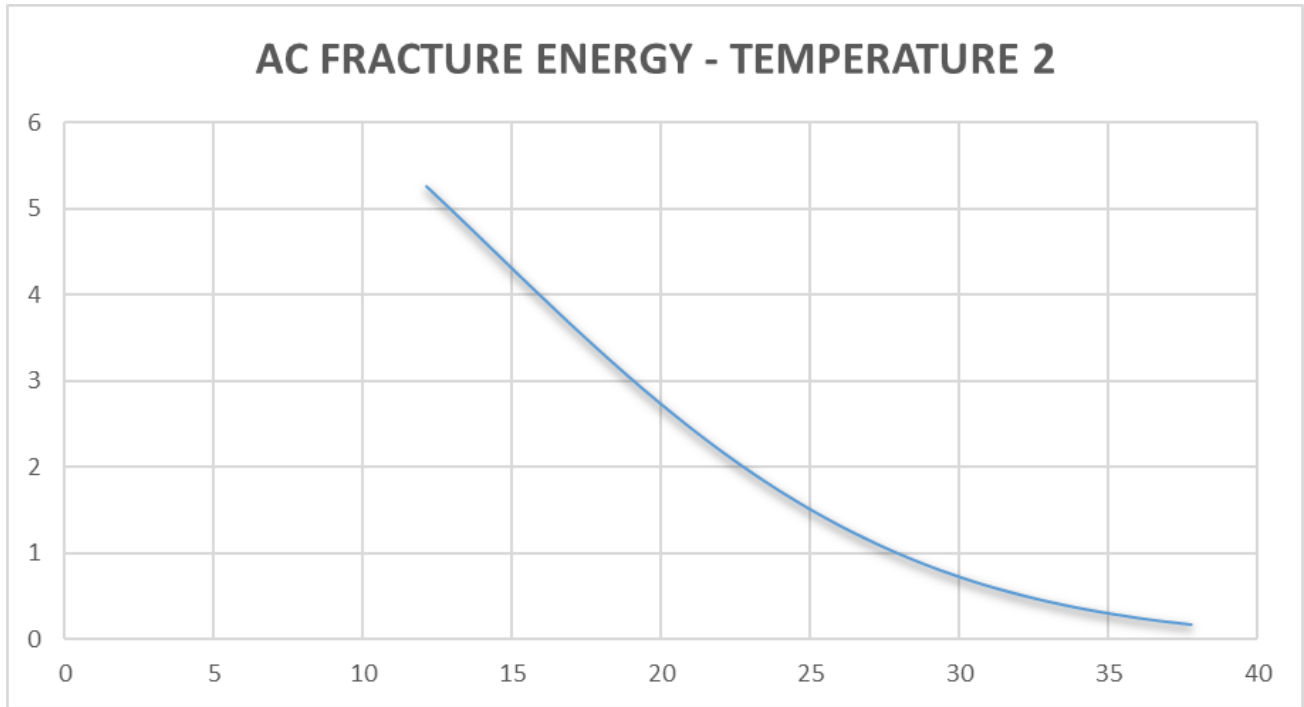


Figure 5.6: Asphalt Concrete Temperature Gradient Sensor II and Fracture Energy

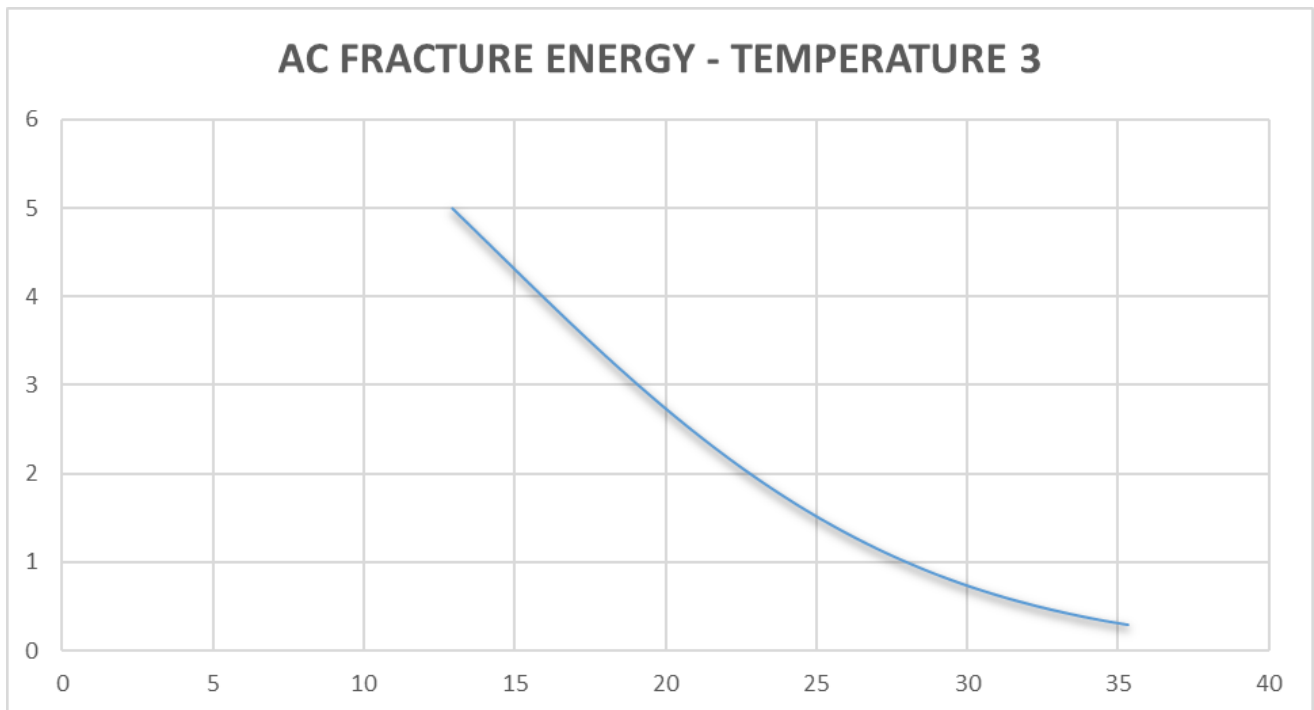


Figure 5.7: Asphalt Concrete Temperature Gradient Sensor III and Fracture Energy

From the data collected over the instrumentation period on the road pavement while in service; it is observed that the temperature gradient has an effect in the resulting modulus of the asphalt concrete. This further explains that; increasing temperature gradient results to decrease in the Asphalt Modulus as well as resulting effective stiffness of the Asphalt Concrete Pavement. Moreover, a reduction in the Asphalt Concrete Temperature results in Increasing Asphalt Concrete Modulus. This scenario is confined to the regional location where the sensors were installed. The results indicate a high correlation between the Asphalt Concrete Temperature and Modulus of Asphalt Concrete is presented in Figure 5.8 – 5.10. the full numerical details is as provided in *Appendix I*.

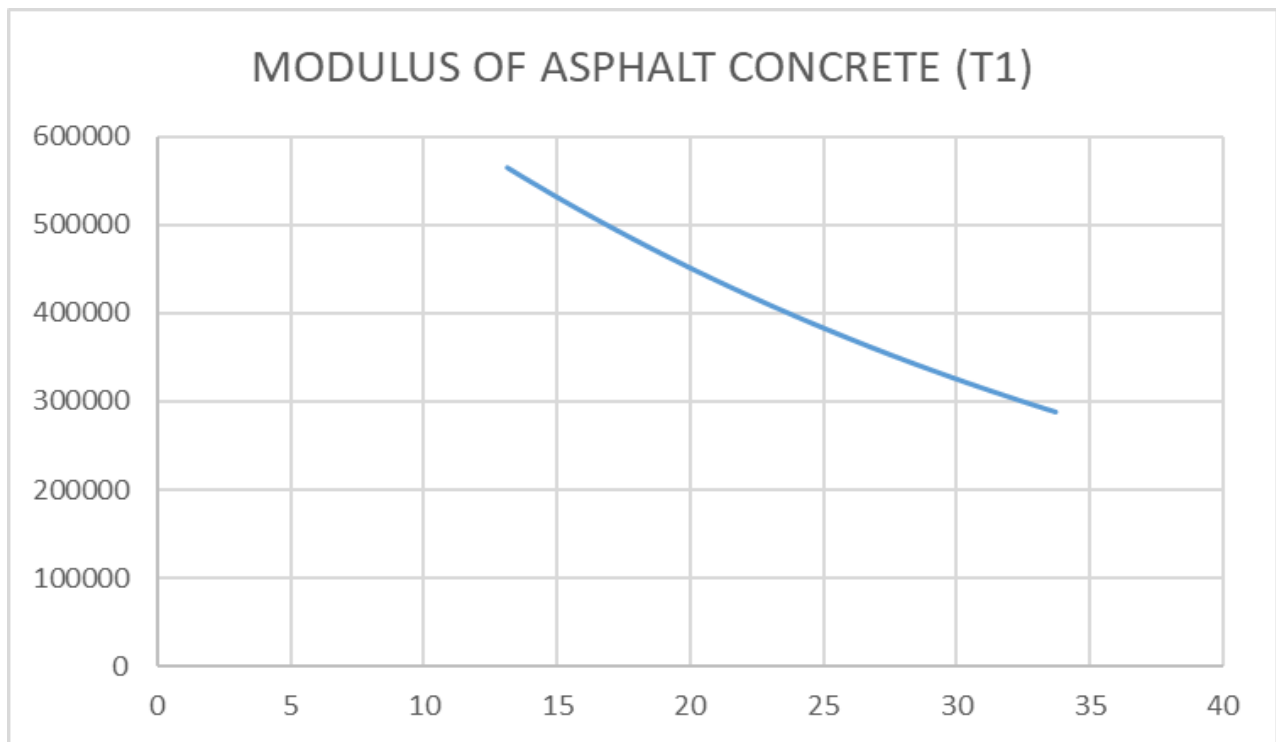


Figure 5.8: AC Temperature Gradient Sensor I and Resilient Modulus

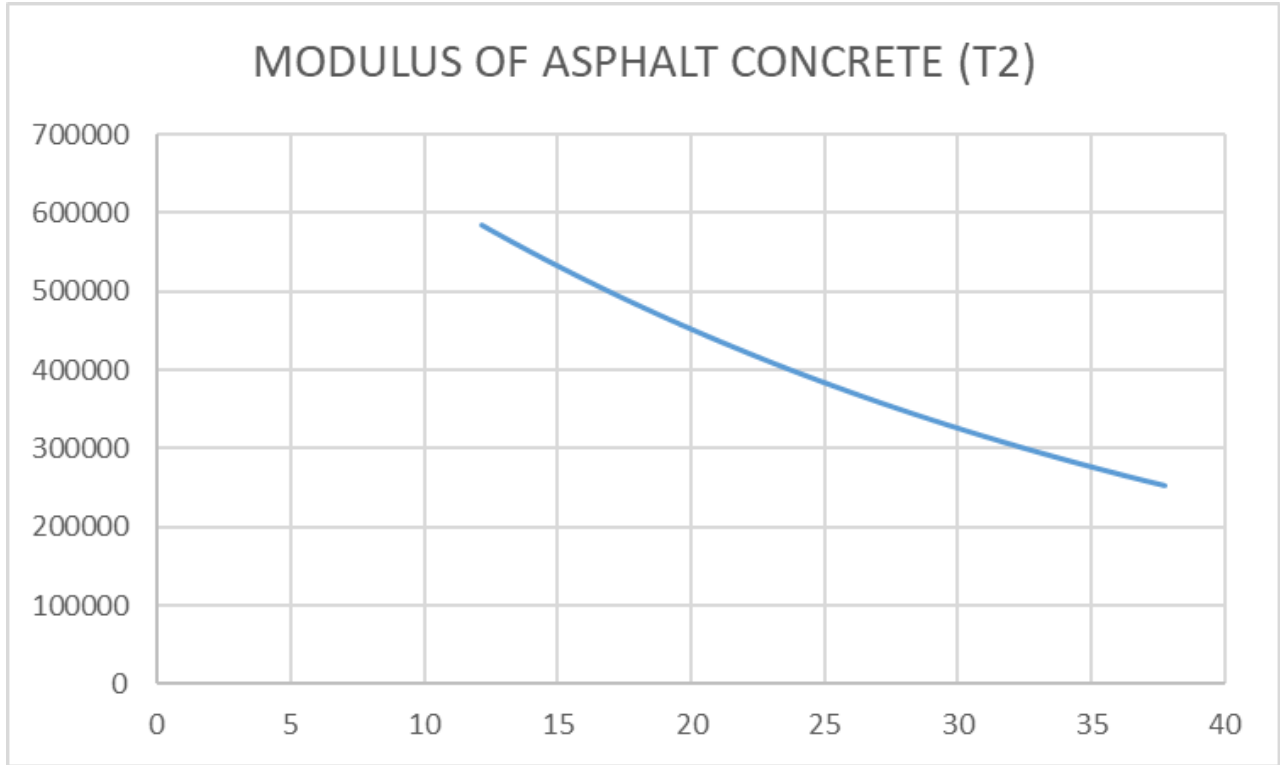


Figure 5.9: AC Temperature Gradient Sensor II and Resilient Modulus

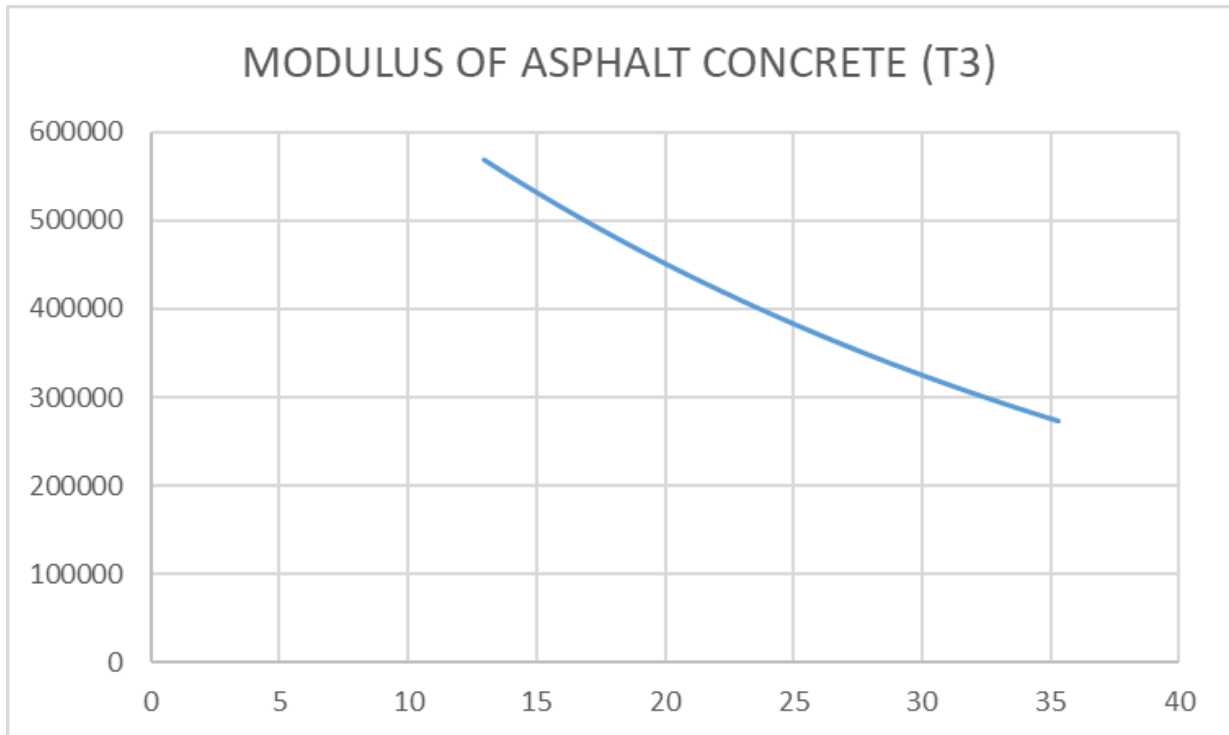


Figure 5.10: AC Temperature Gradient Sensor III and Resilient Modulus

However, a relationship also exists between Asphalt Concrete Fracture Energy as well as the Resilient Modulus of the Asphalt Concrete. The results as shown in Figures 5.11 – 5.13 indicates that a linear relationship exists between Asphalt Concrete Fracture Energy as well as Modulus of Asphalt Concrete. Details on the analysis is presented in Appendix I. The higher the Fracture Energy, the Higher the Resilient Modulus. At a temperature of $23.87^{\circ}C$ the Griffith fracture energy is $1.751691J$ with a resulting Elastic Modulus of AC as (3985738.2 ksi) while at a temperature of $26.25^{\circ}C$, the Griffith Fracture Energy is $1.203068J$ with a resulting modulus of (360173.7ksi) This implies that at lower temperatures, the pavement will perform much better and its material bonding matrix is stable when the Fracture energy is high with a high Resilient Modulus while this scenario is vice versa with increasing temperature gradient. This gives a full indication of the stiffness of the Asphalt Concrete Mix while in service. In addition, this will further result in a stable roadway over the design life. It is thus recommended to monitor the pavement temperature closely so be able to withstand the varying temperature and humidity changes.

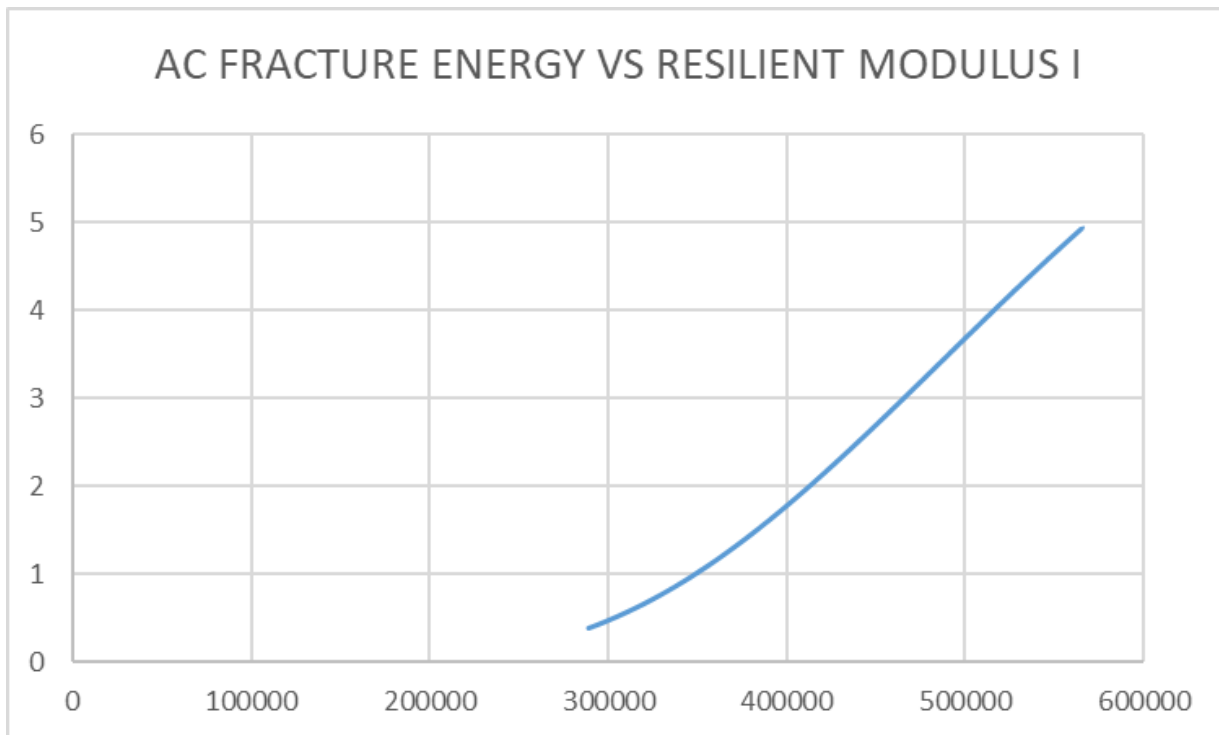


Figure 5.11: AC Fracture Energy and Resilient Modulus I

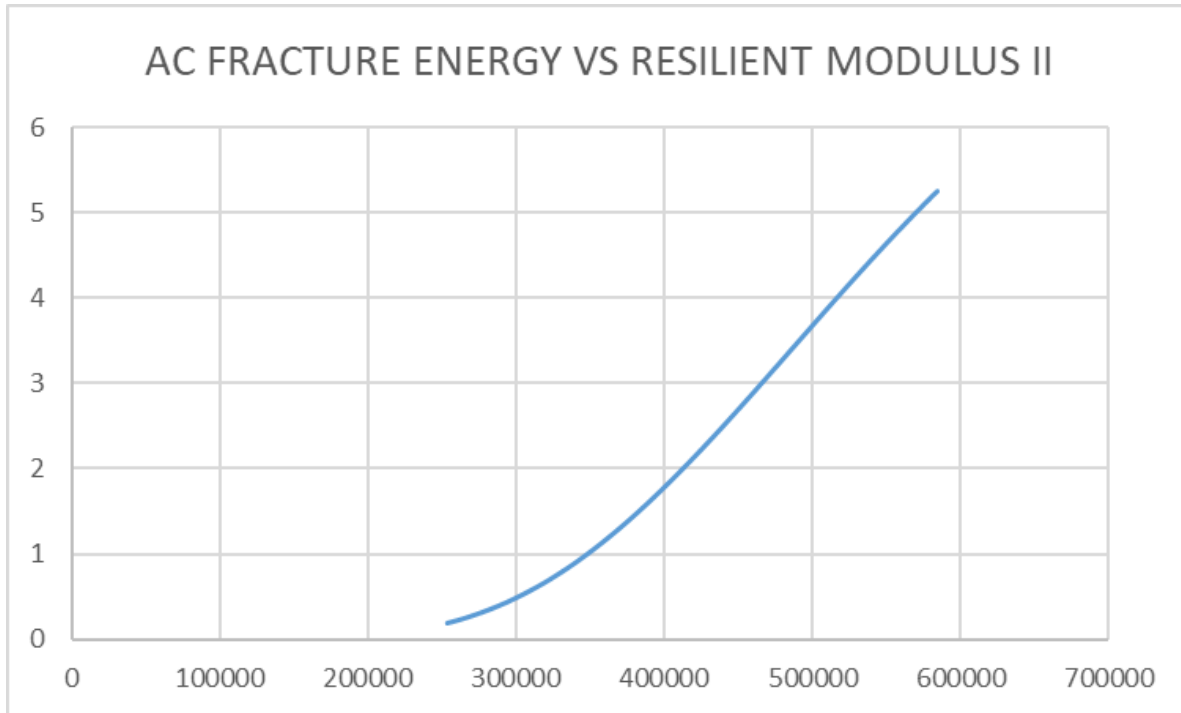


Figure 5.12: AC Fracture Energy and Resilient Modulus II

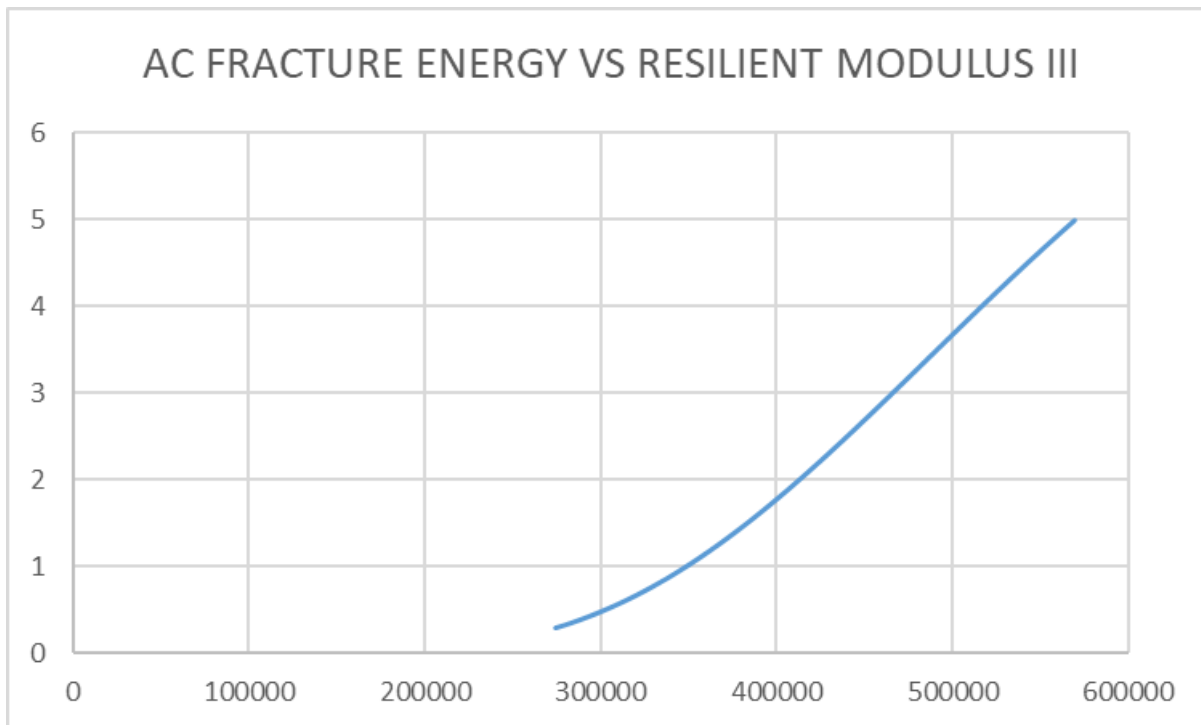


Figure 5.13: AC Fracture Energy and Resilient Modulus III

5.2.1 Damage model for delamination onset and crack propagation

This section summarises the transfer functions for the proposed flexible pavement analysis which provides a preliminary guide to the development of the software interface for the performance computational analysis.

This computation used makes reference to the South African Pavement Engineering Manual (SAPEM) as well as the South Carolina Department of Transportation.

The SAPEM manual serves as a reference guide for all aspects of pavement engineering. SAPEM can be taken in consideration for a sustainable best practice guide. South Carolina Department of Transportation highway pavement design procedures as set forth by the Guide for Mechanistic-Empirical Design of New and Rehabilitated Pavement Structures, Final Report (NCRRP, 2004) is adopted.

The runtime subroutine pavement design equation solver takes account of major aspects of Hot Mix Asphalt design. This also includes design considerations, estimating design traffic, pavement investigation and design processes, structural capacity estimation, and development of software graphic user interface available for pavement deterioration. Standard principles of pavement design for flexible should be made reference to as per SAPEM Chapter 10 and TMH 4,17,20. The traffic design estimation puts forward various methods of obtaining traffic load data and the procedures for estimating the cumulative design traffic load throughout the structural design period. The pavement investigation and design process sections cover both new and rehabilitation design and look at material availability, constructability, performance and maintainability. Economic assessments necessary for evaluating alternative pavement designs are not covered in this document. The structural capacity evaluation methods for flexible pavements and prediction of pavement failure runtime equation is provided.

The equations provided are as documented in the AASHTO interim guide 1972 and AASHTO 1986 and 1993. This report gives requirements for flexible pavement input that include soil support value, design lane equivalent standard axle loads (ESALS), regional factor assumed (1.0), terminal serviceability value and material layer coefficients.

The design approach introduces a strategic change in design constitutive models from input-output to real-time design input-output simulation. The input as specified for the geometry of design

makes use of trial pavement design values and computes the variables used to predict the distress and deformation of the pavement due to response with changing temperature and moisture content values. The procedure to compute rutting, or plastic vertical deformation, in HMA layers is shown in Equation 5.

$$\Delta_{p(HMA)} = \beta_{1r} k_z \varepsilon_{rHMA} 10^{K_{1r}} n^{k_{2r}} \beta_{2r} T^{k_{3r}} \beta_{3r} \quad (5.1)$$

where:

$\Delta_{p(HMA)}$ = Accumulated permanent or plastic vertical displacement in the HMA layer/sublayer, in

$\varepsilon_{p(HMA)}$ = Accumulated permanent or plastic axial strain in the HMA layer/sublayer, in/in

$\varepsilon_{r(HMA)}$ = Resilient or elastic strain calculated by the structural response model at the mid-depth of each HMA layer/sublayer, in/in

β_{1r} = local or mixture field calibration constants; for the global calibration these constants were all set to 1.0

$k_{1r,2r,3r}$ = Global field calibration parameters (from the NCHRP 1-40D recalibration; $K_{1r} = 3.35412$, $K_{2r} = 0.4791$, $k_{3r} = 1.5606$)

k_z = Depth confinement factor

h_{HMA} = Thickness of HMA layer/sublayer, in

T = Pavement Temperature

$$k_z = (C_1 + C_2 D) 0.328196^D$$

$$C_1 = -0.1039(H_{hma})^2 + 2.4868H_{hma} - 17.342$$

$$C_2 = 0.0172(H_{hma})^2 - 1.7331H_{hma} + 27.428$$

where:

D = depth below the surface, in

H_{HMA} = total HMA thickness, in

$$C_1 = -0.1039(H_{hma})^2 + 2.4868H_{hma} - 17.342 \quad (5.2)$$

$$C_1 = 0.0172(H_{hma})^2 - 1.7331H_{hma} + 27.428 \quad (5.3)$$

$$N_r = 1.365 \times 10^{-9} (E_c)^{-4.477} \quad (5.4)$$

Assuming $h_{HMA} = 40\text{mm}$ Equivalent to 1.575inches

Depth $D = 560\text{mm}$ Equivalent to 22.05inches

$$C_1 = -13.68$$

$$C_2 = 24.68$$

$$K_z = 1.1\text{E-}8$$

Temperature of asphalt is 40 degrees assumed as 104 degrees Fahrenheit.

Substitute to Equation 4

$$\Delta_{p(HMA)} = \beta_{1r} k_z \varepsilon_{rHMA} 10^{K_{1r}} n^{K_{2r}} \beta_{2r} T^{K_{3r}} \beta_{3r} \quad (5.5)$$

$$\Delta_{p(HMA)} = 1.2 \times 10^{-5} \text{mm}$$

The equation below represents the field-calibration for rutting in the foundation and all unbound pavement layers.

$$\Delta_{p(soil)} = \beta_{s1} k_{s1} \varepsilon_v h_{soil} \left(\frac{\varepsilon_0}{\varepsilon_r} \right) e^{-\left(\frac{p}{n} \right)^\beta} \quad (5.6)$$

where:

$\Delta_{p(soil)}$ = Permanent or plastic deformation for the layer/sublayer, in

n = Number of axle-load repetition

ε_0 = Intercept determination from laboratory repeated load permanent deformation tests, in/in

ε_r = Resilient strain imposed in laboratory test to obtain material properties ε_0 , ε_r and p , in/in

ε_v = Average vertical resilient or elastic strain in the layer/sublayer and calculated by the structural response model, in/in

Hsoil = Thickness of the unbound layer/sublayer, in

ϵ_{s1} = local calibration constant for the rutting in the unbound layers; the local calibration constant was set to 1.0 for the global calibration effort

K_{s1} = Global calibration coefficient; $k_1 = 1.673$ for granular materials and 1.35 for fine grained materials

B_{s1} = local or mixture field calibration constant; for the global calibration these constants were all set to 1.0

$$\log\beta = (-0.6119 - 0.017638W_c)$$

$$\rho = 10^9 \left[\frac{C_0}{(1 - (10^9)\beta)} \right]^{\frac{1}{\beta}}$$

$$C_0 = \ln \left[\frac{a_1 M_r^{b_1}}{a_9 M_r^{b_9}} \right] = 0.0075$$

W_c = water content, %

M_R = resilient modulus

$a_{1,9}$ = Regression constant; $a_1 = 0.15$ and $a_9 = 20.0$

$b_{1,9}$ = Regression constant; $b_1 = 0.0$ and $a_9 = 0.0$

$$W_c = \left(\frac{51.712}{\left[\frac{0.64 \sqrt{E_r}}{2555} \right]^{(0.3586xGWT^{0.1192})}} \right) \quad (5.7)$$

$$E_r = 2555x \left[\frac{(51.712) \left(\frac{1}{(0.3586xGWT^{0.1192})} \right)}{W_c} \right]^{0.64} \quad (5.8)$$

where:

W_c and GWT are varying parameters

$W_c = 40\%$

$$GWT = 600\text{mm}$$

$$E_r = 6.44 \times 10^3$$

$$\log \beta = (-0.6119 - 0.017638W_c) \quad (5.9)$$

$$B = 0.04818$$

$$C_0 = \ln \left[\frac{a_1 E_r^{b_1}}{a_9 E_r^{b_9}} \right] = 0.0075 \quad (5.10)$$

$$\rho = 10^9 \left[\frac{C_0}{(1 - (10^9)^\beta)} \right]^{\frac{1}{\beta}} \quad (5.11)$$

$$\rho = 1.095 \times 10^{-40}$$

$$\left(\frac{\varepsilon_0}{\varepsilon_r} \right) = \left(\frac{(e^{(\rho)^\beta} x a_1 E_r^{b_1}) + \left(e^{\left(\frac{\rho}{10^9} \right)^\beta} x a_9 E_r^{b_9} \right)}{2} \right) \quad (5.12)$$

$$\frac{\varepsilon_0}{\varepsilon_r} = 1.008 \quad (5.13)$$

,

$$\Delta_{p(soil)} = \beta_{s1} k_{s1} \varepsilon_v h_{soil} \left(\frac{\varepsilon_0}{\varepsilon_r} \right) e^{\left(\frac{\rho}{n} \right)^\beta} \quad (5.14)$$

$$\Delta_{p(soil)} = 0.1526 \text{ €} = \underline{\underline{3.87604\text{mm}}}$$

5.2.2 Damage Criterion and growth prediction in HMA flexible pavement

Due to increasing loading over time and fatigue, the top layer suffers fatigue in the form of alligator crack assumed to initiate at the bottom of the HMA layer, while longitudinal cracks are assumed to initiate at the surface of the pavement. An approach to calculate the extent of incremental pavement damage as provided by the incremental damage is presented. The design equation for flexible pavement is adopted.

$$\log(W_{18}) = Z_R \cdot S_0 + 9.36 \cdot \log(SN + 1) - 0.20 + \frac{\log(\Delta PSI)/(4.2 - 1.5)}{0.4 + 1094/(SN + 1)^{5.19}} + 2.32 \cdot \log(MR) - 8.07 \quad (5.15)$$

where:

W_{18} = predicted number of 18kip equivalent single axle load application

Z_R = standard normal deviate

S_0 = combined standard error of the traffic prediction and performance prediction

SN = structural number indicative of the total pavement thickness required

$SN = a_1D_1 + a_2D_2m_2 + a_3D_3m_3$

a_i = i th layer coefficient

D_i = i th layer thickness (inches)

M_i = i th layer drainage coefficient

ΔPSI = difference between the initial serviceability index, P_0 and the design terminal serviceability index, P_t

M_R = resilient modulus

The environmental design procedure accounts for the damage of pavement considering two strategic input variables, temperature and increasing moisture content. It is recommended that an effective subgrade Resilient Modulus (M_R) for stiffness requirement be used to represent the effect of seasonal variations, especially for moisture-sensitive fine-grained soils for locations with significant freeze-thaw cycles (AASHTO, 1993) and increasing precipitation and areas at the tropics subjected to an increasing temperature gradient. The relative damage U_f is described by the following equation:

$$u_f = 1.18 \times 10^8 \cdot M_R^{-2.23} \quad (5.16)$$

However, the relative damage is computed by the average damage value experienced across all season during the year. The effective subgrade resilient modulus is then given by:

$$M_f = 3015. u_f^{-0.431} \tag{5.17}$$

Previously, the M-EPDG developed a mechanistic-empirical method for designing and evaluating pavement structures. The design process is not as straight forward as that obtained from the empirical design presented by 1993 AASHTO guide. The MEPDG developed a software algorithm to automatically perform pavement design.

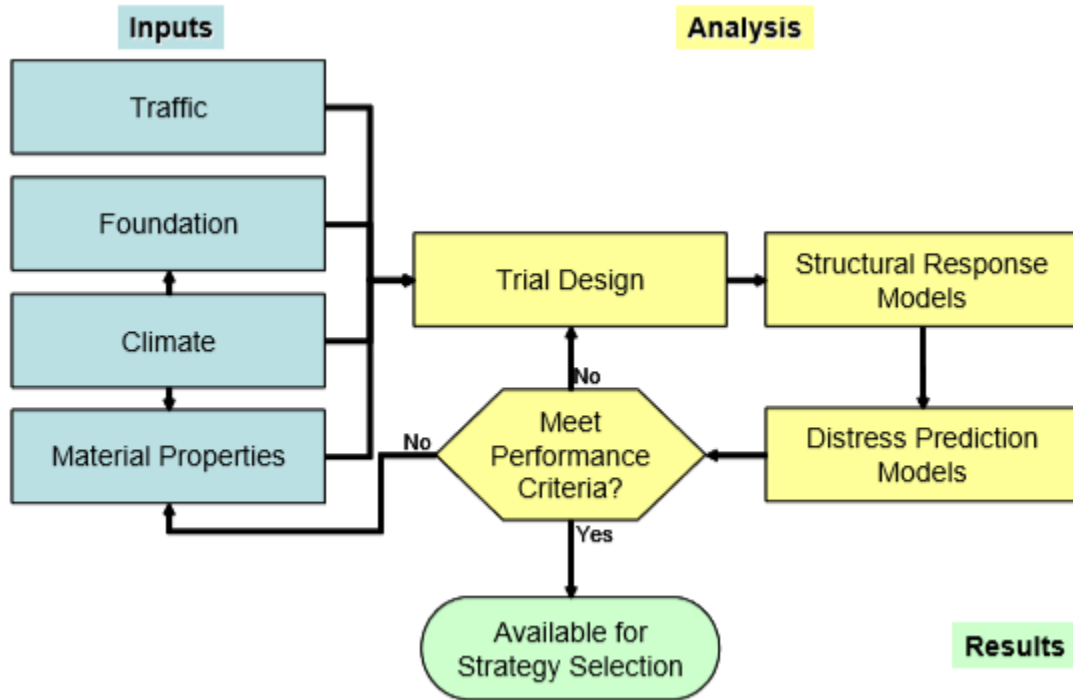


Figure 5.14: M-E flexible pavement design flow chat (Source: MEPDG: 2004)

The design input variables in the M-E design does not specifically consider moisture ingress and increasing temperature variations over time. This study developed an algorithm for designing pavement taking note of the input values mentioned in Figure 5.14.

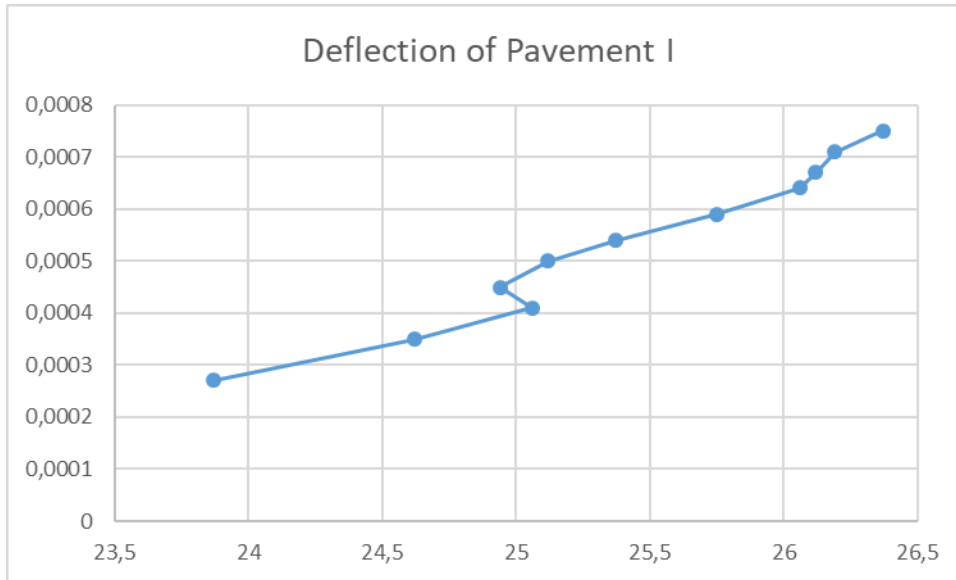


Table 5.15: Relationship between pavement deflection and temperature gradient I

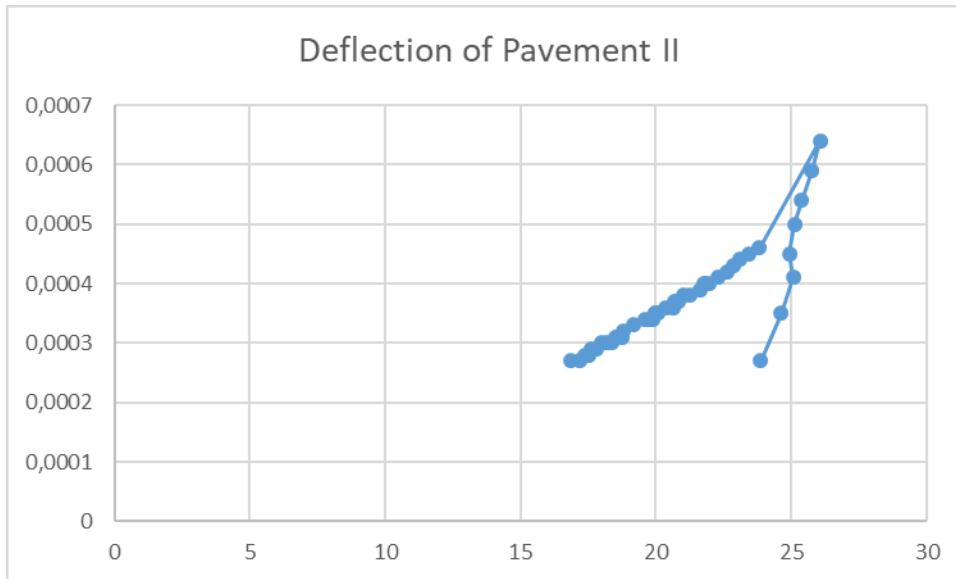


Table 5.16: Relationship between pavement deflection and temperature gradient II

On the contrary, reduced temperature gradient increases the fracture Energy making the pavement stiffness high and resistant to failure, but on very low temperatures a compromise is reached, and the strength is breached resulting in a brittle material (Glass). Although the failure is not visible at the onset of crack propagation, continual exposure to increasing temperatures as well as increasing

moisture content will lead to failure of the pavement before the design life is reached. There is also a strong linear relationship between Pavement Fracture Energy and the Pavement Resilient Modulus. The Table 5.15 and 5.16 indicated that; the higher the temperature, the higher the rate of deflection and the lower the temperature, the lower the deflection.

In addition, the deformation of the pavement is nonlinear owing to the fact that road pavement experiences complex stress-strain variables which are time-dependent resulting in multiple phase deformation based on the following failure modes within the pavement structural matrix. An energy-based constitutive model for the pavement matrix is based on plastic strain energy model and this is represented by a unique relationship between the modified plastic strain energy and the stress parameter. The evaluation of pavement using smart models in computing methods (Data Engine, programming, instrumentation and monitoring devices) gives rise to an evaluation matrix as defined by major constitutive pavement quality indices to determine the safety index as well as the prediction of failure during service load.

An Expert Shell System algorithm is presented in Figure 5.17. the Expert Shell System shows the analysis for pavement design which is referred to as Pavement Design Infographics. This infographic shows the logical approach in designing pavement using real-time environmental data. The data is collected via the sensors, firstly sorted out for errors and then mined within the sub-system using data Mining tools. The refined data is passed to the next phase where finite element analysis is performed as well as layered elastic design of pavement. The output is published. For this study, a number of pavement failure indices are presented in Table 5.0 to take account of the respective measure to counter pavement deformations as they occur.

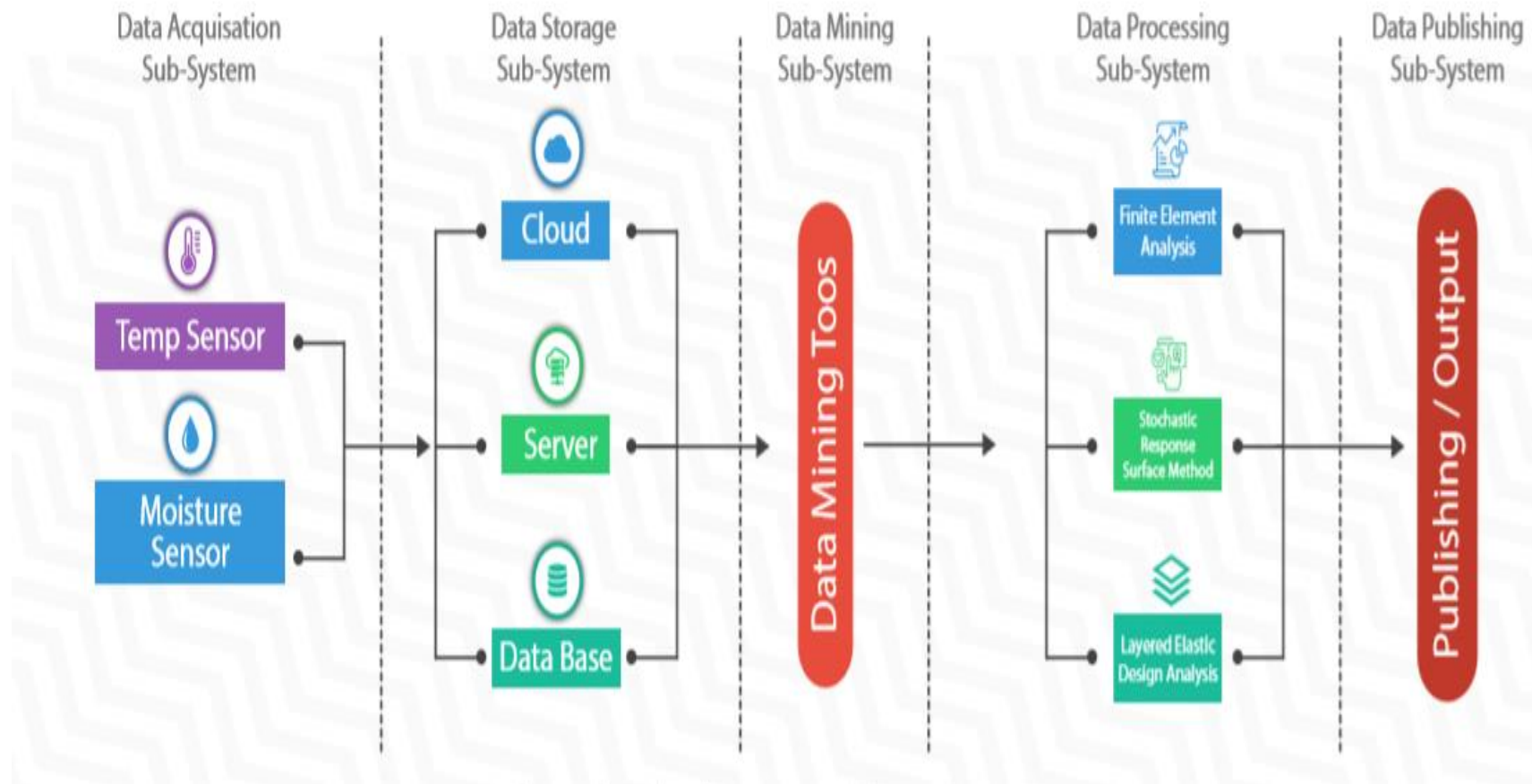


Figure 5.17: Design infographic for moisture and temperature pavement instrumentation algorithm (Researcher, 2019)

Furthermore, a confidence level algorithm was developed in this study. Unfortunately, this algorithm has been forwarded to the United States for Patent Registration and will not be presented since the application is already in process otherwise it will render the patent null and void. In addition, the algorithm developed is proposed to provide a life expectancy value for the road pavement as well as predict the time to failure of the roadway over a period of time at any given time “*t*” within the design life of the pavement.

Table 5.0 Pavement Failure Modes (Researcher, 2019)

| Failure Modes | |
|--------------------------|--------------------------------|
| <i>Pavement Distress</i> | <i>Pavement Deterioration</i> |
| Pavement Cracking | Traffic Loading |
| Pavement Distortion | Environmental/Climatic factors |
| Pavement Disintegration | Drainage effect |
| Skidding hazard | Material quality |
| Surfacing/roughness | Utility/Service cuts |
| | Construction defects |

Vocabulary for the development of a smart technology domain in pavement analysis using a web-based data architecture semantics is presented. This domain includes tools and technology within the software development life cycle in the Database Management System (DBMS). The Database Management System developed will serve as the anchor to the smart road Pavement Management System. Consequently, a confidence rating for Network Level Pavement Management System will be generated in a further study.

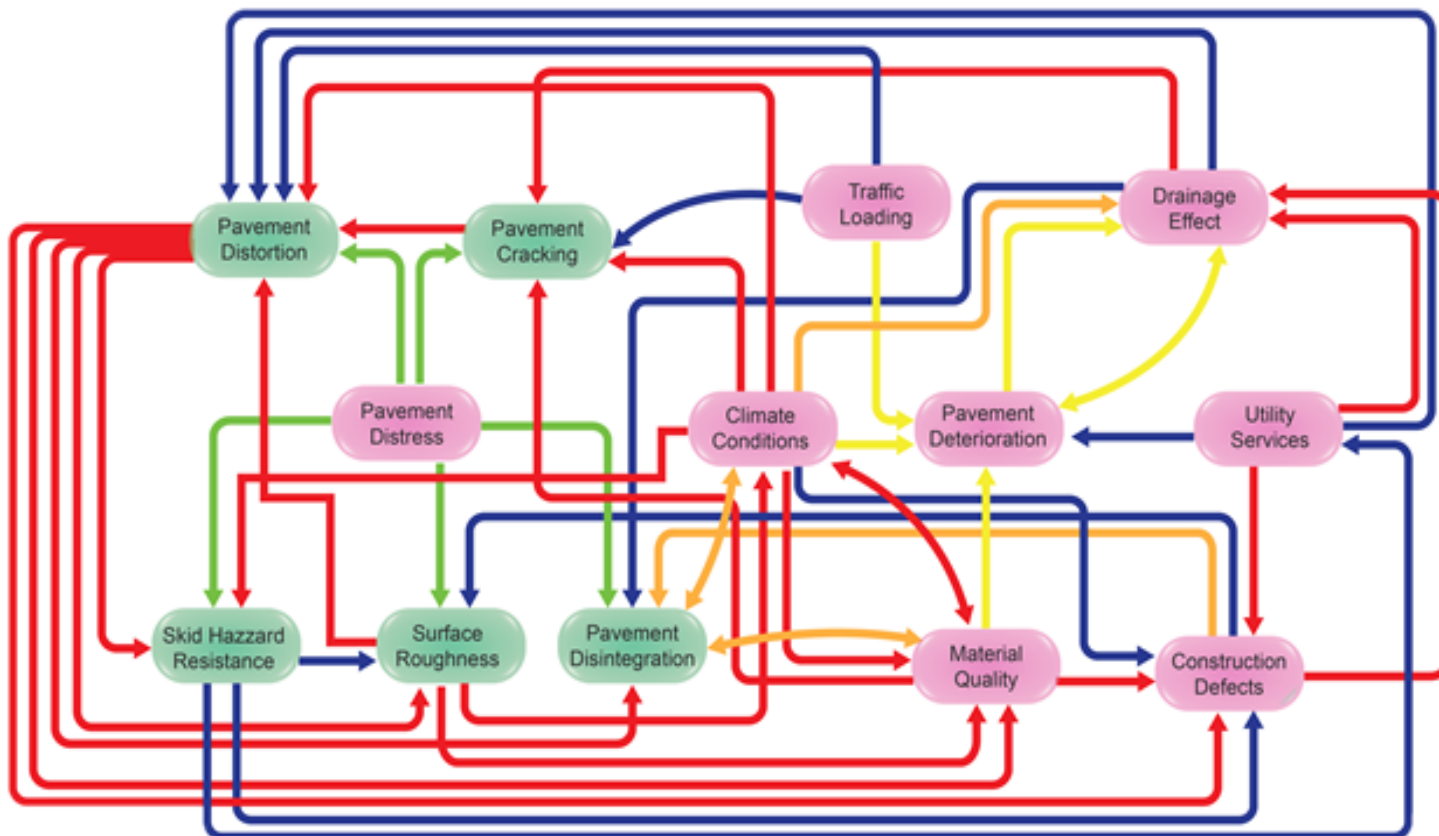


Figure 5.18: Web Data Architecture Model for HMA pavement failure mode. (Researcher, 2019)

A web data architecture is a system of parameters that can be used to assess pavement performance based on failure parameters (pavement distress and pavement deterioration) as presented in Table 5.0. Furthermore, Figure 5.18: Shows the data architecture between pavement condition and pavement deterioration response model. The web architecture indicates that, pavement distress (traffic loading, climate conditions, utility services) results to pavement disintegration (material quality, pavement cracking, drainage defect, surface roughness), and pavement disintegration (construction defects, drainage defect) results to pavement distortion (utility services, skid resistance, traffic loading, and pavement deterioration). The resulting failure stages arise from interaction between the pavement and the surrounding exposure conditions.

This scenario is a relationship between different failure parameters and the corresponding/associated failure mode. Going back to the Griffith (1920) Fracture Energy relationship: it can be concluded that Griffith’s theorem as related to brittle and glass materials can be applied to pavement response.

Figure 5.18 further indicates that certain factors have the ability to influence pavement failure. This scenario put forward the fact that; the failure initiated at the time of initiation (Mode I) may not result to pavement damage; but with time, this will result to exponentially distorted changes in the pavement matrix.

The classification of failure based on Mode I, Mode II and Mode III can be regrouped again from the Data Architecture Model in Table 5.1.

Table 5.1: Relationship between Griffiths Failure Mode and Asphalt Concrete Failure Mode

| Mode I | Mode II | Mode III |
|--------------------|----------------------|-------------------------|
| Surface Roughness | Pavement Cracking | Pavement Distortion |
| Climate Conditions | Construction Defects | Utility Services |
| Traffic Loading | Drainage Effect | Pavement Disintegration |
| Skid resistance | | |
| Material Quality | | |

5.3 Summary

The algorithm presented in Figure 5.17 provides a novel approach for pavement analysis as compared with the conventional Mechanistic-Empirical Pavement Design procedure since the algorithm incorporates real-time pavement environmental characteristics into the design equation considering the transfer functions for analysis. The significance of this algorithm is seen to serve as a mitigation plan to predict pavement performance while recalculating the design parameters over a given road section without necessarily travelling to the site or taking core drills which tend to disrupt the road section and also reduce cost incurred in such activities.

The analysis from the algorithm is presented and discussed using graphs. Fracture Energy as well as real-time Resilient Modulus of the asphalt concrete is presented. The findings indicate that there is a strong relationship between environmental condition and road pavement strength/stiffness ratio (Modulus of Asphalt Concrete). The result in Figure 5.11 – 5.13 indicates that; increasing temperature gradient of the pavement reduces the fracture energy of the Pavement which results in delamination and collapse over a longer period of time. Although the failure is not visible at the onset of crack propagation, continual exposure to increasing temperatures as well as increasing moisture content will lead to failure of the pavement before the design life is reached. There is also a strong linear relationship between Pavement Fracture Energy and the Pavement Resilient Modulus.

CHAPTER SIX: DISCUSSION OF RESULTS

6.0 Introduction

In line with the previously stated objectives, this section provides a relationship between the objectives and the effort to bring about providing a solution to the problem statement based on the methodology presented in Chapter Three.

From the problem statement, it is observed that temperature gradient, as well as increasing moisture or humidity which results to increasing the saturation of the pavement, has an effect in the resilient modulus of the asphalt concrete. This further explains that increasing temperature gradient and moisture/humidity results to decrease in the Asphalt Modulus as well as resulting effective stiffness of the asphalt concrete pavement. In addition, reduction in the Asphalt Concrete Temperature and Moisture Content results in Increasing Asphalt Concrete Modulus. Since pavement behaves like a viscoelastic material (Hasan *et al.*, 2015), the performance of the pavement is significantly influenced by variations in moisture and temperature gradient. The modulus of the Asphalt Concrete has greatly affected hence a reduction in strength over a period of time. This scenario might not be valid for temperature ranges at freeze point. The data from the instrumentation process was analysed using data mining tools and fracture energy principle. The humidity values were from 0 to 1022. To improve efficiency. Consequently, temperature values varied. the three sensors combined generated over 5000 data output results. About 5.5% of the results were rendered invalid due to error in readings. The results indicate the efficiency of collecting real-time data from pavement using sensor probes (microcontrollers, data memory card powered with a solar system) within a period of time. The results also presented serves as input data for high-level time analysis and the results with regards to changing moisture is presented. Temperature variation based on fracture energy criteria is presented. The effect of the critical stress of the asphalt concrete is generated from the temperature gradient and the resulting effect on the pavement performance clearly indicates a strong relationship between pavement temperature changes and pavement strength considering the effective modulus of the asphalt concrete while in service. The resultant effect of the moisture gradient indicated a reduction in strength of the subgrade with increasing moisture due to crack failure opening.

6.1 Discussion of Objectives

6.1.1 Build/Fabricate Sensor Probes to Collect Moisture and Temperature Data from Hot Mix Asphalt Flexible Pavement using Smart Technology.

The sensor used for the conducted study was fabricated in the Research Group in Evolvable Manufacturing Systems (RGEMS) Laboratory, Department of Electrical and Mechatronics Engineering, Central University of Technology, Bloemfontein. The sensor description is as detailed in Chapter Four. The sensor operating system sends data via USB connection synchronized with the Micro Processor. The data is collected every 10 minutes' interval recorded in an Excel Sheet format (.CSV file). The entire system used a +5V voltage regulator looped to the USB port and the Battery. The version of the setup was Named (*MISRA v1.1*). A pictorial view is indicated in the figure below. A link to indicate the process of data transfer can be viewed on the Arduino web page:

<https://www.gammon.au/forum/?id=11497>.

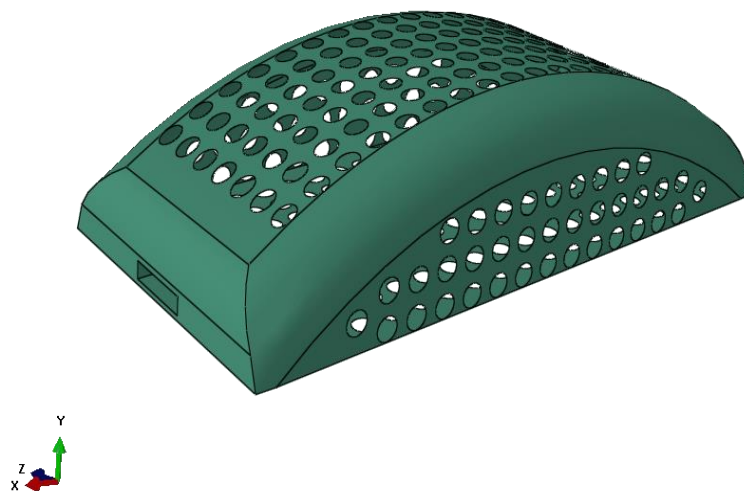


Figure 6.0: Front Elevation of MISRA v1.1

Figures 6.0 - 6.2 show the front elevation, full elevation and aerial view of the device enclosure respectively for MISRA sensor v1.1. The drawing was done using Abaqus 6.13 (CAE) and the material properties selected is that of a Faraday Steel Casing which is designed to resist heavy traffic loading that will arise from moving traffic over the instrumented road section. The casing is perforated to allow soil sample to be absorbed into the casing to enhance contact between the sensor device and the material for accurate readings. The perforation holes are 7.5mm on one side at the tail end, the sensors are driven into the case and secured with a fastener. The wire extension is drawn to allow for the embedded battery to receive constant charge while buried in the underlying pavement layer.

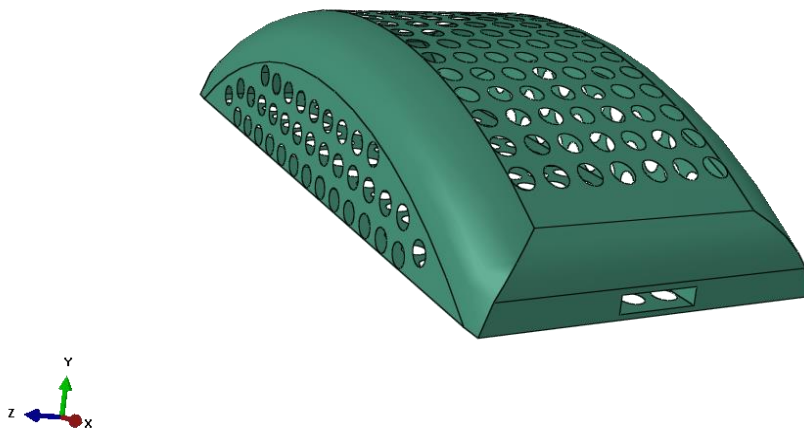


Figure 6.1: Full Elevation MISRA v1.1

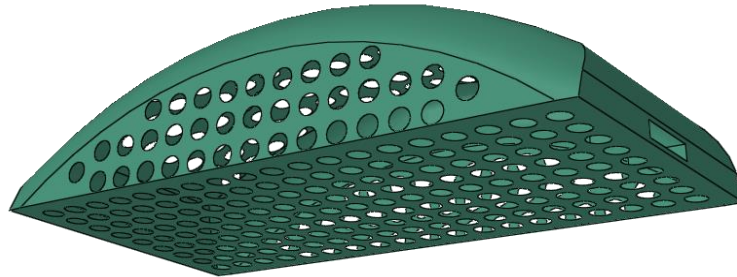


Figure 6.2: Aerial View of MISRA v1.1



Figure 6.3: Moisture Sensor Detector



Figure 6.4: Temperature Sensor



Figure 6.5: MISRA v1.1 Microprocessor



Figure 6.6: MISRA v1.1 Prototype Developed



Figure 6.7: MISRA v1.1 Full Setup with Solar Panel

6.1.2 Install sensor probes to a road pavement test section to collect pavement response

The sensor was installed into a road test section in the eastern cape region. The probes were installed along the tyre path. This process is to be able to collect exact stress and strain data over the moving traffic. The data collected is as indicated in Figure 5.1 and Figure 5.2. Response values were noted and analysed using moisture and temperature damage models to predict failure response. The damage deflection response is as indicated in results. The sequence clearly indicates that increasing temperature overtime causes a reduction on the resilient modulus of the concrete by the increasing strain values with an increasing temperature gradient. However, the pavement may perform better in a reduced temperature environment; the researcher proposes that a viscoelastic analysis of the pavement in low temperature should be considered to analyse the pavement behaviour as a brittle material susceptible to failure like a glass material over moving traffic.

6.1.3 Examine the response of the pavement using Finite element method and multi layered elastic transfer functions for appropriate pavement design.

The data was analysed based on the South Carolina Method of Pavement Design which is in line with the South African pavement design method obtained in the NCHRP -47 Pavement Design Guide. The results are as indicated in Chapter 5. A program was developed using an Integrated Engineering System (*IES*). The program can be run by inputting certain parameters:

- i. The resilient strain of the pavement obtained at time of construction using the results from the laboratory Indirect Tensile Strength (*ITS*) during Asphalt mixing and compaction
- ii. The number of axle loadings estimated during the Pavement Analysis Period observed at time of construction.
- iii. The temperature parameter of the Hot Mix Asphalt surface as well as the underlying pavement layers obtained from the sensor in real time on site.
- iv. The global field parameters k_1 , k_2 , and k_3 for the Hot Mix Asphalt.
- v. The total depth of the pavement below the surface taking account of the underlying layers (Base layer, subbase layer and asphalt concrete surface layer).

- vi. The thickness of The asphalt surface layer at time of construction or assumed thickness of the Hot Mix Asphalt Concrete layer obtained using a venire calliper from in-situ core drills.

6.1.3.1 Web Integrated Source Code Program To Calculate Pavement Failure Using Moisture And Temperature Stress Intensity Propagators

The source code for the web integrated model is presented in the sequence below. The code was written using C++ Programming language and this is solvable using a web compiler link: https://www.onlinegdb.com/online_c++_compiler. This will run the program when the code is copied and pasted on the web link. The corresponding result is generated providing the desired input varying outcome.

```
//Program Moisture and Temperature Stress Intensity Propagators for predicting Pavement
Damage
#include <iostream>
#include <cmath>
using namespace std;
/*
int work1(int z1, int z2, int z3)
{

}
*/

int main()
{
    double B1 = 1, K, E, K1 = -3.35412, K2 = 0.4791, B2 = 1, T, K3 = 1.5606, B3 = 1, n,
D, H, C1, C2, DEF;
    cout << "Enter resilient strain: ";
    cin >> E;
    cout << "Enter number of axle loads: ";
    cin >> n;
    //cout << "Enter thickness of HMA, in: ";
    //cin >> ;
    cout << "Enter mix or pavement temperature, F: ";
    cin >> T;
    //cout << "Enter depth confinement factor: ";
    //cin >> K;
    //cout << "Enter global field calibration parameter k1, k2 and k3: ";
    //cin >> K1 >> K2 >> K3;
    cout << "Enter Local field calibration constants: ";

    cout << "Enter the depth below the surface, in: ";
    cin >> D;
    cout << "Enter total HMA thickness: ";
    cin >> H;

    C1 = -0.1039 * (H * H) + 2.4868 * H - 17.342;
    C2 = 0.0172 * (H * H) - 1.7331 * H + 27.428;

    K = (C1 + C2) * pow(0.328196, D);

    //    DEF = B1 * K * E * pow(10, K1) * pow(n, (K2 * B2)) * pow(T, (K3 * B3));
    DEF = 1 * K * E * pow(10, K1) * pow(n, (K2 * 1)) * pow(T, (K3 * 1));

    cout << "The Deformation in the slab is: " << DEF;
    return 0;
}
```

6.1.4 Develop a program to run pavement failure considering Temperature and moisture variables using Visual Studio Software package and propose a frame work for pavement failure response and maintenance plans based on pavement environmental conditions.

Crack propagation and crack growth were analysed using the Griffith Energy relation. The development of the sensors made use of a reverse engineering deterministic method for determining the resilient modulus of the pavement using stress and strain value components obtained from the pavement in real-time over a period of time. In extremely cold regions, further analysis needs to be performed due to the fact that the pavement will behave like glass and break at very low temperatures. This study provided an efficient way to analyse pavement deterioration in real-time considering temperature and humidity values from the sensor in such a way that the data is sent and analysed in real-time while generating an inference or confidence level of the pavement over a period of time. This process will be analysed daily in a cumulative format and where there is a drastic change in temperature and humidity readings, such values at that specific time is analysed in other to generate maintenance report plans to be used by various departments of Transportation and Road regulation agencies. A Road Asset management report is generated fortnightly and submitted to the authority concerned; however, actions will be weighted over time in line with government budget allocation for road maintenance. This measure will allow the roads to be maintained prior to visible failure and predict deterioration during the design service life.

CHAPTER SEVEN: CONCLUSION AND RECOMMENDATION

7.0 Conclusion

The results from the instrumentation indicate that: there is a strong relationship between the effect of climatic/environmental variations on pavement resilient modulus, stiffness, behaviour during traffic loading and service life performance. The sensor probes indicate that pavement response can be monitored in real-time while subjected to moving traffic load as opposed to methods of determining pavement response using FWD, core drills and mobile field observation devices. The concluded study further seeks to incorporate pavement design and analysis with Information Technology. The instrumentation of the pavement allows for proper communication between the road and the Pavement Design Engineer. The communication enhances that the roadway is given some form of life via the instrumentation process (initiation of 4IR). This helps to better communicate with the road and provide proper maintenance plans much ahead of time before the onset of visible potholes and failure damage due to distress modes formed which might not be visible at the point of initiation. The analysis further leads to developing an expert shell system for analysis of flexible pavement and to predict the service life of a roadway considering its structural adequacy.

A report is proposed to be generated after the expert shell system analysis in order to develop a Road Pavement Management System to assist the Department of Transportation as well as to cut cost on trolley trips for pavement structural health survey and investigation. From the study conducted, it can be seen that smart pavement in sustainable transportation provides a better way to analyse pavement and predict the effective service life over any period of time. The use of the sensors serves to monitor the pavement condition, especially when subjected to hazardous unforeseen conditions like burst pipes and failed drainage lines or excessive rainfall precipitation as well as increasing temperature gradients. With the use of the sensors, it gives the Department of Transportation a heads up failure mitigation plan to cater for any damage that will occur in the future resulting from the previously outlined effects.

This study paved the way for advanced computations in pavement engineering which entail the creation of semantics of pavement domain during its design life through artificial intelligence and high-level expert system shell analysis in JAVA programming.

This model as presented in this study synchronises Pavement Management System with a Web-Based Data Architecture System.

For future recommendation, a confidence rating for Network Level Pavement Management System will be generated in a further study. Together with the JESS algorithm developed in this study, this will enhance pavement sustainability and reduction in maintenance cost.

REFERENCES

AASHTO. 1993. AASHTO Guide for Design of Pavement Structures. American Association of State Highway and Transportation Officials. Washington, DC.

Abaqus 6.13 CAE 2013 Finite Element Design Drawing Environment for deformation of structures. Simulia. 2013.

Abejide, S. O. and Hassan. M. M. 2017. “Moisture Content Numerical Simulation on Structural Damage of Hot Mix Asphaltic Pavement” Accepted for Proceedings of the Second International Conference on Civil Engineering and Materials Science (ICCEMS 2017), May 26-28, Seoul, South Korea

Adu-Osei, A. 2001. Characterization of Unbound Granular Layers in Flexible Pavements. Technical Reported, Texas A&M University Texas Transportation Institute College Station, Texas.

Ahmed, M.Y, Nury, A, H, Islam, F. and Alam, MMJ. B. 2012 Evaluation of geotechnical properties and structural strength enhancing road pavement failure along Sylhet-Sunamganj Highway, Bangladesh. Journal of Soil Science and Environmental Management. Vol.3 (5), pp: 110-117, May 2012.

Ahuja, L. R. and Swartzendruber, D. 1973. Horizontal soil-water intake through a thin zone of reduced permeability. J Hydrol. 19. 71-89

Akhter, G. F. and Witezak, M. W. 1985. Sensitivity of Flexible Pavement Performance to Bituminous Mix Properties. In Transportation Research Record 1034, TRB, National Research Council, Washington, D.C., pp. 70-79.

Al-Azzawi, A. A. 2012. Finite Element Analysis of flexible pavements strengthened with geogrid. ARPN Journal of Engineering and Applied Sciences, 7(10), pp.1295-1299.

Alexander A. Ponizovsky & Olga A. Salimgaryeyeva 2001. Estimating soil water potential from TDR measurements, Communications in Soil Science and Plant Analysis, 32:11-12, 1829-1839, DOI: 10.1081/CSS-120000253

- Alfatlawi, T. J. M 2015 Study on Roadway Subsurface Drainage System and Related Performance Using Fem, *International Journal of Civil Engineering and Technology*, 6(9), pp. 128–138.
- Al-Khateeb, L A., Saoud, A. and Al-Msouti, M. F. 2011. Rutting prediction of flexible pavements using finite element modelling. *Jordan Journal of Civil Engineering*, 5(2), pp.173-189.
- Al-Qadi, I. L., Elseifi, M. A. and Yoo, P.J.. 2004. Pavement Damage due to Different Tire and Vehicle Configurations. Virginia Tech Transportation Institute, Blacksburg, 2004.
- Al-Qadi, I. L., T. L. Brandon, and S. A. Bhutta. Geosynthetically Stabilized Flexible Pavement. *Geosynthetics '97*, Long Beach, Calif., 1992, pp. 647–662.
- Al-Qadi, I. L., T. L. Brandon, R. J. Valentine, B. A. Lacina, and T. E. Smith. 1994. Laboratory Evaluation of Geosynthetic-Reinforced Pavement Sections. In *Transportation Research Record 1439*, TRB, National Research Council, Washington, D.C., 1994, pp. 25–31. 2.
- Al-Qadi, I. L., T. L. Brandon, S. A. Bhutta, and A. K. Appea. 1996. Field Testing of Geosynthetically Stabilized Pavement Sections. Virginia Tech, Blacksburg, 1996.
- Ameri, M., Salehabadi, E.G., Nejad, F.M. and Rostami, T. 2012. Assessment of Analytical Techniques of Flexible Pavements by Final Element Method and Theory of Multi-Layer System. *Journal Basic Applied Science Research*, 2(11), pp.11743-11748.
- Amini, F., 2005a. Potential applications of paving fabrics to reduce reflective cracking. Jackson, MS: Mississippi Department of Transportation, Report No. FHWA/MS-DOT-RD-05-174, Feb.
- Amini, F., 2005b. Potential applications of paving fabrics to reduce reflective cracking. Washington, DC: Dep. Civ. Environ. Eng. State Univ. Coop. with Mississippi Dep. Transp. U.S. Dep. Transp. Fed. Highw. Adm., Final Rep. FHWA/MS-DOT-RD-05-174.
- Amit, K. D. 2016. Drainage system in highways. Term paper in transportation engineering. Lovely professional University. Punjab-India.
- Araya, A. A. 2011. Characterization of Unbound Granular Materials for Pavement., Master's Thesis, Road and Railway Engineering Section, Faculty of Civil Engineering and Geosciences, Delft University of Technology.

Ariza, P and Birgisson, B., 2002, “Evaluation of water flow through pavement systems”, Minnesota Department of Transportation, report no MN/RC - 2002-30.

Ashteyat, A. 2004. Characterization of Drainable Base and Subbase Materials, PhD. Dissertation, The University of Akron, 2004, Akron, Ohio.

Asphalt Institute. 1982. Research and Development of Asphalt Institute’s Thickness Design Manual. 9th Ed., Research Report 82-2, the Asphalt Institute.

ASTM D7369 2011 Standard Test Method for Determining the Resilient Modulus of Bituminous Mixtures by Indirect Tension Test (West Conshohocken PA USA: ASTM International)

Athanasios, I. K. 2010. A Multi-Configuration approach to reliability based structural integrity assessment for ultimate strength. Doctoral Thesis, Cranfield University. Department of Offshore, process and Energy Engineering.

Áurea, S. H., Evandro, P. J. and Lucas, T. B. 2006. Finite Element Modelling of Flexible Pavement.

Averjanov, S. F. 1950. About Permeability of subsurface soils in case of incomplete saturation, *Eng. Collect.*, 7, 1950

Babashamsi, P., Nur, I. M. Y Yusoff, I Ceylan, H. Nor, G. M. N., and Jenatabadi, H. S. “Evaluation of Pavement Life Cycle Cost Analysis: Review and Analysis.” *International Journal of Pavement Research and Technology* 9, no. 4 (July 2016): 241–254. doi: 10.1016/j.ijprt.2016.08.004

Barksdale, R. D. 1991. “Fabrics in Asphalt Overlays and Pavement Maintenance,” Transportation Research Board, Report No. NCHRP 171, Washington, D.C.

Battikha, N. E. 2004. The Condensed Handbook of Measurement and Control, 2nd ed., ISA, pp. 1–8

Bath and North East Somerset Council, Corporate Strategy 2016-2020.

Belegundu, A. D. and Chandrupatla, T. R. 1999. “Optimization Concepts and Applications in Engineering”, Upper Saddle River, New Jersey: Prentice Hall,

Bergström, M. 2006. “Life Cycle Behaviour of Concrete Bridges”, Lulea University of Technology, Department of Civil and Environmental Engineering, Division of Structural

Engineering. 2006:59|ISSN 1402-1757| ISRN: LTU-LIC 06/59, SE-971 87 Lulea Sweden, <http://www.cee.ltu.se>

Birgisson, B., Roque, R., Tia, M. and Masad, E. 2005. Development and Evaluation of Test Methods to Evaluate Water Damage and Effectiveness of Anti-Stripping Agents. Florida Department of Transportation, FL, 2005.

Black, T. N, Gardner, W. R and Thurtell, G. W. 1969. The prediction of evaporation, drainage and soil water storage for a bare soil. *Soil Sci. Soc. Amer. Proc.*, 33, 655-660.

Brooks, R., H., and Corey, A. T. 1964, Hydraulic properties of porous media, Hydrol. Pap3. Colorado State Univ., Fort Collins 19 64.

Bourquin, J., Schmidli, H., Van Hoogevest, P. and Leuenberger, H. (1997) Basic Concepts of Artificial Neural Networks (ANN) Modeling in the Application to Pharmaceutical Development, *Pharmaceutical Development and Technology*, 2:2, 95-109, DOI: 10.3109/10837459709022615

Brooks, R. H., and Corey, A. T. 1966. Properties of porous media affecting fluid flow. *Journal of Irrigation and Drainage. Division. American Society of Civil Engineers*. 92(1R2) 61-88, 1966

Brutsaert, W. 1967. Some Methods of calculating unsaturated permeability. *Trans. ASAE*, 10, 400-404, 1967.

Bumjoon Kang, A, V. Moudon, P. M. Hurvitz, B., and Saelens, E. 2017. Differences in behavior, time, location, and built environment between objectively measured utilitarian and recreational walking. *Transportation Research Part D: Transport and Environment*, Volume 57, 2017, pp. 185-194

Can, J., Yang, X. and Zhanping, Y (2017) Automated real aggregate modelling approach in discrete element method based on X-ray computed tomography images. *International Journal of Pavement Engineering*, 18:9, 837-850, DOI: 10.1080/10298436.2015.1066006

Charlier, R., Horny, P., Sršen, M., Hermansson, Å., Bjarnason, G., Erlingsson, S., and Pavšič, P. 2009. Water influence on bearing capacity and pavement performance: Field observations. In Dawson (Ed.), *Water in road structures—movement, drainage & effects* (pp.175–192). Heidelberg, Germany: Springer Science Business Media.

Cheng, D., Little, D. N. Lytton, R. L. and Holste, J. C. 2002. Surface Energy Measurement of Asphalt and Its Application to Predicting Fatigue and Healing in Asphalt Mixtures. In *Transportation Research Record: Journal of the Transportation Research Board*, No. 1810, TRB, National Research Council, Washington, D.C., pp. 44–53, 2002.

Cho, D.-W. and Kim, K. 2010. The mechanisms of moisture damage in asphalt pavement by applying chemistry aspects. *SCE Journal of Civil Engineering*. 2010", May", "01", Volume="14", number="3", pages="333--341

Christison, T. J. 1972. “The Response of Asphalt Concrete Pavements to Low Temperature” Dissertation Submitted in Partial Fulfilment for Requirements for the Ph.D. in Civil Engineering, University of Alberta, Canada.

Chuan Gu, Yongzheng Wang, YuJun Cui, Yuanqiang Cai. 2019. One-way cyclic behaviour of saturated clay in 3D stress state. *Journal of Geotechnical and Geoenvironmental Engineering*. Volume 145 Issue 10. October 2019.

Colliander, A., Jackson, T. J. Bindlish, R., Chan, S., Das, N., Kim, S. B.et. al., 2017. Validation of SMAP surface soil moisture products with core validation sites. *Remote Sens. Environ.* 191,215–231.

Construction and Building Materials, Volume 152, 2017, pp. 731-745.

Continuum Damage Model for Asphalt Mixtures. Publication FHWA-HRT-08-073,

Cortes, D. D, Shin, H, and Santamarina, J. C 2012. “Numerical simulation of Inverted pavement systems”. *Journal of Transportation Engineering ASCE/December 2012/1507*. DOI: 10.1061/(ASCE)TE.1943-5436.0000472.

Crampton, D., Zhang, Z, Fowler, D. W. and Hudson. W. .. 2001. Development of a formal forensic investigation procedure for pavements. Research Report 1731-3F, Centre for Transportation Research, The University of Texas at Austin, 2001.

Croney, D. and Croney, P. 1998. *The design and performance of road pavements*. 3rd edition, New York, NY.

David, W. IOWA State University, 2004. Determination of the Optimum Base Characteristics for Pavements (TR-482). djwhite@iastate.edu. 515-294-1463.

Davies, B. O. A. 2004. A model for the prediction of subgrade soil resilient modulus for flexible pavement design: Influence of moisture content and climate change. Master of Science Thesis in Civil Engineering. University of Toledo December 2004.

De Beer, M., Sadzik, E M, Fisher, C and Coetzee, C H. 2005. Tyre-Pavement Contact Stress Patterns from the Test Tyres of the Gautrans Heavy Vehicle Simulator (HVS) MK IV+, Proceedings of the 24th Southern African Conference (SATC 2005). ISBN: 1-920-01712-7, Pretoria, South Africa, pp 413-430, 2005.

De Lima, R., Júnior, E., Prata, B., and Weissmann, J., 2013. Distribution of materials in road earthmoving and paving: mathematical programming approach. *J. Constr. Eng. Manag.* 139, 1046e1054.

Dempsey, B. J., Herlach, W. A. and J. Patel, 1985. “The Climatic Material-Structural-Pavement Analysis Program, Federal Highway Administration”, Final Report Vol. 3., FHWA-RD-84-115.

Ditlevsen, O. and Madsen, H. O. 2005. “Structural Reliability Methods”, Coastal, Maritime and Structural Engineering, Department of Mechanical Engineering, Technical University of Denmark.

Dobriyal, P., Qureshi, A., Badola, R., and Hussain, S. A., 2012. A review of the methods available for estimating soil moisture and its implications for water resource management. *J. Hydrol.* 458, 110–117.

Doré, G. & Zubeck, H. K. 2009. *Cold Regions Pavement Engineering*. 1st ed. American Society of Civil Engineers, 1801 Alexander Bell Drive, Reston, USA.

Dubourg, V., Bourinet, J., and Sudret, B. 2012. Reliability-based design optimization of imperfect shells using adaptive kriging meta-models. PUBLISHING DETAILS?

Dunn, W. C. 2006. Introduction to instrumentation, sensors and process control. Artech House Sensors Library. ISBN-1-: 1-58053-011-7. United states of America.

Duong, N., Blanc, J.te & Hornych, P. 2016. Instrumentation of an Innovative Pavement Section on Motorway A10. 10.1007/978-3-319-42797-3_46.

ECMT, 1998. Transport infrastructure in ECMT countries profiles and prospects (monographs). In: The European Conference of Ministers of Transport Paris, France.

Ekblad, J. 2007. *Influence of water on coarse granular road material properties*. Stockholm, Sweden: KTH Royal Institute of Technology.

Ekwulo, E. O., and Eme, D. B. 2009. Fatigue and rutting strain analysis of flexible pavements designed using CBR methods. *African Journal of Environmental Science and Technology*, 3(12), pp.412-421.

Erlingsson, S. 2007. Numerical modelling of thin pavements behaviour in accelerated HVS tests. *Road Materials and Pavement Design*. 8/4, 719-744.

Erlingsson, S. 2010. Impact of water on the response and performance of a pavement structure in an accelerated test. *Road Materials and Pavement Design*. 11/4, 863-880. doi: 10.1080/14680629.2010.9690310.

EshkeveriSalimi, S, Abbo, A. J., and Kouretzis, G. 2019. Bearing capacity of strip footing on sand over clay. *Canadian Geotechnical Journal*, 2019, Vol. 56, No. 5: pp, 699-709.

Feng, M., Lei, C., Dongqing, L. and Xiaobin. W. 2020 Estimation of hydraulic conductivity of saturated frozen soil from the soil freezing characteristic curve. *Science of The Total Environment*, 10.1016/j.scitotenv.2019.134132, 698, (134132), (2020).

Ferrand, J. *et al.*, 2003. Les chaussées urbaines démontables – étude bibliographique. Internal LCPC report, 39 p., December, in French. Available from: <http://heberge.lcpc.fr/cud/>.

FHWA, 2009. Development of Multiaxial Viscoelastoplastic Continuum Damage Model for Asphalt Mixtures. Publication Number: FHWA-HRT-08-073.

FHWA, 2013. Status of the Nation's Highways, Bridges, and Transit: Conditions & Performance. U.S. Department of Transportation Federal Highway Administration.

Field, R.D., Kim, D., LeGrande, A. N. Worden, J. Kelley, M. and Schmidt, G.A. 2014. Evaluating climate model performance in the tropics with retrievals of water isotopic composition from Aura TES. *Geophys. Res. Lett.*, 41, no. 16, 6030-6036, doi:10.1002/2014GL060572.

Fini E. H, Al-Qadi I. L, Abu-Lebdeh. T. and Masson, J. 2011. Use of Surface Energy to evaluate Adhesion of Bituminous Crack Sealants to Aggregates. *American Journal of Engineering and Applied Sciences*. 4 (2):244-252, 2011. ISSN 1941-7020. 2011 Science Publications

Finn, G., Buckley, D., Kelly, K., McDaid, J., Mullaney, D., and ower, J. Guidelines for Road Drainage, Technical Document, Department of the Environment, Heritage and Local Government, 2004.

Fischer, H., Meissner, K., Mix, A., Abram, N. et al.. 2018. Palaeoclimate constraints on the impact of 2 °C anthropogenic warming and beyond. *Nature Geoscience*. 11. 474–485. 10.1038/s41561-018-0146-0.

Fischer, P., Azimi, S. M., Roschlaub, R., and Krau, T. 2018. Towards HD Maps from Aerial Imagery: Robust lane marking segmentation using country-scale imagery. *International Journal of Geo-Information*. ISPRS. 2018, 7, 458; DOI: 10.3390/ijgl710458.

Foundation for Pavement Preservation, Pavement Preservation Glossary of Terms, 2012

Gang Z. 2003. "Impacts of Environmental Factors on Flexible Pavements. " PhD diss., University of Tennessee, 2003. https://trace.tennessee.edu/utk_graddiss/2349

Ger, F., Donal, B. Kieran, K., John, M., Dominic, M. and Jim, P. 2004. Guidelines for road drainage. Department of the Environment, Heritage and Local Governmen. Roinn- U.S.A.

Ghosni. N, Samali, B. and Valipour, H. 2014. Flexural behaviour of high strength concrete composite incorporating long hooked-end steel fibres. 23rd Australian Conference on the Mechanocs of Structures and Materials. Southern Cross University. (ACMSM23), Vol I, Byron Bay, NSW, 9-12 December, Southern Cross University, Lismore, NSW, pp 327-332. ISBN: 9780994152008.

Golestani,,B. Nam, B., Noori, M. An, J. and Tatari, O. (2016): An optimum selection strategy of reflective cracking mitigation methods for an asphalt concrete overlay over flexible pavements. *International Journal of Pavement Engineering*, DOI: 10.1080/10298436.2016.1155709

- Gollwitzer, S. & R. Rackwitz. 1995. Comparison of Numerical Schemes for the Multi-normal Integral. Springer Verlag. In Proceedings of the first IFIP WG 6.5 Working Conference on Reliability and Optimization of Structural Systems, P. Thoft-Christensen (ed.) pp.157-174, 1995
- Green, R. E and Corey, J. C. 1971. Calculations of Hydraulic conductivity. A further evaluation of some predictive methods. Soils Science Society. America, Proceedings. 35, 3-8, 1971.
- Green, R. E. and Corey, C. J. Calculation of hydraulic conductivity: A further evaluation of some predictive methods. *Soil Sci. Soc. Amer. Proc.*, 35, 3-8, 1971.
- Greene, J., *et al.* 2012. Effect of asphalt rubber membrane interlayer (ARMI) on instability rutting and reflection cracking of asphalt mixture. Gainesville, FL: State Materials Office, Research Report Number, FL/ DOT/SMO/12-552.
- Griffith A. A. 1920. “The Phenomena of Rapture and Flow in Solids”. *Philosophical Transactions*, series A, Vol. 221, 1920, p. 163-198.
- Gupta, A. and Kumar, A. 2014. Comparative Structural Analysis of Flexible Pavements Using Finite Element Method. *International Journal on Pavement Engineering & Asphalt Technology*. 15. 10.2478/ijpeat-2013-0005.
- Hajek J. J and Haas, R. C. G. 1987. Factor analysis of pavement distress for surface condition predictions. Transportation Research RECORD 1117. PP 125 – 133.
- Hall, K. T. and Croveti, J. A. 2000. LTPP Data Analysis: Relative Performance of Jointed Plain Concrete Pavement with Sealed and Unsealed Joints, NCHRP Web Document 32 (Project SP20-50(2)), National Cooperative Highway Research Program, Washington, DC.
- Hallin, J. P., Teng, T. P., Scofield, L. A. and Quintus, H. V. 2007. Pavement Design in the Post AASHO Road Test Era, *Transportation Research Circular*, E-C118, July 2007.
- Hasofer, A.M. & Lind, N. C. An Exact and Invariant First Order Reliability Format. ASCE, *Journal. Eng. Mech. Div*, 1974, pp. 111-121.
- Hesp, S., Soleimani, A., Subramani, S. et al. 2009. Asphalt pavement cracking: Analysis of extraordinary life cycle variability in eastern and north-eastern Ontario. *International Journal of Pavement Engineering - INT J PAVEMENT ENG*. 10. 209-227. 10.1080/10298430802343169.

Heyns, M., Hassan, M. M., and Abejide, O. S. 2018. Sustainable waste alternative as cement replacement in pavement stabilization *Journal of Construction Project Management and Innovation* 8 (1), 1767-1778

Hicks, R.G., "Moisture Damage in Asphalt Concrete," NCHRP Synthesis of Highway Practice 175, Transportation Research Board, Washington, D.C., 1991.

Himeno K, Watnabe T 1987. "Design of Asphalt Pavements" Six International Conference on Structural Design of Asphalt Pavements, Ann-Arbour, Michigan.

Holanda, A. S, Araujo, T. D. Melo, L. T. Junior, F. E, Junior, E. P. 2006 Finite Element Modelling of Flexible Pavement.

Hosseini, H. R. A., Darban, A. K.. and Fakhri, K. 2009. The Effects of Geosynthetic Reinforcement on the Damage Propagation Rate of Asphalt Pavements. *Journal of Scientia Iranica*, Vol. 16, No. 1, pp. 26-32.

HRB, 1962. Highway Research Board, The AASHO Road Test- History and Description of Project, Special Report 61, National Academy of Sciences – National Research Council, Publication NO. 816, 1961. Highway Research Board, Washington, DC.

Huang, Y. H. 1993. *Pavement Analysis and Design*. Englewood Cliffs, NJ. Prentice Hall.

Huang, Y. H. 2004. *Pavement Analysis and Design*. 2nd ed. Upper Saddle River, New Jersey, USA: Pearson Education Inc., Prentice Hall and Education Inc.

Morel-Seytoux, H. J., Meyer, P. D. et al.. 1996. Parameter equivalence for the Brooks-Corey and van Genuchten soil characteristics: Preserving the effective capillary drive. *Water Resources Research*, Vol. 32; No. 5, Pages 1251-1258, May 1996 in *Transportation*, American Society of Civil Engineering, pp. 481-488, Boston, MA, 2002.

IOWA State University, 2003. Development of In-Situ Detection Methods for Materials-Related Distress (MRD) in Concrete Pavements" Phase I Report (July 2003). Available on: <http://www.ctre.iastate.edu/reports/mrd.pdf> (.pdf, 5.2 mb)

IOWA State University, 2005. Development of In Situ Detection Methods for Materials-Related Distress (MRD) in Concrete Pavements: Phase II. Final Report (August 2005). Available on: http://www.ctre.iastate.edu/reports/mrd_phase2.pdf (.pdf, 0.5 mb)

Irmay S. 1954. On the hydraulic conductivity of unsaturated soils, E, os Trans. AGU, 35, 463-467, 195

Irwin G. R. 1957. Analysis of stresses and strains near the end of a crack traversing a plate. *Journal of Applied Mechanics, Transaction ASME*. Vol. 79, 1957, pp 361-364.

Jadoun F. M. 2011. Calibration of the Flexible Pavement Distress Prediction Models in the Mechanistic Empirical Pavement Design Guide (MEPDG) for North Carolina. Doctorate Dissertation Graduate Faculty of North Carolina State University in partial fulfilment of the requirements for the degree of Doctor of Philosophy.

Jagtap, P. S. and Nagrale, P. P. 2013. Benefits of mechanistic approach for low volume rural roads. Proceedings of Indian Geotechnical Conference, Roorkee. pp. 1-8.

Jain, S., Joshi, Y. P. & Golia. S. S. 2013. Design of Rigid and Flexible Pavements by Various Methods and Their Cost Analysis of Each Method. *International Journal of Engineering Research and Applications*, vol. 3(5), pp. 119-123.

Jain, S. S., Gupta, A. K., and Sanjeev, R., 1992. Study of Influencing Parameters for Efficient Maintenance Management of Flexible Pavements. *IRC Journal*, Vol 53-1, pp. 93-143.

Janani, L., Sunitha, V. and & Samson, M. (2020) Influence of surface distresses on smartphone-based pavement roughness evaluation, *International Journal of Pavement Engineering*, DOI: 10.1080/10298436.2020.1714045

Jayawickrama P. W., Lytton R. L. "Methodology for predicting asphalt concrete overlay life against reflection cracking", Proceeding of the Sixth International Conference on Structural Design of Pavements, Ann Arbor, Michigan, 13-17 July 1987, p. 912-924

Jia-Der Perng, B. S. 1989. Analysis of crack propagation in asphalt concrete using a cohesive crack model. Master Degree Thesis. Graduate School of Ohio State University.

Jun M, Qiang Z., Laosheng W., and Lingzao Z. 2019. Improving parameter estimation with an efficient sequential probabilistic collocation-based optimal design method. *Journal of Hydrology*, 10.1016/j.jhydrol.2018.11.056, 569, (1-11), 2019

Karim, F. M. A., Rubasi, K. A. H. and Saleh, A. A. “The road pavement condition index (PCI) evaluation and maintenance: a case study of Yemen.” *Organization, Technology and Management in Construction: An International Journal*, vol. 8, no. 1, (2016): 1446 – 1455. doi: 10.1515/otmcj-2016-0008.

Kazmierowski, T. J., Bradbury, A., Hajek, J., Jones, G. 2010. Effectiveness of High Performance Thin Surfacing in a Wet-Freeze Environment, 72nd Transportation Research Board Annual Meeting, 113

Kerkhoven, R. E. and Dormon, G. M. 1953, “Some Considerations on the California Bearing Ratio Method for the Design of Flexible Pavement”, Shell Bitumen Monograph No.1.

Khodaii, A., Fallah, S. and Moghadas Nejad, F. 2009. Effects of Geosynthetics on Reduction of Reflection Cracking in Asphalt Overlays. *Journal of Geotextiles and Geomembranes*, Vol. 27, pp. 1-8.

Khosla, N. P., Birdsall, G. B., and Kawaguchi, S. An In-Depth Evaluation of Moisture Sensitivity of Asphalt Mixtures. NCDOT Research Project 1998-08 FHWA/NC/2002-102, 1999.

Khoury, C., Miller, G. A. and Abousleiman, Y. N. . 2010. “Effect of Suction Hysteresis on Resilient Modulus of Fine-grained Cohesionless Soil.” 8th Int. Conf. Bearing Capacity Roads, Railways, and Airfields, Univ. of Illinois–Urban Champaign, Champaign, IL, pp. 71–78

Khoury, N.N. and M.M. Zaman. 2004. “Correlation between Resilient Modulus, Moisture Variation, and Soil Suction for Subgrade Soils.” In *Transportation Research Record*, Vol. 1874, pp. 99–107. Transportation Research Board, Washington, DC.

Khurram Kamal, Senthan Mathavan, Tayyab Zafar, Imran Moazzam, Ahsan Ali, S. Usman Ahmad & Mujib Rahman (2018) Performance assessment of Kinect as a sensor for pothole imaging and metrology, *International Journal of Pavement Engineering*, 19:7, 565-576, DOI: 10.1080/10298436.2016.1187730.

Kiehl, J. T. and Briegleb, B. P. 2011. Pavement Surface Condition Field Rating Manual for Asphalt Pavement, ARPN. J. Sci. Technology, 2(1):17-25, 2011

Kim, D. S. and Drabkin, S. 1994. “Accuracy Improvement of External Resilient Modulus Measurements Using Specimen Grouting to End Platens,” Transportation Research Record No 1462, Transportation Research Board, National Research Council, 1994, pp. 65-71.

Kim, M. 2007. Three-Dimensional Finite Element Analysis of Flexible Pavements Considering Nonlinear Pavement Foundation Behaviour. Department of Civil Engineering, Graduate College of the University of Illinois at Urbana-Champaign.

Kim, M; Buttlar, G. W; Baek J; Al-Qadi, I. L. 2009. Field and Laboratory Evaluation of Fracture Resistance of Illinois Hot-Mix Asphalt Overlay Mixtures. Transportation Research Record; Journal of the Transportation Research Board. No 2127, Transportation Research Board of the National Academics, Washington, D.C, 2009. Pp 146-154. DOI: 103141/2127-17.

Kim, Y., Lee, H. Heitzman, 2009. M. Dynamic modulus and repeated load tests of cold in-place recycling mixtures using foamed asphalt. *Journal of Materials in Civil Engineering*, 21 (6) (2009), pp. 279-285).

Kim, Y.R., Guddati, M. N., Underwood, B. S., Yun, T. Y., Subramanian, V., Savadatti, S. and Thirunavukkarasu, S. 2009. “Development of a Multiaxial Viscoelastoplastic Continuum Damage Model (VEPCD_FEP++) Final report FHWA-HRT-08-073. Federal Highway Administration.

Kordi, N. E., Endut, I. R. and Baharom, B. 2010. Types of Damages on Flexible Pavement for Malaysian Federal Road. In: Proceeding of Malaysian Universities Transportation Research Forum and Conferences.

Ksaibati, K. and Mahmood, S. 2002, “Utilizing the Long-Term Pavement Performance Database in Evaluating the Effectiveness of Pavement Smoothness”, Department of Civil and Architectural Engineering, The University of Wyoming, Laramie, Wyoming.

Kucukvar, M. et al., 2014. Stochastic decision modelling for sustainable pavement designs. The International Journal of Life Cycle Assessment, 19 (6), 1185–1199.

Kutuk, B. 1998. “Performance of Flexible Pavements Reinforced with Geogrids,” Department of Civil and Environmental Engineering, West Virginia University, Morgantown, West Virginia.

Lean, J. 2010 “Cycles and trends in solar irradiance and climate,” Wiley Interdisciplinary Reviews: Climate Change, vol. 1, January/February 2010, 111-122.

Lekarp, F., Isacsson, U. & Dawson, A. 2000b. State of the art. II: Permanent strain response of unbound aggregates. *Journal of Transportation Engineering, ASCE*. 126/1, 76-83.

Lekarp, F., Isacsson, U., and Dawson, A. 2000a. State of the art I: Resilient response of unbound aggregates. *Journal of Transportation Engineering, ASCE*, 126(1), 66–75, 76-83.

Ling Yang & Zhaoba Wang (2019) Artificial neural network (ANN) modelling of thermal conductivity of supercritical ethane, *Energy Sources, Part A: Recovery, Utilization, and Environmental Effects*, 41:4, 396-404, DOI: 10.1080/15567036.2018.1518358 Sort out initials, etc.

Little, N. D., and Jones, R. D. 2003. Chemical and Mechanical Processes of Moisture Damage in HotMix Asphalt Pavements. Moisture Sensitivity of Asphalt Pavements- A National Seminar, February 4–6, 2003 San Diego, California. Transportation Research Board of the National Academics, 2003.

Liu R., Chen, X., Li, J., Xing, H., Chen J., Aditya Ekbote and Bingbing Wen. 2004. Remote monitoring moisture content in test pavement in Waco and Bryan Districts. Technical Report 0-4415-2. Subsurface sensing laboratory, Department of Electrical and Computer Engineering University of Houston.

Liu, H. S. and Lytton, R., L 1985. “Environmental Effects on Pavement Drainage”, Volume IV. Federal Highway Administration, Report FHWA-DTFH-61-87-C-00057.

Lockwood, M. 2009 “Solar Change and Climate: an update in the light of the current exceptional solar minimum,” *Proceedings of the Royal Society A*, 2 December 2009, doi 10.1098/rspa.2009.0519;

Lu, Y. J, Yang, S. P, Wang, J. X. 2014. Research on pavement longitudinal crack propagation under non-uniform vehicle loading. *Engineering Failure Analysis* 42. 22-31

Lytton, R. L. Back calculation of Pavement Layer Properties. In *Non-destructive Testing of Pavements and Back calculation of Moduli*. ASTM STP 1026. American Society for Testing and Materials, Philadelphia, Pa., 1989, pp.7–38.

- Lytton, R. L., Uzan, J., Fernando, E. G., Roque, R., Hiltunen, D. and Stoffels, S.M. 1993. “Development and Validation of Performance Prediction Models and Specifications for Asphalt Binders and Paving Mixes.” Strategic Highway Research Program, SHRP A-357. National Research Council, Washington, DC
- Magdi, M. and Zumrawi, E. 2016 Investigating Causes of Pavement Deterioration In Khartoum State, *International Journal of Civil Engineering and Technology*, 7(2), 2016, pp. 203–214.
- Maharaj, R. Mahase, M. & Maharaj, C.. (2019). The Performance and Durability of Polyethylene Terephthalate and Crumb Rubber Modified Road Pavement Surfaces. *Progress in Rubber Plastics Recycling Technology*. 35. pp 3-22. 10.1177/1477760618798425.
- Majidzadeh, K., and F. N. Brovold. 1968. Special Report 98: State of the Art: Effect of Water on Bitumen–Aggregate Mixtures. HRB, National Research Council, Washington, D.C., 1968.
- Mamlouk, M. and Mobasher, B. 2004. Cracking Resistance of Asphalt Rubber Mix versus Hot-Mix Asphalt. *International Journal of Road Materials and Pavement Design*, 5(4), pp.435-452.
- Mazumder, M., Kim, H. & Lee, S-J.. (2015). Perpetual Pavement: Future Pavement Network. *Journal of Advanced Construction Materials*. 19. 2015.
- Melchers, R. E. 1987.: “Structural Reliability Analysis and Prediction New York, USA: John Wiley, ISBN: 0-85312-930-4, pp: 401
- MEPDG, 2004; ARA, Inc., ERES Consultants Division. Guide for Mechanistic–Empirical Design of New and Rehabilitated Pavement Structures. Final report, NCHRP Project 1-37A. Transportation Research Board of the National Academies, Washington, DC, 2004.
- Miller, J. S. and Bellinger W. Y. 2014 Distress Identification Manual for the Long- Term Pavement Performance Program FHWA-HRT-13-092 (McLean, Virginia: Federal Highway Administration
- Mohamed, N., Maharaj, R. and Ramlochan D. Rutting and fatigue cracking susceptibility of polystyrene modified asphalt. *Am J Appl Sci*. 2017; 14(5): 583–591.
- Mohammad J. K, Corey L, Jared V. & Zhang, Z. (2013) Rigid and composite pavement index-based performance models for network pavement management system in the state of

Louisiana, *International Journal of Pavement Engineering*, 14:7, 612-628, DOI: 10.1080/10298436.2012.715643

Mohammad R. J, Alesheikh, A. A, Alimohammadi, A., Abolghasem S & Kyehyun K 2011. An approach for automatic updating of GIS road segments for a pavement management system (PMS), *Journal of Spatial Science*, 56:2, 253-267, DOI: 10.1080/14498596.2011.623346.

Mostafa, A. A. 2005 “The Stripping Susceptibility of Airfield Asphalt Mixes: The Development of Guidelines for a Laboratory Test Method”, a Ph.D. thesis Submitted In partial fulfillment of the requirements for the degree of Doctor of Philosophy, Carleton University, January 2005, Ottawa, Canada.

Mostafa, A. A, Bekheet, A.O, El Halim, A. and Easa, S. 2005. Reducing the susceptibility of flexible pavements to moisture-induced damage through superior compaction technology. 6th Transportation Specialty Conference 6 e Conférence spécialisée sur le génie des transports. Toronto, Ontario, Canada June 2-4, 2005/2-4 juin 2005.

Mualem, Y. 1976. A New model for predicting the hydraulic conductivity of unsaturated porous media. *Water Resource Research*. Volume 12, Issue 3. DOI.ORG/10.1029/WR12i003p00513

Mukherjee. D. 2014. Highway Surface Drainage System & Problems of Water Logging in Road Section. *The International Journal of Engineering and Science (IJES)*, 3(11), 44-51.

Muñoz-Carpena, R. 2004. Field devices for monitoring soil water content1. *Bull. Inst. Food Agric. Sci. Univ. Fla.*. 343.

Murana A. A. and Olowosulu, A. T. 2012. Fatigue models for Mechanistic-Empirical Design of flexible pavement. *World Journal of Engineering and Pure and Applied Sci.* 2012; 2(2);74. ISSN 2249-0582.

Kim, N., Kim, S. Y., and Lee, J. (2019) A novel 3D GPR image arrangement for deep learning-based underground object classification, *International Journal of Pavement Engineering*, DOI: 10.1080/10298436.2019.1645846

Nascimento, L.A. H. 2015. Implementation and Validation of the Viscoelastic Continuum Damage Theory for Asphalt Mixture and Pavement Analysis in Brazil. (Under the direction of Dr. Y. Richard Kim). IS THIS A THESIS? Which UNIVERSITY?

National Highway Authority of Pakistan (2019) NHA road network & maps of projects parti - <http://nha.gov.pk/wp-content/uploads/2016/04/NHA-Road-Network-Maps-of-Projects-02.01.2012-Part-01.pdf>. [Retrieved on April 09, 2019].

NCHRP, 2004. Guide for Mechanistic-Empirical Design of New and Rehabilitated Pavement Structures: Appendix RR-Finite Element Procedures for Flexible Pavement Analysis, Transportation Research Board, National Research Council, Washington D.C.

NCHRP, 2010. National Cooperative Highway Research Program. Mechanistic-Empirical Pavement Design Guide, Transportation Research Board, Washington, DC. Obtained from: <http://onlinepubs.trb.org/onlinepubs/archive/mepdg/home.htm>. Site last accessed April 14, 2010.

Ndebele, S. J. 2012. Keynote address by the Minister of TRANSPORT. Presented at the occasion of department's budget vote, 25 April 2012.

Ningyi S, Xiao, F. Wang, J and Amirkhanian, S. 2017. Characterizations of base and subbase layers for Mechanistic-Empirical Pavement Design

Noori, M. *et al.*, 2014. A stochastic optimization approach for the selection of reflective cracking mitigation techniques. *Transportation Research Part A*, 69 (2014), 367–378.

Norouzi, A. Sabouri, M. and Kim, Y. 2014. Evaluation of the fatigue performance of high RAP asphalt mixtures. *Asphalt Pavements*. 9. 1069-1077. 10.1201/b17219-132.

Arslan, O & Yetik, O. 2014. ANN Modelling of an ORC-Binary Geothermal Power Plant: Simav Case Study, *Energy Sources, Part A: Recovery, Utilization, and Environmental Effects*, 36:4, 418-428, DOI: 10.1080/15567036.2010.542437 THIS MUST MOVE UNDER A (ARSLAN, O.

O'Connor, J. S. 1995. "Review of Life Cycle Cost Issue Relating to Prefabricated Aluminium Bridge Decks", Paper for Reynolds Metal Company, Los Angeles.

O'Flaherty, C. A. 2002. *Highways*, 4th Ed. Oxford, UK: Butterworth-Heinemann, 2002, pp. 185–209.

OECD, 1985. Organisation for Economic Co-operation and Development; Washington, D.C. OECD Publications and Information Center, [distributor], 1985 101 p.: ill. ; 27 cm.

Oglesby, C. H. 1976. “Dilemmas in the administration, planning, design, construction, and maintenance of low-volume roads,” Transportation Research Board Special Report, 160, 7-16.

Oglesby, C.H., Highway Engineering, 3rd Edition, New York:John Wiley & Sons, 1975

Olowosulu AT. A Framework for Mechanistic-Empirical Pavement Design for Tropical Climate. *Journal of Civil Engineering*, 2005; Vol. 5, No.1. pp.44-51.

Oscarsson, E. 2011. Evaluation of the Mechanistic-Empirical Pavement Design Guide model for permanent deformations in asphalt concrete. *International Journal of Pavement Engineering*, 12/1, 1-12. doi:10.1080/10298430903578952.

Padmini P. G, Shane U. B, Zalghout, A. 2017. Impact of climate change on pavement structural performance in the united states. Transportation Research Part D: Transport Environment. Vol 57, December 2017. Pg 172-184.

Papadopoulos, E. and Santamarina, J. C. (2019) Inverted base pavements: construction and performance, *International Journal of Pavement Engineering*, 20:6, 697-703, DOI: 10.1080/10298436.2017.1326237

Papagiannakis, A.T. and Masad, E. A “Pavement Design and Materials”, Hoboken, NJ. : Wiley and Sons, ISBN: 978-0471214618.

Papagiannakis, A.T. 2013. Mechanistic-Empirical Pavement Design; A brief Overview. *Geotechnical Engineering Journal of the SEAGS & AGSSEA* Vol. 44 No 1 March 2013. ISSN 0046-5828.

Paris, P. C., and Erdogan, F. A. 1963. “Critical Analysis of Crack Propagation Laws,” Transactions of ASME, *Journal of Basic Engineering*, Series D, 85, No. 3, pp. 528-534.

Park, K., Thomas, N., Lee, W. 2007. Applicability of the International Roughness Index as a Predictor of Asphalt Pavement Condition. *Journal of Transportation Engineering*, 2007

Parris K. 2015. Extension of Stress-Based Finite Element Model Using Resilient Modulus Material Characterization to Develop A Theoretical Framework for Realistic Response Modelling of Flexible Pavements on Cohesive Subgrades. Degree Doctor of Philosophy in the Graduate School of The Ohio State University. The Ohio State University.

Paruelo, J., William, L., Ingrid, B., and Sala, O. E. 1999. Grassland Precipitation-Use Efficiency Varies Across a Resource Gradient. *ECOSYSTEMS*. 2. 64-68. 10.1007/s100219900058.

Paruelo, J. M, Aguiar, M. R and Golluscio, R. A. 1999 Soil water availability in the Patagonian arid steppe: Gravel content effect, *Arid Soil Research and Rehabilitation*, 2:1, 67-74, DOI: 10.1080/15324988809381159

Pavement Interactive. 2008. Flexible pavement mechanistic models. [Online] Available at: www.pavement-interactive.org/article/flexible-pavement-mechanistic-models/ [Accessed: 27 March 2014].

Pavement Interactive. Web page. <https://pavementinteractive.org/>

Peng, Y. and He, Y. 2009. Structural characteristic of cement-stabilized soil bases with 3D finite element method. *Front Architect Civil Engineering China*, 3(4), pp.428-434.

Ponizovsky, A. A and Salimgaryeyeva, O. A. 2001. Estimating soil water potential from TDR measurements. *Communications in Soil Science and Plant Analysis*, 32 (2001) 1829–1839. <https://doi.org/10.1081/CSS-120000253>

Porous Asphalt Pavement. (2015). Wisconsin asphalt pavement association[WAPA].

Proceedings of the Seventh International Conference Applications of Advanced Technology
MORE DETAILS

Promotes, S. and Ksaibati, k. (2016) A risk-based optimisation methodology for pavement management system of county roads, *International Journal of Pavement Engineering*, 17:10, 913-923, DOI: 10.1080/10298436.2015.1065992

Prozzi, J. A., Gossain, V., and Manuel, L. 2005. Reliability of pavement structures using empirical-Mechanistic Models. TRB 2005 Annual Meeting CD-ROM.

QIN, JIANFENG, M.S., June 2010, Civil Engineering Predicting Flexible Pavement Structural Response Using Falling Weight Deflectometer Deflections (94 pp.) Director of Thesis: Shad M. Sargand.

Quebec, C.d.t., 2014. The Quebec Infrastructure Plan, 2014e2024. Ramezaniapour, A.A., Kazemian, A., Moghaddam, M.A., Moodi, F., Ramezaniapour, A.M., 2015. Studying effects of

low-reactivity GGBFS on chloride resistance of conventional and high strength concretes. *Mater. Struct.*

Rabab'ah, A. R. 2007. Integrated Assessment of free drainage base and subbase materials under flexible pavement. Dissertation for Doctor of Philosophy, Graduate Faculty of the University of Akron.

Rahman, M.T., Mahmud, K. and Ahsan, S. 2011. Stress-Strain characteristics of flexible pavement using Finite Element Analysis. *International Journal of Civil and Structural Engineering*, 2(1), pp.233-240.

Rahman, S., & Erlingsson, S. (2014). Predicting permanent deformation behaviour of unbound granular materials. *International Journal of Pavement Engineering*. doi:10.1080/10298436.2014.94320

Rahman, S., & Erlingsson, S. 2012. Moisture sensitivity of unbound granular materials. Proceedings of the 4th European Pavement and Asset Management Conference (EPAM4), Malmö, Sweden (CD-ROM). 2012, September 5-7.

Ramandeep, S. J. 2012. Network-Level Pavement Performance and Management Study in Connecticut. Master's Thesis, University of Connecticut Graduate School. 2012.

Rameshwar S and Franzini, J. B 2012. Unsteady flow in unsaturated soils from a cylindrical source of finite radius, *Journal of Geophysical Research*, 72, 4, (1207-1215), 2012.

Reza F, Boriboonsomsin K and Bazlamit S. 2006. Development of a pavement quality index for the State of Ohio. Paper for 85th Annual meeting of The Transportation Research Board. Washington D.C. January 2006.

Rodrigue, J. P., Comtois, C., and Slack, B. 2006 *The Geography of Transport Systems*. (London and New York: Routledge, 2006). [Pp. 284.] \$ 51.95. ISBN 0-415-35441-2

Rodrigue, J. P. Comtois, C. and Slack E. 2016. *The geography of transport systems*. 10.4324/9781315618159.

Saevarsdottir B, 2014. Performance Modelling of flexible pavements tested in a heavy vehicle simulator. Faculty of civil and environmental engineering, University of Iceland. 2014. Dissertation submitted in partial fulfilment of a Philosophiae Doctor Degree in Civil Engineering

Saevarsdottir, T. and Elingsson, S. 2013 Water impact on the behavior of flexible pavement structure in an accelerated test. *Roads Materials and Pavement Design* 2013, Vol.14, No. 2,225-227. Taylor and Francis.

Sakhaei, M.S, Underwood, B. S., Kim, Y. R., Jackson, N. 2009. Application of artificial Neural networks for estimating dynamic modulus of asphalt concrete. *Journal of transportation research board*, No 2127, National Research Council, Washington, D.C. pp. 173-186.

Salour, F., & Erlingsson, S. 2013. Investigation of a pavement structural behaviour during spring thaw using falling weight deflectometer. *Road Materials and Pavement Design*, 14(1), 141–158. doi:10.1080/14680629.2012.754600

Scazziga, I., Dumont, A. G. and W. Knobel 1987, “Strain Measurements in Bituminous Layers”, Proceedings of the 6th International Conference on the Structural Design of Asphalt Pavements, pp. 574-89. University of Michigan, Ann Arbor.

Scholz, T.V. “Durability of Bituminous Paving Mixtures,” Doctor of Philosophy Thesis, University of Nottingham, October 1995.

Shafabakhsh, G.A., Motamedi, M. and Family, A. 2013a, “Influence of Asphalt Concrete Thickness on Settlement of Flexible Pavements”, *Electronic Journal of Geotechnical Engineering*, Vol.18, Bund C, pp.473-483.

Shapery, R. A 1984. Correspondence principles and generalized J-integral for large deformation and fracture analysis of viscoelastic media. *International Journal of fracture*, vol. 25, pp. 195-223.

Sharma, A. and Sharma, D. (2017). Laboratory Performance of Porous Asphalt Pavement. PUBLISHING DETAILS?

Skjong, R, Gregersen, E. B, Cramer, E. Croker, A., Hagen, O. Korneliussen, G., Lacasse, S., Lotsberg, I., Nadim, F., and Ronold, K. O. 1995. Guide line for Offshore Structural Reliability Analysis - General. DNV. Report No. 95-2018. 1995.

Sohm J., Horny P., Kerzrého J.P., Cottineau L.M., Le Cam V., Hautière N., De La Roche C., and Van Damme H. (2012b), “Remote Monitoring of an Experimental Motorway Section – An Enabling Technology of the 5th Generation Road”. *International Journal of Pavement Research and Technology*, 5 (5): 289-294.

South African National Road Agency Ltd (SANRAL). 2013. Pavement Design: South African Pavement Engineering Manual. An initiative of the South African national roads agency ltd, South Africa.

South African Pavement Engineering Manual. 2014. The South African National Roads Agency. AN initiative of the South African National Roads Agency SOC LTD. Second edition. ISBN 978-1-920611-00-2

Steiakakis, E., Gamvroudis, C., and Alevizos, G. 2012. Kozeny-Carman Equation and Hydraulic Conductivity of Compacted Clayey Soils}, Steiakakis2012KozenyCarmanEA.

Stuart K. D. Moisture Damage in Asphalt Mixtures- A State-of-Art Report, FHWARD-90-019, Federal Highway Administration, U.S Department of Transportation, Washington, D.C., 20001., 1990.

Sung-Hee Kim, Jidong Yang & Jayhyun Kwon (2017) Effects of using screening materials in the graded aggregate base layer of flexible pavements. *International Journal of Pavement Engineering*, 18:2, 97-107, DOI: 10.1080/10298436.2015.1036868

Symons, M. and Herrin, S., 2009. Techniques for Mitigation of Reflective Cracks, Technical Guide. APTP, 05–04, 217.

Tabatabee, N., Al-Qadi, I. L., Sebaaly, P. EE. 1992. Field Investigation of pavement Instrumentation Methods. “Journal of Testing and Evaluation” JTEVA. Vol 20, No 2. March 1992. Pp 144-151.

Tam, T. H., Ibrahim, A. L, Rahman, M. Z. A. and Mazura, Z. 2014 Flood Loss Assessment in the Kota Tinggi 8th Int. Symp. of the Digital Earth pp 1-5

Tarrer, A. R. and V. Wagh. The Effect of the Physical and Chemical Characteristics of the Aggregate on Bonding. Strategic Highway Research Program, National Research Council, Washington, D.C., 1991.

- Taylor, M. A., and N. P. Khosla. Stripping of Asphalt Pavements: State of the Art. In Transportation Research Record 911, TRB, National Research Council, Washington, D.C., pp. 150–158, 1983.
- Terrel, R.L., and S. Al-Swailmi. 1994. “Water Sensitivity of Asphalt-Aggregate Mixes: Test Selection.” SHRP-A-403. National Research Council. Washington, DC, 1994.
- Theyse, H. L. (2002). Stiffness, strength and performance of unbound aggregate material: Application of South African HVS and laboratory results of California flexible pavements (Report for the California Pavement Research Program). Richmond, VA: University of California, Pavement Research Center.
- Tiliouine, B. and Sandjak, K. 2014. Numerical simulation of granular materials behavior for unbound base layers used in Algerian pavement structures. *International Journal of Civil and Structural Engineering*, Vol. 4(3), pp.419-429.
- Tindall, J.A. and J.R. Kunkel. 1999. *Unsaturated Zone Hydrology for Scientists and Engineers*. New Jersey: Prentice Hall.
- Toryila, T. 2016. The effects of poor drainage system on road pavement: a review. *International Journal for Innovative Research in Multidisciplinary Field*. 2. 216-223.
- Tseng, K. and Lytton, R. 1989. “Prediction of Permanent Deformation in Flexible Pavement Materials. Implications of Aggregates in the Design, Construction and Performance of Asphalt Pavements”, ASTM STP 1016, pp. 154-172, American Society for Testing of Materials. (18) (PDF) Mechanistic-Empirical Pavement Design; A Brief Overview. Available from: U.S. Department of Transportation, Federal Highway Administration.
- Underwood. B.S, Kim, Y.R, Savadatti, S. Thirunavukkarasu, S. and Guddati, M. N. 2009. Response and fatigue performance modelling of ALF pavements using 3-D finite element analysis and a simplified viscoelastic continuum damage model. *Journal of the association of asphalt paving technologist*. Vol. 78, pp. 829-868
- van Genuchten, M. T. 1980. A closed-form equation for predicting the hydraulic conductivity of unsaturated soils. *Soil Sci. Soc. Am.*, 44, 892-898. 1980.

Vasconcellos, E.A., 2014. Urban Transport Environment and Equity: The Case for Developing Countries. New York, USA: Routledge.

Von Quintus, H.L., Mallela, J., and Lytton, R., 2003. Techniques for mitigation of reflective cracks. FAA worldwide airport technology transfer conference, April 2010. Atlantic City, NJ.

Walubita, L.F. and van de Ven, M.F. 2000. Stresses and Strains in Asphalt-Surfacing Pavements. South African Transport Conference Organised by: Conference Planners, 'Action in Transport for the New Millennium'.

Wang F, Hassan, A. N., and Fanzini, J. B. 1964. A method of analyzing unsteady, unsaturated flow in soils. *Journal of Geophysical Research*. Vol 69, Issue 12. June 1964 pp 2569-2577.

Wang, F. *et al.*, 2002. A survey study of current pavement related truck characteristics in Texas. Proceedings of the 30th Annual Canadian Society of Civil Engineering, CSCE, Conference, Montreal, Quebec, Canada.

Wang, L. P and Grandhi, R. V. 1995. Improved Two-point Function Approximation for Design Optimizaation. *AIAA Journal*. Vol. 32. 1995.

Wu, L., *et al.*, 2014. Improvement of Crack-Detection Accuracy Using a Novel Crack Defragmentation Technique in Image-Based Road Assessment. *Journal of Computing in Civil Engineering*, 30 (1).

Yang, C., Cui, Y. J., Pereira, J. M. & Huang, M. S. 2008. A constitutive model for unsaturated cemented soils under cyclic loading. *Computers and Geotechnics*, 35, pp. 853-859.

Yang, S., Lin, H., Kung, J. H. S. and Huang, W. 2008. Suction-controlled laboratory tests o resilient modulus of unsaturated compacted subgrade soils. *Journal of Geotechnical and Environmental Engineering*, 134 (9), pp. 1375-184.

Yesuf, G. Y. 2014. Implications of Nonlinear Behaviour of Subgrade Soils in Flexible Pavement Design. *International Journal of Pavement Engineering*, (Submitted).

Yin, H. 2013. The Impact of Strain Gage Instrumentation on Localized Strain Responses in Asphalt Concrete Pavements. *International Journal of Pavement Research and Technology*, 6(3), pp.225-234.

Witczak, M. W., Yoder, E. J. “Principles of Pavement Design” New York: John Wiley & Sons Inc., Second Edition, pp. 24-125, 1975.

Zafar R., Nassar, W. and Elbella, A. 2005. Interaction between Pavement Instrumentation and Hot-Mix-Asphalt in Flexible Pavements. *Emirates Journal for Engineering Research*, 10(1), pp.49-55.

Zafar, M., Shah, S. N. R., Jaffar, M., Rind, T. and Soomro, M. (2019). Condition Survey for Evaluation of Pavement Condition Index of a Highway. *Civil Engineering Journal*. 5. 1367-1383. 10.28991/cej-2019-03091338.

Zapata, P. and Gambatese, J. A., 2005. Energy consumption of asphalt and reinforced concrete pavement materials and construction. *ASCE Journal of Infrastructure Systems*, 11, 9–20.

Zhang C., Wang, H., You, Z. and Ma, B. 2015. Sensitivity Analysis of longitudinal cracking on asphalt pavement using MEPDG in Permafrost region. *Journal of Traffic and Transportation Engineering*. 2015; 2 (1); 40-47. 2095-7564/ ©2015 Periodical Offices of Chang'an University. Production and hosting by Elsevier B.V. on behalf of Owner. This is an open access article under the CC BY-NC-ND license (<http://creativecommons.org/licenses/by-nc-nd/4.0/>).

Zhang, J. 2006. A laboratory scale study of infiltration from Pervious Pavements. A thesis submitted in fulfillment of the requirements for the degree of Master of Engineering. School of Civil, Environmental and Chemical Engineering Science, Engineering and Technology Portfolio RMIT University.

Wu Z, Yang X and Zhang, Z. 2013 Evaluation of MEPDG flexible pavement design using pavement management system data: Louisiana experience, *International Journal of Pavement Engineering*, 14:7, 674-685, DOI: 10.1080/10298436.2012.723709

Zhang, Z. Gaspard, K. and Mostafa A. E. (2016) Evaluating pavement management treatment selection utilising continuous deflection measurements in flexible pavements, *International Journal of Pavement Engineering*, 17:5, 414-422, DOI: 10.1080/10298436.2014.993198

Zhou, F. and Sun, L. 2002. Reflection Cracking in Asphalt Overlay on Existing PCC, Proceedings of the 9th International Conference on Asphalt Pavements, Copenhagen.

Zubeck, H. and Doré, G. 2009. Introduction to Cold Regions Pavement Engineering. 337-345. 10.1061/41072(359)33.

Zumrawi, M. 2016. Investigating surface drainage problem of roads in Khartoum state. Available from: https://www.researchgate.net/publication/303443909_Investigating_surface_drainage_problem_of_roads_in_Khartoum_state [accessed Jan 13, 2020].

APPENDIX I

GRIFFITH ENERGY RELEASE FOR PAVEMENT FAILURE CONSIDERING TEMPERATURE AS ENVIRONMENTAL INPUT PARAMETERS

| Time | Temperature 1 | Temperature 2 | Temperature 3 | GT (T1) | GT(T2) | GT(T3) | E (T1) | E(T2) | E(T3) |
|------|---------------|---------------|---------------|----------|----------|----------|----------|----------|----------|
| 10 | 23,87 | 24,06 | 23,44 | 1,751691 | 1,710227 | 1,847944 | 398204,4 | 395738,2 | 403842,5 |
| 20 | 24,62 | 24,75 | 24,25 | 1,59182 | 1,565145 | 1,669416 | 388558,1 | 386910 | 393287,4 |
| 30 | 25,06 | 25 | 24,69 | 1,502769 | 1,514706 | 1,577419 | 383008,1 | 383760,3 | 387669,8 |
| 40 | 24,94 | 24,87 | 24,69 | 1,526708 | 1,540793 | 1,577419 | 384513,9 | 385394,9 | 387669,8 |
| 50 | 25,12 | 25,06 | 24,87 | 1,490896 | 1,502769 | 1,540793 | 382257,5 | 383008,1 | 385394,9 |
| 60 | 25,37 | 25,19 | 25,19 | 1,442125 | 1,477127 | 1,477127 | 379145,6 | 381383,6 | 381383,6 |
| 70 | 25,75 | 25,62 | 25,5 | 1,370139 | 1,394475 | 1,417207 | 374463,9 | 376059 | 377537,4 |
| 80 | 26,06 | 25,94 | 25,81 | 1,31332 | 1,335112 | 1,359008 | 370687,6 | 372144,8 | 373730 |
| 90 | 26,12 | 25,94 | 25,94 | 1,302519 | 1,335112 | 1,335112 | 369961 | 372144,8 | 372144,8 |
| 100 | 26,19 | 26 | 26 | 1,289999 | 1,324184 | 1,324184 | 369115,3 | 371415,5 | 371415,5 |
| 110 | 26,37 | 26,25 | 26,19 | 1,2582 | 1,279336 | 1,289999 | 366949,2 | 368391,8 | 369115,3 |
| 120 | 26,69 | 26,56 | 26,5 | 1,203068 | 1,22525 | 1,235587 | 363129,9 | 364676,7 | 365392,8 |

| | | | | | | | | | |
|-----|-------|-------|-------|----------|----------|----------|----------|----------|----------|
| 130 | 26,94 | 26,81 | 26,75 | 1,161233 | 1,182852 | 1,192929 | 360173,7 | 361707,9 | 362418,2 |
| 140 | 27,12 | 26,75 | 26,87 | 1,131777 | 1,192929 | 1,172838 | 358060,2 | 362418,2 | 360999 |
| 150 | 27,12 | 26,75 | 26,87 | 1,131777 | 1,192929 | 1,172838 | 358060,2 | 362418,2 | 360999 |
| 160 | 27,12 | 26,69 | 26,94 | 1,131777 | 1,203068 | 1,161233 | 358060,2 | 363129,9 | 360173,7 |
| 170 | 27,06 | 26,62 | 26,87 | 1,141534 | 1,214976 | 1,172838 | 358763,3 | 363962 | 360999 |
| 180 | 27,25 | 26,94 | 27,06 | 1,110848 | 1,161233 | 1,141534 | 356541,4 | 360173,7 | 358763,3 |
| 190 | 27,5 | 27,06 | 27,25 | 1,071404 | 1,141534 | 1,110848 | 353638,9 | 358763,3 | 356541,4 |
| 201 | 27,75 | 27,12 | 27,44 | 1,03301 | 1,131777 | 1,080775 | 350760 | 358060,2 | 354333,3 |
| 211 | 28,19 | 27,56 | 27,81 | 0,967949 | 1,062094 | 1,02395 | 345749,8 | 352945,8 | 350072,5 |
| 221 | 28,62 | 27,75 | 28,19 | 0,907405 | 1,03301 | 0,967949 | 340922,8 | 350760 | 345749,8 |
| 231 | 28,56 | 27,56 | 28,12 | 0,915675 | 1,062094 | 0,978088 | 341592,2 | 352945,8 | 346542,1 |
| 241 | 28,81 | 27,87 | 28,37 | 0,881591 | 1,01495 | 0,942244 | 338811,4 | 349386,4 | 343720,9 |
| 251 | 28,44 | 27,56 | 28,19 | 0,932388 | 1,062094 | 0,967949 | 342935,1 | 352945,8 | 345749,8 |
| 261 | 27,62 | 26,94 | 27,62 | 1,052845 | 1,161233 | 1,052845 | 352254,1 | 360173,7 | 352254,1 |
| 271 | 27,12 | 26,69 | 27,12 | 1,131777 | 1,203068 | 1,131777 | 358060,2 | 363129,9 | 358060,2 |
| 281 | 26,81 | 26,31 | 26,81 | 1,182852 | 1,268736 | 1,182852 | 361707,9 | 367669,8 | 361707,9 |
| 291 | 26,37 | 25,94 | 26,37 | 1,2582 | 1,335112 | 1,2582 | 366949,2 | 372144,8 | 366949,2 |
| 301 | 26,25 | 25,94 | 26,19 | 1,279336 | 1,335112 | 1,289999 | 368391,8 | 372144,8 | 369115,3 |

| | | | | | | | | | |
|-----|-------|-------|-------|----------|----------|----------|----------|----------|----------|
| 311 | 26,31 | 26,06 | 26,25 | 1,268736 | 1,31332 | 1,279336 | 367669,8 | 370687,6 | 368391,8 |
| 321 | 26,75 | 26,25 | 26,62 | 1,192929 | 1,279336 | 1,214976 | 362418,2 | 368391,8 | 363962 |
| 331 | 27,25 | 26,31 | 27,19 | 1,110848 | 1,268736 | 1,120472 | 356541,4 | 367669,8 | 357241,6 |
| 341 | 27,62 | 26,5 | 27,5 | 1,052845 | 1,235587 | 1,071404 | 352254,1 | 365392,8 | 353638,9 |
| 351 | 27,75 | 26,56 | 27,62 | 1,03301 | 1,22525 | 1,052845 | 350760 | 364676,7 | 352254,1 |
| 361 | 27,87 | 26,69 | 27,81 | 1,01495 | 1,203068 | 1,02395 | 349386,4 | 363129,9 | 350072,5 |
| 372 | 27,87 | 26,69 | 27,81 | 1,01495 | 1,203068 | 1,02395 | 349386,4 | 363129,9 | 350072,5 |
| 382 | 27,56 | 26,37 | 27,56 | 1,062094 | 1,2582 | 1,062094 | 352945,8 | 366949,2 | 352945,8 |
| 392 | 27,44 | 26,06 | 27,37 | 1,080775 | 1,31332 | 1,091783 | 354333,3 | 370687,6 | 355145,2 |
| 402 | 27,19 | 25,81 | 27,12 | 1,120472 | 1,359008 | 1,131777 | 357241,6 | 373730 | 358060,2 |
| 412 | 26,5 | 25,56 | 26,62 | 1,235587 | 1,405809 | 1,214976 | 365392,8 | 376797,5 | 363962 |
| 422 | 25,75 | 25 | 25,94 | 1,370139 | 1,514706 | 1,335112 | 374463,9 | 383760,3 | 372144,8 |
| 432 | 25,19 | 24,5 | 25,37 | 1,477127 | 1,616715 | 1,442125 | 381383,6 | 390085,7 | 379145,6 |
| 442 | 24,81 | 24,25 | 25 | 1,552937 | 1,669416 | 1,514706 | 386151,7 | 393287,4 | 383760,3 |
| 452 | 24,56 | 23,94 | 24,69 | 1,604235 | 1,736339 | 1,577419 | 389321,2 | 397294 | 387669,8 |
| 462 | 24,37 | 23,75 | 24,5 | 1,643978 | 1,778216 | 1,616715 | 391747,3 | 399769,8 | 390085,7 |
| 472 | 24,12 | 23,44 | 24,25 | 1,697269 | 1,847944 | 1,669416 | 394962,6 | 403842,5 | 393287,4 |
| 482 | 23,81 | 23,12 | 24 | 1,764921 | 1,921736 | 1,72325 | 398986,3 | 408090 | 396515,3 |

| | | | | | | | | | |
|-----|-------|-------|-------|----------|----------|----------|----------|----------|----------|
| 492 | 23,44 | 22,75 | 23,69 | 1,847944 | 2,009345 | 1,791576 | 403842,5 | 413057 | 400554,9 |
| 502 | 23,12 | 22,37 | 23,31 | 1,921736 | 2,101853 | 1,8777 | 408090 | 418221,2 | 405562,7 |
| 512 | 22,87 | 22,06 | 23,06 | 1,980664 | 2,179199 | 1,935777 | 411439,5 | 422481,8 | 408891,4 |
| 522 | 22,62 | 21,94 | 22,81 | 2,040706 | 2,209588 | 1,994973 | 414816,5 | 424142,7 | 412247,5 |
| 532 | 22,31 | 21,5 | 22,56 | 2,116692 | 2,323129 | 2,055281 | 419042,4 | 430288,8 | 415631,1 |
| 542 | 21,94 | 21,19 | 22,25 | 2,209588 | 2,40509 | 2,131595 | 424142,7 | 434672,3 | 419865,3 |
| 553 | 21,81 | 21,06 | 22,06 | 2,24279 | 2,439936 | 2,179199 | 425949,4 | 436523,9 | 422481,8 |
| 563 | 21,75 | 21 | 22 | 2,258211 | 2,456113 | 2,194362 | 426785,8 | 437381,1 | 423311,4 |
| 573 | 21,62 | 20,87 | 21,87 | 2,291836 | 2,491364 | 2,22743 | 428603,8 | 439244,2 | 425114,6 |
| 583 | 21,25 | 20,37 | 21,56 | 2,389102 | 2,629474 | 2,307452 | 433820,4 | 446484,1 | 429445,4 |
| 593 | 21 | 20,12 | 21,31 | 2,456113 | 2,699997 | 2,373173 | 437381,1 | 450148,7 | 432970,2 |
| 603 | 20,81 | 20 | 21,12 | 2,507726 | 2,734188 | 2,423819 | 440106,7 | 451918,4 | 435668,3 |
| 613 | 20,75 | 19,94 | 21,06 | 2,524147 | 2,751364 | 2,439936 | 440971 | 452805,8 | 436523,9 |
| 623 | 20,69 | 19,81 | 20,94 | 2,540625 | 2,788764 | 2,472349 | 441836,9 | 454734,6 | 438240 |
| 633 | 20,62 | 19,75 | 20,87 | 2,559922 | 2,806109 | 2,491364 | 442849,3 | 455627,6 | 439244,2 |
| 643 | 20,37 | 19,5 | 20,69 | 2,629474 | 2,878945 | 2,540625 | 446484,1 | 459367,2 | 441836,9 |
| 653 | 20,06 | 19,31 | 20,44 | 2,717065 | 2,934895 | 2,6099 | 451032,7 | 462229,9 | 445463,4 |
| 663 | 19,81 | 19,12 | 20,31 | 2,788764 | 2,991345 | 2,646311 | 454734,6 | 465110,3 | 447360,9 |

| | | | | | | | | | |
|-----|-------|-------|-------|----------|----------|----------|----------|----------|----------|
| 673 | 19,87 | 19,06 | 20,25 | 2,771471 | 3,009274 | 2,663205 | 453843,4 | 466023,7 | 448239,4 |
| 683 | 20 | 19,06 | 20,12 | 2,734188 | 3,009274 | 2,699997 | 451918,4 | 466023,7 | 450148,7 |
| 693 | 20 | 19 | 19,94 | 2,734188 | 3,02725 | 2,751364 | 451918,4 | 466938,8 | 452805,8 |
| 703 | 19,62 | 18,69 | 19,75 | 2,843871 | 3,120882 | 2,806109 | 457568,4 | 471695,8 | 455627,6 |
| 713 | 19,19 | 18,31 | 19,5 | 2,97049 | 3,237309 | 2,878945 | 464047 | 477593,1 | 459367,2 |
| 724 | 18,81 | 18,12 | 19,25 | 3,08449 | 3,296171 | 2,952668 | 469848,7 | 480569,3 | 463137,6 |
| 734 | 18,75 | 18 | 19,12 | 3,102663 | 3,333561 | 2,991345 | 470771,3 | 482458,5 | 465110,3 |
| 744 | 18,62 | 17,87 | 19 | 3,142195 | 3,374247 | 3,02725 | 472776,6 | 484513,6 | 466938,8 |
| 754 | 18,56 | 17,81 | 18,94 | 3,160512 | 3,393087 | 3,045275 | 473705 | 485465,1 | 467855,8 |
| 764 | 18,56 | 17,81 | 18,87 | 3,160512 | 3,393087 | 3,066363 | 473705 | 485465,1 | 468927,8 |
| 774 | 18,5 | 17,75 | 18,87 | 3,178874 | 3,411965 | 3,066363 | 474635,3 | 486418,4 | 468927,8 |
| 784 | 18,37 | 17,56 | 18,75 | 3,218809 | 3,471995 | 3,102663 | 476657 | 489449,6 | 470771,3 |
| 794 | 18,19 | 17,37 | 18,56 | 3,274436 | 3,532388 | 3,160512 | 479470,6 | 492499,7 | 473705 |
| 804 | 18 | 17,25 | 18,37 | 3,333561 | 3,57071 | 3,218809 | 482458,5 | 494435,9 | 476657 |
| 814 | 17,81 | 17,06 | 18,25 | 3,393087 | 3,631658 | 3,255852 | 485465,1 | 497517,1 | 478530,9 |
| 824 | 17,62 | 16,94 | 18,12 | 3,452998 | 3,670315 | 3,296171 | 488490,4 | 499473 | 480569,3 |
| 834 | 17,5 | 16,81 | 18 | 3,491028 | 3,71233 | 3,333561 | 490410,8 | 501600,5 | 482458,5 |
| 844 | 17,37 | 16,69 | 17,87 | 3,532388 | 3,751234 | 3,374247 | 492499,7 | 503572,5 | 484513,6 |

| | | | | | | | | | |
|------|-------|-------|-------|----------|----------|----------|----------|----------|----------|
| 854 | 17,19 | 16,44 | 17,69 | 3,589922 | 3,832635 | 3,430882 | 495406,8 | 507705,7 | 487373,6 |
| 864 | 16,87 | 16,19 | 17,37 | 3,692921 | 3,914473 | 3,532388 | 500617,5 | 511872,7 | 492499,7 |
| 874 | 16,56 | 15,88 | 17,12 | 3,793505 | 4,016489 | 3,612376 | 505717,5 | 517087,5 | 496542 |
| 884 | 16,31 | 15,56 | 16,87 | 3,87514 | 4,122326 | 3,692921 | 509868,3 | 522526,1 | 500617,5 |
| 894 | 16,12 | 15,31 | 16,62 | 3,93746 | 4,205319 | 3,77398 | 513045,6 | 526814,8 | 504726,4 |
| 905 | 15,94 | 15,19 | 16,5 | 3,996701 | 4,245235 | 3,813057 | 516074 | 528885,9 | 506710,6 |
| 915 | 15,94 | 15,19 | 16,37 | 3,996701 | 4,245235 | 3,855508 | 516074 | 528885,9 | 508869 |
| 925 | 16,06 | 15,19 | 16,25 | 3,957186 | 4,245235 | 3,894795 | 514053,1 | 528885,9 | 510869,5 |
| 935 | 16,25 | 15,25 | 16,19 | 3,894795 | 4,225271 | 3,914473 | 510869,5 | 527849,4 | 511872,7 |
| 945 | 16,37 | 15,25 | 16,06 | 3,855508 | 4,225271 | 3,957186 | 508869 | 527849,4 | 514053,1 |
| 955 | 16,37 | 15,19 | 15,94 | 3,855508 | 4,245235 | 3,996701 | 508869 | 528885,9 | 516074 |
| 965 | 16,31 | 15 | 15,81 | 3,87514 | 4,308522 | 4,039598 | 509868,3 | 532181,8 | 518272,3 |
| 975 | 16,19 | 14,94 | 15,63 | 3,914473 | 4,328527 | 4,099133 | 511872,7 | 533226,8 | 521331,5 |
| 985 | 16 | 14,75 | 15,44 | 3,976934 | 4,391922 | 4,162133 | 515062,6 | 536549,8 | 524580,3 |
| 995 | 15,88 | 14,63 | 15,31 | 4,016489 | 4,43199 | 4,205319 | 517087,5 | 538659,1 | 526814,8 |
| 1005 | 15,5 | 14,44 | 15,25 | 4,142222 | 4,495462 | 4,225271 | 523552,2 | 542015,9 | 527849,4 |
| 1015 | 15,19 | 14,31 | 15,25 | 4,245235 | 4,538899 | 4,225271 | 528885,9 | 544324,6 | 527849,4 |
| 1025 | 15,13 | 14,13 | 15,13 | 4,26521 | 4,59904 | 4,26521 | 529924,5 | 547537,7 | 529924,5 |

| | | | | | | | | | |
|------|-------|-------|-------|----------|----------|----------|----------|----------|----------|
| 1035 | 15,13 | 14,13 | 15,06 | 4,26521 | 4,59904 | 4,288527 | 529924,5 | 547537,7 | 531138,8 |
| 1045 | 15,25 | 14,06 | 15 | 4,225271 | 4,622423 | 4,308522 | 527849,4 | 548792,3 | 532181,8 |
| 1055 | 15,31 | 14,06 | 14,88 | 4,205319 | 4,622423 | 4,348539 | 526814,8 | 548792,3 | 534274 |
| 1065 | 15,31 | 13,94 | 14,69 | 4,205319 | 4,662496 | 4,411954 | 526814,8 | 550949,8 | 537603,4 |
| 1076 | 15,25 | 13,88 | 14,5 | 4,225271 | 4,682526 | 4,475415 | 527849,4 | 552031,7 | 540953,6 |
| 1086 | 15,19 | 13,75 | 14,38 | 4,245235 | 4,725901 | 4,51551 | 528885,9 | 554383,1 | 543080,2 |
| 1096 | 15,06 | 13,63 | 14,31 | 4,288527 | 4,765908 | 4,538899 | 531138,8 | 556562,6 | 544324,6 |
| 1106 | 15 | 13,5 | 14,19 | 4,308522 | 4,809206 | 4,578995 | 532181,8 | 558933,3 | 546464,6 |
| 1116 | 14,88 | 13,38 | 14 | 4,348539 | 4,849127 | 4,642462 | 534274 | 561130,7 | 549870 |
| 1126 | 14,69 | 13,19 | 13,88 | 4,411954 | 4,912228 | 4,682526 | 537603,4 | 564627,5 | 552031,7 |
| 1136 | 14,5 | 13 | 13,63 | 4,475415 | 4,975175 | 4,765908 | 540953,6 | 568146,1 | 556562,6 |
| 1146 | 14,31 | 12,88 | 13,44 | 4,538899 | 5,014839 | 4,829172 | 544324,6 | 570379,6 | 560030,9 |
| 1156 | 14,19 | 12,63 | 13,25 | 4,578995 | 5,097209 | 4,892317 | 546464,6 | 575061,1 | 563520,9 |
| 1166 | 14 | 12,5 | 13,19 | 4,642462 | 5,139884 | 4,912228 | 549870 | 577510,7 | 564627,5 |
| 1176 | 13,88 | 12,38 | 13,06 | 4,682526 | 5,179172 | 4,955315 | 552031,7 | 579781 | 567032,6 |
| 1186 | 13,81 | 12,25 | 12,94 | 4,705885 | 5,221612 | 4,995016 | 553296,6 | 582250,7 | 569261,7 |
| 1196 | 13,69 | 12,25 | 13 | 4,745908 | 5,221612 | 4,975175 | 555471,8 | 582250,7 | 568146,1 |
| 1206 | 13,5 | 12,19 | 13,13 | 4,809206 | 5,241154 | 4,932124 | 558933,3 | 583394,1 | 565736,2 |

| | | | | | | | | | |
|------|-------|-------|-------|----------|----------|----------|----------|----------|----------|
| 1216 | 13,25 | 12,13 | 13,19 | 4,892317 | 5,260667 | 4,912228 | 563520,9 | 584539,7 | 564627,5 |
| 1226 | 13,13 | 12,19 | 13,25 | 4,932124 | 5,241154 | 4,892317 | 565736,2 | 583394,1 | 563520,9 |
| 1236 | 13,31 | 12,31 | 13,38 | 4,872391 | 5,202041 | 4,849127 | 562416,4 | 581109,5 | 561130,7 |
| 1247 | 13,69 | 12,63 | 13,63 | 4,745908 | 5,097209 | 4,765908 | 555471,8 | 575061,1 | 556562,6 |
| 1257 | 14,13 | 13,13 | 13,94 | 4,59904 | 4,932124 | 4,662496 | 547537,7 | 565736,2 | 550949,8 |
| 1267 | 14,5 | 13,63 | 14,31 | 4,475415 | 4,765908 | 4,538899 | 540953,6 | 556562,6 | 544324,6 |
| 1277 | 14,81 | 14,06 | 14,63 | 4,371895 | 4,622423 | 4,43199 | 535498,2 | 548792,3 | 538659,1 |
| 1287 | 15,13 | 14,38 | 14,94 | 4,26521 | 4,51551 | 4,328527 | 529924,5 | 543080,2 | 533226,8 |
| 1297 | 15,44 | 14,88 | 15,31 | 4,162133 | 4,348539 | 4,205319 | 524580,3 | 534274 | 526814,8 |
| 1307 | 15,81 | 15,31 | 15,69 | 4,039598 | 4,205319 | 4,079271 | 518272,3 | 526814,8 | 520309,8 |
| 1317 | 16,25 | 15,88 | 16,19 | 3,894795 | 4,016489 | 3,914473 | 510869,5 | 517087,5 | 511872,7 |
| 1327 | 16,69 | 16,44 | 16,62 | 3,751234 | 3,832635 | 3,77398 | 503572,5 | 507705,7 | 504726,4 |
| 1337 | 17,06 | 16,94 | 17 | 3,631658 | 3,670315 | 3,650971 | 497517,1 | 499473 | 498494,1 |
| 1347 | 17,44 | 17,31 | 17,37 | 3,510097 | 3,551532 | 3,532388 | 491373,8 | 493466,9 | 492499,7 |
| 1357 | 17,75 | 17,69 | 17,69 | 3,411965 | 3,430882 | 3,430882 | 486418,4 | 487373,6 | 487373,6 |
| 1367 | 18 | 18,06 | 18 | 3,333561 | 3,314846 | 3,333561 | 482458,5 | 481513 | 482458,5 |
| 1377 | 18,31 | 18,37 | 18,31 | 3,237309 | 3,218809 | 3,237309 | 477593,1 | 476657 | 477593,1 |
| 1387 | 18,62 | 18,69 | 18,62 | 3,142195 | 3,120882 | 3,142195 | 472776,6 | 471695,8 | 472776,6 |

| | | | | | | | | | |
|------|-------|-------|-------|----------|----------|----------|----------|----------|----------|
| 1397 | 18,87 | 19,06 | 18,94 | 3,066363 | 3,009274 | 3,045275 | 468927,8 | 466023,7 | 467855,8 |
| 1407 | 19,19 | 19,37 | 19,25 | 2,97049 | 2,917172 | 2,952668 | 464047 | 461323,9 | 463137,6 |
| 1418 | 19,44 | 19,75 | 19,62 | 2,896559 | 2,806109 | 2,843871 | 460269,3 | 455627,6 | 457568,4 |
| 1428 | 20,12 | 20,5 | 20,25 | 2,699997 | 2,593184 | 2,663205 | 450148,7 | 444590,3 | 448239,4 |
| 1438 | 21,06 | 21,5 | 21 | 2,439936 | 2,323129 | 2,456113 | 436523,9 | 430288,8 | 437381,1 |
| 1448 | 21,87 | 22,31 | 21,69 | 2,22743 | 2,116692 | 2,273695 | 425114,6 | 419042,4 | 427623,9 |
| 1458 | 22,37 | 23 | 22,12 | 2,101853 | 1,949882 | 2,164098 | 418221,2 | 409694,4 | 421653,8 |
| 1468 | 22,69 | 23,12 | 22,44 | 2,023782 | 1,921736 | 2,084621 | 413868,1 | 408090 | 417265 |
| 1478 | 23,12 | 23,62 | 22,94 | 1,921736 | 1,807246 | 1,964052 | 408090 | 401472,7 | 410498,9 |
| 1488 | 23,56 | 24,25 | 23,56 | 1,820747 | 1,669416 | 1,820747 | 402261,1 | 393287,4 | 402261,1 |
| 1498 | 24,12 | 25,12 | 24,19 | 1,697269 | 1,490896 | 1,682233 | 394962,6 | 382257,5 | 394059,7 |
| 1508 | 24,81 | 25,87 | 24,75 | 1,552937 | 1,347942 | 1,565145 | 386151,7 | 372997,6 | 386910 |
| 1518 | 25,44 | 26,31 | 25,37 | 1,42867 | 1,268736 | 1,442125 | 378278,8 | 367669,8 | 379145,6 |
| 1528 | 25,62 | 26,25 | 25,69 | 1,394475 | 1,279336 | 1,381334 | 376059 | 368391,8 | 375199,3 |
| 1538 | 25,87 | 26,25 | 26,06 | 1,347942 | 1,279336 | 1,31332 | 372997,6 | 368391,8 | 370687,6 |
| 1548 | 26,31 | 27,25 | 26,44 | 1,268736 | 1,110848 | 1,245987 | 367669,8 | 356541,4 | 366110,3 |
| 1558 | 26,75 | 27,69 | 26,87 | 1,192929 | 1,04213 | 1,172838 | 362418,2 | 351448,7 | 360999 |
| 1568 | 27,25 | 28,37 | 27,31 | 1,110848 | 0,942244 | 1,101285 | 356541,4 | 343720,9 | 355842,7 |

| | | | | | | | | | |
|------|-------|-------|-------|----------|----------|----------|----------|----------|----------|
| 1578 | 27,94 | 28,94 | 27,87 | 1,004525 | 0,864256 | 1,01495 | 348587,7 | 337374,3 | 349386,4 |
| 1588 | 28,44 | 29,31 | 28,44 | 0,932388 | 0,81635 | 0,932388 | 342935,1 | 333317,4 | 342935,1 |
| 1599 | 28,94 | 30 | 28,81 | 0,864256 | 0,732535 | 0,881591 | 337374,3 | 325881,7 | 338811,4 |
| 1609 | 29,06 | 30,06 | 29,12 | 0,848488 | 0,725578 | 0,840687 | 336053,2 | 325243 | 335394,5 |
| 1619 | 29,31 | 30,69 | 29,75 | 0,81635 | 0,655627 | 0,762087 | 333317,4 | 318611,9 | 328556,5 |
| 1629 | 29,87 | 31,5 | 30,37 | 0,747788 | 0,573685 | 0,690457 | 327269,9 | 310284,4 | 321963 |
| 1639 | 30,81 | 32,56 | 31,12 | 0,642931 | 0,479132 | 0,611038 | 317364,2 | 299714,7 | 314163,7 |
| 1649 | 31,69 | 33,63 | 31,94 | 0,55571 | 0,397017 | 0,532755 | 308362,8 | 289410,3 | 305852,5 |
| 1659 | 32,5 | 34,38 | 32,75 | 0,48412 | 0,346714 | 0,463612 | 300303,2 | 282399,5 | 297858,5 |
| 1669 | 33,25 | 35,19 | 33,13 | 0,424732 | 0,298493 | 0,433808 | 293028,6 | 275018,6 | 294180,6 |
| 1679 | 33,5 | 34,81 | 33,25 | 0,406325 | 0,32036 | 0,424732 | 290643,1 | 278456,9 | 293028,6 |
| 1689 | 32,94 | 34 | 32,56 | 0,448507 | 0,371491 | 0,479132 | 296013,8 | 285930,2 | 299714,7 |
| 1699 | 31,75 | 32,38 | 31,31 | 0,550129 | 0,494225 | 0,592125 | 307758,5 | 301483,8 | 312218 |
| 1709 | 30,94 | 31 | 30,31 | 0,629399 | 0,62323 | 0,697148 | 316018,1 | 315398,8 | 322595,3 |
| 1719 | 30,19 | 30,06 | 29,62 | 0,710683 | 0,725578 | 0,777818 | 323863,5 | 325243 | 329956 |
| 1729 | 29,75 | 29,56 | 29,25 | 0,762087 | 0,785163 | 0,823976 | 328556,5 | 330603,9 | 333972 |
| 1739 | 29,69 | 29,5 | 29,25 | 0,769316 | 0,792562 | 0,823976 | 329201,6 | 331253,1 | 333972 |
| 1749 | 29,81 | 29,75 | 29,69 | 0,754911 | 0,762087 | 0,769316 | 327912,5 | 328556,5 | 329201,6 |

| | | | | | | | | | |
|------|-------|-------|-------|----------|----------|----------|----------|----------|----------|
| 1759 | 30,25 | 31,06 | 30,62 | 0,70389 | 0,61711 | 0,663124 | 323228,8 | 314780,6 | 319342 |
| 1770 | 30,94 | 33,25 | 31,94 | 0,629399 | 0,424732 | 0,532755 | 316018,1 | 293028,6 | 305852,5 |
| 1780 | 32,31 | 35,56 | 33,5 | 0,500198 | 0,278426 | 0,406325 | 302174,6 | 271711,5 | 290643,1 |
| 1790 | 33,06 | 36,88 | 34,38 | 0,439177 | 0,215901 | 0,346714 | 294854,7 | 260234 | 282399,5 |
| 1800 | 33,5 | 37,38 | 34,88 | 0,406325 | 0,195587 | 0,316233 | 290643,1 | 256014,2 | 277820,3 |
| 1810 | 33,38 | 37,75 | 35,13 | 0,415076 | 0,181637 | 0,301859 | 291785,7 | 252935,6 | 275558,6 |
| 1820 | 33,56 | 36,88 | 35,31 | 0,402007 | 0,215901 | 0,291855 | 290073,5 | 260234 | 273941,6 |
| 1830 | 33,69 | 37,5 | 35,06 | 0,392782 | 0,190965 | 0,305827 | 288843,1 | 255011,6 | 276190 |
| 1840 | 33,31 | 36,19 | 34,25 | 0,420252 | 0,246891 | 0,35503 | 292454,3 | 266171,8 | 283602,5 |
| 1850 | 32,44 | 34,13 | 32,94 | 0,489151 | 0,362853 | 0,448507 | 300892,9 | 284717,4 | 296013,8 |
| 1860 | 31,62 | 32,44 | 31,62 | 0,562279 | 0,489151 | 0,562279 | 309069,4 | 300892,9 | 309069,4 |
| 1870 | 30,81 | 31,19 | 30,75 | 0,642931 | 0,604014 | 0,649254 | 317364,2 | 313445,5 | 317987,5 |
| 1880 | 30,12 | 30,19 | 30 | 0,718673 | 0,710683 | 0,732535 | 324605,6 | 323863,5 | 325881,7 |
| 1890 | 29,62 | 29,44 | 29,44 | 0,777818 | 0,800015 | 0,800015 | 329956 | 331903,6 | 331903,6 |
| 1900 | 29,19 | 28,94 | 29 | 0,831657 | 0,864256 | 0,856344 | 334627,8 | 337374,3 | 336713,1 |
| 1910 | 28,81 | 28,44 | 28,56 | 0,881591 | 0,932388 | 0,915675 | 338811,4 | 342935,1 | 341592,2 |
| 1920 | 28,37 | 27,94 | 28,19 | 0,942244 | 1,004525 | 0,967949 | 343720,9 | 348587,7 | 345749,8 |
| 1930 | 28 | 27,5 | 27,87 | 0,995654 | 1,071404 | 1,01495 | 347904,5 | 353638,9 | 349386,4 |

| | | | | | | | | | |
|------|-------|-------|-------|----------|----------|----------|----------|----------|----------|
| 1941 | 27,56 | 27,06 | 27,5 | 1,062094 | 1,141534 | 1,071404 | 352945,8 | 358763,3 | 353638,9 |
| 1951 | 27,06 | 26,62 | 27,12 | 1,141534 | 1,214976 | 1,131777 | 358763,3 | 363962 | 358060,2 |
| 1961 | 26,44 | 26,06 | 26,69 | 1,245987 | 1,31332 | 1,203068 | 366110,3 | 370687,6 | 363129,9 |
| 1971 | 25,81 | 25,5 | 26,25 | 1,359008 | 1,417207 | 1,279336 | 373730 | 377537,4 | 368391,8 |
| 1981 | 25,12 | 24,94 | 25,75 | 1,490896 | 1,526708 | 1,370139 | 382257,5 | 384513,9 | 374463,9 |
| 1991 | 24,69 | 24,44 | 25,31 | 1,577419 | 1,62926 | 1,453727 | 387669,8 | 390851,7 | 379890,1 |
| 2001 | 24,37 | 24,06 | 25 | 1,643978 | 1,710227 | 1,514706 | 391747,3 | 395738,2 | 383760,3 |
| 2011 | 24,25 | 23,75 | 24,62 | 1,669416 | 1,778216 | 1,59182 | 393287,4 | 399769,8 | 388558,1 |
| 2021 | 24,06 | 23,37 | 24,31 | 1,710227 | 1,863928 | 1,656664 | 395738,2 | 404767,8 | 392516,6 |
| 2031 | 23,81 | 23,06 | 23,94 | 1,764921 | 1,935777 | 1,736339 | 398986,3 | 408891,4 | 397294 |
| 2041 | 23,44 | 22,75 | 23,62 | 1,847944 | 2,009345 | 1,807246 | 403842,5 | 413057 | 401472,7 |
| 2051 | 22,87 | 22,37 | 23,31 | 1,980664 | 2,101853 | 1,8777 | 411439,5 | 418221,2 | 405562,7 |
| 2061 | 22,56 | 21,81 | 22,94 | 2,055281 | 2,24279 | 1,964052 | 415631,1 | 425949,4 | 410498,9 |
| 2071 | 22,56 | 21,56 | 22,44 | 2,055281 | 2,307452 | 2,084621 | 415631,1 | 429445,4 | 417265 |
| 2081 | 22,44 | 21,31 | 22,12 | 2,084621 | 2,373173 | 2,164098 | 417265 | 432970,2 | 421653,8 |
| 2091 | 22,19 | 20,94 | 21,81 | 2,14656 | 2,472349 | 2,24279 | 420689,8 | 438240 | 425949,4 |
| 2101 | 22,12 | 20,75 | 21,5 | 2,164098 | 2,524147 | 2,323129 | 421653,8 | 440971 | 430288,8 |
| 2112 | 22,06 | 20,56 | 21,37 | 2,179199 | 2,576525 | 2,357304 | 422481,8 | 443719 | 432121,6 |

| | | | | | | | | | |
|------|-------|-------|-------|----------|----------|----------|----------|----------|----------|
| 2122 | 22 | 20,5 | 21,25 | 2,194362 | 2,593184 | 2,389102 | 423311,4 | 444590,3 | 433820,4 |
| 2132 | 21,87 | 20,5 | 21,19 | 2,22743 | 2,593184 | 2,40509 | 425114,6 | 444590,3 | 434672,3 |
| 2142 | 21,75 | 20,31 | 21,06 | 2,258211 | 2,646311 | 2,439936 | 426785,8 | 447360,9 | 436523,9 |
| 2152 | 21,56 | 20,12 | 20,87 | 2,307452 | 2,699997 | 2,491364 | 429445,4 | 450148,7 | 439244,2 |
| 2162 | 21,37 | 20 | 20,69 | 2,357304 | 2,734188 | 2,540625 | 432121,6 | 451918,4 | 441836,9 |
| 2172 | 21,19 | 19,75 | 20,5 | 2,40509 | 2,806109 | 2,593184 | 434672,3 | 455627,6 | 444590,3 |
| 2182 | 20,94 | 19,5 | 20,25 | 2,472349 | 2,878945 | 2,663205 | 438240 | 459367,2 | 448239,4 |
| 2192 | 20,69 | 19,31 | 20 | 2,540625 | 2,934895 | 2,734188 | 441836,9 | 462229,9 | 451918,4 |
| 2202 | 20,44 | 19 | 19,69 | 2,6099 | 3,02725 | 2,823508 | 445463,4 | 466938,8 | 456522,3 |
| 2212 | 20,19 | 18,69 | 19,44 | 2,680154 | 3,120882 | 2,896559 | 449119,6 | 471695,8 | 460269,3 |
| 2222 | 20 | 18,5 | 19,25 | 2,734188 | 3,178874 | 2,952668 | 451918,4 | 474635,3 | 463137,6 |
| 2232 | 19,81 | 18,37 | 19,12 | 2,788764 | 3,218809 | 2,991345 | 454734,6 | 476657 | 465110,3 |
| 2242 | 19,69 | 18,25 | 18,94 | 2,823508 | 3,255852 | 3,045275 | 456522,3 | 478530,9 | 467855,8 |
| 2252 | 19,56 | 18,12 | 18,81 | 2,861382 | 3,296171 | 3,08449 | 458466,9 | 480569,3 | 469848,7 |
| 2262 | 19,37 | 17,94 | 18,62 | 2,917172 | 3,352316 | 3,142195 | 461323,9 | 483406 | 472776,6 |
| 2272 | 19,25 | 17,81 | 18,5 | 2,952668 | 3,393087 | 3,178874 | 463137,6 | 485465,1 | 474635,3 |
| 2283 | 19,06 | 17,62 | 18,31 | 3,009274 | 3,452998 | 3,237309 | 466023,7 | 488490,4 | 477593,1 |
| 2293 | 18,94 | 17,5 | 18,19 | 3,045275 | 3,491028 | 3,274436 | 467855,8 | 490410,8 | 479470,6 |

| | | | | | | | | | |
|------|-------|-------|-------|----------|----------|----------|----------|----------|----------|
| 2303 | 18,75 | 17,37 | 18 | 3,102663 | 3,532388 | 3,333561 | 470771,3 | 492499,7 | 482458,5 |
| 2313 | 18,69 | 17,25 | 17,94 | 3,120882 | 3,57071 | 3,352316 | 471695,8 | 494435,9 | 483406 |
| 2323 | 18,56 | 17,12 | 17,81 | 3,160512 | 3,612376 | 3,393087 | 473705 | 496542 | 485465,1 |
| 2333 | 18,44 | 17,06 | 17,69 | 3,19728 | 3,631658 | 3,430882 | 475567,3 | 497517,1 | 487373,6 |
| 2343 | 18,25 | 16,81 | 17,5 | 3,255852 | 3,71233 | 3,491028 | 478530,9 | 501600,5 | 490410,8 |
| 2353 | 18,06 | 16,69 | 17,37 | 3,314846 | 3,751234 | 3,532388 | 481513 | 503572,5 | 492499,7 |
| 2363 | 17,94 | 16,5 | 17,25 | 3,352316 | 3,813057 | 3,57071 | 483406 | 506710,6 | 494435,9 |
| 2373 | 17,75 | 16,31 | 17,06 | 3,411965 | 3,87514 | 3,631658 | 486418,4 | 509868,3 | 497517,1 |
| 2383 | 17,69 | 16,25 | 17 | 3,430882 | 3,894795 | 3,650971 | 487373,6 | 510869,5 | 498494,1 |
| 2393 | 17,56 | 16,12 | 16,87 | 3,471995 | 3,93746 | 3,692921 | 489449,6 | 513045,6 | 500617,5 |
| 2403 | 17,5 | 16,06 | 16,75 | 3,491028 | 3,957186 | 3,731768 | 490410,8 | 514053,1 | 502585,6 |
| 2413 | 17,37 | 15,94 | 16,62 | 3,532388 | 3,996701 | 3,77398 | 492499,7 | 516074 | 504726,4 |
| 2423 | 17,13 | 15,88 | 16,56 | 3,609166 | 4,016489 | 3,793505 | 496379,7 | 517087,5 | 505717,5 |
| 2433 | 17,25 | 15,75 | 16,5 | 3,57071 | 4,059426 | 3,813057 | 494435,9 | 519290 | 506710,6 |
| 2443 | 17,19 | 15,75 | 16,44 | 3,589922 | 4,059426 | 3,832635 | 495406,8 | 519290 | 507705,7 |
| 2454 | 17,06 | 15,69 | 16,37 | 3,631658 | 4,079271 | 3,855508 | 497517,1 | 520309,8 | 508869 |
| 2464 | 17 | 15,63 | 16,31 | 3,650971 | 4,099133 | 3,87514 | 498494,1 | 521331,5 | 509868,3 |
| 2474 | 16,94 | 15,56 | 16,25 | 3,670315 | 4,122326 | 3,894795 | 499473 | 522526,1 | 510869,5 |

| | | | | | | | | | |
|------|-------|-------|-------|----------|----------|----------|----------|----------|----------|
| 2484 | 16,87 | 15,5 | 16,19 | 3,692921 | 4,142222 | 3,914473 | 500617,5 | 523552,2 | 511872,7 |
| 2494 | 16,81 | 15,38 | 16,06 | 3,71233 | 4,182057 | 3,957186 | 501600,5 | 525610,5 | 514053,1 |
| 2504 | 16,69 | 15,31 | 15,94 | 3,751234 | 4,205319 | 3,996701 | 503572,5 | 526814,8 | 516074 |
| 2514 | 16,56 | 15,19 | 15,81 | 3,793505 | 4,245235 | 4,039598 | 505717,5 | 528885,9 | 518272,3 |

APPENDIX II

INPUT VALUES FOR CALCULATING PAVEMENT DEFLECTION CONSIDERING TEMPERATURE AND AXLE LOAD

| Resilient Strain in HMA | Axle Load | Pavement Temperature | Axle Load Constant | Temperature Constant | Deflection of Pavement |
|-------------------------|-----------|----------------------|--------------------|----------------------|-------------------------|
| K1 | N (kN) | T (Degrees) | K2 | K3 | Δ_{HMA} (inches) |
| 0,00000007 | 1000 | 23,87 | 0,4791 | 1,5606 | 0,00027 |
| 0,00000007 | 1500 | 24,62 | 0,4791 | 1,5606 | 0,00035 |
| 0,00000007 | 2000 | 25,06 | 0,4791 | 1,5606 | 0,00041 |
| 0,00000007 | 2500 | 24,94 | 0,4791 | 1,5606 | 0,00045 |
| 0,00000007 | 3000 | 25,12 | 0,4791 | 1,5606 | 0,00050 |
| 0,00000007 | 3500 | 25,37 | 0,4791 | 1,5606 | 0,00054 |
| 0,00000007 | 4000 | 25,75 | 0,4791 | 1,5606 | 0,00059 |
| 0,00000007 | 4500 | 26,06 | 0,4791 | 1,5606 | 0,00064 |
| 0,00000007 | 5000 | 26,12 | 0,4791 | 1,5606 | 0,00067 |
| 0,00000007 | 5500 | 26,19 | 0,4791 | 1,5606 | 0,00071 |
| 0,00000007 | 6000 | 26,37 | 0,4791 | 1,5606 | 0,00075 |
| 0,00000007 | 1000 | 23,87 | 0,4791 | 1,5606 | 0,00027 |
| 0,00000007 | 1500 | 24,62 | 0,4791 | 1,5606 | 0,00035 |

| | | | | | |
|------------|------|-------|--------|--------|---------|
| 0,00000007 | 2000 | 25,06 | 0,4791 | 1,5606 | 0,00041 |
| 0,00000007 | 2500 | 24,94 | 0,4791 | 1,5606 | 0,00045 |
| 0,00000007 | 3000 | 25,12 | 0,4791 | 1,5606 | 0,00050 |
| 0,00000007 | 3500 | 25,37 | 0,4791 | 1,5606 | 0,00054 |
| 0,00000007 | 4000 | 25,75 | 0,4791 | 1,5606 | 0,00059 |
| 0,00000007 | 4500 | 26,06 | 0,4791 | 1,5606 | 0,00064 |
| 0,00000007 | 5000 | 26,12 | 0,4791 | 1,5606 | 0,00067 |
| 0,00000007 | 5500 | 26,19 | 0,4791 | 1,5606 | 0,00071 |
| 0,00000007 | 6000 | 26,37 | 0,4791 | 1,5606 | 0,00075 |
| 0,00000007 | 1000 | 23,87 | 0,4791 | 1,5606 | 0,00027 |
| 0,00000007 | 1500 | 24,62 | 0,4791 | 1,5606 | 0,00035 |
| 0,00000007 | 2000 | 25,06 | 0,4791 | 1,5606 | 0,00041 |
| 0,00000007 | 2500 | 24,94 | 0,4791 | 1,5606 | 0,00045 |
| 0,00000007 | 3000 | 25,12 | 0,4791 | 1,5606 | 0,00050 |
| 0,00000007 | 3500 | 25,37 | 0,4791 | 1,5606 | 0,00054 |
| 0,00000007 | 4000 | 25,75 | 0,4791 | 1,5606 | 0,00059 |
| 0,00000007 | 4500 | 26,06 | 0,4791 | 1,5606 | 0,00064 |

| | | | | | |
|------------|-------|-------|--------|--------|---------|
| 0,00000007 | 5000 | 26,12 | 0,4791 | 1,5606 | 0,00067 |
| 0,00000007 | 5500 | 26,19 | 0,4791 | 1,5606 | 0,00071 |
| 0,00000007 | 6000 | 26,37 | 0,4791 | 1,5606 | 0,00075 |
| 0,00000007 | 6500 | 26,69 | 0,4791 | 1,5606 | 0,00079 |
| 0,00000007 | 7000 | 26,94 | 0,4791 | 1,5606 | 0,00083 |
| 0,00000007 | 7500 | 27,12 | 0,4791 | 1,5606 | 0,00087 |
| 0,00000007 | 8000 | 27,12 | 0,4791 | 1,5606 | 0,00090 |
| 0,00000007 | 8500 | 27,12 | 0,4791 | 1,5606 | 0,00092 |
| 0,00000007 | 9000 | 27,06 | 0,4791 | 1,5606 | 0,00094 |
| 0,00000007 | 10000 | 27,25 | 0,4791 | 1,5606 | 0,00100 |
| 0,00000007 | 10500 | 27,50 | 0,4791 | 1,5606 | 0,00104 |
| 0,00000007 | 11000 | 27,75 | 0,4791 | 1,5606 | 0,00108 |
| 0,00000007 | 11500 | 28,19 | 0,4791 | 1,5606 | 0,00113 |
| 0,00000007 | 12000 | 28,62 | 0,4791 | 1,5606 | 0,00118 |
| 0,00000007 | 12500 | 28,56 | 0,4791 | 1,5606 | 0,00120 |
| 0,00000007 | 13000 | 28,81 | 0,4791 | 1,5606 | 0,00124 |

APPENDIX III: INPUT VALUES FOR FIELD CALIBRATION CONSTANT KZ

| Kz | C1 | C2 | K1r | K2r | K3r |
|--------------|--------------|--------------|--------------|-------------|-------------|
| 1 | - 57,5815 | - 12,1605 | - 3,35412 | - 0,4791 | - 1,5606 |
| -1,28444E-09 | - 57,5815 | - 12,1605 | - 3,35412 | - 0,4791 | - 1,5606 |
| -1,28444E-09 | - 57,5815 | - 12,1605 | - 3,35412 | - 0,4791 | - 1,5606 |
| -1,28444E-09 | - 57,5815 | - 12,1605 | - 3,35412 | - 0,4791 | - 1,5606 |
| -1,28444E-09 | - 57,5815 | - 12,1605 | - 3,35412 | - 0,4791 | - 1,5606 |
| -1,28444E-09 | - 57,5815 | - 12,1605 | - 3,35412 | - 0,4791 | - 1,5606 |
| -1,28444E-09 | - 57,5815 | - 12,1605 | - 3,35412 | - 0,4791 | - 1,5606 |
| -1,28444E-09 | - 57,5815 | - 12,1605 | - 3,35412 | - 0,4791 | - 1,5606 |
| -1,28444E-09 | - 57,5815 | - 12,1605 | - 3,35412 | - 0,4791 | - 1,5606 |
| -1,28444E-09 | - 57,5815 | - 12,1605 | - 3,35412 | - 0,4791 | - 1,5606 |
| -1,28444E-09 | - 57,5815 | - 12,1605 | - 3,35412 | - 0,4791 | - 1,5606 |
| | | | | | |

APPENDIX IV: PROCEDURE FOR INSTRUMENTATION AND INSTALLATION

Road IOT Instrumentation Notes

1. Installation

- Pull the two wires (power and antenna) through the PVC pipe.
- Before connecting the **20mm** male and female PVC pipes, apply the provided PVC Weld thoroughly. Connect the male and female.
- Place the device and pipes in the ground.
- Connect the power cable to the solar panel.
- Take down the current GPS location of the device as well as the device ID for the software developer to implement. This will ensure that the location of each device is known should the GPS fail.

2. SigFox Backend

The device transmits the reading to the SigFox backend. This information can be seen at:

<https://backend.sigfox.com/>

Username: bskrtell@gmail.com

Password: banksZA111/

3. Data package

The data will be sent to the backend as follow:

| Bytes | Example | Description |
|------------------|--------------------------|---------------------------------------|
| RAW DATA | 0f5444330f9313750c2810d6 | |
| BYTE 0,1,2 and 3 | 0F 54 44 33 | *Latitude |
| BYTE 4,5,6 and 7 | 0F 93 13 75 | *Longitude |
| BYTE 8 | 0C | Temperature (degree Celsius) |
| BYTE 9 | 28 | Humidity (%) |
| BYTE 10 and 11 | 10 D6 | Battery Voltage (Milli-Volts) |

* Latitude data should be divided by 10 000 000 to get the correct floating number

* Longitude data should be divided by 10 000 000 to get the correct floating number

4. Do's and Don'ts

- Do not pull too hard on the cables.
- If ever an error occurs, disconnect the power cable and leave for the battery to deplete before connecting again. This will cause the device to reset.
- Since the battery will be connected from assembly ensure the batteries are kept on charge when receiving the devices. This is done by connecting the power cable to the solar panel and placing it in the sun.

APPENDIX V: MOISTURE AND TEMPERATURE SENSOR DATA OBTAINED FROM PAVEMENT SUBGRADE LAYER

| | time | Temperature | Humidity | Battery Voltage |
|----|---------------------|-------------|----------|-----------------|
| 0 | 2019-12-01 18:18:56 | 20 | 47 | 3697 |
| 1 | 2019-12-01 18:29:06 | 20 | 47 | 3697 |
| 2 | 2019-12-01 18:39:17 | 20 | 47 | 3697 |
| 3 | 2019-12-01 18:49:27 | 20 | 47 | 3690 |
| 4 | 2019-12-01 18:59:39 | 20 | 47 | 3692 |
| 5 | 2019-12-01 19:09:49 | 20 | 47 | 3692 |
| 6 | 2019-12-01 19:20:00 | 19 | 46 | 3689 |
| 7 | 2019-12-01 19:30:11 | 20 | 46 | 3687 |
| 8 | 2019-12-01 19:40:21 | 19 | 47 | 3688 |
| 9 | 2019-12-01 19:50:32 | 19 | 47 | 3689 |
| 10 | 2019-12-01 20:00:43 | 19 | 47 | 3684 |
| 11 | 2019-12-01 20:10:53 | 19 | 47 | 3682 |
| 12 | 2019-12-01 20:21:04 | 19 | 48 | 3682 |
| 13 | 2019-12-01 20:31:15 | 19 | 48 | 3683 |
| 14 | 2019-12-01 20:41:25 | 19 | 48 | 3676 |
| 15 | 2019-12-01 20:51:36 | 19 | 49 | 3683 |
| 16 | 2019-12-01 21:01:47 | 19 | 49 | 3674 |
| 17 | 2019-12-01 21:11:58 | 19 | 49 | 3684 |
| 18 | 2019-12-01 21:22:08 | 19 | 49 | 3677 |
| 19 | 2019-12-01 21:32:19 | 19 | 49 | 3680 |
| 20 | 2019-12-01 21:42:30 | 19 | 50 | 3678 |
| 21 | 2019-12-01 21:52:40 | 19 | 49 | 3670 |
| 22 | 2019-12-01 22:02:51 | 19 | 49 | 3677 |
| 23 | 2019-12-01 22:13:02 | 19 | 50 | 3671 |
| 24 | 2019-12-01 22:23:13 | 19 | 50 | 3676 |
| 25 | 2019-12-01 22:33:23 | 19 | 50 | 3669 |
| 26 | 2019-12-01 22:43:34 | 19 | 50 | 3671 |
| 27 | 2019-12-01 22:53:44 | 19 | 50 | 3670 |
| 28 | 2019-12-01 23:03:55 | 19 | 50 | 3671 |
| 29 | 2019-12-01 23:14:05 | 19 | 50 | 3663 |
| 30 | 2019-12-01 23:24:15 | 19 | 50 | 3664 |
| 31 | 2019-12-01 23:34:26 | 19 | 50 | 3673 |
| 32 | 2019-12-01 23:44:38 | 19 | 50 | 3671 |
| 33 | 2019-12-01 23:54:48 | 19 | 50 | 3662 |
| 34 | 2019-12-02 00:04:58 | 19 | 50 | 3660 |
| 35 | 2019-12-02 00:15:09 | 19 | 50 | 3662 |
| 36 | 2019-12-02 00:25:19 | 19 | 50 | 3663 |

| | | | | |
|----|---------------------|----|----|------|
| 37 | 2019-12-02 00:35:30 | 19 | 49 | 3660 |
| 38 | 2019-12-02 00:45:41 | 19 | 49 | 3662 |
| 39 | 2019-12-02 00:55:51 | 19 | 49 | 3662 |
| 40 | 2019-12-02 01:06:02 | 19 | 49 | 3655 |
| 41 | 2019-12-02 01:16:13 | 19 | 49 | 3657 |
| 42 | 2019-12-02 01:26:23 | 19 | 49 | 3665 |
| 43 | 2019-12-02 01:36:34 | 19 | 49 | 3661 |
| 44 | 2019-12-02 01:46:44 | 19 | 49 | 3662 |
| 45 | 2019-12-02 01:56:55 | 19 | 49 | 3659 |
| 46 | 2019-12-02 02:07:05 | 19 | 49 | 3664 |
| 47 | 2019-12-02 02:17:16 | 19 | 49 | 3653 |
| 48 | 2019-12-02 02:27:27 | 19 | 49 | 3654 |
| 49 | 2019-12-02 02:37:37 | 19 | 49 | 3654 |
| 50 | 2019-12-02 02:47:48 | 19 | 49 | 3650 |
| 51 | 2019-12-02 02:57:58 | 19 | 48 | 3648 |
| 52 | 2019-12-02 03:08:09 | 19 | 49 | 3657 |
| 53 | 2019-12-02 03:18:19 | 19 | 49 | 3650 |
| 54 | 2019-12-02 03:28:29 | 19 | 49 | 3654 |
| 55 | 2019-12-02 03:38:40 | 19 | 49 | 3653 |
| 56 | 2019-12-02 03:48:51 | 19 | 49 | 3651 |
| 57 | 2019-12-02 03:59:01 | 19 | 49 | 3649 |
| 58 | 2019-12-02 04:09:12 | 20 | 48 | 3655 |
| 59 | 2019-12-02 04:19:23 | 20 | 49 | 3649 |
| 60 | 2019-12-02 04:29:33 | 20 | 48 | 3656 |
| 61 | 2019-12-02 04:39:44 | 20 | 48 | 3648 |
| 62 | 2019-12-02 04:49:54 | 20 | 49 | 3654 |
| 63 | 2019-12-02 05:00:05 | 20 | 48 | 3658 |
| 64 | 2019-12-02 05:10:16 | 20 | 48 | 3665 |
| 65 | 2019-12-02 05:20:26 | 21 | 47 | 3663 |
| 66 | 2019-12-02 05:30:36 | 21 | 46 | 3664 |
| 67 | 2019-12-02 05:40:48 | 21 | 46 | 3672 |
| 68 | 2019-12-02 05:50:58 | 21 | 44 | 3664 |
| 69 | 2019-12-02 06:01:08 | 22 | 43 | 3671 |
| 70 | 2019-12-02 06:11:20 | 22 | 44 | 3673 |
| 71 | 2019-12-02 06:21:30 | 22 | 43 | 3661 |
| 72 | 2019-12-02 06:31:41 | 22 | 42 | 3677 |
| 73 | 2019-12-02 06:41:52 | 22 | 42 | 3666 |
| 74 | 2019-12-02 06:52:03 | 22 | 42 | 3668 |
| 75 | 2019-12-02 07:02:13 | 22 | 42 | 3665 |
| 76 | 2019-12-02 07:12:24 | 22 | 40 | 3668 |
| 77 | 2019-12-02 07:22:35 | 23 | 41 | 3667 |

| | | | | |
|-----|---------------------|----|----|------|
| 78 | 2019-12-02 07:32:45 | 23 | 40 | 3675 |
| 79 | 2019-12-02 07:42:57 | 23 | 40 | 3670 |
| 80 | 2019-12-02 07:53:07 | 23 | 41 | 3671 |
| 81 | 2019-12-02 08:03:18 | 23 | 41 | 3668 |
| 82 | 2019-12-02 08:13:29 | 23 | 40 | 3674 |
| 83 | 2019-12-02 08:23:40 | 24 | 40 | 3676 |
| 84 | 2019-12-02 08:33:50 | 24 | 40 | 3682 |
| 85 | 2019-12-02 08:44:02 | 24 | 39 | 3680 |
| 86 | 2019-12-02 08:54:12 | 24 | 39 | 3683 |
| 87 | 2019-12-02 09:04:23 | 24 | 37 | 3684 |
| 88 | 2019-12-02 09:14:35 | 25 | 37 | 3692 |
| 89 | 2019-12-02 09:24:45 | 25 | 36 | 3676 |
| 90 | 2019-12-02 09:34:56 | 25 | 36 | 3683 |
| 91 | 2019-12-02 09:45:07 | 25 | 37 | 3679 |
| 92 | 2019-12-02 09:55:18 | 25 | 37 | 3688 |
| 93 | 2019-12-02 10:05:29 | 25 | 38 | 3687 |
| 94 | 2019-12-02 10:15:40 | 25 | 36 | 3688 |
| 95 | 2019-12-02 10:25:51 | 25 | 37 | 3693 |
| 96 | 2019-12-02 10:36:02 | 25 | 38 | 3692 |
| 97 | 2019-12-02 10:46:13 | 25 | 39 | 3689 |
| 98 | 2019-12-02 10:56:24 | 25 | 38 | 3700 |
| 99 | 2019-12-02 11:06:35 | 25 | 38 | 3712 |
| 100 | 2019-12-02 11:16:47 | 26 | 38 | 3724 |
| 101 | 2019-12-02 11:26:57 | 26 | 37 | 3723 |
| 102 | 2019-12-02 11:37:09 | 27 | 35 | 3727 |
| 103 | 2019-12-02 11:47:21 | 27 | 35 | 3734 |
| 104 | 2019-12-02 11:57:32 | 27 | 35 | 3744 |
| 105 | 2019-12-02 12:07:44 | 28 | 34 | 3743 |
| 106 | 2019-12-02 12:17:56 | 28 | 33 | 3768 |
| 107 | 2019-12-02 12:28:08 | 28 | 31 | 3681 |
| 108 | 2019-12-02 12:38:19 | 29 | 29 | 3765 |
| 109 | 2019-12-02 12:48:32 | 30 | 27 | 3692 |
| 110 | 2019-12-02 12:58:43 | 30 | 28 | 3778 |
| 111 | 2019-12-02 13:08:55 | 30 | 32 | 3639 |
| 112 | 2019-12-02 13:19:08 | 30 | 27 | 3674 |
| 113 | 2019-12-02 13:29:19 | 30 | 28 | 3796 |
| 114 | 2019-12-02 13:39:32 | 30 | 28 | 3797 |
| 115 | 2019-12-02 13:49:44 | 30 | 28 | 3814 |
| 116 | 2019-12-02 13:59:56 | 30 | 28 | 3817 |
| 117 | 2019-12-02 14:10:08 | 30 | 27 | 3822 |
| 118 | 2019-12-02 14:20:21 | 30 | 24 | 3470 |

| | | | | |
|-----|---------------------|----|----|------|
| 119 | 2019-12-02 14:30:33 | 30 | 28 | 3833 |
| 120 | 2019-12-02 14:40:44 | 31 | 27 | 3836 |
| 121 | 2019-12-02 14:50:57 | 31 | 26 | 3844 |
| 122 | 2019-12-02 15:01:10 | 31 | 26 | 3827 |
| 123 | 2019-12-02 15:11:21 | 31 | 27 | 3849 |
| 124 | 2019-12-02 15:21:34 | 30 | 27 | 3821 |
| 125 | 2019-12-02 15:31:46 | 29 | 30 | 3446 |
| 126 | 2019-12-02 15:41:59 | 28 | 32 | 3712 |
| 127 | 2019-12-02 15:52:11 | 27 | 35 | 3812 |
| 128 | 2019-12-02 16:02:23 | 27 | 34 | 3682 |
| 129 | 2019-12-02 16:12:35 | 26 | 35 | 3707 |
| 130 | 2019-12-02 16:22:46 | 26 | 36 | 3718 |
| 131 | 2019-12-02 16:32:58 | 26 | 39 | 3791 |
| 132 | 2019-12-02 16:43:10 | 25 | 40 | 3793 |
| 133 | 2019-12-02 16:53:22 | 25 | 41 | 3730 |
| 134 | 2019-12-02 17:03:33 | 25 | 41 | 3727 |
| 135 | 2019-12-02 17:13:45 | 25 | 42 | 3789 |
| 136 | 2019-12-02 17:23:57 | 24 | 43 | 3783 |
| 137 | 2019-12-02 17:34:09 | 24 | 42 | 3777 |
| 138 | 2019-12-02 17:44:21 | 24 | 43 | 3780 |
| 139 | 2019-12-02 17:54:32 | 24 | 45 | 3780 |
| 140 | 2019-12-02 18:04:44 | 24 | 45 | 3776 |
| 141 | 2019-12-02 18:14:56 | 24 | 45 | 3776 |
| 142 | 2019-12-02 18:25:08 | 24 | 43 | 3637 |
| 143 | 2019-12-02 18:35:20 | 24 | 46 | 3768 |
| 144 | 2019-12-02 18:45:31 | 24 | 49 | 3690 |
| 145 | 2019-12-02 18:55:42 | 24 | 46 | 3766 |
| 146 | 2019-12-02 19:05:54 | 23 | 47 | 3770 |
| 147 | 2019-12-02 19:16:05 | 23 | 46 | 3764 |
| 148 | 2019-12-02 19:26:17 | 23 | 46 | 3763 |
| 149 | 2019-12-02 19:36:29 | 23 | 46 | 3759 |
| 150 | 2019-12-02 19:46:40 | 23 | 46 | 3759 |
| 151 | 2019-12-02 19:56:52 | 23 | 45 | 3642 |
| 152 | 2019-12-02 20:07:03 | 23 | 45 | 3671 |
| 153 | 2019-12-02 20:17:16 | 22 | 46 | 3681 |
| 154 | 2019-12-02 20:27:26 | 23 | 47 | 3747 |
| 155 | 2019-12-02 20:37:38 | 22 | 48 | 3752 |
| 156 | 2019-12-02 20:47:50 | 22 | 48 | 3751 |
| 157 | 2019-12-02 20:58:01 | 22 | 46 | 3748 |
| 158 | 2019-12-02 21:08:12 | 22 | 44 | 3746 |
| 159 | 2019-12-02 21:18:24 | 22 | 45 | 3745 |

| | | | | |
|-----|---------------------|----|----|------|
| 160 | 2019-12-02 21:28:36 | 21 | 43 | 3746 |
| 161 | 2019-12-02 21:38:47 | 21 | 43 | 3740 |
| 162 | 2019-12-02 21:48:59 | 21 | 39 | 3741 |
| 163 | 2019-12-02 21:59:10 | 22 | 38 | 3733 |
| 164 | 2019-12-02 22:09:21 | 22 | 36 | 3738 |
| 165 | 2019-12-02 22:19:33 | 22 | 34 | 3732 |
| 166 | 2019-12-02 22:29:43 | 22 | 34 | 3733 |
| 167 | 2019-12-02 22:39:55 | 21 | 33 | 3730 |
| 168 | 2019-12-02 22:50:06 | 21 | 33 | 3730 |
| 169 | 2019-12-02 23:00:17 | 21 | 32 | 3730 |
| 170 | 2019-12-02 23:10:27 | 21 | 33 | 3729 |
| 171 | 2019-12-02 23:20:38 | 21 | 32 | 3725 |
| 172 | 2019-12-02 23:30:48 | 21 | 32 | 3726 |
| 173 | 2019-12-02 23:40:59 | 21 | 31 | 3647 |
| 174 | 2019-12-02 23:51:10 | 21 | 33 | 3728 |
| 175 | 2019-12-03 00:01:21 | 21 | 32 | 3722 |
| 176 | 2019-12-03 00:11:32 | 20 | 26 | 3714 |
| 177 | 2019-12-03 00:21:42 | 20 | 25 | 3720 |
| 178 | 2019-12-03 00:31:53 | 20 | 27 | 3719 |
| 179 | 2019-12-03 00:42:04 | 20 | 27 | 3693 |
| 180 | 2019-12-03 00:52:14 | 20 | 30 | 3720 |
| 181 | 2019-12-03 01:02:25 | 19 | 33 | 3714 |
| 182 | 2019-12-03 01:12:36 | 19 | 34 | 3714 |
| 183 | 2019-12-03 01:22:46 | 19 | 35 | 3712 |
| 184 | 2019-12-03 01:32:56 | 19 | 35 | 3710 |
| 185 | 2019-12-03 01:43:08 | 19 | 35 | 3709 |
| 186 | 2019-12-03 01:53:18 | 19 | 37 | 3708 |
| 187 | 2019-12-03 02:03:28 | 19 | 39 | 3707 |
| 188 | 2019-12-03 02:13:40 | 18 | 40 | 3704 |
| 189 | 2019-12-03 02:23:51 | 18 | 42 | 3704 |
| 190 | 2019-12-03 02:34:01 | 18 | 41 | 3703 |
| 191 | 2019-12-03 02:44:13 | 18 | 41 | 3703 |
| 192 | 2019-12-03 02:54:24 | 18 | 41 | 3703 |
| 193 | 2019-12-03 03:04:35 | 18 | 40 | 3697 |
| 194 | 2019-12-03 03:14:46 | 18 | 41 | 3696 |
| 195 | 2019-12-03 03:24:57 | 18 | 42 | 3696 |
| 196 | 2019-12-03 03:35:08 | 18 | 40 | 3694 |
| 197 | 2019-12-03 03:45:20 | 18 | 36 | 3694 |
| 198 | 2019-12-03 03:55:30 | 18 | 34 | 3696 |
| 199 | 2019-12-03 04:05:41 | 18 | 34 | 3690 |
| 200 | 2019-12-03 04:15:51 | 18 | 34 | 3690 |

| | | | | |
|-----|---------------------|----|----|------|
| 201 | 2019-12-03 04:26:02 | 19 | 33 | 3690 |
| 202 | 2019-12-03 04:36:12 | 19 | 33 | 3696 |
| 203 | 2019-12-03 04:46:23 | 19 | 33 | 3691 |
| 204 | 2019-12-03 04:56:34 | 19 | 33 | 3692 |
| 205 | 2019-12-03 05:16:55 | 19 | 33 | 3695 |
| 206 | 2019-12-03 05:27:05 | 19 | 46 | 3618 |
| 207 | 2019-12-03 05:37:16 | 19 | 32 | 3699 |
| 208 | 2019-12-03 05:47:27 | 19 | 32 | 3689 |
| 209 | 2019-12-03 05:57:38 | 19 | 33 | 3699 |
| 210 | 2019-12-03 06:07:48 | 20 | 32 | 3702 |
| 211 | 2019-12-03 06:17:59 | 20 | 31 | 3709 |
| 212 | 2019-12-03 06:28:09 | 20 | 32 | 3695 |
| 213 | 2019-12-03 06:38:20 | 20 | 31 | 3704 |
| 214 | 2019-12-03 06:48:31 | 20 | 31 | 3694 |
| 215 | 2019-12-03 06:58:41 | 19 | 36 | 3710 |
| 216 | 2019-12-03 07:08:52 | 19 | 38 | 3665 |
| 217 | 2019-12-03 07:19:03 | 18 | 39 | 3704 |
| 218 | 2019-12-03 07:29:14 | 18 | 38 | 3698 |
| 219 | 2019-12-03 07:39:25 | 18 | 37 | 3698 |
| 220 | 2019-12-03 07:49:36 | 18 | 38 | 3702 |
| 221 | 2019-12-03 07:59:47 | 18 | 37 | 3705 |
| 222 | 2019-12-03 08:09:59 | 18 | 35 | 3658 |
| 223 | 2019-12-03 08:20:10 | 18 | 35 | 3705 |
| 224 | 2019-12-03 08:30:20 | 18 | 30 | 3704 |
| 225 | 2019-12-03 09:00:54 | 18 | 30 | 3713 |
| 226 | 2019-12-03 09:11:04 | 18 | 28 | 3713 |
| 227 | 2019-12-03 09:21:16 | 18 | 29 | 3715 |
| 228 | 2019-12-03 09:31:27 | 18 | 31 | 3704 |
| 229 | 2019-12-03 09:41:38 | 18 | 27 | 3715 |
| 230 | 2019-12-03 09:51:49 | 18 | 26 | 3712 |
| 231 | 2019-12-03 10:02:00 | 18 | 27 | 3719 |
| 232 | 2019-12-03 10:12:11 | 18 | 24 | 3733 |
| 233 | 2019-12-03 10:22:22 | 18 | 22 | 3627 |
| 234 | 2019-12-03 10:32:32 | 18 | 25 | 3725 |
| 235 | 2019-12-03 10:42:44 | 18 | 23 | 3733 |
| 236 | 2019-12-03 10:52:55 | 18 | 22 | 3724 |
| 237 | 2019-12-03 11:03:06 | 18 | 24 | 3728 |
| 238 | 2019-12-03 11:13:17 | 18 | 26 | 3726 |
| 239 | 2019-12-03 11:23:28 | 18 | 27 | 3731 |
| 240 | 2019-12-03 11:33:39 | 18 | 29 | 3734 |
| 241 | 2019-12-03 11:43:51 | 18 | 29 | 3716 |

| | | | | |
|-----|---------------------|----|----|------|
| 242 | 2019-12-03 11:54:02 | 18 | 29 | 3733 |
| 243 | 2019-12-03 12:04:13 | 18 | 28 | 3732 |
| 244 | 2019-12-03 12:14:25 | 18 | 29 | 3738 |
| 245 | 2019-12-03 12:24:36 | 18 | 29 | 3739 |
| 246 | 2019-12-03 12:34:47 | 18 | 28 | 3736 |
| 247 | 2019-12-03 12:44:59 | 18 | 28 | 3744 |
| 248 | 2019-12-03 12:55:09 | 18 | 28 | 3741 |
| 249 | 2019-12-03 13:05:21 | 18 | 29 | 3739 |
| 250 | 2019-12-03 13:15:33 | 18 | 31 | 3743 |
| 251 | 2019-12-03 13:25:43 | 18 | 30 | 3738 |
| 252 | 2019-12-03 13:35:55 | 18 | 31 | 3740 |
| 253 | 2019-12-03 13:46:06 | 18 | 29 | 3744 |
| 254 | 2019-12-03 13:56:17 | 18 | 28 | 3749 |
| 255 | 2019-12-03 14:06:28 | 18 | 26 | 3750 |
| 256 | 2019-12-03 14:16:41 | 18 | 25 | 3745 |
| 257 | 2019-12-03 14:26:52 | 18 | 29 | 3742 |
| 258 | 2019-12-03 14:37:03 | 18 | 27 | 3736 |
| 259 | 2019-12-03 14:47:15 | 18 | 27 | 3744 |
| 260 | 2019-12-03 14:57:26 | 18 | 23 | 3742 |
| 261 | 2019-12-03 15:07:37 | 18 | 25 | 3749 |
| 262 | 2019-12-03 15:17:49 | 18 | 28 | 3739 |
| 263 | 2019-12-03 15:28:00 | 18 | 29 | 3735 |
| 264 | 2019-12-03 15:38:10 | 17 | 31 | 3740 |
| 265 | 2019-12-03 15:48:22 | 17 | 33 | 3737 |
| 266 | 2019-12-03 15:58:32 | 17 | 33 | 3736 |
| 267 | 2019-12-03 16:08:42 | 17 | 32 | 3747 |
| 268 | 2019-12-03 16:18:54 | 18 | 33 | 3591 |
| 269 | 2019-12-03 16:29:05 | 18 | 29 | 3749 |
| 270 | 2019-12-03 16:39:17 | 18 | 31 | 3739 |
| 271 | 2019-12-03 16:49:28 | 17 | 32 | 3660 |
| 272 | 2019-12-03 16:59:38 | 17 | 33 | 3733 |
| 273 | 2019-12-03 17:09:49 | 17 | 33 | 3733 |
| 274 | 2019-12-03 17:20:00 | 17 | 30 | 3728 |
| 275 | 2019-12-03 17:30:10 | 17 | 29 | 3727 |
| 276 | 2019-12-03 17:40:20 | 17 | 29 | 3725 |
| 277 | 2019-12-03 17:50:32 | 17 | 29 | 3724 |
| 278 | 2019-12-03 18:00:42 | 17 | 28 | 3722 |
| 279 | 2019-12-03 18:10:52 | 17 | 31 | 3568 |
| 280 | 2019-12-03 18:21:04 | 16 | 28 | 3718 |
| 281 | 2019-12-03 18:31:14 | 16 | 28 | 3719 |
| 282 | 2019-12-03 18:41:24 | 16 | 28 | 3716 |

| | | | | |
|-----|---------------------|----|----|------|
| 283 | 2019-12-03 18:51:35 | 16 | 28 | 3715 |
| 284 | 2019-12-03 19:01:45 | 16 | 28 | 3714 |
| 285 | 2019-12-03 19:11:55 | 16 | 27 | 3712 |
| 286 | 2019-12-03 19:22:06 | 16 | 28 | 3711 |
| 287 | 2019-12-03 19:32:17 | 16 | 28 | 3709 |
| 288 | 2019-12-03 19:42:27 | 16 | 28 | 3708 |
| 289 | 2019-12-03 19:52:38 | 16 | 28 | 3706 |
| 290 | 2019-12-03 20:02:48 | 16 | 28 | 3707 |
| 291 | 2019-12-03 20:12:58 | 16 | 28 | 3700 |
| 292 | 2019-12-03 20:23:09 | 15 | 27 | 3698 |
| 293 | 2019-12-03 20:33:19 | 15 | 26 | 3697 |
| 294 | 2019-12-03 20:43:29 | 15 | 26 | 3695 |
| 295 | 2019-12-03 20:53:40 | 15 | 26 | 3694 |
| 296 | 2019-12-03 21:03:50 | 15 | 25 | 3700 |
| 297 | 2019-12-03 21:14:00 | 15 | 24 | 3693 |
| 298 | 2019-12-03 21:24:11 | 15 | 24 | 3693 |
| 299 | 2019-12-03 21:34:21 | 15 | 23 | 3696 |
| 300 | 2019-12-03 21:44:31 | 14 | 22 | 3688 |
| 301 | 2019-12-03 21:54:42 | 14 | 21 | 3685 |
| 302 | 2019-12-03 22:04:52 | 15 | 19 | 3692 |
| 303 | 2019-12-03 22:15:03 | 15 | 18 | 3688 |
| 304 | 2019-12-03 22:25:13 | 16 | 18 | 3685 |
| 305 | 2019-12-03 22:35:23 | 15 | 19 | 3687 |
| 306 | 2019-12-03 22:45:34 | 16 | 19 | 3685 |
| 307 | 2019-12-03 22:55:44 | 15 | 19 | 3694 |
| 308 | 2019-12-03 23:05:54 | 15 | 19 | 3679 |
| 309 | 2019-12-03 23:16:05 | 15 | 19 | 3680 |
| 310 | 2019-12-03 23:26:14 | 15 | 20 | 3675 |
| 311 | 2019-12-03 23:36:24 | 15 | 21 | 3675 |
| 312 | 2019-12-03 23:46:35 | 15 | 21 | 3674 |
| 313 | 2019-12-03 23:56:45 | 15 | 22 | 3670 |
| 314 | 2019-12-04 00:06:55 | 15 | 23 | 3672 |
| 315 | 2019-12-04 00:17:05 | 15 | 23 | 3664 |
| 316 | 2019-12-04 00:27:16 | 15 | 23 | 3661 |
| 317 | 2019-12-04 00:37:27 | 15 | 24 | 3673 |
| 318 | 2019-12-04 00:47:36 | 14 | 24 | 3668 |
| 319 | 2019-12-04 00:57:47 | 15 | 24 | 3674 |
| 320 | 2019-12-04 01:07:57 | 15 | 25 | 3673 |
| 321 | 2019-12-04 01:18:07 | 15 | 25 | 3664 |
| 322 | 2019-12-04 01:28:17 | 15 | 25 | 3667 |
| 323 | 2019-12-04 01:38:28 | 15 | 25 | 3674 |

| | | | | |
|-----|---------------------|----|----|------|
| 324 | 2019-12-04 01:48:38 | 15 | 26 | 3667 |
| 325 | 2019-12-04 01:58:48 | 15 | 26 | 3670 |
| 326 | 2019-12-04 02:08:58 | 14 | 26 | 3665 |
| 327 | 2019-12-04 02:19:09 | 15 | 27 | 3675 |
| 328 | 2019-12-04 02:29:19 | 14 | 27 | 3656 |
| 329 | 2019-12-04 02:39:29 | 14 | 27 | 3661 |
| 330 | 2019-12-04 02:49:39 | 15 | 27 | 3667 |
| 331 | 2019-12-04 02:59:49 | 14 | 27 | 3662 |
| 332 | 2019-12-04 03:10:00 | 14 | 27 | 3653 |
| 333 | 2019-12-04 03:20:10 | 15 | 27 | 3660 |
| 334 | 2019-12-04 03:30:20 | 14 | 28 | 3658 |
| 335 | 2019-12-04 03:40:31 | 15 | 28 | 3659 |
| 336 | 2019-12-04 03:50:40 | 14 | 28 | 3658 |
| 337 | 2019-12-04 04:00:50 | 15 | 28 | 3655 |
| 338 | 2019-12-04 04:11:01 | 15 | 28 | 3660 |
| 339 | 2019-12-04 04:21:11 | 15 | 27 | 3655 |
| 340 | 2019-12-04 04:31:22 | 15 | 27 | 3661 |
| 341 | 2019-12-04 04:41:32 | 15 | 27 | 3662 |
| 342 | 2019-12-04 04:51:41 | 16 | 26 | 3671 |
| 343 | 2019-12-04 05:01:53 | 16 | 25 | 3664 |
| 344 | 2019-12-04 05:12:03 | 16 | 25 | 3672 |
| 345 | 2019-12-04 05:22:13 | 16 | 23 | 3660 |
| 346 | 2019-12-04 05:32:23 | 17 | 21 | 3683 |
| 347 | 2019-12-04 05:42:34 | 16 | 22 | 3674 |
| 348 | 2019-12-04 05:52:43 | 16 | 22 | 3675 |
| 349 | 2019-12-04 06:02:55 | 16 | 24 | 3687 |
| 350 | 2019-12-04 06:13:05 | 17 | 23 | 3677 |
| 351 | 2019-12-04 06:23:15 | 17 | 23 | 3686 |
| 352 | 2019-12-04 06:33:26 | 17 | 21 | 3677 |
| 353 | 2019-12-04 06:43:35 | 17 | 20 | 3686 |
| 354 | 2019-12-04 06:53:46 | 17 | 21 | 3694 |
| 355 | 2019-12-04 07:03:57 | 18 | 20 | 3687 |
| 356 | 2019-12-04 07:14:08 | 18 | 21 | 3695 |
| 357 | 2019-12-04 07:24:19 | 18 | 22 | 3698 |
| 358 | 2019-12-04 07:34:30 | 18 | 21 | 3710 |
| 359 | 2019-12-04 07:44:41 | 18 | 21 | 3708 |
| 360 | 2019-12-04 08:05:03 | 19 | 25 | 3717 |
| 361 | 2019-12-04 08:15:13 | 19 | 21 | 3723 |
| 362 | 2019-12-04 08:25:23 | 19 | 23 | 3726 |
| 363 | 2019-12-04 08:35:34 | 19 | 22 | 3731 |
| 364 | 2019-12-04 08:45:45 | 19 | 23 | 3708 |

| | | | | |
|-----|---------------------|----|----|------|
| 365 | 2019-12-04 08:55:56 | 19 | 24 | 3746 |
| 366 | 2019-12-04 09:06:08 | 19 | 24 | 3747 |
| 367 | 2019-12-04 09:16:20 | 19 | 28 | 3753 |
| 368 | 2019-12-04 09:26:31 | 19 | 25 | 3749 |
| 369 | 2019-12-04 09:36:43 | 19 | 27 | 3763 |
| 370 | 2019-12-04 09:46:54 | 19 | 26 | 3768 |
| 371 | 2019-12-04 09:57:05 | 19 | 33 | 3616 |
| 372 | 2019-12-04 10:07:17 | 19 | 31 | 3777 |
| 373 | 2019-12-04 10:17:28 | 19 | 34 | 3634 |
| 374 | 2019-12-04 10:27:39 | 18 | 33 | 3784 |
| 375 | 2019-12-04 10:48:03 | 19 | 32 | 3811 |
| 376 | 2019-12-04 10:58:14 | 19 | 30 | 3787 |
| 377 | 2019-12-04 11:08:26 | 19 | 32 | 3808 |
| 378 | 2019-12-04 11:18:38 | 20 | 32 | 3795 |
| 379 | 2019-12-04 11:28:50 | 20 | 28 | 3805 |
| 380 | 2019-12-04 11:39:01 | 21 | 29 | 3822 |
| 381 | 2019-12-04 11:49:13 | 20 | 30 | 3815 |
| 382 | 2019-12-04 11:59:24 | 19 | 32 | 3816 |
| 383 | 2019-12-04 12:09:36 | 20 | 31 | 3814 |
| 384 | 2019-12-04 12:19:47 | 19 | 30 | 3733 |
| 385 | 2019-12-04 12:29:59 | 20 | 31 | 3851 |
| 386 | 2019-12-04 12:40:11 | 21 | 29 | 3852 |
| 387 | 2019-12-04 12:50:23 | 22 | 26 | 3877 |
| 388 | 2019-12-04 13:00:35 | 23 | 23 | 3878 |
| 389 | 2019-12-04 13:10:47 | 23 | 20 | 3889 |
| 390 | 2019-12-04 13:20:59 | 24 | 19 | 3872 |
| 391 | 2019-12-04 13:31:11 | 24 | 22 | 3814 |
| 392 | 2019-12-04 13:41:24 | 23 | 25 | 3887 |
| 393 | 2019-12-04 13:51:36 | 23 | 25 | 3901 |
| 394 | 2019-12-04 14:01:48 | 24 | 21 | 3896 |
| 395 | 2019-12-04 14:12:01 | 25 | 56 | 3781 |
| 396 | 2019-12-04 14:22:12 | 25 | 20 | 3902 |
| 397 | 2019-12-04 14:32:25 | 25 | 19 | 3886 |
| 398 | 2019-12-04 14:42:37 | 24 | 18 | 3883 |
| 399 | 2019-12-04 14:52:49 | 25 | 20 | 3705 |
| 400 | 2019-12-04 15:03:01 | 24 | 19 | 3914 |
| 401 | 2019-12-04 15:13:14 | 23 | 19 | 3877 |
| 402 | 2019-12-04 15:23:26 | 22 | 22 | 3869 |
| 403 | 2019-12-04 15:33:38 | 22 | 23 | 3868 |
| 404 | 2019-12-04 15:43:50 | 21 | 23 | 3871 |
| 405 | 2019-12-04 15:54:02 | 21 | 24 | 3866 |

| | | | | |
|-----|---------------------|----|----|------|
| 406 | 2019-12-04 16:04:14 | 20 | 25 | 3865 |
| 407 | 2019-12-04 16:14:26 | 20 | 26 | 3862 |
| 408 | 2019-12-04 16:24:38 | 20 | 26 | 3858 |
| 409 | 2019-12-04 16:34:49 | 20 | 25 | 3847 |
| 410 | 2019-12-04 16:45:02 | 20 | 28 | 3601 |
| 411 | 2019-12-04 16:55:13 | 20 | 27 | 3858 |
| 412 | 2019-12-04 17:05:25 | 19 | 27 | 3854 |
| 413 | 2019-12-04 17:15:37 | 19 | 27 | 3851 |
| 414 | 2019-12-04 17:25:49 | 19 | 27 | 3850 |
| 415 | 2019-12-04 17:36:00 | 19 | 27 | 3833 |
| 416 | 2019-12-04 17:46:12 | 19 | 27 | 3852 |
| 417 | 2019-12-04 17:56:24 | 19 | 28 | 3850 |
| 418 | 2019-12-04 18:06:35 | 19 | 27 | 3751 |
| 419 | 2019-12-04 18:16:48 | 19 | 28 | 3842 |
| 420 | 2019-12-04 18:26:59 | 19 | 28 | 3842 |
| 421 | 2019-12-04 18:37:10 | 19 | 28 | 3842 |
| 422 | 2019-12-04 18:47:23 | 19 | 28 | 3839 |
| 423 | 2019-12-04 18:57:34 | 19 | 28 | 3837 |
| 424 | 2019-12-04 19:07:45 | 18 | 28 | 3817 |
| 425 | 2019-12-04 19:17:57 | 18 | 28 | 3839 |
| 426 | 2019-12-04 19:28:09 | 18 | 28 | 3835 |
| 427 | 2019-12-04 19:38:21 | 18 | 29 | 3829 |
| 428 | 2019-12-04 19:48:32 | 18 | 29 | 3831 |
| 429 | 2019-12-04 19:58:44 | 18 | 30 | 3829 |
| 430 | 2019-12-04 20:08:56 | 18 | 29 | 3668 |
| 431 | 2019-12-04 20:19:07 | 18 | 30 | 3829 |
| 432 | 2019-12-04 20:29:19 | 18 | 31 | 3828 |
| 433 | 2019-12-04 20:39:31 | 17 | 31 | 3502 |
| 434 | 2019-12-04 20:49:42 | 17 | 33 | 3825 |
| 435 | 2019-12-04 20:59:53 | 17 | 33 | 3659 |
| 436 | 2019-12-04 21:10:05 | 17 | 33 | 3824 |
| 437 | 2019-12-04 21:20:17 | 17 | 33 | 3810 |
| 438 | 2019-12-04 21:30:28 | 17 | 33 | 3815 |
| 439 | 2019-12-04 21:40:40 | 17 | 33 | 3584 |
| 440 | 2019-12-04 21:50:51 | 17 | 34 | 3815 |
| 441 | 2019-12-04 22:01:02 | 17 | 32 | 3719 |
| 442 | 2019-12-04 22:11:15 | 17 | 34 | 3812 |
| 443 | 2019-12-04 22:21:26 | 17 | 34 | 3809 |
| 444 | 2019-12-04 22:31:37 | 17 | 34 | 3807 |
| 445 | 2019-12-04 22:41:48 | 17 | 34 | 3803 |
| 446 | 2019-12-04 22:52:01 | 17 | 33 | 3804 |

| | | | | |
|-----|---------------------|----|----|------|
| 447 | 2019-12-04 23:02:12 | 17 | 33 | 3753 |
| 448 | 2019-12-04 23:12:23 | 17 | 34 | 3799 |
| 449 | 2019-12-04 23:22:35 | 17 | 33 | 3777 |
| 450 | 2019-12-04 23:32:47 | 17 | 33 | 3796 |
| 451 | 2019-12-04 23:42:58 | 17 | 32 | 3655 |
| 452 | 2019-12-04 23:53:09 | 17 | 33 | 3791 |
| 453 | 2019-12-05 00:03:20 | 16 | 33 | 3791 |
| 454 | 2019-12-05 00:13:32 | 16 | 34 | 3782 |
| 455 | 2019-12-05 00:23:43 | 16 | 33 | 3792 |
| 456 | 2019-12-05 00:33:54 | 16 | 33 | 3780 |
| 457 | 2019-12-05 00:44:06 | 16 | 35 | 3786 |
| 458 | 2019-12-05 00:54:18 | 16 | 35 | 3668 |
| 459 | 2019-12-05 01:04:28 | 16 | 36 | 3784 |
| 460 | 2019-12-05 01:14:40 | 15 | 37 | 3782 |
| 461 | 2019-12-05 01:24:52 | 15 | 33 | 3627 |
| 462 | 2019-12-05 01:35:03 | 15 | 37 | 3779 |
| 463 | 2019-12-05 01:45:15 | 15 | 36 | 3779 |
| 464 | 2019-12-05 01:55:26 | 15 | 38 | 3761 |
| 465 | 2019-12-05 02:05:37 | 15 | 38 | 3778 |
| 466 | 2019-12-05 02:15:49 | 15 | 37 | 3640 |
| 467 | 2019-12-05 02:26:00 | 15 | 42 | 3610 |
| 468 | 2019-12-05 02:36:11 | 15 | 38 | 3621 |
| 469 | 2019-12-05 02:46:22 | 15 | 37 | 3769 |
| 470 | 2019-12-05 02:56:34 | 14 | 36 | 3639 |
| 471 | 2019-12-05 03:06:45 | 14 | 39 | 3765 |
| 472 | 2019-12-05 03:16:56 | 14 | 38 | 3709 |
| 473 | 2019-12-05 03:27:07 | 14 | 39 | 3765 |
| 474 | 2019-12-05 03:37:18 | 14 | 39 | 3766 |
| 475 | 2019-12-05 03:47:30 | 14 | 38 | 3759 |
| 476 | 2019-12-05 03:57:42 | 14 | 38 | 3759 |
| 477 | 2019-12-05 04:07:53 | 15 | 61 | 3542 |
| 478 | 2019-12-05 04:18:04 | 15 | 37 | 3759 |
| 479 | 2019-12-05 04:28:15 | 15 | 37 | 3756 |
| 480 | 2019-12-05 04:38:27 | 16 | 36 | 3740 |
| 481 | 2019-12-05 04:48:38 | 16 | 36 | 3758 |
| 482 | 2019-12-05 04:58:49 | 16 | 35 | 3745 |
| 483 | 2019-12-05 05:09:01 | 16 | 34 | 3752 |
| 484 | 2019-12-05 05:19:11 | 17 | 34 | 3753 |
| 485 | 2019-12-05 05:29:23 | 17 | 32 | 3752 |
| 486 | 2019-12-05 05:39:34 | 17 | 33 | 3751 |
| 487 | 2019-12-05 05:49:45 | 18 | 31 | 3699 |

| | | | | |
|------|---------------------|----|----|------|
| 488 | 2019-12-05 05:59:57 | 18 | 31 | 3749 |
| 489 | 2019-12-05 06:10:09 | 18 | 30 | 3756 |
| 490 | 2019-12-05 06:20:20 | 18 | 31 | 3751 |
| 491 | 2019-12-05 06:30:31 | 19 | 30 | 3708 |
| 492 | 2019-12-05 06:40:43 | 19 | 29 | 3756 |
| 493 | 2019-12-05 06:50:54 | 19 | 28 | 3753 |
| 494 | 2019-12-05 07:01:05 | 19 | 29 | 3759 |
| 495 | 2019-12-05 07:11:16 | 20 | 29 | 3752 |
| 496 | 2019-12-05 07:21:28 | 20 | 29 | 3751 |
| 497 | 2019-12-05 07:31:39 | 20 | 28 | 3744 |
| 498 | 2019-12-05 07:41:51 | 20 | 29 | 3744 |
| 499 | 2019-12-05 07:52:02 | 20 | 27 | 3750 |
| 500 | 2019-12-05 08:02:13 | 20 | 28 | 3749 |
| - | - | - | - | - |
| - | - | - | - | - |
| - | - | - | - | - |
| - | - | - | - | - |
| 4202 | 2019-12-31 15:11:22 | 25 | 27 | 3552 |
| 4203 | 2019-12-31 15:21:33 | 25 | 28 | 3551 |
| 4204 | 2019-12-31 15:31:44 | 25 | 27 | 3551 |
| 4205 | 2019-12-31 15:41:54 | 25 | 27 | 3551 |
| 4206 | 2019-12-31 15:52:04 | 25 | 27 | 3551 |
| 4207 | 2019-12-31 16:02:15 | 25 | 27 | 3551 |
| 4208 | 2019-12-31 16:12:25 | 25 | 27 | 3551 |
| 4209 | 2019-12-31 16:22:36 | 25 | 26 | 3550 |
| 4210 | 2019-12-31 16:32:46 | 25 | 27 | 3550 |
| 4211 | 2019-12-31 16:42:57 | 25 | 27 | 3549 |
| 4212 | 2019-12-31 16:53:07 | 25 | 27 | 3548 |
| 4213 | 2019-12-31 17:03:18 | 24 | 27 | 3548 |
| 4214 | 2019-12-31 17:13:29 | 24 | 27 | 3549 |
| 4215 | 2019-12-31 17:23:39 | 24 | 27 | 3548 |
| 4216 | 2019-12-31 17:33:50 | 24 | 27 | 3548 |
| 4217 | 2019-12-31 17:43:59 | 24 | 27 | 3548 |
| 4218 | 2019-12-31 17:54:10 | 24 | 27 | 3548 |
| 4219 | 2019-12-31 18:04:21 | 24 | 27 | 3547 |